Structure and Function of the Human RecQ DNA Helicases

Dissertation
zur
Erlangung der naturwissenschaftlichen Doktorwürde
(Dr. sc. nat.)
vorgelegt der
Mathematisch-naturwissenschaftlichen Fakultät
der
Universität Zürich

von
Patrick L. Garcia
aus
Unterseen BE

Promotionskomitee
Prof. Dr. Josef Jiricny (Vorsitz)
Prof. Dr. Ulrich Hübscher
Dr. Pavel Janscak (Leitung der Dissertation)

Zürich, 2005

For my parents

Summary

The RecQ DNA helicases are highly conserved from bacteria to man and are required for the maintenance of genomic stability. All unicellular organisms contain a single RecQ helicase, whereas the number of RecQ homologues in higher organisms can vary. Mutations in the genes encoding three of the five human members of the RecQ family give rise to autosomal recessive disorders called Bloom syndrome, Werner syndrome and Rothmund-Thomson syndrome. These diseases manifest commonly with genomic instability and a high predisposition to cancer. However, the genetic alterations vary as well as the types of tumours in these syndromes. Furthermore, distinct clinical features are observed, like short stature and immunodeficiency in Bloom syndrome patients or premature ageing in Werner Syndrome patients. Also, the biochemical features of the human RecQ-like DNA helicases are diverse, pointing to different roles in the maintenance of genomic stability.

The goal of my thesis was to explore the functions of the human RecQ homologues BLM, WRN and especially the so far biochemically uncharacterised RECQ5, with a focus on the identification of functional domains of these proteins, their biochemical properties and modes of action.

To characterise the domain organisation of the BLM protein, Janscak *et al.* (1) purified from *E. coli* and biochemically characterised a deletion variant of BLM, encompassing amino acids 642-1290. This truncated version contained the DEAH, the RecQ-Ct and the HRDC domains. This fragment was proficient in DNA-stimulated ATPase and DNA helicase activity displaying the same substrate specificity as the full-size protein. Gel-filtration experiments revealed that it exists as a monomer in solution both free and in its DNA-bound form, even in the presence of Mg^{2+} and ATPγS. With a λ Spi^- assay, it could be shown that $BLM^{642\text{-}1290}$ is able to partially suppress the illegitimate recombination in *E. coli recQ*$^-$ strains. Furthermore, the RecQ-Ct domain was identified as a region essential for activity of the protein, and the HRDC domain as an auxiliary DNA binding domain.

With my work on RECQ5β (2), I could show the first biochemical characterisation of this RecQ DNA helicase. After overexpression in *E. coli*, I purified the protein to high homogeneity and subjected it to various biochemical assays. The protein showed the predicted ATP-dependent 3'-5' helicase activity and was also able to promote the

migration of Holliday juntions. Surprisingly, RECQ5β displayed a DNA strand-annealing activity residing in the C-terminal half of the protein. This activity was strongly inhibited by RPA. Inhibition of the annealing activity could also be observed in the presence of the poorly hydrolysable ATPγS, which was alleviated by mutations in the ATP binding motif of RECQ5β, indicating an inability of RECQ5β to anneal DNA strands in the ATP-bound form.

BLM and WRN are classified as SF2 helicases and show ATPase activity with single and double stranded DNA as effectors, indicating that translocation along the DNA is mediated by contacts with the phosphodiester backbone. SF1 helicases like the PcrA from *B. stearothermophilus* make contacts with the bases of the DNA, which is dependent on the rotational flexibility of the DNA backbone. I have shown that DNA unwinding by BLM and WRN was inhibited by vinylphosphonate internucleotide linkages in the DNA that reduce the rotational flexibility of the phosphodiester backbone; an effect also observed with PcrA (3). However, in contrast to PcrA, a single stranded DNA binding protein RPA could alleviate the inhibitory effect of these modifications on BLM and WRN-mediated unwinding, pointing to mechanistic differences between SF1 and SF2 helicases.

One of the functions of BLM is to act together with Topoisomerase IIIα to process recombination intermediates containing double Holliday junctions using a strand-passage mechanism that prevents the formation of cross-over products (4). Wu *et al.* (5) have shown that this dissolution reaction is highly specific to BLM amongst the human RecQ helicases and that it requires the HRDC domain of BLM. The HRDC domain is essential for the efficient binding to and unwinding of double Holliday junctions by BLM. The unwinding of simple duplexes is not an activity of the protein that is required for this reaction. The lysine 1270 of BLM located in the HRDC domain is required for efficient dissolution and is predicted to majorly contribute to the interaction with DNA.

Cheok *et al.* have shown that, in addition to the highly conserved DNA unwinding activity, BLM also contains a strand-annealing activity that does not require Mg^{2+}, is inhibited by ssDNA binding proteins and ATP, and is dependent on DNA length. Through deletion analysis we have shown that a 60 amino acid stretch in the C-terminal part of BLM is important for strand annealing (6).

Zusammenfassung

Die RecQ DNS Helikasen sind hochkonserviert in Bakterien bis zum Menschen und sind wichtig für die Bewahrung genomischer Stabilität. Alle unizellulären Organismen beinhalten eine einzige RecQ Helikase, während die Anzahl in höheren Organismen variieren kann. Mutationen in drei der fünf menschlichen RecQ-Homologen resultieren in den seltenen autosomal rezessiven Krankheiten Bloom Syndrom, Werner Syndrom und Rothmund-Thompson Syndrom. Diese Krankheiten zeichnen sich alle durch genomische Instabilität und hohe Krebsdisposition aus. Jedoch zeigen Syndrome Unterschiede bezüglich der genetischen Veränderungen, Art der Tumore und klinischen Befunden. Die biochemischen Eigenschaften der humanen RecQ DNS Helikasen sind auch verschieden, auf deren unterschiedlichen Aufgaben in verschiedenen Ketten und Rollen in Gewährleistung der genomischen Stabilität hin weisend.

Das Ziel meiner Dissertation war es, die Funktionen der RecQ Homologen BLM, WRN und besonders die des bis dahin spärlich charakterisierten RECQ5 zu erforschen mit speziellem Augenmerk auf die Identifikation funktioneller Domänen, biochemische Eigenschaften und Reaktionsmechanismen.

Um die Domänorganisationsstruktur des BLM Proteins zu definieren, haben Janscak *et al.* (1) eine Deletionsvariante von BLM, das Peptid der Aminosäuren 642-1290, nach Überexpression in *E. coli* aufgereinigt und biochemisch charakterisiert. Die Variante enthält die DEAH Helikasen-, die RecQ-Ct und die HRDC Domänen. Dieses Fragment zeigte DNS-stimulierte ATPase Aktvität mit derselben Substratspezifität wie das Protein der ganzen Länge. Durch Gel-filtrationsexperimente konnte gezeigt werden, dass das Protein in Lösung frei und in DNS gebundener Form als Monomer vorlag, was nicht durch die Präsenz von Mg^{2+} sowie von ATPγS beeinflusst wurde. In einem λ Spi$^-$ Versuch hat sich gezeigt, dass BLM$^{642\text{-}1290}$ partiell die illegitime Rekombination in *E. ColiRecQ*$^-$ unterdrücken konnte. Des Weiteren wurde die RecQ-Ct Domäne als eine für die Aktivität des Proteins essentielle Region und die HRDC Domäne als auxiliäre Bindungsdomäne identifiziert werden.

Durch meine Arbeit mit RECQ5β, konnte ich die erste biochemische Charakterisierung dieser RecQ-ähnlichen DNS Helikase zeigen (2). Nach Überexprimierung in *E. coli* habe ich das Protein zu hoher Homogenität aufgereinigt und es mittels klassischen Helikasenversuchen charakterisiert. Das Protein hat die vorausgesagte ATP-abhängige

3'-5' Helikasenaktivität gezeigt, und vermochte auch Holliday Strukturen zu migrieren. Erstaunlicherweise zeigte dieses Protein eine DNS-Paarungsaktivität im C-terminalen Teil, welche durch RPA inhibiert werden konnte. Die Inhibition der Paarungsaktivität konnte ebenfalls durch das schwach hydrolysierbare ATPγS beobachtet werden, was wiederum duch Mutationen im ATP-Bindungsmotiv aufgehoben wurde, darauf hindeutend, dass das Protein in ATP-gebundener Form nicht in der Lage ist, DNS Stränge aneinanderzuführen.

BLM und WRN sind als SF2 Helikasen klassifiziert und zeigen ATPase Aktivitäten mit einzelsträngiger sowie doppelsträngiger DNS als Effektoren, auf einen Translokationsmechanismus deutend, welcher durch Kontakte mit dem Phosphodiestergerüst bewerkstelligt wird. SF1 Helikasen wie PcrA aus *B. stearothermophilus* gehen Kontakte mit den Basen ein, was eine Rotationsflexibilität der DNS benötigt. Ich konnte zeigen, dass die Helikasenaktivität von BLM und WRN durch den Einbau von Vinylphosphonaten, welche die Rotationsflexibilität des Phosphodiestergerüsts der DNS vermindern, inhibiert wurde; ein Effekt, der auch mit PcrA beobachtet wurde (3). Im Gegensatz zu PcrA konnte der inhibitorische Effekt durch das humane einzelstrangbindende RPA aufgehoben werden, auf mechanistische Unterschiede zwischen SF1 und SF2 Helikasen hindeutend (3).

Eine der Funktionen von BLM ist, Rekombinationsintermediate mit doppel Holliday Strukturen zusammen mit TOPOIIIα aufzulösen (4) um die Entstehung von "cross-over"-Produkten zu verhindern. Wu *et al.* (5) haben gezeigt, dass diese Reaktion, im Englischen "double Holliday junction dissolution" genannt, hochspezifisch für BLM ist unter den humanen RecQ Helikasen und dass die HRDC Domäne von BLM benötigt. Wir konnten des Weiteren zeigen, dass die HRDC Domäne von BLM essenziell fuer die Bindung an und Aufwindung von doppel Holliday Strukturen ist. Das Aufschmelzen simpler DNS Duplexe ist nicht eine Aktivität, welche für diese Reaktion benötigt wird. Lysin 1270 in BLM ist wichtig fuer die effiziente Dissolution und scheint einen wichtigen Beitrag zur Interaktion mit der DNS zu leisten.

Cheok *et al.* haben gezeigt, dass BLM, zusätzlich zu der hochkonservierten Helikasenaktivtität, eine DNS-Basenpaarungsaktivität besitzt. Diese durch BLM bewerkstelligte Basenpaarung ist Mg^{2+}-unabhängig, wird durch einzelsträngige DNS inhibiert und ist von der DNS-Länge abhängig. Durch Deletionsanalyse konnte gezeigt werden, dass die C-Terminale Domäne dafür essenziell ist, und 60 Aminosäuren davon für die

Bindung einzelsträngiger DNS und für die Basenpaarung wichtig ist (6).

Contents

1 Helicases - Classification and Mode of Action

Helicases are ubiquitous enzymes that use the free energy from NTP hydrolysis to separate the two component strands of double-stranded nucleic acids (DNA-DNA, RNA-DNA, RNA-RNA). These enzymes play essential roles in all aspects of nucleic acid metabolism (7).

Helicases are classified according to sequence homology and directionality. The directionality is defined with respect to the nucleic acid strand on which the enzyme translocates (3'-5' or 5'-3') (8). Based on amino acid sequence homology, helicases are classified into five majour groups, denoted superfamilies 1-5 (SF1-5) (Table 1). SF1 and SF2 are the largest and are characterised by a set of similar amino acid motifs called Q, I, Ia and II-VI (Figure 1). SF3 helicases harbour only three different conserved helicase motifs called A, B and C and the SF4 helicases are known to have the five motifs called 1, 1a and 2-4 (9). The motifs of the SF5 members have not been well described.

Superfamily	Helicase	Organism	nucleic acid	Reference
SF1	Rep	*E. coli*	DNA	(10; 11)
	PcrA	*B. stearothermophilus*	DNA	(10; 12)
	UvrD	*E. coli*	DNA	(10)
SF2	RecQ	*E. coli*	DNA	(10)
	NS3	*Hepatitis C Virus*	RNA	(10; 13)
SF3	T antigen	*SV40 papovavirus*	DNA/RNA	(10)
SF4	DnaB	*E. coli*	DNA	(10)
SF5	Rho	*E. coli*	DNA/RNA	(10)

Table 1: Classification of Helicases based on sequence homology, with some examples.

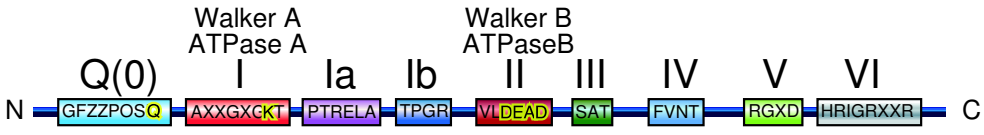

Figure 1: Schematic representation of the domain organisation of the DEAD box helicases. boxes represent conserved helicase motifs showing consensus sequences by single-letter amino acid code. (Z=D, E, H, K, R; O=S, T; X=any aa). Adapted from Ref. (14).

In Figure 1, the domain organisation of DEAD box helicases is schematically depicted. The Q-motif is characteristic of the DEAD box family (15; 16). It contains a highly conserved glutamine which is also present in the ”0” motif of the RecQ helicases that belong to the DExH helicase family. In *E. coli* RecQ the conserved glutamine has been shown to bind to the adenine moiety of the ATP cofactor (17). For a number of helicases it has been shown by mutational anlalysis that this conserved residue is essential for ATPase and helicase activity of the enzyme. Moreover, a missense mutation at the equivalent residue of the BLM helicase is sufficient to cause the Bloom syndrome (18). Motif I is also referred to as the Walker A motif found in ATPases (19). This domain is also essential for ATP binding; a conserved lysine residue makes contacts with the β and the γ phosphates of the ATP molecule (20). The motif Ia has been shown to contribute to ssDNA binding in the UL9 helicase from the Herpes Simplex Virus (HSV) and is present in many SF1 and SF2 helicases (21). In the DEAD and DExH helicases an additional motif named Ib motif is found with a consensus sequence of TxGx (14). Motif II is equivalent to Walker B motif also found in other ATPases. Based on the sequence of this motif, helicases are further classified into the DExH and the DEAD families. The highly conserved aspartate residue in Motif I (D of DE) coordinates Mg^{2+}, and is required for ATP hydrolysis but not binding (20). Motif III is very likely to be important for coupling ATPase to helicase activity (22). Motif IV seems to be essential for the later steps of the ATPase reaction as it binds ADP. Motif V is likely to serve as an additional domain for binding DNA, since it has been shown to make contacts with the sugar-phosphate backbone (9). The motif VI has been proposed to be required for the helicase to move along the DNA substrate by mediating conformational changes associated with nucleotide binding (14).

For the mode of action of helicases, several models have been proposed and are depicted schematically in Figure 2. In the inchworm model, the enzyme binds to ssDNA and translocates along the strand until it reaches the duplex which is then invaded and unwound (23). The modified inchworm model has been proposed for the monomeric UvrD helicase. The enzyme consists of two DNA binding subdomains, a leading domain that binds to ssDNA and dsDNA and a trailing domain that only binds to ssDNA. ATP binding induces a closed conformation of the enzyme by pulling the trailing domain towards the leading domain. Upon ATP hydrolysis, the trailing domain remains on ssDNA and the leading domain is moved forward into the duplex and mediates strand

separation (24; 25). In the active rolling model, the helicase consists of two identical subunits that can both bind to ssDNA and dsDNA. One subunit stays bound on ssDNA and the subunit behind will detach from the DNA and rotate around the bound subunit to bind dsDNA. A conformational change upon ATP hydrolysis will then lead to the separation of the duplex (26).

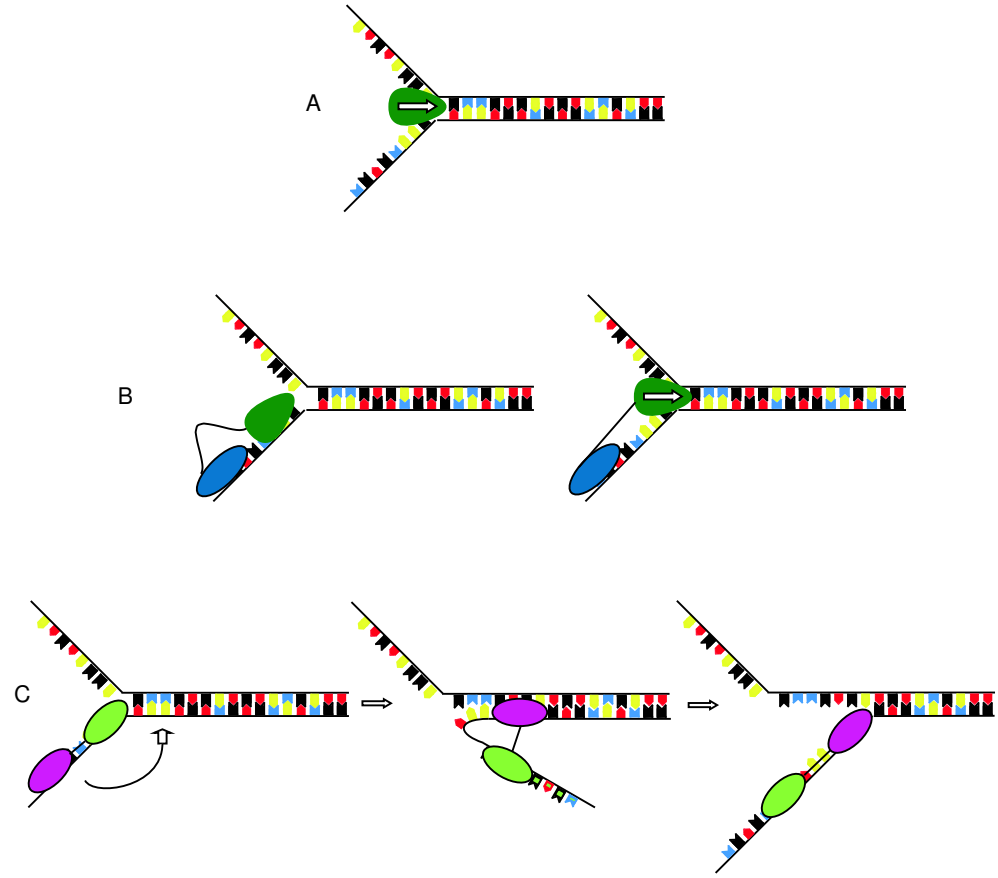

Figure 2: Models for DNA helicase translocation and unwinding. (A) Inchworm model. (B) Modified inchworm model. Leading domain in green, trailing domain in blue. (C) Active rolling model. Two identical subunits in green and purple.

2 The RecQ Family of DNA Helicases

2.1 General Features and Structural Organisation

The RecQ helicases, named after the DNA helicase RecQ of *Escherichia coli*, are highly conserved from bacteria to man. Defective functions of these proteins lead to genomic instability that generally manifests as hyperrecombination. In humans, defects in the *BLM* , *WRN* and *RTS/RECQ4* genes are associated with the autosomal recessive, cancer-prone diseases Bloom syndrome (BS) (27; 28), Werner syndrome (WS) (29; 30) and Rothmund Thompson syndrome (RTS) (31; 32; 33), respectively. Higher organisms contain several RecQ homologues, with five homologues identified in humans. These proteins presumably play specialised roles in genome maintenance since distinctions in the clinical as well as the cellular manifestations of BS, WS and RTS have been observed. Furthermore, the multiple RecQ homologues also display differences at the biochemical level with overlapping, but also very distinct substrate specificities mostly due to the presence of various additional functional domains. The diverse protein interaction partners observed further implicate different human RecQ homologues in different DNA transactions. It seems that the cellular functions of the sole RecQ homologues in unicellular organisms are divided up into and extended on several homologues in higher organisms.

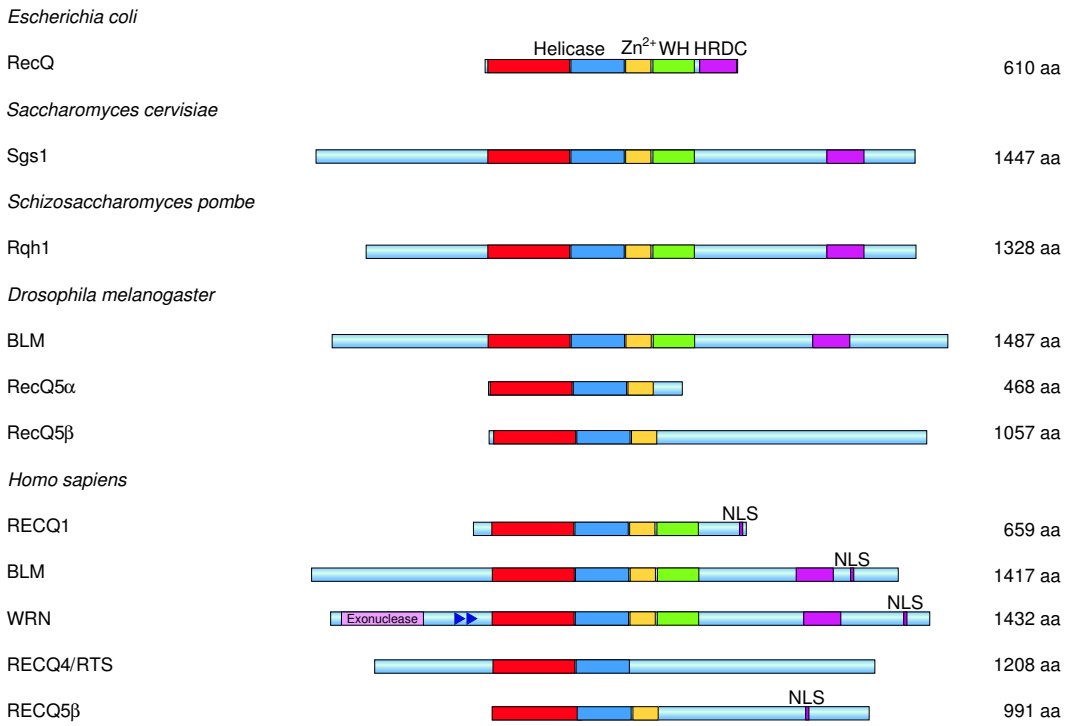

Figure 3: Schematic representation of the RecQ helicases of selected organisms. The domains of the RecQ from *E. coli* are labelled; helicase domains in red and blue, Zinc-binding domain in yellow, the winged helix domain in green and the HRDC domain in purple, according to the crystal structure of the *E. coli* RecQ helicase (34). The putative nuclear localisation signals (NLS) are marked by red boxes. WRN contains an additional exonuclease domain and a direct repeat (blue triangles). The lengths of the proteins are given to the right in number of amino acids.

In Figure 3, selected RecQ helicases are drawn schematically. All RecQ members contain the helicase domains characteristic of the DEAH subgroup of SF2 helicases (10). The adjacent Zn^{2+} binding domain has been found in all RecQ helicases examined, except for RECQ4. Another characteristic of the RecQ members is the winged helix (WH) domain, which has only been found to be absent in the human RECQ4 and RECQ5 and their orthologues. Furthermore, distal to the WH domain, the **H**elicase and **R**NAse **D** **C**-terminal (HRDC) domain is found. This domain is absent in RECQ1, RECQ4 and REQ5. The WRN helicase contains an additional 3'-5' exonuclease at the aminoterminus of the protein and a 27 amino acid repeat between the exonuclease and the helicase domains. All unicellular organisms examined contain a single RecQ homologue that harbours all the common conserved motifs, such as the helicase domains, the Zn^{2+} binding domain, the WH domain and the HRDC domain (34).

Some biochemical characteristics of selected members of the RecQ family are listed in Table 2. Figure 4 schematically shows some substrates that have been used to study

the substrate specificities of RecQ helicases in Table 2.

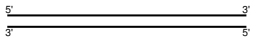	Blunt-ended duplex Enzymes that require a free ssDNA tail or load to a specific structure do normally not unwind such a structure by themselves.
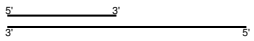	5‘- tailed duplex A substrate for 5’-3‘ helicases that load on free ssDNA or to the ssDNA/dsDNA interface.
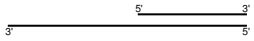	3‘- tailed duplex A substrate for 3’-5‘ helicases that load on free ssDNA or to the ssDNA/dsDNA interface.
	Duplex containing a bubble This substrate mimicks a duplex with a distortion of the helix or DNA containing a loop.
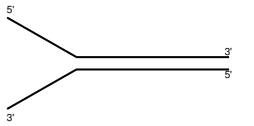	Splayed arm or forked duplex 5'-3' and 3'-5' helicases that require free ssDNA or load on this specific junction will unwind such a substrate.
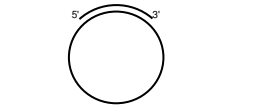	A classic helicase substrate Large circular ssDNA containing a partial duplex. This substrate has been mostly prepared from M13 ssDNA annealed to a synthetic oligonucleotide
	D-loop structure This substrate mimicks an intermediate from homologous recombination, a ssDNA strand invades the duplex to form this structure. Disruption of D-loops can be monitored if the enzyme does not unwind from blunt ends.
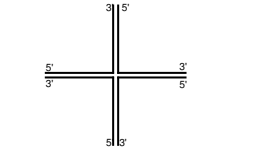	Holliday junction or 4-way junction A synthetic Holliday junction resulting from annealing of four oligonucleotides. Used to test for Holliday junction branch migration. A preferred substrate for BLM.
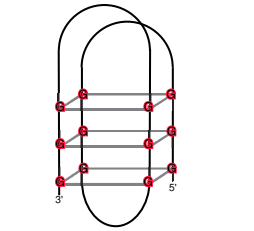	G4 DNA, also called G quadruplex DNA. G-rich sequences, especially at telomeres, can form such a structure through Hogsteen-bonds between Gs. This structure is biochemically formed from one oligonucleotide and is stable at room-temperature. A preferred structure for BLM, WRN and Sgs1.

Figure 4: Various DNA substrates used to biochemically assay DNA helicases and explanatory to Table 2.

Substrate	**RECQ1**	**BLM**	**WRN**	**Sgs1**	*E. coli* RecQ
Blunt-ended duplex	- (35)	- (36; 37)	- (36; 38; 39)		+ (40; 41; 42)
5'-tailed duplex	- (35)	- (36; 37)	- (39)	- (43)	+ (42)
3'-tailed duplex	+ (35; 44)	-+ (36)	-+ (36; 45)	+ (43)	+ (42)
Splayed arm	+ (44)	+ (36; 46; 47; 48)	+ (36; 46; 47; 49)	+ (43; 50; 51)	+ (42; 52)
Bubble-substrate 4nt		- (36)			
Bubble-substrate 8nt and larger	-+ (35)	+ (36)	++ (36; 38)		
D-loop	+ (44)	+ (37)	+ (53)		
circular ssDNA/partial duplex 17-30 bp	+ (35)	+ (54; 55)	+ (56; 57; 58; 59)	+ (60)	
circular ssDNA/partial duplex 42-100 bp	+ (61)	+ (54; 37; 55; 62)	- (56; 58; 63; 64)	+ (60)	+ (40; 65)
Holliday junction	+ (44)	++ (36; 66)	+ (36)	+ (43; 66)	+ (42)
G4 DNA 3' tail		++ (36; 48; 66)	++ (36)	++ (50; 51; 66)	+ (52)
G4 DNA blunt		- (48)	- (36; 67)	- (50)	
G4 DNA 5' tail			+ (67)		

Table 2: Substrate specificities for some RecQ helicases. + indicates unwinding ability, - no unwinding observed, ++ strong activity, -+ weak activity. The substrates are explained in Figure 4

2.2 The *Escherichia coli* RecQ

2.2.1 Genetics

The RecQ protein from *Escherichia coli* is the founding member of the RecQ DNA helicase family and was discovered in 1984 by Nakayama *et al.* in a screen for mutations that confer resistance to thymineless death (68; 69). RecQ acts in the RecF pathway of homologous recombination that operates in the repair of stalled replication forks. *RecQ* mutations in a *recBC sbcB* background lead to an enhanced UV sensitivity and lower the efficiency of conjugal recombination (68). RecQ and RecJ are required for lagging strand degradation at stalled replication forks. (70; 71; 72). RecQ is involved in the supression of illegitimate recombination, which is enhanced 30-300 fold in *recQ*$^-$ mutants (73). A recent study shows that RecQ is needed for the fast degradation of the LexA repressor in response to UV irradiation to induce the SOS response (74), reviewed in Ref. (75). The SOS response is a mechanism of bacteria strongly enhanced by the formation of RecA filaments and induces the expression of roughly 30 DNA repair genes as a response to DNA damage (76).

2.2.2 Biochemical Properties of RecQ

The *RecQ* gene codes for a 610 amino acids long protein that is an ATP-dependent 3'-5' helicase. In an initial biochemical characterisation of RecQ, Umezu *et al.* observed that the protein is able of unwinding partial duplexes as long as 143 bp in an ATP-dependent manner (40). Harmon and Kowalczykowski found that RecQ is capable of unwinding a wide variety of abnormal DNA structures including D-loops, indicative of a role in suppressing illegitimate recombination by disrupting aberrant recombination intermediates (42). Furthermore, RecQ was shown to unwind a covalently closed double-stranded DNA substrate which can activate the strand-passage activity of DNA topoisomerase III (77). Further biochemical properties are in another chapter (Chapter 2).

2.2.3 Models for RecQ-mediated DNA Transactions

Based on genetic and biochemical evidences, four roles for RecQ in the maintenance of genomic stability in *E. coli* have been proposed (Figure 5): In a model for the initiation of recombination, RecQ unwinds DNA at gaps (in wt cells) or double-strand breaks

(in *recBC*$^{-}$ *cells*) allowing RecA filament formation to initiate recombination and D-loop formation (42). In the anti-recombination model, RecQ can disrupt D-loops formed by RecA (42). RecQ is very likely to perform the double Holliday junction (DHJ) dissolution, as it has been shown that RecQ in concert with Topo III can catenate/decatenate duplex DNA (77), and that BLM together TOPOIIIα can perform the DHJ dissolution (4) it is likely that RecQ can, together with Topo III perform this reaction as well *in vivo*. In the SOS model of Hishida *et al.* (74), RecQ binds a gap on the leading strand of a stalled replication fork and unwinds the duplex template ahead of the fork, in a 3'-5' direction. The ensuing topological stress may be relieved by the combined action with a type I topoisomerase such as Topo III. Subsequently, RecQ switches to the lagging strand template, generating a single-stranded DNA gap on the lagging strand, on which a RecA filament is assembled in the 3' direction, leading to SOS induction. Subsequent repair of the blocking lesion, trans-lesion synthesis, or recombinational restart may lead to the resumption of DNA replication.

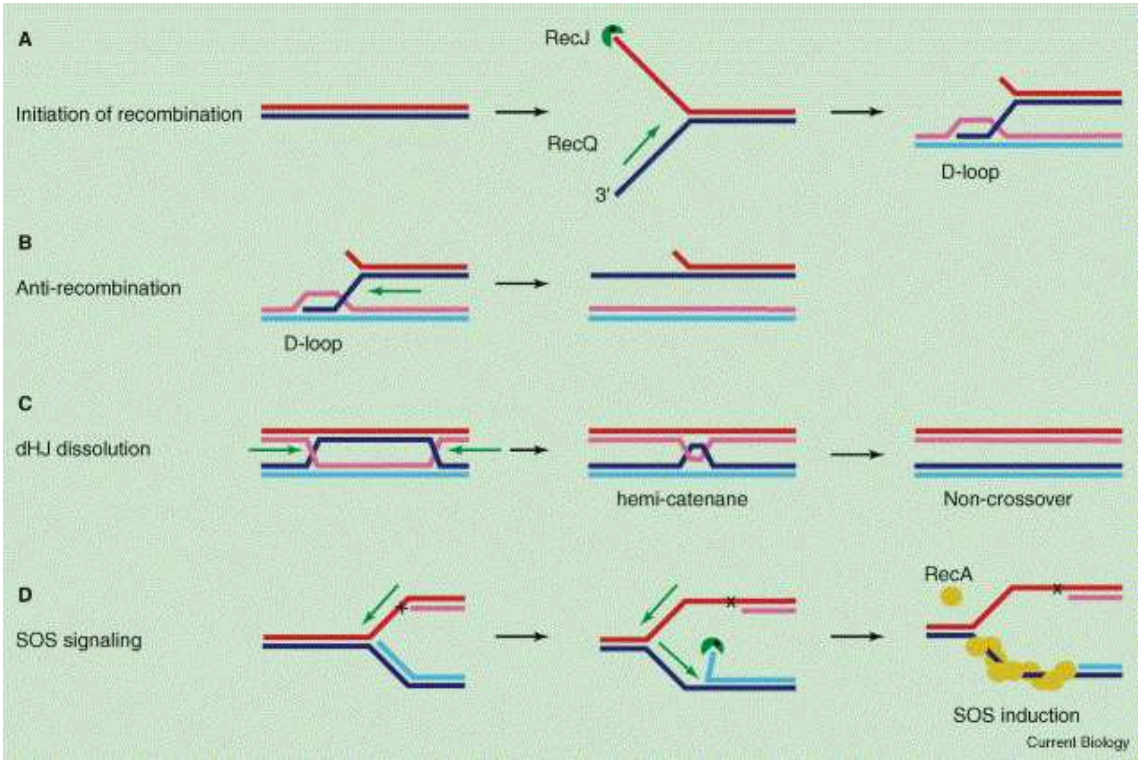

Figure 5: Roles of the RecQ DNA helicase in genomic maintenance. Adapted from Ref. (75) (A) Initiation of recombination. (B) Anti-recombination. (C) DHJ dissolution. (D) The SOS model.

2.2.4 Structure of RecQ

Bernstein and Keck have crystallized the catalytic core of the *E. coli* RecQ protein and resolved its structure (34). The crystal structure of RecQ is shown in Figure 6. In this work, the authors show that C-terminally adjacent to the helicase domains, there are two additional structural motifs that are not present in other helicases: The Zn^{2+}-binding domain contains four highly conserved cysteines which coordinate a zinc ion. Adjacent to that lies the winged helix (WH) domain forming a helix-turn-helix fold, found to act as a DNA binding motif in many proteins (78). The HRDC was not present on the polypeptide crystallized and its function is not yet fully elucidated. Liu *et al.* have resolved the 3-dimensional structure of the HRDC of Sgs1 from *Saccharomyces cervisiae*, but were not able to draw functional conclusions from this work (79).

Recently, Liu *et al.* have characterised the importance of the Zn^{2+}-binding domain. They show that the highly conserved cysteines form a complex with the Zn^{2+}. This complex is essential for DNA binding and helicase activity, but not for ATP binding. Furthermore, they show that this zinc finger binding motif is important in maintaining the integrity of the protein structure. They further discuss that this Zn^{2+} finger is unique to the RecQ family (80).

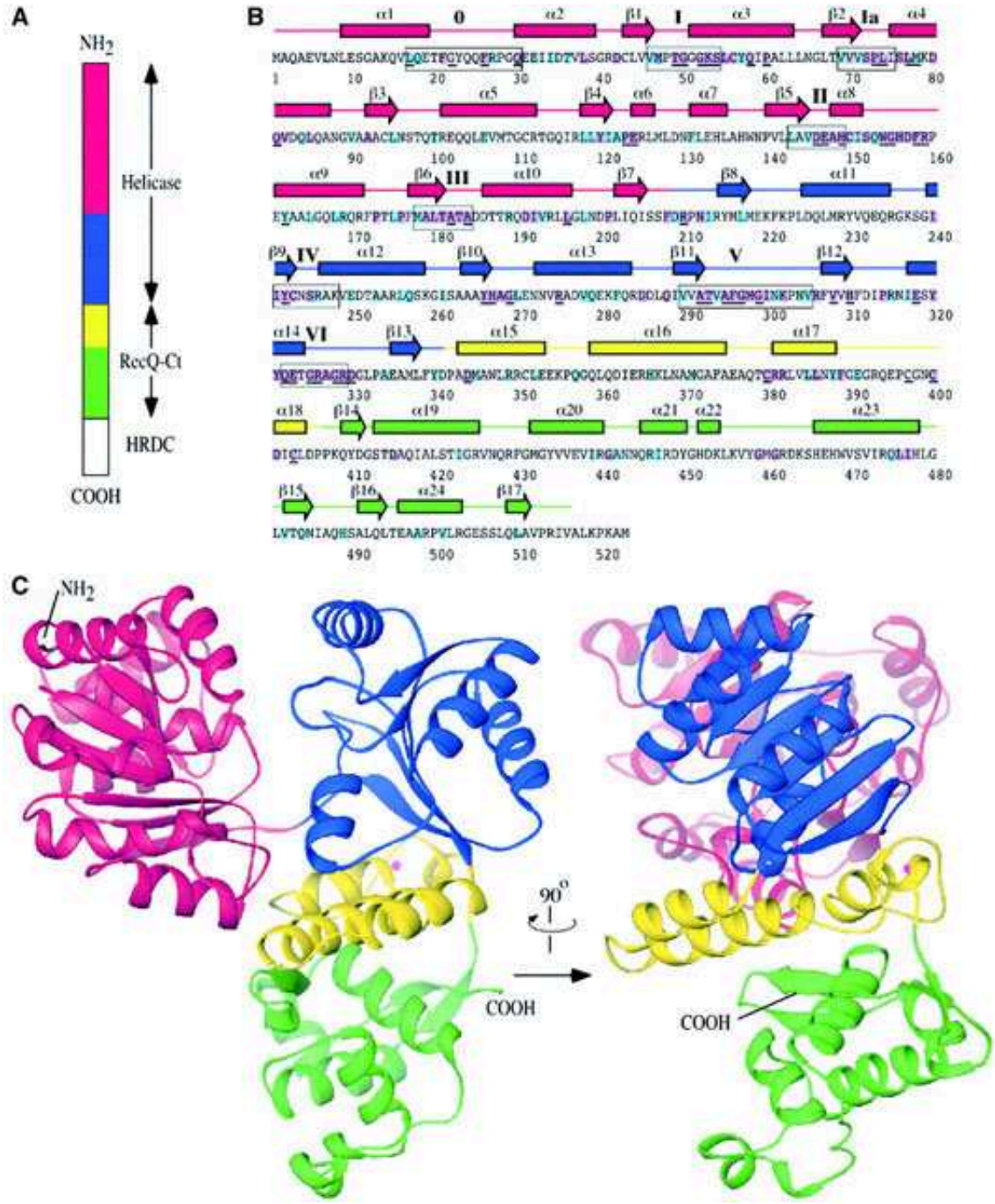

Figure 6: The structure of the RecQ catalytic core. Adapted from Ref. (34). (A) Schematic diagram of *E. coli*. Three conserved regions, helicase, RecQ-conserved (RecQ-Ct), and Helicase-and-RNase-D-C-terminal (HRDC) (81), are labelled. The catalytic core of *E. coli* RecQ (RecQΔC) includes only the helicase and RecQ-Ct regions, and comprises four apparent subdomains in the structure: residues 1-208 in red, 209-340 in blue, 341-406 in yellow and 407-516 in green. (B) Sequence and secondary structure of RecQΔC. Helices (boxes) and β-strands (arrows) are shown above the sequence and labelled sequentially. Colour coding is the same as in (A). Conserved helicase motifs (motifs 0-VI) are labelled and enclosed in boxes. Residues that are invariant among 65 bacterial RecQ proteins are underlined, and residues that are invariant or highly conserved with a subset of eukaryotic RecQ proteins (human WRN, BLM, and *S.cervisiae*) are highlighted in purple or light-blue boxes, respectively. (C) Orthogonal views of a ribbon diagram of the crystal structure of RecQΔC, colour-coded as in (A). A bound Zn^{2+} ion is shown as a magenta sphere.

2.3 *Saccharomyces cervisiae* Sgs1

2.3.1 *Sgs1* Cellular Phenotype

Sgs1 was identified as a suppressor of the slow growth phenotype of *top3* mutants (Chapter 2.3.3). *sgs1* mutant budding yeast cells show a 40% decrease in lifespan compared to wild-type cells (82; 83). McVey *et al.* have shown that *sgs1* mutants in fact arrest in G_2 or in G_1 (84). *sgs1* mutants do not show differences in telomere lenghts, compared to wild-type cells (85), but the double mutants *sgs1 tlc1* and *sgs1 est2* show an elevated rate of telomere shortening compared to the single *tlc1* mutant, indicating a role in telomere maintenance (86). *sgs1* cells show increased sensitivity to treatment with MMS (87; 88), UV light (89; 90) and HU (91), but not to γ-radiation (91). At the chromosomal level, *sgs1* mutants display a wide variety of defects as marker loss (85; 92), an elevated rate of sister chromatid exchanges (SCE) (93), gross chromosomal rearrangements (94; 95), a higher rate of loss of heterozygosity (96) and an increased level of illegitimate recombination (97). MMS-induced interchromosomal recombination was found to be reduced in *sgs1* cells and UV light exposure of these mutants only induced little of those events (92).

2.3.2 Biochemical Properties of Sgs1

Sgs1 codes for a protein of 1447 amino acids and has not been purified at the full length yet. Biochemical assays were performed with a deletion variant $Sgs1^{400\text{-}1268}$, which is as the other RecQ helicases an ATP-dependent 3'-5' helicase being able to unwind a wide variety of abnormal DNA structures including Holliday junctions (HJ) and D-loops (Chapter 2). Not only is Sgs1 able to unwind DNA duplexes, it can also disrupt RNA/DNA hybrid molecules (60).

The abundance of Sgs1 is cell-cycle regulated, with low levels in M and G_1, a peak in S and degradation in G_2. Sgs1 forms S-phase specific nuclear foci which partially co-localise with Rad53 and the origin recognition complex (82). Sinclair *et al.* have reported Sgs1 to localise into the nucleolus (82), while Frei and Gasser did not observe this (91).

2.3.3 Interaction Partners and Models for DNA Transactions

Topoisomerases

DNA topoisomerases are enzymes that alter the state of supercoiling of DNA by a strand-passage mechanism involving transient DNA breaks. According to their mode of action, they are classified into the type I topoisomerases which generate ssDNA breaks and into type II topoisomerases that create dsDNA breaks to mediate strand-passage.

The *S. cervisiae Sgs1* was identified by three different groups independently, but always in the context of either a topoisomerase gene or protein. Gangloff *et al.* discovered *Sgs1* in a screen for suppressors of the *top3* slow-growth phenotype (98). Watt *et al.* identified *Sgs1* in a search for interaction partners of Top2 (99) and Lu *et al.* found *Sgs1* because of genetic interaction with Top1 (Type I) (100). *Sgs1* interacts physically and genetically with all three nuclear topoisomerases. Yeast Top1 is required for DNA replication (101), mitotic chromosome condensation (102) and general transcriptional repression in stationary phase (103). Under normal conditions, a deletion of *top1* has no effect on growth. Top1 has been reported to interact with Sgs1, but the role of this complex has not been identified yet (99; 82). Top2 (Type II) is required for the resolution of intertwined chromosomes during mitosis and meiosis and is an essential gene (104; 105; 106). Genetically, *Top2* and *Sgs1* have been reported to be epistatic with regard to reducing chromosome non-disjunction, suggesting that they are involved in the same pathway for chromosome segregation (85).

Top3 mutants grow poorly (107; 108), are sensitive to DNA damaging agents (109; 110), have severe meiotic defects (111; 112) and exhibit hyper-recombination between repetitive sequences such as telomeres and rDNA (101; 108; 111). The G_2 delay, elevated frequency of marker loss and altered morpholgy of a *top3* mutant are suppressed by mutations in the *Sgs1* gene (98; 113). Recombinant Top3 (Type I) only acts on negatively supercoiled dsDNA (107). Ira *et al.* have shown that the deletion of *Sgs1* increases crossovers in yeast cells 2-3 fold. The overexpression of Srs2 nearly eliminates crossovers, whereas overexpression of Rad51 in *srs2* cells almost completely eliminates the noncrossover recombination products. It is very likely that Sgs1 in concert with Top3 performs the same reaction as BLM/TOPOIIIα on DHJs.

Sgs1 and Homologous Recombination

Srs2 is a 3'-5' helicase showing only limited homolgy to the *E. coli* UvrD helicase and no homology to any known human protein (114). Srs2 suppresses homologous recombination (HR) through disrupting Rad51 ssDNA filaments (115; 116). Recently, Pfander *et al.* have demonstrated that SUMO-modified PCNA recruits Srs2 in S phase to prevent unwanted recombination events at replicating chromosomes (117). Furthermore, the *sgs1 srs2* double mutant shows a severe growth which is alleviated upon blocking recombination by mutating *Rad51, Rad52, Rad55* or *Rad57* (89). A recent study from Liberi *et al.* shows that in *sgs1* mutants, recombination-dependent DNA intermediates accumulate at damaged forks, a phenomenon that requires the Rad51 protein, which is counteracted by the Srs2 protein and does not prevent fork movement (118). Sgs1, but not Srs2, promotes the resolution of these recombination intermediates. The integrity of these DNA structures at sister chromatid junctions is protected by the Rad53 checkpoint kinase. They also show that *top3* and *top3 sgs1* mutants accumulate the same structures as *sgs1* cells, arising from defective maturation of the recombination intermediates (118). The accumulation of HJs arising from fork reversal in *rad53* mutants has been shown by Sogo *et al.* (119).

Sgs1 in Checkpoint Activation and Replication Fork Maintenance

Frei and Gasser have observed that the deletion of *Sgs1* partially compromises the intra-S-phase checkpoint, which is largely mediated by the Rad53 kinase (91). Bjergbaek *et al.* later found that Sgs1 functions independently of both Top3 and Rad51 to stimulate the checkpoint kinase Rad53 upon replication fork stalling in response to HU treatment. This checkpoint activation is not dependent on the helicase activity of Sgs1 which correlates with the finding of direct interaction with Rad53. Furthermore, Sgs1 and Mrc1, which serves as mediator or adaptor for Rad53 activation, act in the same pathway for checkpoint activation. Moreover, they find that Top3 and Rad51 are required for DNA polα and DNA pol ϵ stabilisation at stalled replication forks and that Sgs1 and Mrc1 act synergistically to stabilise DNA polα and DNA pol ϵ at stalled forks (120; 121) . The authors conclude that the checkpoint kinase activation requires Sgs1 as a noncatalytic Rad53-binding site, while the Top3/Sgs1 resolvase contributes to recovery of stalled replication forks (121). Fabre *et al.* have further shown that Sgs1 may be involved in the

repair of single-stranded gaps arising from replication (122).

The *SLX* genes and Mus81/Mms4

In a screen for mutations that show synthetic lethality in an *sgs1* background, Mullen *et al.* have found a group of genes that were named *SLX* (123; 124). A synthetic lethality was also found between the *slx* mutants and *top3*, indicative of a function in pathways parallel to that of Sgs1/Top3. *SLX6* was shown to be allelic to *Srs2*. Slx5 and Slx8 are putative RING/finger domain proteins that form a complex and are required for efficient sporulation. Slx1 and Slx4 also form a complex and Slx2 and Slx3 were demonstrated to be the two subunits of the Mus81-Mms4 heterodimeric complex that acts as a structure-specific nuclease (123; 124). Fabre *et al.* have later proposed that the single stranded DNA resulting from the stalling of replication forks can be processed by two competing mechanisms: Either recombination or nonrecombinational translesion synthesis. Srs2 would channel recombination intermediates back into the translesion synthesis pathway, whereas Sgs1/Top3 and Mus81/Mms4 interact in recombination and/or replication to allow replication restart (122).

RAD16

Saffi *et al.* have shown that *Sgs1* is epistatic to the repair protein Rad16 with respect to cell survival after treatments with UVC, 4-NQO and H_2O_2 and that the defect in helicase activity of Sgs1 is essential for most aspects of the *sgs1* mutation phenotype (90; 109). Rad16 has been shown to function in global genome repair of the nucleotide excision repair (125).

RMI1/NCE4

In a recent study, Chang *et al.* show that Rmi1 (RecQ-mediated genome instability, also known as NCE4) physically interacts with Sgs1 and Top3 (126). Cells lacking RMI1 activate the Rad53 checkpoint kinase, undergo a mitotic delay, and display increased re-localisation of the recombination repair protein Rad52, indicating the presence of spontaneous DNA damage. Consistent with a role for RMI1 in maintaining genome integrity, *rmi1* cells exhibit increased recombination frequency and increased frequency of gross

chromosomal rearrangements. In addition, *rmi1* strains fail to fully activate Rad53 upon exposure to DNA-damaging agents, suggesting that Rmi1 is also an important part of the Rad53-dependent DNA damage response (126).

Another recent study identified Rmi1/Nce4 as potential component of the Sgs1/Top3 pathway, based on the observation that strains lacking any one of these genes require Mus81 and Mms4 for viability. *sgs1* and *rmi1* mutants display the same spectrum of synthetic lethal interactions, including the requirements for Slx1, Slx4, Slx5, and Slx8. Like *sgs1 mus81*, the *rmi1 mus81* synthetic lethality is dependent on HR. On their own, mutations in Rmi1 result in phenotypes that mimic those of *sgs1* or *top3* strains including slow growth, hyperrecombination, DNA damage sensitivity and reduced sporulation. And like *top3* strains, most *rmi1* phenotypes are suppressed by mutations in Sgs1. They further show that Rmi1 forms a heteromeric complex with Sgs1-Top3 *in vitro* and *in vivo*. The Rmi1-Top3 complex is stable in the absence of the Sgs1 helicase, but the loss of either Rmi1 or Top3 in yeast compromises the interaction of the other with Sgs1. Further biochemical studies demonstrated that Rmi1 is a structure-specific DNA binding protein with a preference for cruciform structures suggesting that the DNA binding specificity of Rmi1 plays a role in targeting Sgs1-Top3 to appropriate substrates (127).

2.4 RECQ1

RECQ1, sometimes called RECQL or helicase Q1, is the smallest of the human RecQ helicases (see Figure 3) and was originally cloned independently by two groups (128; 129). The human *RECQ1* gene is located on chromosome 12p11-12 (128; 130). Zhang and Xi have described two variants resulting from alternative splicing (131). Interestingly, although a defect in RECQ1 has not been associated with a human disease yet, this chromosomal location has been found to coincide with cytogenetic alterations in testicular germ-cell tumours (132).

The first biochemical charaterisation of RECQ1 was performed before its cDNA was cloned. Yanagisawa *et al.* purified DNA-dependent ATPases from HeLa cells and xeroderma pigmentosum (XP) cells to identify the cause of the disease and found that the ATPases purified from XP cells differed from those from HeLa cells (133). A 73 kDa ATPase, called ATPase Q1, was isolated and found to display 3'-5' helicase activity (134). The identified ATPase Q1 failed to complement XP-cell extracts from XP-C complemention group cells for DNA repair defects (129). The XPC helicase defective in these XP-C complementation group cells was identified in another work (135).

The purified RECQ1 was shown by Cui *et al.* to form dimers in the presence and absence of ssDNA, with an apparent molecular mass of 158 kDa (35; 61). Also, the kinetic studies on RECQ1-mediated unwinding suggested that the enzyme functions as a dimer (35).

RECQ1 is by itself a rather poor helicase, capable of displacing short partial duplexes. However, it displays an enhanced processivity upon interaction with human replication protein A (RPA) being able to unwind duplexes as long as 501 bp. This interaction is specific, as the E. coli single strand binding protein (ESSB) did not stimulate RECQ1-mediated unwinding of long duplexes (61). Therefore, the enhancement of processivity is not achieved through merely coating the single stranded DNA, but rather through a specific protein-protein interaction facilitating the loading of the helicase onto the ssDNA/dsDNA interface. Furthermore, RECQ1 has recently been shown to unwind HJs, D-loops and to promote annealing of short oligonucleotides (44).

In a yeast two-hybrid screen, Seki *et al.* have identified RECQ1 to interact with Qip1 and Rch1, which are two of the three human importin α homologues involved in nuclear-cytoplasmic transport (136). This interaction was confirmed by the finding that Qip1 was

able to mediate nuclear transport of BSA when conjugated to the full RECQ1 nuclear localisation signal (NLS) (137).

2.5 BLM - The Bloom Syndrome Helicase

2.5.1 The Bloom Syndrome

The Bloom syndrome (BS) is a rare autosomal recessive disorder with a high predisposition to cancer development. BS was first observed in 1954 (138) and is caused by defects in the *BLM* gene, located on chromosome 15q26.1 (28). BS is characterised by a stunted growth, including disproportional growth, manifested in a small head and unusual facial and skull growths. Furthermore, male infertility and immunodeficiency, characterised by a decrease in IgA and IgM levels is observed in BS patients. Figure 7 shows a young BS patient who suffers from severe facial telangiectatic erythema. BS patients suffer from a 150-300 fold increase in the risk of developing malignancies of all types.

Figure 7: A BS patient. Adapted from Ref. (139). His sun sensitive telangiectatic erythema cover almost all his face.

2.5.2 BS Cellular Phenotype

The hallmark of cell lines derived from BS patients is the elevated rate of sister chromatid exchanges (SCEs) to about 10 fold. SCEs represent HR events between sister

chromatids during S phase or G_2 resulting in crossovers. In Figure 8, an example for elevated SCE levels in BS cells is shown. Similarly, ES cells as well as lymphocytes, primary or immortalised fibroblasts of *Blm* knockout mice (140; 141), murine *Blm* knockout ES cells (142) and DT40 *BLM*$^{-/-}$ chicken B-cells (143; 144) show an elevated rate of SCEs.

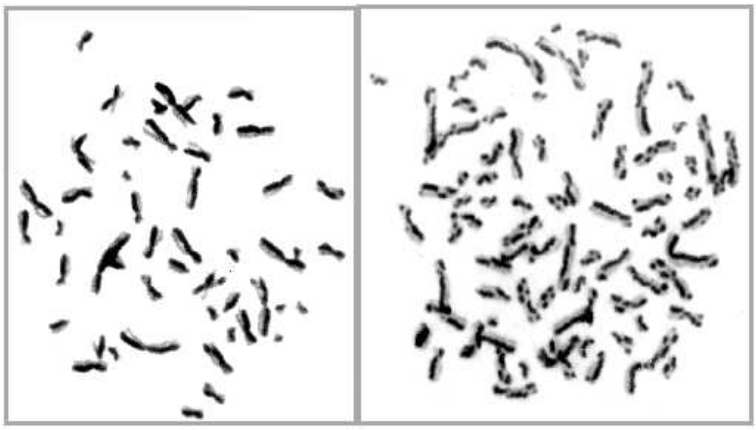

Figure 8: SCE analysis. Adapted from (145). To the left, chromosomes from a normal cell. To the right, chromosomes from a BS cell. Sister chromatids are distinguished through an assay based on differential labelling by BrdU.

It has been observed that BS cells as well as fibroblasts from *BLM*$^{-/+}$ carriers show a tendency for the accumulation of micronuclei (146; 147) or to bud out micronuclei at an abnormally high rate (148). Furthermore, a comparatively high number of gaps, breaks and rearranged chromosomes can be observed in BS cells (149; 150; 143). Moreover, BS cells have been reported to display a significantly lower rate of chain elongation during DNA synthesis (151; 152). BS cells are sensitive to UV radiation (153; 144) and to the ribonucleotide reductase inhibitor hydroxyurea (HU) (154; 155).

2.5.3 BLM - The Protein

The BS protein (BLM) is 1417 amino acids long, was cloned (18) and purified and characterised (62), where it was found that the protein displays ATP-dependent 3'-5' helicase activity. Furthermore, BLM has been found through gel-exclusion chromatography and electron microscopy to form ring-oligomeric structures with hexamers being the most prominent forms (156). BLM is able to unwind a wide variety of structures as depicted in Table 2 with a preference for quadruplex DNA and HJs (48; 157). The most important biochemical finding on BLM to date is, that in conjunction with TOPOIIIα, it is able to

resolve DHJs via a strand passage mechanism that prevents exchanges between flanking sequences (4). This reaction is called DHJ dissolution and is illustrated in Figure 9. DHJs have been described to be intermediates in meiotic recombination (158) and are predicted to form in mitotic cells during repair of DSBs by HR. As BS cells are not hypersensitive to ionizing radiation, BLM presumably does not carry an essential role in DSB repair (159). It is thought that the non-meiotic DHJs arise from HR-dependent repair of daughter strand gaps formed during replication (159; 4). The DHJ dissolution reaction explains many of the phenotypes of BS cells, but most importantly, the cause of the elevated rate of SCEs is revealed. In addition, BLM has also been reported to mediate strand exchange *in vitro* by Machwe *et al.* (160).

The expression of BLM cells is cell-cycle dependent; The protein level peaks in S, persists in G_2/M and is degraded in G_1, consistent with its role in S and G_2. BLM is a phosphoprotein and is phosphorylated during mitosis (154; 161) and in response to γ-radiation (162; 163; 155). The kinase responsible for this posphorylation seems to be ATM (Chapter 2.5.4). Also, BLM can be sumolyated (Chapter 2.5.4). Furthermore, BLM is a downstream target of the ATR-Chk1 pathway.

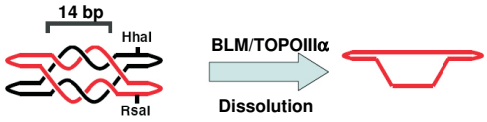

Figure 9: The DHJ dissolution reaction. Adapted from (4). BLM and TOPOIIIα together dissolute the structure depicted to the right into its components. In the experimental setup, one of the component oligonucleotides is labelled radioactively and will be detected as single species upon visualisation of radioactivity.

2.5.4 Interaction Partners of BLM

Many of the interaction partners of BLM listed below indicate that BLM is recruited to and activated at sites of recombination, probably to ensure the correct resolution of aberrant structures without cross-overs.

ATM, ATR and DNA Damage Response

In cells from ataxia telangiectasia (AT) patients - they lack the ataxia telangiectasia mutated protein (ATM) - the mitotic and the γ-radiation-induced phosphorylation of BLM are absent (153; 164; 163), but the ATR-dependent phosphorylation of BLM in response

to HU or UVC treatment is not altered (153; 164). ATM appears to be activated primarily by ionizing radiation or radiomimetic drugs that generate double-strand breaks (165). BLM has been reported to interact with ATM by Beamish *et al.* (154). Also, BLM interacts with ATR and evidences have lead to the suggestion that BLM is also a downstream target of ATR (164). It was shown that BLM forms foci with γH2AX at broken replication forks and that these foci recruit BRCA1 and NBS1 (166). Later, it was found that BLM localises into nuclear foci with phosphorylated γH2Ax and RAD51 and proposed that this is a response to restore productive DNA replication following S-phase arrest (155). BLM is very likely to be required at these cites to resolve the arising recombination intermediates.

Sengupta *et al.* have observed that BLM co-localised with the DNA damage response proteins 53BP1 and H2AX. Furthermore, BLM facilitated the the physical interaction between p53 and 53BP1, but 53BP1 was required for the efficient accumulation of BLM and p53 at sites of stalled replication. The formation of BLM/53BP1-foci was independent of γ-H2AX. The Chk1 active kinase was essential for the focal co-localisation of BLM and 53BP1 and for the consequent stabilisation of BLM. The authors propose that BLM functions in repair processes upon receipt of the signals mediated by 53BP1 and from ATR/Chk1 from replicational stress (167).

The BASC complex

Wang *et al.* have identified a high-order complex consisting of many DNA repair factors, BLM amongst them, and called it BASC, standing for **B**RCA1-**a**ssociated genome **s**urveillance **c**omplex (168). The complex includes tumour supressors and DNA damage repair proteins: BRCA1, BLM, MSH2, MSH6, MLH1, ATM, RAD50-MRE11-Nbs1 (MRN complex) and RFC. Especially, it was found that BRCA1, BLM and the MRN complex form large nuclear foci containing PCNA upon treatment with DNA-synthesis inhibiting agents.

The BRAFT Complex

Upon immunoprecipitation of BLM from HeLa cells, Meetei *et al.* identified by masspectrometric methods a complex that includes BLM, TOPOIIIα, RPA and the five core Fanconi anemia (FA) proteins FANCA, FANCC, FANCE, FANCF and FANCG and called this

complex BRAFT. BLM is responsible for the unwinding activity in this complex (169). Pichierri *et al.* have shown that BLM and FANCD2 colocalise and co-immunoprecipitate upon treatment with DNA crosslinkers or agents inducing replication fork arrest, again indicating a functional interaction (170). The features of the BS are very different to those of the FA, but some aspects of genomic instability in these diseases are similar. For a review on the Fanconi anemia proteins, see Ref. (171).

CAF-1

Jiao *et al.* found that BLM interacts with hp150, the largest subunit of the chromatin assembly factor 1 (CAF-1) *in vivo* and *in vitro*. The two proteins were found to co-localise at nuclear foci at sites of DNA synthesis. The fraction of co-localising foci was increased upon DNA damage or replication inhibition. BLM could inhibit CAF-1-mediated chromatin assembly *in vitro*. The activity of CAF-1 was not affected in BLM deficient cells, CAF-1 could not be mobilized in the nucleus upon hydroxyurea treatment. The authors suggested that BLM and CAF-1 function in a coordinated way to promote survival in response to DNA damage and/or replication blockage (172).

PML

The premyelocytic leukemia protein (PML), is a tumour supressor and has been found to localise into specific structures called PML bodies, where many proteins involved in DNA metabolism localise to (173; 174; 175). BLM trafficks into PML bodies in a manner dependent on SUMO modification (176).

MutSα - the MSH2/MSH6 heterodimer

Marsischky *et al.* observed, that the *S. cervisiae* MSH2/MSH6 heterodimer (MutSα) interacts with HJs and may help resolving them (177), providing a first evidence for a possible role of DNA mismatch repair (MMR) proteins in HR. Later, it was found that BLM associated with the human MutSα through direct interaction with hMSH6 *in vivo*. BLM and MSH6 co-localise at nuclear foci upon exposure to ionizing radiation. The authors did not observe an effect of MutSα on unwinding activity of BLM (178). Yang *et al.* have further investigated this interaction and found that the purified MutSα could

stimulate the BLM-mediated HJ branch migration *in vitro* and that this interaction could be regulated by p53. Furthermore, hMSH6 co-localised with BLM and p53 phosphorylated at Ser-15 in hydroxyurea-induced RAD51 foci. Moreover, they showed hMSH2 and hMSH6 to coimmunoprecipitate with BLM, p53 and RAD51. Moreover, they observed that the number of RAD51 foci and the amount of the BLM-p53-RAD51 complex was increased in cells deficient in hMSH2 or hMSH6 (179). The authors deduct from these data that MutSα forms a complex with BLM-p53-RAD51 in response to the damage of DNA replication forks to promote DSB repair. This assumption may not quite explain why the mismatch-sensor complex MutSα would be required at these sites. An intriguing model would be that the MutSα/BLM interaction serves for preventing homeologous recombination (HR between not perfectly homologous sequences). For a review on MMR, see Ref. (180).

MLH1

MLH1, one of the eukaryotic homologues of the MutL from *E. coli*, is part of the heterodimeric complex MutLα consisting of MLH1 and PMS2 that is recruited to sites of DNA-mismatch-specific bound MutSα or MutSβ complexes during MMR (181). BLM and MLH1 have been found to interact *in vivo* and *in vitro*. Furthermore, BLM and MLH1 co-localise in untreated as well as in aphidicoline-treated cells (182). As BLM deficiency does not result in a MMR defect, BLM is very unlikely to play a role in this reaction (182; 183).

p53

Wang *et al.* found that BLM and p53 are likely to regulate apoptosis since they observed that the ectopic expression of p53 induces apoptosis in normal cells but not in BS cells. As BS cells show normal Fas-induced apoptosis, this effect seems specific for the p53 apoptotic pathway (184). However, Davalos and Campisi claim that p53-induced apoptosis also occurs in BS cells (166)

In vivo, BLM and p53 phosphorylated on Ser-15 partially co-localise (185). BLM and p53 also co-immunoprecipitate from cell extracts (184; 185) and have been shown to physically interact *in vitro* (186). p53 is able to inhibit the unwinding activity of BLM on HJs, but not on standard oligonucleotide substrates. p53 may therefore be involved

in the regulation of HR through modulating the interaction of BLM with recombination intermediates (185). Furthermore, Garkavtsev *et al.* have observed that the ectopic expression of BLM causes an anti-proliferative effect in p53 wild-type cells, but not in p53-deficient cells. Moreover, the p53-mediated transactivation is attenuated in primary BS fibroblasts (186).

Rad51

The eukaryotic Rad51 protein and its paralogs are orthologues of the bacterial RecA protein which is involved in HR and DNA repair. Rad51 forms a nucleoprotein filament on ssDNA to mediate strand exchange. BLM and the human Rad51 have been shown to interact both *in vivo* and *in vitro*. In some untreated cells, BLM and Rad51 co-localise in late S-phase, and this is enhanced upon γ-radiation and aphidicolin treatment (187; 162). Rad51 and BLM have also been observed to co-localise in early meiotic cells at sites of interhomologue-DNA transactions (188).

RPA

The replication protein A (RPA) is a human single-stranded DNA binding protein that exists as a heterotrimer formed by subunits of 14, 32 and 70 kDa. BLM interacts physically with RPA through the p70 subunit (54; 183) and co-localises with the p34 and p70 subunits of RPA at nuclear foci in normal fibroblasts (189). *In vitro*, BLM is able to unwind partial duplexes of up to 100 bp, whereas, in a reaction together with RPA, partial duplexes as long as 259 bp can be unwound. This enhancement of helicase activity is not achieved through stimulation of ATPase activity (54; 47).

TOPOIIIα

The type I topoisomerase TOPOIIIα co-localise with BLM at nuclear foci in growing, normal fibroblasts as well as in transformed human fibroblasts (190) and interacts directly with BLM in the dissolution of DHJs in a non-crossover manner (Chapter 2.5.3) (4).

TRF2

In telomerase-negative cells that maintain their telomeres by a different mechanism called alternative lengthening of telomeres (ALT), BLM colocalises with the telomere repeat binding factor 2 (TRF2) in atypical, telomere-associated PML bodies. Also, TRF2 and BLM could be co-immunoprecipitated, suggesting an *in vivo* role of this association (191). TRF2 also interacts with BLM physically and stimulates its helicase activity on forked duplexes with or without two telomeric repeats. TRF2 is unable to bind these structures, as it requires more telomeric repeats (47).

WRN

WRN and BLM have been reported to interact directly *in vivo* and *in vitro* and that this interaction has a functional consequence in regulating the exonuclease activity of WRN (63). This interaction is certainly not the only way for the two proteins to function, as only a small portion of WRN could be co-immunoprecipitated with BLM (63), and BS is quite different from the Werner syndrome.

2.6 WRN - The Werner Syndrome Helicase

2.6.1 The Werner Syndrome

Like BS, the Werner syndrome (WS) is a rare autosomal disorder associated with high predisposition to cancer. It has been described for the first time in the PhD thesis of Otto Werner in 1904 (29). This syndrome arises from defects in the *WRN* gene. Only by the work of Thannhauser (192) this disease was clearly distinguished from the Rothmund-Thompson syndrome (Chapter 2.7). WS starts to be apparent in adolescence where the usual growth spurt does not take place, leading to a short stature. As also seen with BS patients, the facial features are thin and appear bird-like as a result of the stunted growth. The skin is affected by unusual pigmentation patterns, and hyperkeratoses appear at bony areas of the skin, such as for example at the limbs, and often acquires ulcers at such places. The earliest and clearest signs of WS is the early onset of various features of ageing such as hair greying and thinning, osteoporosis and soft tissue calcification. Furthermore, diabetes mellitus at an unusual early stage can evolve as well as arteriosclerosis, hypermelanosis and cerebral cortical atrophy. WS is not only characterised by premature ageing but also a higher incident of malignancies is observed (193). These malignancies, unlike the ones observed in BS, are mostly of epithelial and mesenchymal origin. Therefore, WS patients have a predisposition to develop soft tissue sarcomas, osteosarcomas, acral lentigenous melanomas, meningiomas and thyroid carcinomas (194). In contrast to the ageing symptoms, it has been observed that WS patients have a lower incidence of Alzheimer-like neuropathologies (195). Figure 10 shows a typical WS patient.

Figure 10: A Japanese-American WS patient as a teenager (left) and at the age of 48 (right). She was patient number 1 in the study of Epstein *et al.* and deceased at the age of 57, a high age for WS patients. Adapted from Ref. (193).

2.6.2 WS Cellular Phenotype

The *WRN* gene has been positionally cloned and is located in the p11-p12 region on chromosome 8, spanning 180 kb (30; 196). In culture, WS cells have been shown to undergo replicative senescence at a faster rate than normal cells which is considered to be the hallmark of WS cells with an average lifespan of only 27% of normal cells (197). A recent study shows that the WS cells are defective in lagging strand synthesis of telomeres and therefore will suffer from a single telomere loss and further argues for WRN being involved in replication, presumably by disrupting quadruplex DNA that may form on the G-rich lagging strand template (198). Furthermore, the growth defects of WS cells are retained after transformation (199). The expression of telomerase hTERT reverses the poor growth and the entry into premature senescence phenotypes of WS cells but seems not quite sufficient to immortalise the cells (200; 199). WS cells have been reported to be sensitive to 4-nitroquinoline 1-oxide (4NQO) (144; 201; 202). This effect can be reverted by expressing hTERT in SV40-transformed WS cells (203). WS cells have further been reported to be sensitive to DNA cross-linking drugs such as mitomicin C and cisplatin (199; 202; 204). Furthermore, WRN-deficient human and murine cells are sensitive to camptothecin, an inhibitor of Topoisomerase I (205; 206). Sensitivity to γ-radiation and radiomimetic drugs is debated, since several groups have shown different responses of WS cells to these treatments (144; 199; 201; 207).

The hallmark of WS cells at the chromosomal level is the elevated rate of extensive

somatic deletions and translocations which can vary in different clones (208; 209). Furthermore, WS cells display a higher number of RAD51 foci than normal cells, which probably indicates the persistence of unprocessed recombination intermediates (210). Unlike in BS cells, no increase in SCE-frequency is seen in WS cells (144; 211; 212).

WRN seems not to be involved in homologous recombination. Instead, its strong interaction with Ku rather suggests a role in non-homologous end-joining, in a manner that Ku regulates the WRN exonuclease in resection of DNA at non-homologous ends (Chapter 2.6.4). This action is likely not to be the sole on DNA ends, as WS cells do not show an obvious DNA double strand break (DSB) repair defect.

2.6.3 WRN - The Protein

The WRN protein is 1432 amino acids long and contains two functional domains: the central helicase domain and the N-terminal exonuclease domain. Furthermore, it carries an unusual direct repeat of 27 amino acids located between the exonuclease and the helicase domains (Figure 3).

WRN displays an ATP-dependent 3'-5' helicase activity. As most other RecQ helicases, it is able to unwind D-loops, G-quadruplex DNA and to migrate Holliday junctions (Table 2). The N-terminal nuclease domain displays 3'-5' polarity and shows low processivity (213). Orren *et al.* have observed that WRN *in vitro* will as helicase unwind the duplex of the invading strand in a D-loop structure and as 3'-5' exonuclease digest the invading strand (53). WRN has also been reported to mediate strand exchange *in vitro* (160), but the activity observed may be debated as the reaction conditions were far from physiological.

The cellular WRN protein levels are elevated during cytologic transformation of B-cells and fibroblasts and decreased when fibroblasts in culture reach confluency, indicative of a role of in proliferating cells (214). The expression of WRN is cell-cycle regulated, with the concentration peaking in the G_2/M phases (215). WRN is present in the nucleolus and migrates from nucleoli to nuclear foci upon treatment with HU, aphidicolin, 4NQO or camptothecin (216; 217; 218; 219; 220).

2.6.4 Interaction Partners of WRN

DNA-PK complex

The DNA-PK complex consists of DNA-PK$_{cs}$ and the Ku70/Ku80 heterodimer. It has been shown that WRN interacts with both the Ku heterodimer (221; 222; 223; 224; 225; 226) and DNA-PK$_{cs}$ (207). WRN is phosphorylated *in vivo* and *in vitro* by DNA-PK (207). The Ku70/Ku80 heterodimer strongly stimulates the exonuclease activity of WRN (223; 224; 207; 227), which is alleviated by poly(ADP-ribosyl)ation of Ku70/Ku80 (228). Not only does the Ku70/Ku80 stimulate the exonuclease activity of WRN, but it also extends the substrate specificity, so that WRN is able to degrade 3' protruding or blunt ends (223). Moreover, the inhibition of WRN exonuclease activity by 8-oxoG and 8-oxoA is alleviated by Ku70/Ku80 (229; 222).

DNA polymerase β

DNA polymerase β (polβ) is a key polymerase in both short and long-patch base excision repair (BER) (for a review on BER, see Ref. (230)). WRN has been shown to physically interact with polβ and to stimulate strand-displacement DNA synthesis of polβ (231). Furthermore a truncated variant consisting mainly of the helicase domain was sufficient to stimulate polβ (231).

DNA polymerase δ

Kamath-Loeb *et al.* could show that WRN interacts with DNA polymerase δ (polδ), a polymerase required for DNA replication and repair. WRN increases the nucleotide incorporation by polδ in the absence of PCNA but not that of the polymerases α or ϵ (232). The same group further showed that this interaction specifically facilitates the polδ-mediated DNA replication of templates forming secondary structures like quadruplex DNA and/or DNA repair (233). This hypothesis correlates with the observed S-phase defects in WS cells, namely defective lagging strand synthesis at telomeres observed after WRN depletion in HeLa cells (198).

EXO1

The human exonuclease 1 (EXO1) is a 5'-3' exonuclease and a 5'-flap-specific endonuclease and it has been proposed to function in DNA recombination and MMR. The exonucleolytic and the endonucleolytic activities have both been shown to be stimulated by WRN (234). Moreover, EXO1 and WRN interact physically *in vivo* and *in vitro* (234).

FEN1

The flap-endonuclease 1 (FEN1) is a protein that acts in DNA replication to remove the 5' overhang that arises at Okazaki fragments (235) and is also responsible for the removal of 5' overhangs arising in strand displacement synthesis during base excision repair (236). Brosh *et al.* have shown that WRN interacts with FEN1 and greatly stimulates the FEN1 nuclease activity (46). Sharma *et al.* further show by FRET (fluorescence resonance energy transfer) that WRN and FEN1 form a complex *in vivo* that co-localises with foci associated with arrested replication forks. WRN stimulates FEN1 cleavage of branch-migrating double-flap structures (237). Moreover, they show that *in vitro*, WRN unwinds Holliday junctions and stimulates FEN1 to cleave the unwound product (237).

MYC

MYC is an oncoprotein and acts as a transcription factor coordinating cell growth and division. When overproduced, it has been found to sensitize cells to agents stimulating apoptosis (238). Grandori *et al.* reported that MYC directly stimulates transcription of WRN and that the overexpression of MYC in WS fibroblasts or after WRN depletion from control fibroblasts led to rapid cellular senescence that could not be suppressed by hTERT expression. They proposed that WRN up-regulation by MYC may promote MYC-driven tumorigenesis by preventing cellular senescence (239). A discussion of the link between MYC and WRN in tumourigenesis is laid out by the same group in Ref. (240).

p53

The tumour suppressor protein p53 interacts physically with WRN both *in vitro* and *in vivo* (241; 185; 217). Yang *et al.* have further shown that this interaction modulates the

activities of both partners. p53 inhibits WRN-mediated unwinding of Holliday junctions, but only if it is not phosphorylated at Ser-378 and is also able to inhibit the exonuclease activity of WRN (217). WRN enhances the transcription of p53-responsive promoters in transfection assays. Ectopic expression of WRN also leads to higher p21 protein levels (241).

RNA polymerase II transcription

Balajee *et al.* found that in permeabilised WS cells the efficiency of transcription of a plasmid template containing the RNA polymerase II- dependent adenovirus major late promoter is reduced to 40-60% compared to normal cells. This reduction in transcription efficiency is reverted by the addition of the WRN protein. This effect seems to be mediated by the direct repeat of 27 amino acids ahead of the helicase motifs, as the authors show that a WRN mutant lacking the direct repeat fails to stimulate the low RNA pol II transcription rate of WS cells (242).

RPA

WRN alone can only unwind partial duplexes up to 40 bp, but in the presence of RPA it is able to unwind partial duplexes as long as 849 bp without an increase in ATPase activity (243). RPA does not effect the exonuclease activity of WRN (222). The physical interaction between WRN and RPA has been shown *in vitro* (243).

TRF2

In telomerase-negative cells that maintain their telomeres through the ALT pathway, WRN co-localises with TRF1, TRF2, PML, RAD52 and NBS1 in nuclear structures called ALT-specific, atypical PML bodies. In HeLa cells, where the telomerase is present, WRN localises to the nucleolus (86). As observed with BLM, TRF2 interacts with WRN physically and stimulates the helicase activity of WRN on forked duplexes with or without two telomeric repeats (47). The exonuclease activity of WRN is not affected by this interaction (47). Opresko *et. al* further showed that WRN associates with telomeres when dissociation of telomeric D-loops is likely during replication and recombination. They observed that most TRF1/PCNA co-localising nuclear foci contain WRN in S

phase ALT cells but not in telomerase-proficient HeLa cells. TRF1 and TRF2 limits the WRN-mediated disruption of D-loops (244). WRN is thus very likely to be involved in ALT.

WHIP

The Werner helicase interacting protein (WHIP) is a protein of 660 amino acids with homology to the replication factor C (RFC) family proteins. WHIP interacts with WRN, but not with BLM or RECQ1. The function of this protein is unknown to date (245).

2.7 RECQ4/RTS- The Rothmund-Thomson Syndrome Protein

2.7.1 The Rothmund-Thomson Syndrome

The Rothmund-Thomson syndrome (RTS) is a rare autosomal recessive disorder with roughly 200 reported patients worldwide. RTS has first been described in 1868 by Rothmund, a german ophtalmologist. Patients from a german family suffered from unusual skin degeneration and cataracts, a condition where the lens of the eye gradually turns opaque and results in a blurred view (31). 68 years later, Thomson, a British dermatologist described a syndrome with skin abnormalities and skeletal malformations and called it Poikiloderma congenitale (32). In 1957, Taylor recognised that the two syndromes are manifestations of the same disease and called it therefore RTS (33).

Through a number of patient studies it is known that RTS confers a high incidence of malignancies, mainly osteosarcomas (246; 247; 248; 249; 250; 251; 252; 253). Patients suffer from retarded postnatal growth and skin abnormalities that manifest as poikiloderma and sun-sensitive rash. Most patients also have sparse hair and eyebrows. Furthermore, diverse skeletal abnormalities arise, such as a decrease in bone density (osteopenia), pathological fractures, dislocations and metaphysis. In many cases, the so-called ”radial ray defect” is immediately apparent, which manifests as appendages of the thumb or small, missing or bifid thumbs. Often, cataracts appear, whereas mental or gonadal problems are varying from patient to patient. RTS has been found in some cases to be associated with a defect in the *RECQ4* gene (254). Wang *et al.* have later classified RTS into RTS type I, which represents RTS without a predisposition to osteosarcomas and with an intact *RECQ4*, and into RTS II that is characterised by a defective RECQ4 and a high predisposition to osteosarcomas (250). Figure 11 shows a female RTS patient.

Figure 11: A female RTS patient. Adapted from Ref. (255). The picture to the left shows the usual strong manifestation of poikiloderma, also the hair is sparse and the eyebrows are missing. The patient's arm suffers from eczematous lesions and bulla formation. The skeletal development of the hand appeares normal. The patient further suffered from severe infections of the respiratory tract.

Another disease associated with a defective *RECQ4* gene has been recently identified: the RAPADILINO syndrome, characterised by **ra**dial hypoplasia, **pa**tella hypoplasia and cleft or arched palate, **di**arrhea and dislocated joints, **li**ttle size and limb malformation, **no**se slender and normal intelligence. Unlike the RTS, RAPADILINO does not display the same high predisposition for malignancies (256).

Interestingly, the distinction between the two syndromes is also seen at the genetic level, as RTS patients with a defective *RECQ4* gene are mainly compound heterozygotes of nonsense or frameshift mutations, resulting in a RECQ4 polypeptide lacking a large part of the helicase domains (248; 254; 257), whereas most of the RAPADILINO patients are compound heterozygotes in which at least one of two defective RECQ4 alleles contains a deletion that causes, upon pre-mRNA splicing, the skipping of exon 7 without frameshift leading to a polypeptide with an intact putative helicase domain of RECQ4 (256).

2.7.2 RTS Cellular Phenotype

RTS cells have been reported to be genetically unstable, displaying a high frequency of chromosomal abnormalities such as translocations and trisomies (258; 259; 260; 261; 262). Cultured cells from RTS patients show normal sensitivity to mitomicin C, bleomycin, vincristine, methotrexate (248), cisplatin and adriamycin (263). The rate of sister chromatid exchanges is also normal in RTS cells (248). However, RTS cells show an increased sensitivity to ionizing radiation (263; 264; 265), probably due to a reduced level of DNA repair synthesis and an abnormally low rate of the removal of radiation-induced DNA lesions (264). The low DNA repair capacity is also an explanation for the UV sensitivity and reduced unscheduled DNA synthesis after UVC exposure observed in RTS cells (266).

2.7.3 RTS/RECQ4 - The Protein

The *RECQ4* gene has been cloned by Kitao *et al.* before it was known to be associated with RTS (215). It lies on the p-arm of chromosome 8 at 24.3 spanning 6.5 kb and includes 21 exons (267). The RECQ4 protein of 1208 amino acids harbours the helicase domains, but seems to lack the Zn^{2+}-binding domain as well as the WH and HRDC domains.

The RECQ4 protein is present in all phases of the cell cycle, but apparently peaks in S and G_2, again indicating replicative or postreplicative roles of RECQ4(267). Yin *et al.* have recently shown that the RECQ4 protein is present in the nucleus as well as in the cytoplasm of HeLa cells and preliminarly characterised biochemical activities of the immunoprecipitated protein. They could observe an ATPase activity with ssDNA or dsDNA as co-effectors but the protein failed to displace synthetic DNA duplexes (268) or to melt a triple helix. The authors conclude that RECQ4 may be similar to the SWI/SNF chromatin-remodelling factors, members of the SF2 family that show ATPase activity but not helicase activity *in vitro*. The absence of the Zn^{2+} binding domain remains enigmatic even in this context.

Using *Xenopus laevis* as a model system, Sangrithi *et al.* have found that xRTS, the *X. laevis* homologue of RECQ4, is essential for DNA replication in egg extracts (269). They observed that xRTS accumulates on chromatin during replication initiation after establishment of the prereplication-complex but before the recruitment of replicative

polymerases. Furthermore, xRTS depletion suppressed the loading of RPA that marks unwound origins before polymerase recruitment. The authors conclude that xRTS functions after the formation of the prereplication-complex to promote loading of replication factors, an activity previously unrecongnised but apparently necessary for initiation of replication (269). This role in replication initiation may explain the cause of chromosomal abberations of type II RTS cells.

2.7.4 Interaction Partners of RECQ4

UBR1 and UBR2

UBR1 and UBR2 are very similar proteins that are the components of ubiquitin (Ub) ligases (E3) of the N-end rule pathway, one pathway of the Ub-proteasome system. Yin *et al.* could isolate a protein complex consisting of RECQ4 UBR1 and UBR2 mainly from the cytoplasm and observed that this complex displayed DNA-stimulated ATPase activity, but failed to display helicase or translocase activities. Furthermore, they showed that RECQ4 is not ubiquitylated *in vivo* and is a long-lived protein in HeLa cells (268).

p53

Recently, p53 has been shown to repress the transcription of *RECQ4* in G_1-arrested cells, both in the absence and presence of DNA damage. Tumour-derived mutant forms of p53 were not able to repress the transcription of *RECQ4*. Arresting the cells by the topoisomerase-inhibitors etoposide (arrest in G_2) or camptothecin (arrest in S) led to further accumulation of p53 and concomitant decrease in the amount of RECQ4. Histone deacetylase 1 (HDAC1) was shown to be normally recruited to the *RECQ4* and *p21* promoter. Trichostatin A (TSA), an inhibitor of all histone deacetylases (HDACs) inhibited the p53-mediated repression of the *RECQ4* promoter, probably due to a conformational change of HDAC1 as it was observed that it was no longer bound to the promoter upon camptothecin treatment. The authors of this work proposed that the p53-mediated repression of *RECQ4* transcription during DNA damage results from the modulation of the *RECQ4* promoter occupancy by transcription activators and repressors (270).

2.8 RECQ5

2.8.1 Discovery of RECQ5

RECQ5 is the fifth human homologue of the *E. coli* RecQ and has not been associated with any syndrome yet. Kitao *et al.* identified a small isoform of RECQ5, which was later denoted RECQ5α (215). In this work, they cloned a cDNA with homology of 48$\%$ to the helicase domain of RecQ. The cloned gene encoded for a 410 amino acids long polypeptide. Because of the relatively small size compared to the other human RecQ homologues, the authors classified this RECQ5 variant as a member of a small group. FISH analysis revealed the corresponding gene to be located on on the q arm of chromosome 17 at the 25 region. The gene was found to be expressed ubiquitously with the highest levels in testis and ovary (215).

A year later, Sekelsky *et al.* reported their work on cloning the *Drosophila melanogaster* RecQ5 (DmRecQ5) (271). The discovery of the DmRecQ5 was coincidental, as they found it while cloning an unrelated cell-cycle checkpoint gene by screening a *Drosophila* embryo cDNA library. They found two RECQ5 isoforms of 54 kDa and 121 kDa generated by alternative splicing. The shorter one consists of the conserved helicase domains and is similar to the previously reported human RECQ5 protein and the longer one, in addition to the helicase region, contains a long C-terminal part bearing many charged residues without homology to any other RecQ helicase. Furthermore, they showed that the long isoform of DmRecQ5 localises to the nucleus. The authors also extended their study to the human RECQ5 and observed that the cDNA from Kitao *et al.* was incomplete at the 5' end and used this clone to screen a brain cDNA library. They found a cDNA coding for a protein of 49 kDa, which would be a bit longer than the 46 kDa protein identified by Kitao *et al.* As both cDNAs contained a polyadenylation signal at the 3' end, it was assured that both constructs were from genuine coding mRNA. Although the two cDNAs were almost identical, the one identified by Sekelsky *et al.* was slightly longer than the other at the 3' end. It was concluded that the resulting protein would be generated from a different alternative splicing to yield a protein containing additional 25 amino acids. The protein variant Sekelsky *et al.* had discovered in this work was actually later denoted RECQ5γ. Furthermore, they speculated on the existence of two additional variants, of which one was later cloned and named RECQ5β (see below) (271). Another attempt to clone RECQ5 DNA from human testis mRNA revealed

three different splice variants named α, β and γ. The structure of these transcripts are shown in Figure 12 (272). Furthermore, it has been shown that RECQ5β localises to the nucleus, whereas the short isoforms RECQ5α and RECQ5γ are only present in the cytoplasm. The authors also report an interaction of RECQ5β with the topoisomerases IIIα and IIIβ (272).

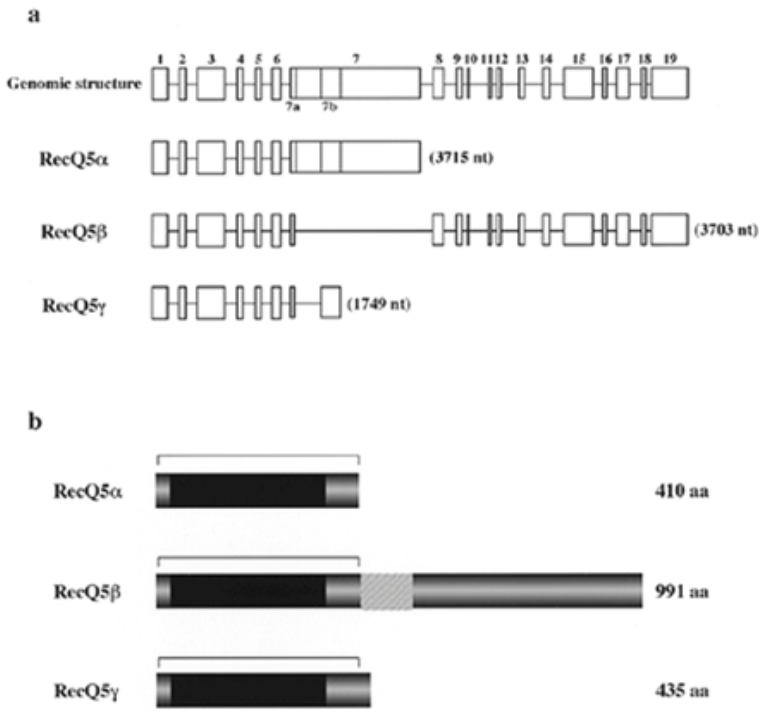

Figure 12: Structure of the *RECQ5* gene and the encoded RECQ5 proteins. Adapted from Ref. (272). (a) Genomic structure of the *RECQ5* gene and the exon organisations of three RECQ5 mRNA isomers, RECQ5α, RECQ5β and RECQ5γ. (b) Schematic representation of the RECQ5 isomers, the sizes are given on the right. The darkened areas indicate the locations of the helicase domains shared by the RecQ helicase family. The hatched areas indicate the extended homologous region to *E.coli* RecQ helicase and correspond to the Zn^{2+}-binding domain. RECQ5γ contains RECQ5α plus an additional 25 unconserved amino acids resulting in 435 amino acids.

2.8.2 *Drosophila melanogaster* RECQ5

Ozsoy *et al.* have performed the first biochemical characterisation of DmRecQ5b, the small *Drosophila melanogaster* RECQ5 isoform of 54 kDa. They subjected it to classical helicase assays and observed that the protein displayed 3'-5' ATP (dATP)- dependent helicase activity on partial duplexes as long as 93 bp. Furthermore, they observed that the protein shows higher helicase activity with dATP than with ATP, with turnover rates of 1380 min^{-1} and 900 min^{-1}, respectively (273). In a later work, the same group

extended the biochemical characterisation of DmRecQ5b and found that it is a structure-specific helicase like the other RecQ helicases. The protein unwound 3'-flaps, three-way junctions and synthetic forks more efficient than 5'-flaps and 12 nt-bubble substrates. DmRecQ5 also unwound synthetic Holliday junctions. Moreover, they observed that the protein shows a preference for unwinding the "lagging-strand arm" in a synthetic structure resembling a replication fork pointing to a role of DmRecQ5 in the recovery of stalled replication forks (274).

Kawasaki *et al.* expressed the large DmRecQ5c isoform of 121 kDa in the baculovirus system and subjected it to various *in vitro* assays. In gel filtration experiments, they observed that the proteins forms oligomers. Furthermore, they observed that DmRecQ5 hydrolyses GTP more efficiently than ATP in the presence of ssDNA. However, the helicase activity of DmRecQ5c was promoted by ATP and not by GTP. Nevertheless, GTP had a stimulatory effect on ATP-driven DNA unwinding (275).

To explore the cellular role of *Drosophila melanogaster* RECQ5, Nakayama *et al.* expressed the DmRECQ5 in an *sgs1* yeast mutant. DmRECQ5 was able to complement the *sgs1* phenotypes of the synthetic growth defect with *srs2*, the hypersensitivity to hydroxyurea and to MMS and also the elevated rate of sister chromatid exchanges (SCEs), but only poorly complemented the suppression of slow growth in *top3*. They further show that the helicase domain and helicase activity of DmRecQ5 was required to complement both the *sgs1 srs2* and the *sgs1 top3* phenotypes. The C-terminus of DmRECQ5 was dispensable for complementig the *sgs1 srs2* phenotype, but was required for complementation of *sgs1 top3*. These data further imply that the RecQ functions are highly conserved. It is still unclear, why the elevated rate of SCEs was complemented, but the slow growth of the *top3* could not be reverted (276).

2.8.3 RECQ5 and SCEs

Wang *et al.* used the chicken B-cell line DT40 to study the consequences of knocking-out the chicken orthologues of alone or in different combinations (277). The DT40 cells are a popular system to study gene knock-outs as the high rate of homologous recombination observed in these cells allows to knock out genes by gene targeting. In this work, the authors generated the following mutants: *RECQ1*$^{-/-}$, *RECQ5*$^{-/-}$, *BLM*$^{-/-}$, *RECQ1*$^{-/-}$*/RECQ5*$^{-/-}$, *RECQ1*$^{-/-}$*/BLM*$^{-/-}$ and *RECQ5*$^{-/-}$*/BLM*$^{-/-}$ and tested them for the sen-

sitivities to MMC, MMS and UV-light treatments, and also monitored the rate of spontaneous or MMC-induced SCEs. They found that both the *RECQ1*$^{-/-}$ *BLM*$^{-/-}$ and the *RECQ5*$^{-/-}$ *BLM*$^{-/-}$ mutants grew slower than the *BLM*$^{-/-}$ cells due to the increase in the number of dead cells, suggesting a role for *RECQ5* and *RECQ1* in cell viability in the absence of BLM. Moreover, the *RECQ5*$^{-/-}$ *BLM*$^{-/-}$ mutant showed an elevated rate of SCEs compared to *BLM*$^{-/-}$ cells, whereas this effect was not seen with the *RECQ1*$^{-/-}$ *BLM*$^{-/-}$ mutant. The authors failed to observe a change in sensitivity to UV upon inactivating *RECQ5* in a *BLM*$^{-/-}$ background. Finally, the *RECQ1*$^{-/-}$ and the *RECQ5*$^{-/-}$ single and double mutants did not show a significant difference from the wild-type cells in growth, sensitivity to DNA-damaging agents and frequency of SCE (277). This suggests that the absence of BLM creates substrates for RECQ5 that do not appear in normal cells. This work shows a first implication of RECQ5 in suppressing SCEs, but the chicken B-cell line DT40 may not be an ideal model system for the elucidation of the role of the human RECQ5 protein as the chicken orthologue is only 649 amino acids long.

Recently, Hu *et al.* have taken the issue of RECQ5 being implicated in suppressing SCEs further into murine ES cells (142). They observed that in *RECQ5*$^{+/-}$ murine ES cells, that grew normally, the level of SCEs is the same as in wild-type cells, whereas in real *RECQ5*$^{-/-}$ cells, which also grew normally, the rate of SCEs is elevated approximately three-fold compared to wild-type or heterozygous cells. A further confirmation of this phenotype was obtained with mouse embryonic fibroblasts (MEFS) derived from the ES cells. This elevated rate of SCEs is comparable to that of BLM-deficient cells. Upon creating the double knock-out *RECQ5*$^{-/-}$*/BLM*$^{-/-}$, the authors could observe a normal growth rate, but a further increase in the rate of SCEs, compared to the single knockouts. Their data imply that RECQ5 and BLM have nonredundant roles in suppressing SCEs. It is not clear, however, in what kind of pathway RECQ5 would function to suppress SCEs (142). These results differ somewhat from those obtained from the chicken DT40 B-cell line, but probably mouse cells are a better model, as the murine and the human RECQ5 share 79% homology.

References

[1] Janscak, P., Garcia, P. L., Hamburger, F., Makuta, Y., Shiraishi, K., Imai, Y., Ikeda, H. & Bickle, T. A. (2003). Characterization and mutational analysis of the RecQ core of the Bloom syndrome protein. *J. Mol. Biol.* **330** (1), 29–42.

[2] Garcia, P. L., Liu, Y., Jiricny, J., West, S. C. & Janscak, P. (2004). Human RECQ5beta, a protein with DNA helicase and strand-annealing activities in a single polypeptide. *EMBO J.* **23** (14), 2882–91.

[3] Garcia, P. L., Bradley, G., Hayes, C. J., Krintel, S., Soultanas, P. & Janscak, P. (2004). RPA alleviates the inhibitory effect of vinylphosphonate internucleotide linkages on DNA unwinding by BLM and WRN helicases. *Nucleic Acids Res.* **32** (12), 3771–8.

[4] Wu, L. & Hickson, I. D. (2003). The Bloom's syndrome helicase suppresses crossing over during homologous recombination. *Nature,* **426** (6968), 870–4.

[5] Wu, L., Lung Chan, K., Ralf, C., Bernstein, D. A., Garcia, P. L., Bohr, V. A., Vindigni, A., Janscak, P., Keck, J. L. & Hickson, I. D. (2005). The HRDC domain of BLM is required for the dissolution of double Holliday junctions. *EMBO J.* **24** (14), 2679–87.

[6] Cheok, C. F., Wu, L., Garcia, P. L., Janscak, P. & Hickson, I. D. (2005). The Bloom's syndrome helicase promotes the annealing of complementary single-stranded DNA. *Nucleic Acids Res,* **33** (12), 3932–41.

[7] Matson, S. W., Bean, D. W. & George, J. W. (1994). Dna helicases: enzymes with essential roles in all aspects of DNA metabolism. *Bioessays,* **16** (1), 13–22.

[8] Singleton, M. R. & Wigley, D. B. (2002). Modularity and specialization in superfamily 1 and 2 helicases. *J. Bacteriol.* **184** (7), 1819–26.

[9] Hall, M. C. & Matson, S. W. (1999). Helicase motifs: the engine that powers DNA unwinding. *Mol. Microbiol.* **34** (5), 867–77.

[10] Gorbalenya, A. & Koonin, E. (1993). Helicases: amino acid sequence comparisons and structure-funtion relationships. *Curr. Opin. Struct. Biol.* **3**, 419–429.

[11] Korolev, S., Hsieh, J., Gauss, G. H., Lohman, T. M. & Waksman, G. (1997). Major domain swiveling revealed by the crystal structures of complexes of *E. coli* rep helicase bound to single-stranded DNA and ADP. *Cell,* **90** (4), 635–47.

[12] Velankar, S. S., Soultanas, P., Dillingham, M. S., Subramanya, H. S. & Wigley, D. B. (1999). Crystal structures of complexes of Pcra DNA helicase with a DNA substrate indicate an inchworm mechanism. *Cell,* **97** (1), 75–84.

[13] Kim, J. L., Morgenstern, K. A., Griffith, J. P., Dwyer, M. D., Thomson, J. A., Murcko, M. A., Lin, C. & Caron, P. R. (1998). Hepatitis C virus NS3 RNA helicase domain with a bound oligonucleotide: the crystal structure provides insights into the mode of unwinding. *Structure,* **6** (1), 89–100.

[14] Tuteja, N. & Tuteja, R. (2004). Unraveling DNA helicases. Motif, structure, mechanism and function. *Eur. J. Biochem.* **271** (10), 1849–63.

[15] Tanner, N. K., Cordin, O., Banroques, J., Doere, M. & Linder, P. (2003). The Q motif: a newly identified motif in DEAD box helicases may regulate ATP binding and hydrolysis. *Mol. Cell.* **11** (1), 127–38.

[16] Cordin, O., Tanner, N. K., Doere, M., Linder, P. & Banroques, J. (2004). The newly discovered Q motif of DEAD-box RNA helicases regulates RNA-binding and helicase activity. *EMBO J.* **23** (13), 2478–87.

[17] Bernstein, D. A. & Keck, J. L. (2003). Domain mapping of Escherichia coli RecQ defines the roles of conserved N- and C-terminal regions in the RecQ family. *Nucleic Acids Res.* **31** (11), 2778–85.

[18] Ellis, N. A., Groden, J., Ye, T. Z., Straughen, J., Lennon, D. J., Ciocci, S., Proytcheva, M. & German, J. (1995). The Bloom's syndrome gene product is homologous to recQ helicases. *Cell,* **83** (4), 655–66.

[19] Walker, J. E., Saraste, M., Runswick, M. J. & Gay, N. J. (1982). Distantly related sequences in the alpha- and beta-subunits of ATP synthase, myosin, kinases and other ATP-requiring enzymes and a common nucleotide binding fold. *EMBO J.* **1** (8), 945–51.

[20] Pause, A. & Sonenberg, N. (1992). Mutational analysis of a DEAD box RNA helicase: the mammalian translation initiation factor eiF-4A. *EMBO J.* **11** (7), 2643–54.

[21] Marintcheva, B. & Weller, S. K. (2003). Helicase motif Ia is involved in single-strand DNA-binding and helicase activities of the herpes simplex virus type 1 origin-binding protein, UL9. *J. Virol.* **77** (4), 2477–88.

[22] Dillingham, M. S., Soultanas, P. & Wigley, D. B. (1999). Site-directed mutagenesis of motif iii in pcra helicase reveals a role in coupling atp hydrolysis to strand separation. *Nucleic Acids Res.* **27** (16), 3310–7.

[23] Yarranton, G. T. & Gefter, M. L. (1979). Enzyme-catalyzed DNA unwinding: studies on escherichia coli rep protein. *Proc. Natl. Acad. Sci. U S A,* **76** (4), 1658–62.

[24] Mechanic, L. E., Hall, M. C. & Matson, S. W. (1999). Escherichia coli DNA helicase II is active as a monomer. *J. Biol. Chem.* **274** (18), 12488–98.

[25] Delagoutte, E. & von Hippel, P. H. (2003). Helicase mechanisms and the coupling of helicases within macromolecular machines. Part ii: Integration of helicases into cellular processes. *Q Rev. Biophys.* **36** (1), 1–69.

[26] Lohman, T. M. (1992). Escherichia coli DNA helicases: mechanisms of DNA unwinding. *Mol. Microbiol.* **6** (1), 5–14.

[27] Bloom, D. (1966). The syndrome of congenital telangiectatic erythema and stunted growth. *J. Pediatr.* **68** (1), 103–13.

[28] McDaniel, L. D. & Schultz, R. A. (1992). Elevated sister chromatid exchange phenotype of bloom syndrome cells is complemented by human chromosome 15. *Proc. Natl. Acad. Sci. U S A,* **89** (17), 7968–72.

[29] Werner, O. (1904). Über Katarakt in Verbindung mit Sklerodermie. *Thesis/Dissertation, Kiel University,* .

[30] Yu, C. E., Oshima, J., Fu, Y. H., Wijsman, E. M., Hisama, F., Alisch, R., Matthews, S., Nakura, J., Miki, T., Ouais, S., Martin, G. M., Mulligan, J. & Schellenberg, G. D. (1996). Positional cloning of the Werner's syndrome gene. *Science,* **272** (5259), 258–62.

[31] Rothmund, A. (1868). Über Cataracten in Verbindung mit einer eigenthümlichen Hautdegeneration. *Arch. Klin. Exp. Ophtalmol.* **4**, 159–182.

[32] Thomson, M. (1936). Poikiloderma congenitale. *Br. J. Dermatol.* **48**, 221–234.

[33] Taylor, W. B. (1957). Rothmund's syndrome; Thomson's syndrome; congenital poikiloderma with or without juvenile cataracts. *AMA Arch. Derm.* **75** (2), 236–44.

[34] Bernstein, D. A., Zittel, M. C. & Keck, J. L. (2003). High-resolution structure of the E.coli RecQ helicase catalytic core. *EMBO J.* **22** (19), 4910–21.

[35] Cui, S., Klima, R., Ochem, A., Arosio, D., Falaschi, A. & Vindigni, A. (2003). Characterization of the DNA-unwinding activity of human RECQ1, a helicase specifically stimulated by human replication protein A. *J. Biol. Chem.* **278** (3), 1424–32.

[36] Mohaghegh, P., Karow, J. K., Brosh Jr, R. M., J., Bohr, V. A. & Hickson, I. D. (2001). The Bloom's and Werner's syndrome proteins are DNA structure-specific helicases. *Nucleic Acids Res.* **29** (13), 2843–9.

[37] van Brabant, A. J., Ye, T., Sanz, M., German, I. J., Ellis, N. A. & Holloman, W. K. (2000). Binding and melting of D-loops by the Bloom syndrome helicase. *Biochemistry,* **39** (47), 14617–25.

[38] Machwe, A., Xiao, L., Theodore, S. & Orren, D. K. (2002). Dnase i footprinting and enhanced exonuclease function of the bipartite werner syndrome protein (wrn) bound to partially melted duplex dna. *J. Biol. Chem.* **277** (6), 4492–504.

[39] Suzuki, N., Shiratori, M., Goto, M. & Furuichi, Y. (1999). Werner syndrome helicase contains a 5'-3' exonuclease activity that digests DNA and RNA strands in DNA/DNA and RNA/DNA duplexes dependent on unwinding. *Nucleic Acids Res.* **27** (11), 2361–8.

[40] Umezu, K., Nakayama, K. & Nakayama, H. (1990). Escherichia coli RecQ protein is a DNA helicase. *Proc. Natl. Acad. Sci. U S A,* **87** (14), 5363–7.

[41] Harmon, F. G. & Kowalczykowski, S. C. (2001). Biochemical characterization of the DNA helicase activity of the escherichia coli RecQ helicase. *J. Biol. Chem.* **276** (1), 232–43.

[42] Harmon, F. G. & Kowalczykowski, S. C. (1998). RecQ helicase, in concert with RecAand SSB proteins, initiates and disrupts DNA recombination. *Genes Dev.* **12** (8), 1134–44.

[43] Bennett, R. J., Keck, J. L. & Wang, J. C. (1999). Binding specificity determines polarity of DNA unwinding by the Sgs1 protein of S. cerevisiae. *J. Mol. Biol.* **289** (2), 235–48.

[44] Sharma, S., Sommers, J. A., Choudhary, S., Faulkner, J. K., Cui, S., Andreoli, L., Muzzolini, L., Vindigni, A. & Brosh, R. M., J. (2005). Biochemical analysis of the DNA unwinding and strand annealing activities catalyzed by human RECQ1. *J. Biol. Chem.* **JBC Papers in Press. Published on May 16, 2005 as Manuscript M500264200**.

[45] Brosh, R. M., J., Waheed, J. & Sommers, J. A. (2002). Biochemical characterization of the DNA substrate specificity of Werner syndrome helicase. *J. Biol. Chem.* **277** (26), 23236–45.

[46] Brosh, R. M., J., Majumdar, A., Desai, S., Hickson, I. D., Bohr, V. A. & Seidman, M. M. (2001). Unwinding of a DNA triple helix by the Werner and Bloom syndrome helicases. *J. Biol. Chem.* **276** (5), 3024–30.

[47] Opresko, P. L., von Kobbe, C., Laine, J. P., Harrigan, J., Hickson, I. D. & Bohr, V. A. (2002). Telomere-binding protein TRF2 binds to and stimulates the Werner and Bloom syndrome helicases. *J. Biol. Chem.* **277** (43), 41110–9.

[48] Sun, H., Karow, J. K., Hickson, I. D. & Maizels, N. (1998). The Bloom's syndrome helicase unwinds G4 DNA. *J. Biol. Chem.* **273** (42), 27587–92.

[49] Opresko, P. L., Laine, J. P., Brosh, R. M., J., Seidman, M. M. & Bohr, V. A. (2001). Coordinate action of the helicase and 3' to 5' exonuclease of Werner syndrome protein. *J. Biol. Chem.* **276** (48), 44677–87.

[50] Sun, H., Bennett, R. J. & Maizels, N. (1999). The Saccharomyces cerevisiae Sgs1 helicase efficiently unwinds G-G paired DNAs. *Nucleic Acids Res.* **27** (9), 1978–84.

[51] Han, H., Bennett, R. J. & Hurley, L. H. (2000). Inhibition of unwinding of G-quadruplex structures by Sgs1 helicase in the presence of N,N'-bis[2-(1-piperidino)ethyl]-3,4,9,10-perylenetetracarboxylic diimide, a G-quadruplex-interactive ligand. *Biochemistry,* **39** (31), 9311–6.

[52] Wu, X. & Maizels, N. (2001). Substrate-specific inhibition of RecQ helicase. *Nucleic Acids Res.* **29** (8), 1765–71.

[53] Orren, D. K., Theodore, S. & Machwe, A. (2002). The Werner syndrome helicase/exonuclease (WRN) disrupts and degrades D-loops in vitro. *Biochemistry,* **41** (46), 13483–8.

[54] Brosh, R. M., J., Li, J. L., Kenny, M. K., Karow, J. K., Cooper, M. P., Kureekattil, R. P., Hickson, I. D. & Bohr, V. A. (2000). Replication protein A physically interacts with the Bloom's syndrome protein and stimulates its helicase activity. *J. Biol. Chem.* **275** (31), 23500–8.

[55] Neff, N. F., Ellis, N. A., Ye, T. Z., Noonan, J., Huang, K., Sanz, M. & Proytcheva, M. (1999). The DNA helicase activity of BLM is necessary for the correction of the genomic instability of bloom syndrome cells. *Mol. Biol. Cell,* **10** (3), 665–76.

[56] Gray, M. D., Shen, J. C., Kamath-Loeb, A. S., Blank, A., Sopher, B. L., Martin, G. M., Oshima, J. & Loeb, L. A. (1997). The Werner syndrome protein is a DNA helicase. *Nat. Genet.* **17** (1), 100–3.

[57] Suzuki, N., Shimamoto, A., Imamura, O., Kuromitsu, J., Kitao, S., Goto, M. & Furuichi, Y. (1997). DNA helicase activity in Werner's syndrome gene product synthesized in a baculovirus system. *Nucleic Acids Res.* **25** (15), 2973–8.

[58] Brosh, R. M., J., Orren, D. K., Nehlin, J. O., Ravn, P. H., Kenny, M. K., Machwe, A. & Bohr, V. A. (1999). Functional and physical interaction between WRN helicase and human replication protein A. *J. Biol. Chem.* **274** (26), 18341–50.

[59] Orren, D. K., Brosh, R. M., J., Nehlin, J. O., Machwe, A., Gray, M. D. & Bohr, V. A. (1999). Enzymatic and DNA binding properties of purified WRN protein: high affinity binding to single-stranded DNA but not to DNA damage induced by 4NQO. *Nucleic Acids Res.* **27** (17), 3557–66.

[60] Bennett, R. J., Sharp, J. A. & Wang, J. C. (1998). Purification and characterization of the Sgs1 DNA helicase activity of Saccharomyces cerevisiae. *J. Biol. Chem.* **273** (16), 9644–50.

[61] Cui, S., Arosio, D., Doherty, K. M., Brosh, R. M., J., Falaschi, A. & Vindigni, A. (2004). Analysis of the unwinding activity of the dimeric RECQ1 helicase in the presence of human replication protein A. *Nucleic Acids Res.* **32** (7), 2158–70.

[62] Karow, J. K., Chakraverty, R. K. & Hickson, I. D. (1997). The Bloom's syndrome gene product is a 3'-5' DNA helicase. *J. Biol. Chem.* **272** (49), 30611–4.

[63] von Kobbe, C., Karmakar, P., Dawut, L., Opresko, P., Zeng, X., Brosh, R. M., J., Hickson, I. D. & Bohr, V. A. (2002). Colocalization, physical, and functional interaction between Werner and Bloom syndrome proteins. *J. Biol. Chem.* **277** (24), 22035–44.

[64] Shen, J. C., Gray, M. D., Oshima, J. & Loeb, L. A. (1998). Characterization of Werner syndrome protein DNA helicase activity: directionality, substrate dependence and stimulation by replication protein A. *Nucleic Acids Res.* **26** (12), 2879–85. 0305-1048 Journal Article.

[65] Umezu, K. & Nakayama, H. (1993). RecQ DNA helicase of Escherichia coli. Characterization of the helix-unwinding activity with emphasis on the effect of single-stranded DNA-binding protein. *J. Mol. Biol.* **230** (4), 1145–50.

[66] Huber, M. D., Lee, D. C. & Maizels, N. (2002). G4 DNA unwinding by BLM and Sgs1p: substrate specificity and substrate-specific inhibition. *Nucleic Acids Res.* **30** (18), 3954–61.

[67] Fry, M. & Loeb, L. A. (1999). Human werner syndrome DNA helicase unwinds tetrahelical structures of the fragile X syndrome repeat sequence d(CGG)n. *J. Biol. Chem.* **274** (18), 12797–802.

[68] Nakayama, H., Nakayama, K., Nakayama, R., Irino, N., Nakayama, Y. & Hanawalt, P. C. (1984). Isolation and genetic characterization of a thymineless death-resistant mutant of Escherichia coli K12: identification of a new mutation (recq1) that blocks the RecF recombination pathway. *Mol. Gen. Genet.* **195** (3), 474–80.

[69] Nakayama, H. (2005). Escherichia coli RecQ helicase: A player in thymineless death. *Mutat. Res.* **Epub ahead of print**.

[70] Courcelle, J., Carswell-Crumpton, C. & Hanawalt, P. C. (1997). recF and recR are required for the resumption of replication at DNA replication forks in Escherichia coli. *Proc. Natl. Acad. Sci. U S A,* **94** (8), 3714–9.

[71] Courcelle, J. & Hanawalt, P. C. (1999). RecQ and RecJ process blocked replication forks prior to the resumption of replication in UV-irradiated Escherichia coli. *Mol. Gen. Genet.* **262** (3), 543–51.

[72] Courcelle, J., Donaldson, J. R., Chow, K. H. & Courcelle, C. T. (2003). DNA damage-induced replication fork regression and processing in Escherichia coli. *Science,* **299** (5609), 1064–7.

[73] Hanada, K., Ukita, T., Kohno, Y., Saito, K., Kato, J. & Ikeda, H. (1997). RecQ DNA helicase is a suppressor of illegitimate recombination in Escherichia coli. *Proc. Natl. Acad. Sci. U S A,* **94** (8), 3860–5.

[74] Hishida, T., Han, Y. W., Shibata, T., Kubota, Y., Ishino, Y., Iwasaki, H. & Shinagawa, H. (2004). Role of the Escherichia coli RecQ DNA helicase in SOS signaling and genome stabilization at stalled replication forks. *Genes Dev.* **18** (15), 1886–97.

[75] Heyer, W. D. (2004). Damage signaling: RecQ sends an SOS to you. *Curr. Biol.* **14** (20), R895–7.

[76] Foster, P. L. (2005). Stress responses and genetic variation in bacteria. *Mutat. Res.* **569** (1-2), 3–11.

[77] Harmon, F. G., DiGate, R. J. & Kowalczykowski, S. C. (1999). RecQ helicase and topoisomerase III comprise a novel DNA strand passage function: a conserved mechanism for control of DNA recombination. *Mol. Cell.* **3** (5), 611–20.

[78] Gajiwala, K. S. & Burley, S. K. (2000). Winged helix proteins. *Curr. Opin. Struct. Biol.* **10** (1), 110–6.

[79] Liu, Z., Macias, M. J., Bottomley, M. J., Stier, G., Linge, J. P., Nilges, M., Bork, P. & Sattler, M. (1999). The three-dimensional structure of the HRDC domain and implications for the Werner and Bloom syndrome proteins. *Structure Fold Des.* **7** (12), 1557–66.

[80] Liu, J. L., Rigolet, P., Dou, S. X., Wang, P. Y. & Xi, X. G. (2004). The zinc finger motif of Escherichia coli RecQ is implicated in both DNA binding and protein folding. *J. Biol. Chem.* **279** (41), 42794–802.

[81] Morozov, V., Mushegian, A. R., Koonin, E. V. & Bork, P. (1997). A putative nucleic acid-binding domain in Bloom's and Werner's syndrome helicases. *Trends Biochem. Sci.* **22** (11), 417–8.

[82] Sinclair, D. A., Mills, K. & Guarente, L. (1997). Accelerated aging and nucleolar fragmentation in yeast sgs1 mutants. *Science,* **277** (5330), 1313–6.

[83] Mankouri, H. W. & Morgan, A. (2001). The DNA helicase activity of yeast Sgs1p is essential for normal lifespan but not for resistance to topoisomerase inhibitors. *Mech. Ageing Dev.* **122** (11), 1107–20.

[84] McVey, M., Kaeberlein, M., Tissenbaum, H. A. & Guarente, L. (2001). The short life span of Saccharomyces cerevisiae sgs1 and srs2 mutants is a composite of normal aging processes and mitotic arrest due to defective recombination. *Genetics,* **157** (4), 1531–42.

[85] Watt, P. M., Hickson, I. D., Borts, R. H. & Louis, E. J. (1996). SGS1, a homologue of the Bloom's and Werner's syndrome genes, is required for maintenance of genome stability in Saccharomyces cerevisiae. *Genetics,* **144** (3), 935–45.

[86] Johnson, F. B., Marciniak, R. A., McVey, M., Stewart, S. A., Hahn, W. C. & Guarente, L. (2001). The Saccharomyces cerevisiae WRN homolog Sgs1p participates in telomere maintenance in cells lacking telomerase. *EMBO J.* **20** (4), 905–13.

[87] Miyajima, A., Seki, M., Onoda, F., Shiratori, M., Odagiri, N., Ohta, K., Kikuchi, Y., Ohno, Y. & Enomoto, T. (2000). Sgs1 helicase activity is required for mitotic but apparently not for meiotic functions. *Mol. Cell. Biol.* **20** (17), 6399–409.

[88] Mullen, J. R., Kaliraman, V. & Brill, S. J. (2000). Bipartite structure of the SGS1 DNA helicase in Saccharomyces cerevisiae. *Genetics,* **154** (3), 1101–14.

[89] Gangloff, S., Soustelle, C. & Fabre, F. (2000). Homologous recombination is responsible for cell death in the absence of the Sgs1 and Srs2 helicases. *Nat. Genet.* **25** (2), 192–4.

[90] Saffi, J., Pereira, V. R. & Henriques, J. A. (2000). Importance of the Sgs1 helicase activity in DNA repair of Saccharomyces cerevisiae. *Curr. Genet.* **37** (2), 75–8.

[91] Frei, C. & Gasser, S. M. (2000). The yeast Sgs1p helicase acts upstream of Rad53p in the DNA replication checkpoint and colocalizes with Rad53p in S-phase-specific foci. *Genes Dev.* **14** (1), 81–96.

[92] Onoda, F., Seki, M., Miyajima, A. & Enomoto, T. (2001). Involvement of SGS1 in DNA damage-induced heteroallelic recombination that requires RAD52 in Saccharomyces cerevisiae. *Mol. Gen. Genet.* **264** (5), 702–8.

[93] Onoda, F., Seki, M., Miyajima, A. & Enomoto, T. (2000). Elevation of sister chromatid exchange in Saccharomyces cerevisiae sgs1 disruptants and the relevance of the disruptants as a system to evaluate mutations in Bloom's syndrome gene. *Mutat. Res.* **459** (3), 203–9.

[94] Myung, K., Datta, A. & Kolodner, R. D. (2001). Suppression of spontaneous chromosomal rearrangements by S phase checkpoint functions in Saccharomyces cerevisiae. *Cell,* **104** (3), 397–408.

[95] Myung, K., Datta, A., Chen, C. & Kolodner, R. D. (2001). SGS1, the Saccharomyces cerevisiae homologue of BLM and WRN, suppresses genome instability and homeologous recombination. *Nat. Genet.* **27** (1), 113–6.

[96] Ajima, J., Umezu, K. & Maki, H. (2002). Elevated incidence of loss of heterozygosity (LOH) in an sgs1 mutant of Saccharomyces cerevisiae: roles of yeast RecQ helicase in suppression of aneuploidy, interchromosomal rearrangement, and the simultaneous incidence of both events during mitotic growth. *Mutat. Res.* **504** (1-2), 157–72.

[97] Yamagata, K., Kato, J., Shimamoto, A., Goto, M., Furuichi, Y. & Ikeda, H. (1998). Bloom's and Werner's syndrome genes suppress hyperrecombination in yeast sgs1 mutant: implication for genomic instability in human diseases. *Proc. Natl. Acad. Sci. U S A,* **95** (15), 8733–8.

[98] Gangloff, S., McDonald, J. P., Bendixen, C., Arthur, L. & Rothstein, R. (1994). The yeast type i topoisomerase Top3 interacts with Sgs1, a DNA helicase homolog: a potential eukaryotic reverse gyrase. *Mol. Cell. Biol.* **14** (12), 8391–8.

[99] Watt, P. M., Louis, E. J., Borts, R. H. & Hickson, I. D. (1995). Sgs1: a eukaryotic homolog of e. coli RecQ that interacts with topoisomerase ii in vivo and is required for faithful chromosome segregation. *Cell,* **81** (2), 253–60.

[100] Lu, J., Mullen, J. R., Brill, S. J., Kleff, S., Romeo, A. M. & Sternglanz, R. (1996). Human homologues of yeast helicase. *Nature,* **383** (6602), 678–9.

[101] Kim, R. A. & Wang, J. C. (1989). A subthreshold level of DNA topoisomerases leads to the excision of yeast rDNA as extrachromosomal rings. *Cell,* **57** (6), 975–85.

[102] Castano, I. B., Brzoska, P. M., Sadoff, B. U., Chen, H. & Christman, M. F. (1996). Mitotic chromosome condensation in the rDNA requires TRF4 and DNA topoisomerase I in Saccharomyces cerevisiae. *Genes Dev.* **10** (20), 2564–76.

[103] Choder, M. (1991). A general topoisomerase I-dependent transcriptional repression in the stationary phase in yeast. *Genes Dev.* **5** (12A), 2315–26.

[104] Holm, C., Goto, T., Wang, J. C. & Botstein, D. (1985). DNA topoisomerase II is required at the time of mitosis in yeast. *Cell,* **41** (2), 553–63.

[105] Holm, C., Stearns, T. & Botstein, D. (1989). DNA topoisomerase II must act at mitosis to prevent nondisjunction and chromosome breakage. *Mol. Cell. Biol.* **9** (1), 159–68.

[106] Uemura, T., Ohkura, H., Adachi, Y., Morino, K., Shiozaki, K. & Yanagida, M. (1987). DNA topoisomerase II is required for condensation and separation of mitotic chromosomes in S. pombe. *Cell,* **50** (6), 917–25.

[107] Kim, R. A. & Wang, J. C. (1992). Identification of the yeast TOP3 gene product as a single strand-specific DNA topoisomerase. *J. Biol. Chem.* **267** (24), 17178–85.

[108] Wallis, J. W., Chrebet, G., Brodsky, G., Rolfe, M. & Rothstein, R. (1989). A hyper-recombination mutation in S. cerevisiae identifies a novel eukaryotic topoisomerase. *Cell,* **58** (2), 409–19.

[109] Saffi, J., Feldmann, H., Winnacker, E. L. & Henriques, J. A. (2001). Interaction of the yeast Pso5/Rad16 and Sgs1 proteins: influences on DNA repair and aging. *Mutat. Res.* **486** (3), 195–206.

[110] Chakraverty, R. K., Kearsey, J. M., Oakley, T. J., Grenon, M., de La Torre Ruiz, M. A., Lowndes, N. F. & Hickson, I. D. (2001). Topoisomerase III acts upstream of Rad53p in the S-phase DNA damage checkpoint. *Mol. Cell. Biol.* **21** (21), 7150–62.

[111] Bailis, A. M., Arthur, L. & Rothstein, R. (1992). Genome rearrangement in top3 mutants of Saccharomyces cerevisiae requires a functional RAD1 excision repair gene. *Mol. Cell. Biol.* **12** (11), 4988–93.

[112] Gangloff, S., de Massy, B., Arthur, L., Rothstein, R. & Fabre, F. (1999). The essential role of yeast topoisomerase III in meiosis depends on recombination. *EMBO J.* **18** (6), 1701–11.

[113] Onodera, R., Seki, M., Ui, A., Satoh, Y., Miyajima, A., Onoda, F. & Enomoto, T. (2002). Functional and physical interaction between Sgs1 and Top3 and Sgs1-independent function of Top3 in DNA recombination repair. *Genes Genet. Syst.* **77** (1), 11–21.

[114] Rong, L. & Klein, H. L. (1993). Purification and characterization of the SRS2 DNA helicase of the yeast Saccharomyces cerevisiae. *J. Biol. Chem.* **268** (2), 1252–9.

[115] Krejci, L., Van Komen, S., Li, Y., Villemain, J., Reddy, M. S., Klein, H., Ellenberger, T. & Sung, P. (2003). DNA helicase Srs2 disrupts the Rad51 presynaptic filament. *Nature,* **423** (6937), 305–9.

[116] Veaute, X., Jeusset, J., Soustelle, C., Kowalczykowski, S. C., Le Cam, E. & Fabre, F. (2003). The Srs2 helicase prevents recombination by disrupting Rad51 nucleoprotein filaments. *Nature,* **423** (6937), 309–12.

[117] Pfander, B., Moldovan, G. L., Sacher, M., Hoege, C. & Jentsch, S. (2005). SUMO-modified PCNA recruits Srs2 to prevent recombination during S phase. *Nature,* **Epub ahead of print**.

[118] Liberi, G., Maffioletti, G., Lucca, C., Chiolo, I., Baryshnikova, A., Cotta-Ramusino, C., Lopes, M., Pellicioli, A., Haber, J. E. & Foiani, M. (2005). Rad51-dependent DNA structures accumulate at damaged replication forks in sgs1 mutants defective in the yeast ortholog of BLM recq helicase. *Genes Dev.* **19** (3), 339–50.

[119] Sogo, J. M., Lopes, M. & Foiani, M. (2002). Fork reversal and ssDNA accumulation at stalled replication forks owing to checkpoint defects. *Science,* **297** (5581), 599–602.

[120] Cobb, J. A., Bjergbaek, L., Shimada, K., Frei, C. & Gasser, S. M. (2003). DNA polymerase stabilization at stalled replication forks requires mec1 and the RecQ helicase Sgs1. *EMBO J.* **22** (16), 4325–36.

[121] Bjergbaek, L., Cobb, J. A., Tsai-Pflugfelder, M. & Gasser, S. M. (2005). Mechanistically distinct roles for Sgs1p in checkpoint activation and replication fork maintenance. *EMBO J.* **24** (2), 405–17.

[122] Fabre, F., Chan, A., Heyer, W. D. & Gangloff, S. (2002). Alternate pathways involving Sgs1/Top3, Mus81/ Mms4, and Srs2 prevent formation of toxic recombination intermediates from single-stranded gaps created by DNA replication. *Proc. Natl. Acad. Sci. U S A,* **99** (26), 16887–92.

[123] Mullen, J. R., Kaliraman, V., Ibrahim, S. S. & Brill, S. J. (2001). Requirement for three novel protein complexes in the absence of the Sgs1 DNA helicase in saccharomyces cerevisiae. *Genetics,* **157** (1), 103–18.

[124] Kaliraman, V., Mullen, J. R., Fricke, W. M., Bastin-Shanower, S. A. & Brill, S. J. (2001). Functional overlap between Sgs1-Top3 and the Mms4-Mus81 endonuclease. *Genes Dev.* **15** (20), 2730–40.

[125] Schild, D., Glassner, B. J., Mortimer, R. K., Carlson, M. & Laurent, B. C. (1992). Identification of RAD16, a yeast excision repair gene homologous to the recombinational repair gene RAD54 and to the SNF2 gene involved in transcriptional activation. *Yeast,* **8** (5), 385–95.

[126] Chang, M., Bellaoui, M., Zhang, C., Desai, R., Morozov, P., Delgado-Cruzata, L., Rothstein, R., Freyer, G. A., Boone, C. & Brown, G. W. (2005). RMI1/NCE4, a suppressor of genome instability, encodes a member of the recQ helicase/Topo III complex. *EMBO J.* **advance online publication** (May, 12).

[127] Mullen, J. R., Nallaseth, F. S., Lan, Y. Q., Slagle, C. E. & Brill, S. J. (2005). Yeast rmi1/nce4 controls genome stability as a subunit of the sgs1-top3 complex. *Mol. Cell. Biol.* **25** (11), 4476–87.

[128] Puranam, K. L. & Blackshear, P. J. (1994). Cloning and characterization of RECQL, a potential human homologue of the escherichia coli DNA helicase RecQ. *J. Biol. Chem.* **269** (47), 29838–45.

[129] Seki, M., Miyazawa, H., Tada, S., Yanagisawa, J., Yamaoka, T., Hoshino, S., Ozawa, K., Eki, T., Nogami, M., Okumura, K. & et al. (1994). Molecular cloning of cDNA encoding human DNA helicase Q1 which has homology to Escherichia coli Rec Q helicase and localization of the gene at chromosome 12p12. *Nucleic Acids Res.* **22** (22), 4566–73.

[130] Puranam, K. L., Kennington, E., Sait, S. N., Shows, T. B., Rochelle, J. M., Seldin, M. F. & Blackshear, P. J. (1995). Chromosomal localization of the gene encoding the human DNA helicase RECQL and its mouse homologue. *Genomics,* **26** (3), 595–8.

[131] Zhang, A. H. & Xi, X. (2002). Molecular cloning of a splicing variant of human RECQL helicase. *Biochem. Biophys. Res. Commun.* **298** (5), 789–92.

[132] Suijkerbuijk, R. F., Sinke, R. J., Meloni, A. M., Parrington, J. M., van Echten, J., de Jong, B., Oosterhuis, J. W., Sandberg, A. A. & Geurts van Kessel, A. (1993). Overrepresentation of chromosome 12p sequences and karyotypic evolution in i(12p)-negative testicular germ-cell tumors revealed by fluorescence in situ hybridization. *Cancer Genet. Cytogenet.* **70** (2), 85–93.

[133] Yanagisawa, J., Seki, M., Ui, M. & Enomoto, T. (1992). Alteration of a DNA-dependent ATPase activity in xeroderma pigmentosum complementation group C cells. *J. Biol. Chem.* **267** (6), 3585–8.

[134] Seki, M., Yanagisawa, J., Kohda, T., Sonoyama, T., Ui, M. & Enomoto, T. (1994). Purification of two DNA-dependent adenosinetriphosphatases having DNA helicase activity from HeLa cells and comparison of the properties of the two enzymes. *J. Biochem. (Tokyo),* **115** (3), 523–31.

[135] Masutani, C., Sugasawa, K., Yanagisawa, J., Sonoyama, T., Ui, M., Enomoto, T., Takio, K., Tanaka, K., van der Spek, P. J., Bootsma, D. & et al. (1994). Purification and cloning of a nucleotide excision repair complex involving the xeroderma pigmentosum group C protein and a human homologue of yeast RAD23. *EMBO J.* **13** (8), 1831–43.

[136] Seki, T., Tada, S., Katada, T. & Enomoto, T. (1997). Cloning of a cDNA encoding a novel importin-alpha homologue, Qip1: discrimination of Qip1 and Rch1 from hSrp1 by their ability to interact with DNA helicase Q1/recQL. *Biochem. Biophys. Res. Commun.* **234** (1), 48–53.

[137] Miyamoto, Y., Imamoto, N., Sekimoto, T., Tachibana, T., Seki, T., Tada, S., Enomoto, T. & Yoneda, Y. (1997). Differential modes of nuclear localization signal (NLS) recognition by three distinct classes of NLS receptors. *J. Biol. Chem.* **272** (42), 26375–81.

[138] Bloom, D. (1954). Congenital telangiectatic erythema resembling lupus erythematosus in dwarfs; probably a syndrome entity. *AMA Am. J. Dis. Child.* **88** (6), 754–8.

[139] Guarente-Lab, H. (2005). Ageing in humans. Found at URL: http://web.mit.edu/biology/guarente/human/human.html.

[140] Chester, N., Kuo, F., Kozak, C., O'Hara, C. D. & Leder, P. (1998). Stage-specific apoptosis, developmental delay, and embryonic lethality in mice homozygous for a targeted disruption in the murine Bloom's syndrome gene. *Genes Dev.* **12** (21), 3382–93.

[141] Luo, G., Santoro, I. M., McDaniel, L. D., Nishijima, I., Mills, M., Youssoufian, H., Vogel, H., Schultz, R. A. & Bradley, A. (2000). Cancer predisposition caused by elevated mitotic recombination in Bloom mice. *Nat. Genet.* **26** (4), 424–9.

[142] Hu, Y., Lu, X., Barnes, E., Yan, M., Lou, H. & Luo, G. (2005). Recql5 and Blm RecQ DNA Helicases Have Nonredundant Roles in Suppressing Crossovers. *Mol Cell Biol,* **25** (9), 3431–42.

[143] Wang, W., Seki, M., Narita, Y., Sonoda, E., Takeda, S., Yamada, K., Masuko, T., Katada, T. & Enomoto, T. (2000). Possible association of BLM in decreasing DNA double strand breaks during DNA replication. *EMBO J.* **19** (13), 3428–35.

[144] Imamura, O., Fujita, K., Itoh, C., Takeda, S., Furuichi, Y. & Matsumoto, T. (2002). Werner and Bloom helicases are involved in DNA repair in a complementary fashion. *Oncogene,* **21** (6), 954–63.

[145] Amor-Guéret, M. (2005). Bloom syndrome. *Atlas Genet. Cytogenet. Oncol. Haematol.* , URL: http://www.infobiogen.fr/services/chromcancer/Tumors/BLO10002.html.

[146] Rosin, M. P. & German, J. (1985). Evidence for chromosome instability in vivo in Bloom syndrome: increased numbers of micronuclei in exfoliated cells. *Hum. Genet.* **71** (3), 187–91.

[147] Frorath, B., Schmidt-Preuss, U., Siemers, U., Zollner, M. & Rudiger, H. W. (1984). Heterozygous carriers for Bloom syndrome exhibit a spontaneously increased micronucleus formation in cultured fibroblasts. *Hum. Genet.* **67** (1), 52–5.

[148] Yankiwski, V., Marciniak, R. A., Guarente, L. & Neff, N. F. (2000). Nuclear structure in normal and Bloom syndrome cells. *Proc. Natl. Acad. Sci. U S A,* **97** (10), 5214–9.

[149] German, J. (1969). Bloom's syndrome. I. Genetical and clinical observations in the first twenty-seven patients. *Am. J. Hum. Genet.* **21** (2), 196–227.

[150] Poppe, B., Van Limbergen, H., Van Roy, N., Vandecruys, E., De Paepe, A., Benoit, Y. & Speleman, F. (2001). Chromosomal aberrations in Bloom syndrome patients with myeloid malignancies. *Cancer Genet. Cytogenet.* **128** (1), 39–42.

[151] Hand, R. & German, J. (1975). A retarded rate of DNA chain growth in Bloom's syndrome. *Proc. Natl. Acad. Sci. U S A,* **72** (2), 758–62.

[152] Waters, R., Regan, J. D. & German, J. (1978). Increased amounts of hybrid (heavy/heavy) DNA in Bloom's syndrome fibroblasts. *Biochem. Biophys. Res. Commun.* **83** (2), 536–41.

[153] Ababou, M., Dumaire, V., Lecluse, Y. & Amor-Gueret, M. (2002). Bloom's syndrome protein response to ultraviolet-C radiation and hydroxyurea-mediated DNA synthesis inhibition. *Oncogene,* **21** (13), 2079–88.

[154] Beamish, H., Kedar, P., Kaneko, H., Chen, P., Fukao, T., Peng, C., Beresten, S., Gueven, N., Purdie, D., Lees-Miller, S., Ellis, N., Kondo, N. & Lavin, M. F. (2002). Functional link between BLM defective in Bloom's syndrome and the ataxia-telangiectasia-mutated protein, ATM. *J. Biol. Chem.* **277** (34), 30515–23.

[155] Davies, S. L., North, P. S., Dart, A., Lakin, N. D. & Hickson, I. D. (2004). Phosphorylation of the Bloom's syndrome helicase and its role in recovery from S-phase arrest. *Mol. Cell. Biol.* **24** (3), 1279–91.

[156] Karow, J. K., Newman, R. H., Freemont, P. S. & Hickson, I. D. (1999). Oligomeric ring structure of the Bloom's syndrome helicase. *Curr. Biol.* **9** (11), 597–600.

[157] Karow, J. K., Constantinou, A., Li, J. L., West, S. C. & Hickson, I. D. (2000). The Bloom's syndrome gene product promotes branch migration of holliday junctions. *Proc. Natl. Acad. Sci. U S A,* **97** (12), 6504–8.

[158] Schwacha, A. & Kleckner, N. (1995). Identification of double Holliday junctions as intermediates in meiotic recombination. *Cell,* **83** (5), 783–91.

[159] Bachrati, C. Z. & Hickson, I. D. (2003). RecQ helicases: suppressors of tumorigenesis and premature aging. *Biochem. J.* **374** (Pt 3), 577–606.

[160] Machwe, A., Xiao, L., Groden, J., Matson, S. W. & Orren, D. K. (2005). RECQ family members combine strand pairing and unwinding activities to catalyze strand exchange. *J. Biol. Chem.* **Epub ahead of print**.

[161] Dutertre, S., Ababou, M., Onclercq, R., Delic, J., Chatton, B., Jaulin, C. & Amor-Gueret, M. (2000). Cell cycle regulation of the endogenous wild type Bloom's syndrome DNA helicase. *Oncogene,* **19** (23), 2731–8.

[162] Bischof, O., Kim, S. H., Irving, J., Beresten, S., Ellis, N. A. & Campisi, J. (2001). Regulation and localization of the Bloom syndrome protein in response to DNA damage. *J. Cell. Biol.* **153** (2), 367–80.

[163] Ababou, M., Dutertre, S., Lecluse, Y., Onclercq, R., Chatton, B. & Amor-Gueret, M. (2000). ATM-dependent phosphorylation and accumulation of endogenous BLM protein in response to ionizing radiation. *Oncogene,* **19** (52), 5955–63.

[164] Franchitto, A. & Pichierri, P. (2002). Bloom's syndrome protein is required for correct relocalization of RAD50/MRE11/NBS1 complex after replication fork arrest. *J. Cell. Biol.* **157** (1), 19–30.

[165] Rotman, G. & Shiloh, Y. (1999). ATM: a mediator of multiple responses to genotoxic stress. *Oncogene,* **18** (45), 6135–44.

[166] Davalos, A. R. & Campisi, J. (2003). Bloom syndrome cells undergo p53-dependent apoptosis and delayed assembly of BRCA1 and NBS1 repair complexes at stalled replication forks. *J. Cell. Biol.* **162** (7), 1197–209. 0021-9525 Journal Article.

[167] Sengupta, S., Robles, A. I., Linke, S. P., Sinogeeva, N. I., Zhang, R., Pedeux, R., Ward, I. M., Celeste, A., Nussenzweig, A., Chen, J., Halazonetis, T. D. & Harris, C. C. (2004). Functional interaction between BLM helicase and 53BP1 in a Chk1-mediated pathway during S-phase arrest. *J. Cell. Biol.* **166** (6), 801–13.

[168] Wang, Y., Cortez, D., Yazdi, P., Neff, N., Elledge, S. J. & Qin, J. (2000). BASC, a super complex of BRCA1-associated proteins involved in the recognition and repair of aberrant DNA structures. *Genes Dev.* **14** (8), 927–39.

[169] Meetei, A. R., Sechi, S., Wallisch, M., Yang, D., Young, M. K., Joenje, H., Hoatlin, M. E. & Wang, W. (2003). A multiprotein nuclear complex connects Fanconi anemia and Bloom syndrome. *Mol. Cell. Biol.* **23** (10), 3417–26.

[170] Pichierri, P., Franchitto, A. & Rosselli, F. (2004). BLM and the FANC proteins collaborate in a common pathway in response to stalled replication forks. *EMBO J.* **23** (15), 3154–63.

[171] D'Andrea, A. D. & Grompe, M. (2003). The Fanconi anaemia/BRCA pathway. *Nat. Rev. Cancer,* **3** (1), 23–34.

[172] Jiao, R., Bachrati, C. Z., Pedrazzi, G., Kuster, P., Petkovic, M., Li, J. L., Egli, D., Hickson, I. D. & Stagljar, I. (2004). Physical and functional interaction between the Bloom's syndrome gene product and the largest subunit of chromatin assembly factor 1. *Mol. Cell. Biol.* **24** (11), 4710–9.

[173] Hodges, M., Tissot, C., Howe, K., Grimwade, D. & Freemont, P. S. (1998). Structure, organization, and dynamics of promyelocytic leukemia protein nuclear bodies. *Am. J. Hum. Genet.* **63** (2), 297–304.

[174] Ruggero, D., Wang, Z. G. & Pandolfi, P. P. (2000). The puzzling multiple lives of PML and its role in the genesis of cancer. *Bioessays,* **22** (9), 827–35.

[175] Dellaire, G. & Bazett-Jones, D. P. (2004). PML nuclear bodies: dynamic sensors of DNA damage and cellular stress. *Bioessays,* **26** (9), 963–77.

[176] Eladad, S., Ye, T. Z., Hu, P., Leversha, M., Beresten, S., Matunis, M. J. & Ellis, N. A. (2005). Intra-nuclear trafficking of the BLM helicase to DNA damage-induced foci is regulated by SUMO modification. *Hum. Mol. Genet.* . HMG Advance Access.

[177] Marsischky, G. T., Lee, S., Griffith, J. & Kolodner, R. D. (1999). 'saccharomyces cerevisiae MSH2/6 complex interacts with Holliday junctions and facilitates their cleavage by phage resolution enzymes. *J. Biol. Chem.* **274** (11), 7200–6.

[178] Pedrazzi, G., Bachrati, C. Z., Selak, N., Studer, I., Petkovic, M., Hickson, I. D., Jiricny, J. & Stagljar, I. (2003). The Bloom's syndrome helicase interacts directly with the human DNA mismatch repair protein hMSH6. *Biol. Chem.* **384** (8), 1155–64.

[179] Yang, Q., Zhang, R., Wang, X. W., Linke, S. P., Sengupta, S., Hickson, I. D., Pedrazzi, G., Perrera, C., Stagljar, I., Littman, S. J., Modrich, P. & Harris, C. C. (2004). The mismatch DNA repair heterodimer, hMSH2/6, regulates BLM helicase. *Oncogene,* **23** (21), 3749–56.

[180] Stojic, L., Brun, R. & Jiricny, J. (2004). Mismatch repair and DNA damage signalling. *DNA Repair (Amst),* **3** (8-9), 1091–101.

[181] Li, G. M. & Modrich, P. (1995). Restoration of mismatch repair to nuclear extracts of H6 colorectal tumor cells by a heterodimer of human MutL homologs. *Proc. Natl. Acad. Sci. U S A,* **92** (6), 1950–4.

[182] Pedrazzi, G., Perrera, C., Blaser, H., Kuster, P., Marra, G., Davies, S. L., Ryu, G. H., Freire, R., Hickson, I. D., Jiricny, J. & Stagljar, I. (2001). Direct association of Bloom's syndrome gene product with the human mismatch repair protein MLH1. *Nucleic Acids Res.* **29** (21), 4378–86.

[183] Langland, G., Kordich, J., Creaney, J., Goss, K. H., Lillard-Wetherell, K., Bebenek, K., Kunkel, T. A. & Groden, J. (2001). The bloom's syndrome protein (blm) interacts with mlh1 but is not required for dna mismatch repair. *J. Biol. Chem.* **276** (32), 30031–5.

[184] Wang, X. W., Tseng, A., Ellis, N. A., Spillare, E. A., Linke, S. P., Robles, A. I., Seker, H., Yang, Q., Hu, P., Beresten, S., Bemmels, N. A., Garfield, S. & Harris, C. C. (2001). Functional interaction of p53 and BLM DNA helicase in apoptosis. *J. Biol. Chem.* **276** (35), 32948–55.

[185] Yang, Q., Zhang, R., Wang, X. W., Spillare, E. A., Linke, S. P., Subramanian, D., Griffith, J. D., Li, J. L., Hickson, I. D., Shen, J. C., Loeb, L. A., Mazur, S. J., Appella, E., Brosh, R. M., J., Karmakar, P., Bohr, V. A. & Harris, C. C. (2002). The processing of Holliday junctions by BLM and WRN helicases is regulated by p53. *J. Biol. Chem.* **277** (35), 31980–7.

[186] Garkavtsev, I. V., Kley, N., Grigorian, I. A. & Gudkov, A. V. (2001). The bloom syndrome protein interacts and cooperates with p53 in regulation of transcription and cell growth control. *Oncogene,* **20** (57), 8276–80.

[187] Wu, L., Davies, S. L., Levitt, N. C. & Hickson, I. D. (2001). Potential role for the BLM helicase in recombinational repair via a conserved interaction with RAD51. *J. Biol. Chem.* **276** (22), 19375–81.

[188] Moens, P. B., Kolas, N. K., Tarsounas, M., Marcon, E., Cohen, P. E. & Spyropoulos, B. (2002). The time course and chromosomal localization of recombination-related proteins at meiosis in the mouse are compatible with models that can resolve the early DNA-DNA interactions without reciprocal recombination. *J. Cell. Sci.* **115** (Pt 8), 1611–22.

[189] Sanz, M. M., Proytcheva, M., Ellis, N. A., Holloman, W. K. & German, J. (2000). BLM, the Bloom's syndrome protein, varies during the cell cycle in its amount, distribution, and co-localization with other nuclear proteins. *Cytogenet. Cell. Genet.* **91** (1-4), 217–23.

[190] Johnson, F. B., Lombard, D. B., Neff, N. F., Mastrangelo, M. A., Dewolf, W., Ellis, N. A., Marciniak, R. A., Yin, Y., Jaenisch, R. & Guarente, L. (2000). Association of the Bloom syndrome protein with topoisomerase iiialpha in somatic and meiotic cells. *Cancer Res.* **60** (5), 1162–7.

[191] Stavropoulos, D. J., Bradshaw, P. S., Li, X., Pasic, I., Truong, K., Ikura, M., Ungrin, M. & Meyn, M. S. (2002). The Bloom syndrome helicase BLM interacts with TRF2 in ALT cells and promotes telomeric DNA synthesis. *Hum. Mol. Genet.* **11** (25), 3135–44.

[192] Thannhauser, S. (1945). Werner's syndrome (progeria of the adult) and Rothmund's syndrome: two types of closely related heredo-familial atrophic dermatosis with juvenile cataracts and endocrine features. A critical study with five new cases. *Ann. Intern. Med.* **23**, 559–626.

[193] Epstein, C. J., Martin, G. M., Schultz, A. L. & Motulsky, A. G. (1966). Werner's syndrome a review of its symptomatology, natural history, pathologic features, genetics and relationship to the natural aging process. *Medicine (Baltimore),* **45** (3), 177–221.

[194] Goto, M., Miller, R. W., Ishikawa, Y. & Sugano, H. (1996). Excess of rare cancers in Werner syndrome (adult progeria). *Cancer Epidemiol. Biomarkers Prev.* **5** (4), 239–46.

[195] Salk, D. (1982). Werner's syndrome: a review of recent research with an analysis of connective tissue metabolism, growth control of cultured cells, and chromosomal aberrations. *Hum. Genet.* **62** (1), 1–5.

[196] Matsumoto, T., Imamura, O., Yamabe, Y., Kuromitsu, J., Tokutake, Y., Shimamoto, A., Suzuki, N., Satoh, M., Kitao, S., Ichikawa, K., Kataoka, H., Sugawara, K., Thomas, W., Mason, B., Tsuchihashi, Z., Drayna, D., Sugawara, M., Sugimoto, M., Furuichi, Y. & Goto, M. (1997). Mutation and haplotype analyses of the Werner's syndrome gene based on its genomic structure: genetic epidemiology in the Japanese population. *Hum. Genet.* **100** (1), 123–30.

[197] Salk, D., Bryant, E., Au, K., Hoehn, H. & Martin, G. M. (1981). Systematic growth studies, cocultivation, and cell hybridization studies of Werner syndrome cultured skin fibroblasts. *Hum. Genet.* **58** (3), 310–6.

[198] Crabbe, L., Verdun, R. E., Haggblom, C. I. & Karlseder, J. (2004). Defective telomere lagging strand synthesis in cells lacking WRN helicase activity. *Science,* **306** (5703), 1951–3.

[199] Saintigny, Y., Makienko, K., Swanson, C., Emond, M. J. & Monnat, R. J., J. (2002). Homologous recombination resolution defect in werner syndrome. *Mol. Cell. Biol.* **22** (20), 6971–8.

[200] Wyllie, F. S., Jones, C. J., Skinner, J. W., Haughton, M. F., Wallis, C., Wynford-Thomas, D., Faragher, R. G. & Kipling, D. (2000). Telomerase prevents the accelerated cell ageing of Werner syndrome fibroblasts. *Nat. Genet.* **24** (1), 16–7. 1061-4036 Journal Article.

[201] Prince, P. R., Ogburn, C. E., Moser, M. J., Emond, M. J., Martin, G. M. & Monnat, R. J., J. (1999). Cell fusion corrects the 4-nitroquinoline 1-oxide sensitivity of Werner syndrome fibroblast cell lines. *Hum. Genet.* **105** (1-2), 132–8. 0340-6717 Journal Article.

[202] Poot, M., Gollahon, K. A., Emond, M. J., Silber, J. R. & Rabinovitch, P. S. (2002). Werner syndrome diploid fibroblasts are sensitive to 4-nitroquinoline-n-oxide and 8-methoxypsoralen: implications for the disease phenotype. *FASEB J.* **16** (7), 757–8.

[203] Hisama, F. M., Chen, Y. H., Meyn, M. S., Oshima, J. & Weissman, S. M. (2000). WRN or telomerase constructs reverse 4-nitroquinoline 1-oxide sensitivity in transformed Werner syndrome fibroblasts. *Cancer Res.* **60** (9), 2372–6.

[204] Poot, M., Yom, J. S., Whang, S. H., Kato, J. T., Gollahon, K. A. & Rabinovitch, P. S. (2001). Werner syndrome cells are sensitive to DNA cross-linking drugs. *FASEB J.* **15** (7), 1224–6.

[205] Okada, M., Goto, M., Furuichi, Y. & Sugimoto, M. (1998). Differential effects of cytotoxic drugs on mortal and immortalized B-lymphoblastoid cell lines from normal and Werner's syndrome patients. *Biol. Pharm. Bull.* **21** (3), 235–9.

[206] Lebel, M. & Leder, P. (1998). A deletion within the murine werner syndrome helicase induces sensitivity to inhibitors of topoisomerase and loss of cellular proliferative capacity. *Proc. Natl. Acad. Sci. U S A,* **95** (22), 13097–102.

[207] Yannone, S. M., Roy, S., Chan, D. W., Murphy, M. B., Huang, S., Campisi, J. & Chen, D. J. (2001). Werner syndrome protein is regulated and phosphorylated by DNA-dependent protein kinase. *J. Biol. Chem.* **276** (41), 38242–8.

[208] Fukuchi, K., Martin, G. M. & Monnat, R. J., J. (1989). Mutator phenotype of Werner syndrome is characterized by extensive deletions. *Proc. Natl. Acad. Sci. U S A,* **86** (15), 5893–7.

[209] Salk, D., Au, K., Hoehn, H. & Martin, G. M. (1981). Cytogenetics of Werner's syndrome cultured skin fibroblasts: variegated translocation mosaicism. *Cytogenet. Cell. Genet.* **30** (2), 92–107.

[210] Pichierri, P., Franchitto, A., Mosesso, P. & Palitti, F. (2001). Werner's syndrome protein is required for correct recovery after replication arrest and dna damage induced in s-phase of cell cycle. *Mol. Biol. Cell.* **12** (8), 2412–21.

[211] Darlington, G. J., Dutkowski, R. & Brown, W. T. (1981). Sister chromatid exchange frequencies in Progeria and Werner syndrome patients. *Am. J. Hum. Genet.* **33** (5), 762–6.

[212] Melaragno, M. I., Pagni, D. & Smith, M. A. (1995). Cytogenetic aspects of Werner's syndrome lymphocyte cultures. *Mech. Ageing. Dev.* **78** (2), 117–22.

[213] Huang, S., Beresten, S., Li, B., Oshima, J., Ellis, N. A. & Campisi, J. (2000). Characterization of the human and mouse WRN 3'-5' exonuclease. *Nucleic Acids Res.* **28** (12), 2396–405.

[214] Kawabe, T., Tsuyama, N., Kitao, S., Nishikawa, K., Shimamoto, A., Shiratori, M., Matsumoto, T., Anno, K., Sato, T., Mitsui, Y., Seki, M., Enomoto, T., Goto, M., Ellis, N. A., Ide, T., Furuichi, Y. & Sugimoto, M. (2000). Differential regulation of human RecQ family helicases in cell transformation and cell cycle. *Oncogene,* **19** (41), 4764–72.

[215] Kitao, S., Ohsugi, I., Ichikawa, K., Goto, M., Furuichi, Y. & Shimamoto, A. (1998). Cloning of two new human helicase genes of the RecQ family: biological significance of multiple species in higher eukaryotes. *Genomics,* **54** (3), 443–52.

[216] Constantinou, A., Tarsounas, M., Karow, J. K., Brosh, R. M., Bohr, V. A., Hickson, I. D. & West, S. C. (2000). Werner's syndrome protein (WRN) migrates Holliday junctions and co-localizes with RPA upon replication arrest. *EMBO Rep.* **1** (1), 80–4.

[217] Brosh, R. M., J., Karmakar, P., Sommers, J. A., Yang, Q., Wang, X. W., Spillare, E. A., Harris, C. C. & Bohr, V. A. (2001). p53 modulates the exonuclease activity of Werner syndrome protein. *J. Biol. Chem.* **276** (37), 35093–102.

[218] Blander, G., Zalle, N., Daniely, Y., Taplick, J., Gray, M. D. & Oren, M. (2002). Dna damage-induced translocation of the Werner helicase is regulated by acetylation. *J. Biol. Chem.* **277** (52), 50934–40.

[219] Gray, M. D., Wang, L., Youssoufian, H., Martin, G. M. & Oshima, J. (1998). Werner helicase is localized to transcriptionally active nucleoli of cycling cells. *Exp. Cell. Res.* **242** (2), 487–94.

[220] Sakamoto, S., Nishikawa, K., Heo, S. J., Goto, M., Furuichi, Y. & Shimamoto, A. (2001). Werner helicase relocates into nuclear foci in response to DNA damaging agents and co-localizes with RPA and Rad51. *Genes Cells,* **6** (5), 421–30.

[221] Cooper, M. P., Machwe, A., Orren, D. K., Brosh, R. M., Ramsden, D. & Bohr, V. A. (2000). Ku complex interacts with and stimulates the Werner protein. *Genes Dev.* **14** (8), 907–12.

[222] Orren, D. K., Machwe, A., Karmakar, P., Piotrowski, J., Cooper, M. P. & Bohr, V. A. (2001). A functional interaction of Ku with Werner exonuclease facilitates digestion of damaged DNA. *Nucleic Acids Res.* **29** (9), 1926–34.

[223] Li, B. & Comai, L. (2000). Functional interaction between Ku and the werner syndrome protein in DNA end processing. *J. Biol. Chem.* **275** (50), 39800.

[224] Li, B. & Comai, L. (2001). Requirements for the nucleolytic processing of dna ends by the werner syndrome protein-Ku70/80 complex. *J. Biol. Chem.* **276** (13), 9896–902.

[225] Li, B. & Comai, L. (2002). Displacement of DNA-PKcs from DNA ends by the werner syndrome protein. *Nucleic Acids Res.* **30** (17), 3653–61.

[226] Karmakar, P., Snowden, C. M., Ramsden, D. A. & Bohr, V. A. (2002). Ku heterodimer binds to both ends of the Werner protein and functional interaction occurs at the Werner N-terminus. *Nucleic Acids Res.* **30** (16), 3583–91.

[227] Karmakar, P., Piotrowski, J., Brosh, R. M., J., Sommers, J. A., Miller, S. P., Cheng, W. H., Snowden, C. M., Ramsden, D. A. & Bohr, V. A. (2002). Werner protein is a target of DNA-dependent protein kinase in vivo and in vitro, and its catalytic activities are regulated by phosphorylation. *J. Biol. Chem.* **277** (21), 18291–302.

[228] Li, B., Navarro, S., Kasahara, N. & Comai, L. (2004). Identification and biochemical characterization of a werner's syndrome protein complex with Ku70/80 and poly(ADP-ribose) polymerase-1. *J. Biol. Chem.* **279** (14), 13659–67.

[229] Stefanini, M., Scappaticci, S., Lagomarsini, P., Borroni, G., Berardesca, E. & Nuzzo, F. (1989). Chromosome instability in lymphocytes from a patient with Werner's syndrome is not associated with DNA repair defects. *Mutat. Res.* **219** (3), 179–85.

[230] Barnes, D. E. & Lindahl, T. (2004). Repair and genetic consequences of endogenous dna base damage in mammalian cells. *Annu. Rev. Genet.* **38**, 445–76.

[231] Harrigan, J. A., Opresko, P. L., von Kobbe, C., Kedar, P. S., Prasad, R., Wilson, S. H. & Bohr, V. A. (2003). The Werner syndrome protein stimulates DNA polymerase beta strand displacement synthesis via its helicase activity. *J. Biol. Chem.* **278** (25), 22686–95.

[232] Kamath-Loeb, A. S., Johansson, E., Burgers, P. M. & Loeb, L. A. (2000). Functional interaction between the Werner syndrome protein and DNA polymerase delta. *Proc. Natl. Acad. Sci. U S A,* **97** (9), 4603–8.

[233] Kamath-Loeb, A. S., Loeb, L. A., Johansson, E., Burgers, P. M. & Fry, M. (2001). Interactions between the Werner syndrome helicase and DNA polymerase delta specifically facilitate copying of tetraplex and hairpin structures of the d(CGG)n trinucleotide repeat sequence. *J. Biol. Chem.* **276** (19), 16439–46.

[234] Sharma, S., Sommers, J. A., Driscoll, H. C., Uzdilla, L., Wilson, T. M. & Brosh, R. M., J. (2003). The exonucleolytic and endonucleolytic cleavage activities of human exonuclease 1 are stimulated by an interaction with the carboxyl-terminal region of the Werner syndrome protein. *J. Biol. Chem.* **278** (26), 23487–96.

[235] Bambara, R. A., Murante, R. S. & Henricksen, L. A. (1997). Enzymes and reactions at the eukaryotic DNA replication fork. *J. Biol. Chem.* **272** (8), 4647–50.

[236] Klungland, A. & Lindahl, T. (1997). Second pathway for completion of human DNA base excision-repair: reconstitution with purified proteins and requirement for DNase IV (FEN1). *EMBO J.* **16** (11), 3341–8.

[237] Sharma, S., Otterlei, M., Sommers, J. A., Driscoll, H. C., Dianov, G. L., Kao, H. I., Bambara, R. A. & Brosh, R. M., J. (2004). Wrn helicase and fen-1 form a complex upon replication arrest and together process branchmigrating dna structures associated with the replication fork. *Mol. Biol. Cell.* **15** (2), 734–50.

[238] Evan, G. I., Wyllie, A. H., Gilbert, C. S., Littlewood, T. D., Land, H., Brooks, M., Waters, C. M., Penn, L. Z. & Hancock, D. C. (1992). Induction of apoptosis in fibroblasts by c-myc protein. *Cell,* **69** (1), 119–28.

[239] Grandori, C., Wu, K. J., Fernandez, P., Ngouenet, C., Grim, J., Clurman, B. E., Moser, M. J., Oshima, J., Russell, D. W., Swisshelm, K., Frank, S., Amati, B., Dalla-Favera, R. & Monnat, R. J., J. (2003). Werner syndrome protein limits MYC-induced cellular senescence. *Genes Dev.* **17** (13), 1569–74.

[240] Grandori, C., Robinson, K. L., Galloway, D. A. & Swisshelm, K. (2004). Functional link between myc and the werner gene in tumorigenesis. *Cell Cycle,* **3** (1), 22–5.

[241] Blander, G., Kipnis, J., Leal, J. F., Yu, C. E., Schellenberg, G. D. & Oren, M. (1999). Physical and functional interaction between p53 and the Werner's syndrome protein. *J. Biol. Chem.* **274** (41), 29463–9.

[242] Balajee, A. S., Machwe, A., May, A., Gray, M. D., Oshima, J., Martin, G. M., Nehlin, J. O., Brosh, R., Orren, D. K. & Bohr, V. A. (1999). The Werner syndrome protein is involved in RNA polymerase ii transcription. *Mol. Biol. Cell.* **10** (8), 2655–68.

[243] Brosh, R. M., J., von Kobbe, C., Sommers, J. A., Karmakar, P., Opresko, P. L., Piotrowski, J., Dianova, I., Dianov, G. L. & Bohr, V. A. (2001). Werner syndrome protein interacts with human flap endonuclease 1 and stimulates its cleavage activity. *EMBO J.* **20** (20), 5791–801.

[244] Opresko, P. L., Otterlei, M., Graakjaer, J., Bruheim, P., Dawut, L., Kolvraa, S., May, A., Seidman, M. M. & Bohr, V. A. (2004). The Werner syndrome helicase and exonuclease cooperate to resolve telomeric D loops in a manner regulated by TRF1 and TRF2. *Mol. Cell.* **14** (6), 763–74.

[245] Kawabe, Y., Branzei, D., Hayashi, T., Suzuki, H., Masuko, T., Onoda, F., Heo, S. J., Ikeda, H., Shimamoto, A., Furuichi, Y., Seki, M. & Enomoto, T. (2001). A novel protein interacts with the Werner's syndrome gene product physically and functionally. *J. Biol. Chem.* **276** (23), 20364–9.

[246] Vennos, E. M., Collins, M. & James, W. D. (1992). Rothmund-Thomson syndrome: review of the world literature. *J. Am. Acad. Dermatol.* **27** (5 Pt 1), 750–62.

[247] Vennos, E. M. & James, W. D. (1995). Rothmund-thomson syndrome. *Dermatol. Clin.* **13** (1), 143–50.

[248] Lindor, N. M., Furuichi, Y., Kitao, S., Shimamoto, A., Arndt, C. & Jalal, S. (2000). Rothmund-Thomson syndrome due to RECQ4 helicase mutations: report and clinical and molecular comparisons with Bloom syndrome and Werner syndrome. *Am. J. Med. Genet.* **90** (3), 223–8.

[249] Wang, L. L., Worley, K., Gannavarapu, A., Chintagumpala, M. M., Levy, M. L. & Plon, S. E. (2002). Intron-size constraint as a mutational mechanism in Rothmund-Thomson syndrome. *Am. J. Hum. Genet.* **71** (1), 165–7.

[250] Wang, L. L., Gannavarapu, A., Kozinetz, C. A., Levy, M. L., Lewis, R. A., Chintagumpala, M. M., Ruiz-Maldanado, R., Contreras-Ruiz, J., Cunniff, C., Erickson, R. P., Lev, D., Rogers, M., Zackai, E. H. & Plon, S. E. (2003). Association between osteosarcoma and deleterious mutations in the RECQL4 gene in Rothmund-Thomson syndrome. *J. Natl. Cancer. Inst.* **95** (9), 669–74.

[251] Drouin, C. A., Mongrain, E., Sasseville, D., Bouchard, H. L. & Drouin, M. (1993). Rothmund-Thomson syndrome with osteosarcoma. *J. Am. Acad. Dermatol.* **28** (2 Pt 2), 301–5.

[252] Dick, D. C., Morley, W. N. & Watson, J. T. (1982). Rothmund-Thomson syndrome and osteogenic sarcoma. *Clin. Exp. Dermatol.* **7** (1), 119–23.

[253] el Khoury, J. M., Haddad, S. N. & Atallah, N. G. (1997). Osteosarcomatosis with Rothmund-Thomson syndrome. *Br. J. Radiol.* **70**, 215–8.

[254] Kitao, S., Shimamoto, A., Goto, M., Miller, R. W., Smithson, W. A., Lindor, N. M. & Furuichi, Y. (1999). Mutations in RECQL4 cause a subset of cases of Rothmund-Thomson syndrome. *Nat. Genet.* **22** (1), 82–4.

[255] Snels, D. G., Bavinck, J. N., Muller, H. & Vermeer, B. J. (1998). A female patient with the Rothmund-Thomson syndrome associated with anhidrosis and severe infections of the respiratory tract. *Dermatology,* **196** (2), 260–3.

[256] Siitonen, H. A., Kopra, O., Kaariainen, H., Haravuori, H., Winter, R. M., Saamanen, A. M., Peltonen, L. & Kestila, M. (2003). Molecular defect of RAPADILINO syndrome expands the phenotype spectrum of RECQL diseases. *Hum. Mol. Genet.* **12** (21), 2837–44.

[257] Balraj, P., Concannon, P., Jamal, R., Beghini, A., Hoe, T. S., Khoo, A. S. & Volpi, L. (2002). An unusual mutation in RECQ4 gene leading to Rothmund-Thomson syndrome. *Mutat. Res.* **508** (1-2), 99–105.

[258] Ying, K. L., Oizumi, J. & Curry, C. J. (1990). Rothmund-Thomson syndrome associated with trisomy 8 mosaicism. *J. Med. Genet.* **27** (4), 258–60.

[259] Der Kaloustian, V. M., McGill, J. J., Vekemans, M. & Kopelman, H. R. (1990). Clonal lines of aneuploid cells in Rothmund-Thomson syndrome. *Am. J. Med. Genet.* **37** (3), 336–9.

[260] Orstavik, K. H., McFadden, N., Hagelsteen, J., Ormerod, E. & van der Hagen, C. B. (1994). Instability of lymphocyte chromosomes in a girl with Rothmund-Thomson syndrome. *J. Med. Genet.* **31** (7), 570–2.

[261] Durand, F., Castorina, P., Morant, C., Delobel, B., Barouk, E. & Modiano, P. (2002). Rothmund-Thomson syndrome, trisomy 8 mosaicism and RECQ4 gene mutation. *Ann. Dermatol. Venereol.* **129** (6-7), 892–5.

[262] Miozzo, M., Castorina, P., Riva, P., Dalpra, L., Fuhrman Conti, A. M., Volpi, L., Hoe, T. S., Khoo, A., Wiegant, J., Rosenberg, C. & Larizza, L. (1998). Chromosomal instability in fibroblasts and mesenchymal tumors from 2 sibs with Rothmund-Thomson syndrome. *Int. J. Cancer.* **77** (4), 504–10.

[263] Varughese, M., Leavey, P., Smith, P., Sneath, R., Breatnach, F. & O'Meara, A. (1992). Osteogenic sarcoma and Rothmund Thomson syndrome. *J. Cancer Res. Clin. Oncol.* **118** (5), 389–90.

[264] Smith, P. J. & Paterson, M. C. (1982). Enhanced radiosensitivity and defective DNA repair in cultured fibroblasts derived from Rothmund Thomson syndrome patients. *Mutat. Res.* **94** (1), 213–28.

[265] Kerr, B., Ashcroft, G. S., Scott, D., Horan, M. A., Ferguson, M. W. & Donnai, D. (1996). Rothmund-Thomson syndrome: two case reports show heterogeneous cutaneous abnormalities, an association with genetically programmed ageing changes, and increased chromosomal radiosensitivity. *J. Med. Genet.* **33** (11), 928–34.

[266] Shinya, A., Nishigori, C., Moriwaki, S., Takebe, H., Kubota, M., Ogino, A. & Imamura, S. (1993). A case of Rothmund-Thomson syndrome with reduced DNA repair capacity. *Arch. Dermatol.* **129** (3), 332–6.

[267] Kitao, S., Lindor, N. M., Shiratori, M., Furuichi, Y. & Shimamoto, A. (1999). Rothmund-thomson syndrome responsible gene, RECQL4: genomic structure and products. *Genomics,* **61** (3), 268–76.

[268] Yin, J., Kwon, Y. T., Varshavsky, A. & Wang, W. (2004). RECQL4, mutated in the Rothmund-Thomson and RAPADILINO syndromes, interacts with ubiquitin ligases UBR1 and UBR2 of the N-end rule pathway. *Hum. Mol. Genet.* **13** (20), 2421–30.

[269] Sangrithi, M. N., Bernal, J. A., Madine, M., Philpott, A., Lee, J., Dunphy, W. G. & Venkitaraman, A. R. (2005). Initiation of DNA Replication Requires the RECQL4 Protein Mutated in Rothmund-Thomson Syndrome. *Cell,* **121** (6), 887–898.

[270] Sengupta, S., Shimamoto, A., Koshiji, M., Pedeux, R., Rusin, M., Spillare, E. A., Shen, J. C., Huang, L. E., Lindor, N. M., Furuichi, Y. & Harris, C. C. (2005). Tumor suppressor p53 represses transcription of RECQ4 helicase. *Oncogene,* **24** (10), 1738–48.

[271] Sekelsky, J. J., Brodsky, M. H., Rubin, G. M. & Hawley, R. S. (1999). Drosophila and human RecQ5 exist in different isoforms generated by alternative splicing. *Nucleic Acids Res.* **27** (18), 3762–9.

[272] Shimamoto, A., Nishikawa, K., Kitao, S. & Furuichi, Y. (2000). Human RecQ5beta, a large isomer of RecQ5 DNA helicase, localizes in the nucleoplasm and interacts with topoisomerases 3alpha and 3beta. *Nucleic Acids Res.* **28** (7), 1647–55.

[273] Ozsoy, A. Z., Sekelsky, J. J. & Matson, S. W. (2001). Biochemical characterization of the small isoform of Drosophila melanogaster RECQ5 helicase. *Nucleic Acids Res.* **29** (14), 2986–93.

[274] Ozsoy, A. Z., Ragonese, H. M. & Matson, S. W. (2003). Analysis of helicase activity and substrate specificity of Drosophila RECQ5. *Nucleic Acids Res.* **31** (5), 1554–64.

[275] Kawasaki, K., Maruyama, S., Nakayama, M., Matsumoto, K. & Shibata, T. (2002). Drosophila melanogaster RECQ5/QE DNA helicase: stimulation by GTP binding. *Nucleic Acids Res.* **30** (17), 3682–91.

[276] Nakayama, M., Kawasaki, K., Matsumoto, K. & Shibata, T. (2004). The possible roles of the DNA helicase and C-terminal domains in RECQ5/QE: complementation study in yeast. *DNA Repair (Amst),* **3** (4), 369–78.

[277] Wang, W., Seki, M., Narita, Y., Nakagawa, T., Yoshimura, A., Otsuki, M., Kawabe, Y., Tada, S., Yagi, H., Ishii, Y. & Enomoto, T. (2003). Functional relation among RecQ family helicases RecQL1, RecQL5, and BLM in cell growth and sister chromatid exchange formation. *Mol. Cell. Biol.* **23** (10), 3527–35.

Abbreviations

Abbreviation	Explanation
4NQO	4-nitroquinoline 1-oxide
ALT	Alternative lengthening of telomeres
ATP	Adenosine-triphosphate
BER	Base excision repair
BLM	Bloom syndrome protein
bp	Base pairs
BS	Bloom syndrome
eto	Etoposide
DHJ	Double Holliday junction
DSB	Double strand break
dsDNA	Double-stranded DNA
ES cells	Embryonic stem cells
FA	Fanconi anemia
FRET	Fluorescence resonance energy transfer
GTP	Guanosine-triphosphate
HJ	Hollday junction
HSV	Herpes simplex virus
HU	Hydroxyurea
HDAC	Histone deacteylase
HRDC	Helicase and Rnase D C-terminal domain
IgA	Immunoglobulin A
IgM	Immunoglobulin M
MMC	Mitomycin C
MMS	Methyl methanosulfonate
MMR	Mismatch repair
MRN	The MRE11/RAD50/NBS1 complex
MutSα	The MSH2/MSH6 heterodimer
MutSβ	The MSH2/MSH3 heterodimer
MutLα	The MLH1/PMS2 heterodimer
NLS	Nuclear localisation signal
nt	Nucleotides
NTP	Nucleoside-triphosphate

PCNA	Proliferating cell nuclear antigen
PML	Premyelocytic leukemia protein
RFC	Replication factor C
RPA	Replication protein A
RTS	Rothmund-Thomson syndrome
SCE	Sister-chromatid exchange
SF	Superfamily
ssDNA	Single-stranded DNA
SUMO	Small ubiquitin-like modifier
TSA	Trichostatin A
Ub	Ubiquitin
UV	Ultraviolet
WH	Winged helix
WHIP	Werner helicase interacting protein
WRN	Werner syndrome protein

3 Results

Article I

Characterization and Mutational Analysis of the RecQ
Core of the Bloom Syndrome Protein

Pavel Janscak, Patrick L. Garcia, Fabienne Hamburger, Yoko Makuta, Kouya Shiraishi, Yukiho Imai, Hideo Ikeda and Thomas A. Bickle *J Mol Biol.* 2003, **1**: 29-42

My contribution to this work was some help with protein purifications and the experiments for figure 3 c.

doi:10.1016/S0022-2836(03)00534-5 J. Mol. Biol. (2003) 330, 29–42

JMB

Available online at www.sciencedirect.com

SCIENCE DIRECT®

Characterization and Mutational Analysis of the RecQ Core of the Bloom Syndrome Protein

Pavel Janscak[1,2]*, Patrick L. Garcia[2], Fabienne Hamburger[1], Yoko Makuta[3], Kouya Shiraishi[3], Yukiho Imai[3], Hideo Ikeda[3] and Thomas A. Bickle[1]

[1]*Division of Molecular Microbiology, Biozentrum University of Basel Klingelbergstr. 50-70, CH-4056 Basel, Switzerland*

[2]*Institute of Molecular Cancer Research, University of Zurich August Forel-Strasse 7 CH-8008 Zurich, Switzerland*

[3]*Institute of Medical Science Medinet Inc., Tamagawadai 2-2-8, Setagaya-ku, Tokyo 158-0096, Japan*

**Corresponding author*

Bloom syndrome protein forms an oligomeric ring structure and belongs to a group of DNA helicases showing extensive homology to the *Escherichia coli* DNA helicase RecQ, a suppressor of illegitimate recombination. After over-production in *E. coli*, we have purified the RecQ core of BLM consisting of the DEAH, RecQ-Ct and HRDC domains (amino acid residues 642–1290). The $BLM^{642-1290}$ fragment could function as a DNA-stimulated ATPase and as a DNA helicase, displaying the same substrate specificity as the full-size protein. Gel-filtration experiments revealed that $BLM^{642-1290}$ exists as a monomer both in solution and in its single-stranded DNA-bound form, even in the presence of Mg^{2+} and ATPγS. Rates of ATP hydrolysis and DNA unwinding by $BLM^{642-1290}$ showed a hyperbolic dependence on ATP concentration, excluding a co-operative interaction between ATP-binding sites. Using a λ Spi^- assay, we have found that the $BLM^{642-1290}$ fragment is able to partially substitute for the RecQ helicase in suppressing illegitimate recombination in *E. coli*. A deletion of 182 C-terminal amino acid residues of $BLM^{642-1290}$, including the HRDC domain, resulted in helicase and single-stranded DNA-binding defects, whereas kinetic parameters for ATP hydrolysis of this mutant were close to the $BLM^{642-1290}$ values. This confirms the prediction that the HRDC domain serves as an auxiliary DNA-binding domain. Mutations at several conserved residues within the RecQ-Ct domain of BLM reduced ATPase and helicase activities severely as well as single-stranded DNA-binding of the enzyme. Together, these data define a minimal helicase domain of BLM and demonstrate its ability to act as a suppressor of illegitimate recombination.

Keywords: Bloom syndrome; DNA helicase; genomic instability; illegitimate recombination; mutagenesis

Introduction

Helicases are motor proteins that are characterized by the ability to unwind nucleic acid duplexes (DNA–DNA, DNA–RNA and RNA–RNA) in a reaction coupled to the hydrolysis of NTPs.[1–4] Helicases perform a variety of important tasks in nucleic acid metabolism, ranging from a simple strand separation at the replication fork to more sophisticated processes, such as migration of Holliday junctions.[5,6]

Mechanistically, there are two classes of helicases: those that translocate along a nucleic acid strand in a 3′ to 5′ direction; and those that operate with the opposite polarity. Based on amino acid sequence homology, helicases have been grouped into five superfamilies (SF1–SF5).[7] Most 3′-5′ DNA helicases are members of SF1 or SF2. These two superfamilies have similar sets of conserved motifs, and the proteins are generally considered to be monomeric. However, the oligomeric state of

Abbreviations used: ATPγS, adenosine 5′-*O*-(3-thiotriphosphate); BS, Bloom syndrome; CBD, chitin-binding domain; DSB, double-strand break; dsDNA, double-stranded DNA; EMSA, electrophoretic mobility-shift assay; HRDC, helicase and RNAseD C-terminal; P_i, inorganic phosphate; RecQ-Ct, RecQ C-terminal; SCE, sister chromatid exchanges; ssDNA, single-stranded DNA; WS, Werner syndrome.

E-mail address of the corresponding author: pjanscak@imr.unizh.ch

0022-2836/03/$ - see front matter

the functional form of these enzymes has been debated, with both monomeric and oligomeric models being proposed.[8–12] The 5′-3′ DNA helicases belong to SF4 and SF5. They are characterized by fewer conserved motifs and generally form hexameric rings.[13]

The RecQ helicase family belongs to SF2 and includes enzymes that have extensive homology to the 3′-5′ DNA helicase RecQ of *Escherichia coli*. This enzyme is involved in processing nascent DNA at blocked replication forks prior to the resumption of DNA synthesis and in suppressing illegitimate recombination.[14,15] Interestingly, prokaryotes and unicellular eukaryotes possess only a single RecQ helicase, while several RecQ homologues are present in multi-cellular organisms.[16] In humans, five RecQ homologues have been identified thus far. Mutations in three of them have been shown to be associated with autosomal recessive disorders characterized by genomic instability and cancer predisposition. Mutations in BLM result in Bloom syndrome (BS); mutations in WRN result in Werner syndrome (WS); and mutations in RecQL4 result in Rothmund–Thomson syndrome (RTS).[17–19] Genomic instability in BS is evidenced by chromosome breaks, gaps and, most typically, by high rate of sister chromatid exchanges (SCE).[20] Cells from WS and RTS individuals display an increased rate of gross chromosomal rearrangements.[20] Mutations in RecQ homologues in other eukaryotic organisms also are associated with increased rates of chromosomal abnormalities.[21,22]

Although cellular phenotypes of mutants suggest that RecQ DNA helicases act as suppressors of illegitimate recombination, exact DNA transactions mediated by these enzymes to maintain genomic stability remain elusive. Illegitimate recombination takes place between sequences of little or no homology exposed upon exonucleolytic processing of DNA double-strand breaks (DSBs) and it results in DNA rearrangement such as deletions, translocations, duplications or inversions.[23,24] The observations that several RecQ helicases could promote branch migration of Holliday junctions led to the proposal that these enzymes remove Holliday junctions formed at stalled replication forks and thus suppress induction of DSBs through the action of a resolvase.[6] WRN was shown to facilitate copying of tetraplex and hairpin structures of the d(CGG) trinucleotide repeat sequence by DNA polymerase δ, suggesting another mechanism that would minimize formation of DSBs at replication forks stalled by unusual DNA secondary structures.[25] Furthermore, there is evidence suggesting that RecQ DNA helicases promote non-mutagenic repair of DSBs, perhaps by inhibiting extensive exonucleolytic processing of DSBs or by dissociating intermediates of illegitimate recombination produced by single-strand annealing at sites of micro-homology.[24,26,27]

All RecQ family members contain a DEAH helicase domain characterized by a set of seven amino acid sequence motifs that are present in other SF2 helicases. Mutagenesis and structural studies of a number of SF1 and SF2 helicases demonstrated that these motifs are responsible for coupling of ATP hydrolysis to DNA binding, translocation and unwinding.[8,28–31] In addition, all RecQ helicases contain a C-terminal extension that can be divided into two domains.[32] The proximal domain, called the RecQ-Ct (RecQ C-terminal) domain, is unique to the family. The distal domain is present also in RNAseD and its eukaryotic homologues, and is called the HRDC (helicase and RNAseD C-terminal) domain. A recent NMR structure of the HRDC domain of Sgs1 (the single RecQ homologue in *Saccharomyces cerevisiae*) suggested that this domain might function as an auxiliary DNA-binding domain in a manner similar to that of its structural homologue, domain 1B in PcrA.[33] The role of the RecQ-Ct domain in the helicase function remains to be determined. The eukaryotic members of the RecQ family usually have additional N and C-terminal domains that flank the RecQ core, which show little or no sequence homology and vary considerably in size between different RecQ members.[34] These divergent domains are involved in interactions with other proteins and thus most probably serve to differentiate functionally between the multiple RecQ helicases present in higher eukaryotes.[34]

Size-exclusion chromatography and electron microscopic examination of BLM indicated that it forms predominantly a hexameric ring structure.[35] BLM oligomerization is mediated by the N-terminal part of the protein.[36] Similarly, a purified N-terminal exonuclease domain of the WRN protein was found to exist in a trimer/hexamer equilibrium, which was shifted towards the hexameric species upon addition of a DNA substrate.[37] This suggests that the full-size WRN protein may also form a hexamer. Moreover, steady-state kinetic analysis of the helicase activity of the *E. coli* RecQ helicase suggested that the enzyme may act as an oligomer, perhaps a trimer.[38]

Here, we report biochemical characteristics of a recombinant fragment of the Bloom syndrome protein encompassing the amino acid residues 642–1290, which includes the entire RecQ homology region of BLM. We have found that this fragment exists as a monomer both in solution and in a form bound to a 30mer oligonucleotide, even in the presence of adenosine 5′-*O*-(3-thiotriphosphate) (ATPγS) and Mg^{2+}, and can function as a DNA-stimulated ATPase as well as a DNA helicase, displaying the same substrate specificity as the full-size protein. This indicates that the oligomeric ring structure formed by BLM is not essential for the helicase activity of the enzyme. Using a λ Spi^- assay, we have found that expression of $BLM^{642-1290}$ in an *E. coli* strain carrying a *rec*Q mutation partially reduced the elevated illegitimate recombination observed in this strain, suggesting that the RecQ function to suppress illegitimate recombination has been conserved throughout evolution. Furthermore, we have investigated the roles of the

RecQ-Ct and HRDC domains of BLM in helicase activity of the enzyme by mutational analysis. Our data suggest that the RecQ-Ct domain may be involved in coupling of DNA binding to ATP hydrolysis, whereas the HRDC domain may serve as an auxiliary DNA-binding domain.

Results

Expression, purification and determination of the oligomeric state of BLM$^{642-1290}$

The region of the *BLM* cDNA encoding the RecQ portion of BLM (amino acid residues 642–1290, Figure 1(a)) was cloned in the pTXB3 vector to construct a translational fusion of this fragment with a C-terminal Mxe intein and chitin-binding domain, which serves as a self-cleaving affinity tag. Expression of this construct in the BL21-CodonPlus (DE3)-RIL strain yielded large amounts of the fusion protein in soluble form (Figure 1(b)). Usage of the RIL codon plus strain significantly increased the level of protein expression when compared to BL21(DE3) (data not shown). The BLM$^{642-1290}$ protein was purified to more than 95% homogeneity by combining affinity purification on a chitin column with subsequent chromatography on heparin and CM-Sepharose columns (see Materials and Methods). This procedure yielded typically 1–1.5 mg of pure protein per 1 g of cell paste.

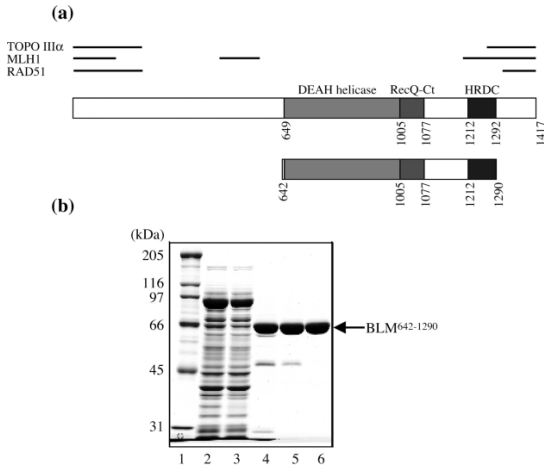

Figure 1. Structure and purification of BLM$^{642-1290}$. (a) A schematic of the Bloom syndrome protein demonstrating the location of the DEAH helicase, RecQ-Ct and HRDC domains. The locations of the protein–protein interaction regions for DNA topoisomerase IIIα (TOPO IIIα), MLH1 and RAD51 are indicated above this scheme by black lines. A schematic of the BLM$^{642-1290}$ fragment is shown below. (b) SDS-PAGE of fractions from purification of BLM$^{642-1290}$. The protein was expressed and purified as described in Materials and Methods. Samples were analyzed on a 10% polyacrylamide gel, which was stained with Coomassie brilliant blue. Lane 1, protein size markers; lane 2, total cell extract; lane 3, soluble part of cell extract; lane 4, pooled fractions from chitin column; lane 5, pooled fractions from heparin column; lane 5, pooled fractions from a CM-Sepharose column.

In order to characterize the oligomeric state of BLM$^{642-1290}$, we carried out size-exclusion chromatography using a Superdex 200 column. We determined apparent molecular masses of BLM$^{642-1290}$ in solution and in a form bound to a 30mer oligonucleotide both in the absence and presence of the poorly hydrolyzable analogue of ATP, ATPγS, and Mg^{2+} (Table 1). The BLM$^{642-1290}$ protein alone was found to elute in a single peak corresponding to a molecular mass of 66.8 kDa and in the presence of ATPγS/Mg^{2+} in a peak corresponding to 69.3 kDa. As the predicted molecular mass of BLM$^{642-1290}$ is 74.1 kDa, these data suggest that BLM$^{642-1290}$ exists as a monomer in solution. Addition of a 30mer oligonucleotide to BLM$^{642-1290}$ (at a BLM to DNA molar ratio of 6) in the absence and in the presence of ATPγS/Mg^{2+} resulted in peaks corresponding to molecular masses of 103.3 kDa and 104.6 kDa, respectively. Since the 30mer oligonucleotide alone eluted from the column at a molecular mass of 33 kDa, these data suggest that BLM$^{642-1290}$ exists as monomer in its single-stranded DNA (ssDNA)-bound form.

Biochemical characterization of the BLM$^{642-1290}$ fragment

The purified BLM$^{642-1290}$ fragment was first tested for its ability to hydrolyze ATP in the presence of various DNA effectors, including circular M13mp18 ssDNA, synthetic 43mer oligonucleotide and plasmid double-stranded DNA (dsDNA). ATPase activity was monitored by measuring the production of inorganic phosphate (P_i) using a malachite green assay (see Materials and Methods). As shown in Figure 2(a), BLM$^{642-1290}$ exhibited a strong DNA-dependent ATPase activity. The rate of ATP hydrolysis in the presence of ssDNA was higher than that in the presence of plasmid dsDNA. Only a weak ATPase activity was observed in the absence of a DNA effector.

The ATPase reaction catalyzed by BLM$^{642-1290}$ in the presence of circular M13mp18 ssDNA displayed classical Michaelis–Menten kinetics over a range of ATP concentrations from 10 μM to 2 mM (Figure 2(b)). The steady-state kinetic parameters

Table 1. Molecular masses of free and DNA-bound forms of BLM$^{642-1290}$ in the presence and in the absence of ATPγS/Mg^{2+} determined by gel-filtration

Sample	Apparent molecular mass (kDa)
30mer	33.0
BLM	66.8
BLM + 30mer	103.3
BLM + Mg^{2+} + ATPγS	69.3
BLM + Mg^{2+} + ATPγS + 30mer	104.6

The predicted molecular mass of BLM$^{642-1290}$ is 74.1 kDa.

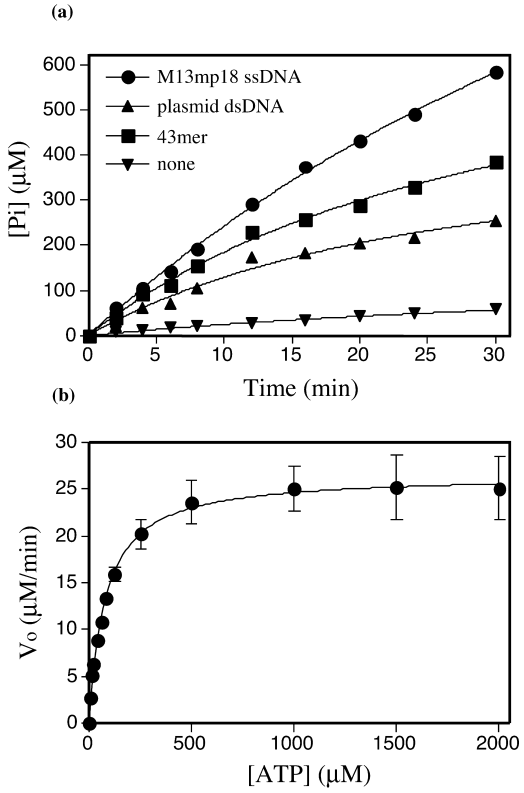

Figure 2. ATPase activity of $BLM^{642-1290}$. (a) Time-course of ATP hydrolysis by 20 nM $BLM^{642-1290}$ in the presence of various DNA co-factors including M13mp18 ssDNA (circle), pTZ18R plasmid dsDNA (upwards pointing triangle), 43mer synthetic oligonucleotide (square) and no DNA (downwards pointing triangle). In each reaction, DNA was present at a concentration of 25 μg/ml and ATP was 2 mM. (b) Dependence of the initial rate of ATP hydrolysis by 20 nM $BLM^{642-1290}$ in the presence of M13mp18 ssDNA (25 μg/ml) on ATP concentration. Reactions were carried out in buffer H at 37 °C and quantified as described in Materials and Methods. The lines in (a) correspond to a fit by an exponential equation:

$$Y = Y_{max}(1 - \exp(-kX)$$

where Y is the concentration of the reaction product, X is time and k is the rate constant. The line in (b) corresponds to a fit by Michaelis–Menten equation:

$$Y = Y_{max}X/(K_M + X)$$

where Y is the initial reaction rate, X is the concentration of substrate and K_M is the Michaelis–Menten constant. Each value represents the mean of at least three independent measurements.

of the ATPase reaction, k_{cat} and K_M, were 22.14 s^{-1} and 77.3 μM, respectively. The fact that the enzyme kinetic curve is hyperbolic rather than sigmoidal suggests that ATP hydrolysis by $BLM^{642-1290}$ is not a co-operative reaction.

The helicase activity of $BLM^{642-1290}$ was first tested on a partial DNA duplex substrate comprising a 44mer radiolabeled oligonucleotide annealed to circular M13mp18 ssDNA. This substrate was incubated with increasing amounts of $BLM^{642-1290}$ in the presence of ATP, which was followed by analysis of the reaction products on a non-denaturing 15% polyacrylamide gel. Figure 3(a) shows that $BLM^{642-1290}$ indeed possesses a DNA-unwinding activity, resulting in displacement of the radiolabeled oligonucleotide from M13mp18 ssDNA.

To estimate the affinity of $BLM^{642-1290}$ helicase for ATP, the initial rate of $BLM^{642-1290}$-mediated unwinding of 25 bp partial M13 duplex was measured over a range of concentrations of ATP from 5 μM to 2 mM. The data displayed a hyperbolic dependence on ATP concentration with a $K_{1/2}$ value of 31.8 μM (Figure 3(b)). The hyperbolic nature of the curve argues against a co-operativity in the helicase reaction of $BLM^{642-1290}$ with respect to ATP concentration.

To compare the substrate specificity of the $BLM^{642-1290}$ fragment to that of the full-size protein, we have examined the ability of these proteins to unwind various 5′ end-labeled synthetic DNA structures with a common duplex region sequence, including blunt-ended duplex, 3′ ssDNA-tailed duplex, forked duplex with two non-complementary single-stranded arms (splayed arm) and blunt-ended duplexes containing either a nick or a 5′-ssDNA flap (20 nt) in the central part of the DNA molecule. The last two DNA molecules have not been tested as substrates for BLM thus far. Like the full-size BLM protein, the $BLM^{642-1290}$ fragment could unwind both 3′-ssDNA-tail duplex and splayed arm, with the latter being unwound more efficiently than the former (Figure 3(c)). The blunt-ended duplex was not unwound by either protein. In contrast, both proteins could efficiently unwind the 5′ flap structure to extents similar to those of the splayed arm, releasing the labeled 5′ flap oligonucleotide (Figure 3(c)). The nicked duplex was a much poorer substrate for unwinding by both enzymes compared to the 5′ flap duplex (Figure 3(c)), indicating a role of the 5′-ssDNA flap in the initiation of duplex unwinding.

The BLM helicase was shown to disrupt synthetic immobile four-way DNA junctions, which resemble Holliday junctions.[39] To investigate whether the $BLM^{642-1290}$ fragment possesses such an activity, a four-way junction substrate prepared by annealing of 50mer oligonucleotides, of which one was 5′ end-labeled, was incubated with increasing amounts of $BLM^{642-1290}$. Figure 3(d) shows that $BLM^{642-1290}$ was able to disrupt four-way junctions to the component single strands, as is evident from the appearance of the free radiolabeled oligonucleotide. As observed with the full-size BLM protein, the unwinding of four-way junctions by $BLM^{642-1290}$ resulted in the accumulation of three-stranded and two-stranded species, suggesting that these species are reaction intermediates.[39] The presence of traces of these species in untreated DNA substrate is most probably due to spontaneous

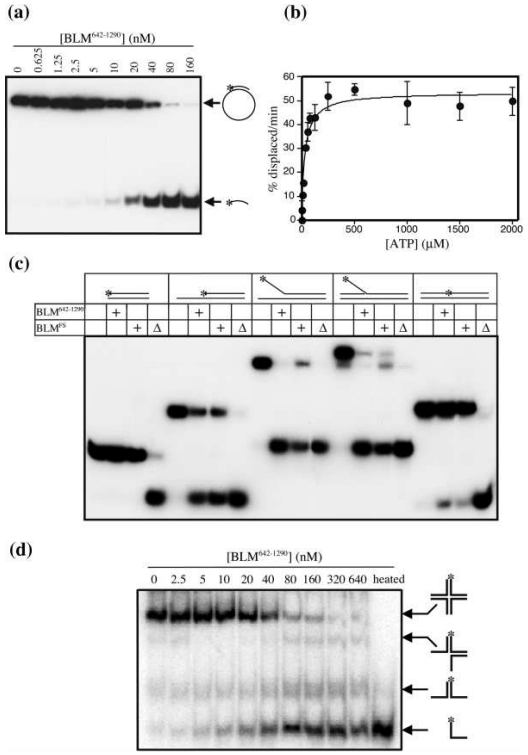

Figure 3. DNA helicase activity of $BLM^{642-1290}$. (a) Unwinding of 44 bp partial M13 duplexes by $BLM^{642-1290}$. Reaction mixtures (10 μl) in buffer H contained 0.5 nM DNA, 2 mM ATP and the indicated amounts of $BLM^{642-1290}$. The reactions were initiated with enzyme and incubated at 37 °C for 30 minutes prior to termination by adding 0.5 reaction volume of buffer S. Samples were analyzed by electrophoresis in non-denaturing 15% polyacrylamide gel followed by autoradiography. (b) Dependence of the initial rate of unwinding of 0.5 nM 25 bp partial M13 duplex by 20 nM $BLM^{642-1290}$ on the concentration of ATP. Reaction rates were measured in buffer H at 37 °C as described in Materials and Methods for concentrations of ATP ranging from 10 μM to 2000 μM. Each value represents the mean of at least three independent measurements. The line in the graph corresponds to a fit by the Michaelis–Menten equation (see the legend to Figure 2). (c) Comparison of the helicase activities of $BLM^{642-1290}$ and BLM^{FS} (full-size BLM) on blunt-ended duplex (lanes 1–4), 3′-ssDNA-tailed duplex (lanes 5–8), splayed arm (lanes 9–12), 5′-ssDNA-flap duplex (lanes 13–16) and nicked duplex (lanes 17–20). Reaction mixtures (10 μl) in buffer H contained 1 nM DNA substrate, 2 mM ATP and 20 nM enzyme. Reactions were carried out and analyzed as described for (a). The triangles mark the lanes that contain heat-denatured DNA. Note that the 5′-flap substrate contains a small fraction of splayed arm, which is due to incomplete annealing of the C_{19} oligonucleotide. (d) Unwinding of the synthetic four-way junction by $BLM^{642-1290}$. Reaction mixtures (10 μl) in buffer H contained 1 nM DNA substrate, 2 mM ATP and the indicated amounts of $BLM^{642-1290}$. Reactions were carried out and analyzed as described for (a). Positions of four-way junction substrate, three-stranded, two-stranded and single-stranded products are indicated to the right. DNA substrates were prepared as described in Materials and Methods. The asterisks (*) indicate the location of the radioactive label.

dissociation of the four-way structure following electroelution from polyacrylamide gel.

Together, these data show that the $BLM^{642-1290}$ fragment can function as an ATP-dependent DNA helicase with the same substrate specificity as the full-size protein. Moreover, the lack of co-operativity in both ATPase and helicase reactions (with respect to ATP concentration) in combination with the gel-filtration data argues that the $BLM^{642-1290}$ helicase may function as a monomer.

The $BLM^{642-1290}$ helicase can suppress elevated illegitimate recombination in *E. coli recQ* mutant

In order to obtain further functional characteristics of $BLM^{642-1290}$, we asked whether it is able to substitute *in vivo* for the *E. coli* RecQ helicase in suppressing illegitimate recombination. Using the λ Spi^- assay, it has been demonstrated that *E. coli recQ* mutations enhance frequency of spontaneous and UV-induced illegitimate recombination, indicating that RecQ plays a suppressive role in illegitimate recombination.[15] In the λ Spi^- assay, the frequency of formation of specialized λ*bio* transducing phages, which result from abnormal excision of the chromosome by illegitimate recombination, is measured.[40] Most of the λ*bio* transducing phages lack the *red-gam* region of λ phage and show the Spi^- phenotype, which is the ability to form plaques on a lawn of *E. coli* P2 lysogen. On the other hand, normal λ phages cannot grow in P2 lysogen. Therefore, the frequency of illegitimate recombination can be calculated as a ratio of the number of Spi^- phages to the number of total phages in a given lysate. To examine whether the $BLM^{642-1290}$ helicase can suppress the hyper-recombination phenotype of RecQ-deficient cells, the corresponding region of the *BLM* cDNA was cloned into pBluescript SK(+) under control of the *lac* promoter. The resulting plasmid construct was introduced into the HI2776 Δ*recQ101* λ*cI857* lysogen and the frequencies of the λ Spi^- phage formation in this strain prior to and after UV irradiation were compared with those displayed by the Δ*recQ101* mutant transformed with the pBluescript SK(+) vector. We found that $BLM^{642-1290}$ significantly reduced the rate of illegitimate recombination in the Δ*recQ101* mutant under both the non-irradiated (tenfold) and the irradiated (4.1-fold) conditions, although it did not restore the wild-type levels completely (Table 2). Interestingly, the wild-type strain (HI1162 λ*cI857* lysogen) harboring the *BLM* plasmid showed a higher frequency of λ Spi^- phage formation than the wild-type strain harboring the pBluescript SK(+) vector (Table 2), suggesting that the BLM fragment may also have a negative effect on the DNA metabolism in *E. coli*.

Table 2. Effect of $BLM^{642-1290}$ on spontaneous and UV-induced illegitimate recombination in the wild-type and *recQ* mutation background

Strain	UV dose (J/m^2)	λ Spi^- phages (10^{-9}) per total λ phage (SE)	Relative frequency λ Spi^- to control	Burst size
Wild-type[a] [pBluescript SK(+)]	0	1.0 (0.33)	1	114
Wild-type[a] [pJP79 (*BLM*$^+$)]	0	12 (1.0)	12	91
Δ*recQ101*[b] [pBluescript SK(+)]	0	130 (16)	1	52
Δ*recQ101*[b] [pJP79 (*BLM*$^+$)]	0	13 (1.5)	0.1	91
Wild-type[a] [pBluescript SK(+)]	25	80 (4.7)	1	95
Wild-type[a] [pJP79 (*BLM*$^+$)]	25	120 (26)	1.5	85
Δ*recQ101*[b] [pBluescript SK(+)]	25	1200 (100)	1	53
Δ*recQ101*[b] [pJP79 (*BLM*$^+$)]	25	290 (21)	0.24	98

The frequency of Spi^- phages per total phages was measured as described in Materials and Methods. Values are the average of four independent measurements. (SE) indicates the standard error of the mean. Burst size is the number of total phages per cell.
[a] HI1162 λ*cI857* lysogen.
[b] HI2776 Δ*recQ101* :: *cat* λ*cI857* lysogen.

Together, these results indicate that the BLM fragment can indeed function as a suppressor of spontaneous and UV-induced illegitimate recombination in *E. coli*, although the compensation of the *rec*Q mutation was partial.

C-terminal deletion mutagenesis of $BLM^{642-1290}$

As mentioned above, the homology region of RecQ family members consists of the DEAH helicase, RecQ-Ct and HRDC domains. The DEAH helicase domain contains a set of seven amino acid sequence motifs that have been studied extensively in other SF1 and SF2 DNA helicases, and shown to mediate coupling of ATP hydrolysis to DNA translocation and unwinding.[8,28–31] The roles of the RecQ-Ct and HRDC domains, which are present only in the RecQ family of DNA helicases, remain to be investigated. To address the importance of the RecQ-Ct and HRDC domains of BLM for the helicase activity of the enzyme, we have generated a series of C-terminal truncations of $BLM^{642-1290}$, including $BLM^{642-1167}$, $BLM^{642-1108}$, $BLM^{642-1056}$, $BLM^{642-1036}$ and $BLM^{642-997}$, by cloning corresponding regions of the BLM cDNA into pTXB3 to construct translational fusions with a C-terminal Mxe intein and a chitin-binding domain. However, only one of those constructs, lacking the HRDC domain and a part of the linker connecting the HRDC and RecQ-Ct domains ($BLM^{642-1108}$) was found to produce stable soluble protein when expressed in the *E. coli* BL21 (RIL) strain. The shorter deletion variants lacking a part of or the entire RecQ-Ct domain were found to be insoluble when expressed as fusions with Mxe–CBD. The $BLM^{642-1167}$ mutant ending at the beginning of the HRDC domain could not be expressed in *E. coli* BL21 (RIL), perhaps due to its sensitivity to degradation.

The $BLM^{642-1108}$ variant was subjected to the same purification procedure as $BLM^{642-1290}$. However, it was not bound to the heparin column. Measuring steady-state parameters for ATP hydrolysis in the presence of a 43mer oligonucleotide revealed that the $BLM^{642-1108}$ mutant displayed nearly the same ssDNA-dependent ATPase activity as $BLM^{642-1290}$ (Table 3). In contrast, it showed about threefold decrease in helicase activity on 25 bp partial M13 duplex substrate with respect to $BLM^{642-1290}$ and even more pronounced defect in the ability to disrupt four-way junctions (Figure 4(a) and (b)). An electrophoretic mobility-shift assay (EMSA) employing 5′ end-labeled 30mer oligonucleotide (also used for the S200 gel-filtration experiments) revealed that the $BLM^{642-1108}$ mutant had reduced ssDNA binding activity dramatically as compared to $BLM^{642-1290}$ (Figure 7).

Thus, the data from biochemical characterization of $BLM^{642-1108}$ support the prediction that the HRDC domain serves as an auxiliary DNA-binding domain.[33]

Site-directed mutagenesis of the RecQ-Ct domain

Because of the insolubility of BLM fragments lacking the RecQ-Ct domain, we examined the importance of this region using a site-directed approach. We altered several residues in this

Table 3. Steady-state kinetic parameters for ssDNA-dependent ATP hydrolysis by BLM mutants

Protein	k_{cat} (s^{-1})	k_{cat} decrease factor	K_m (μm)	K_m(wt)/K_m(mut)
Wild-type	25.79	1.00	63.5	1.00
R1038A	1.36	18.96	66.6	1.00
F1045A	4.76	5.42	62.8	0.99
E1047Q	18.62	1.39	59.0	0.93
E1047A	14.72	1.75	148.1	2.33
D1064N	23.48	1.10	74.0	1.17
D1064A	0.12	214.92	58.5	0.92
R1108A	25.97	0.99	51.2	0.81
K1125A	27.01	0.95	54.3	0.86
$BLM^{642-1108}$	19.63	1.31	51.9	0.82

$BLM^{642-1290}$ is referred to as wild-type in this table. The point mutants are derivatives of $BLM^{642-1290}$. ATPase reactions were carried out in the presence of 43mer oligonucleotide as described under Materials and Methods.

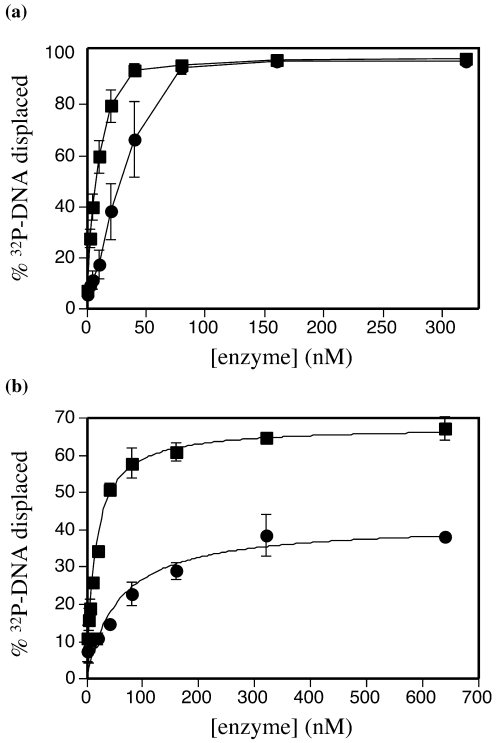

Figure 4. DNA helicase activity of the $BLM^{642-1108}$ mutant. Unwinding of (a) 0.5 nM 25 bp partial M13 duplex and (b) 1 nM synthetic four-way junction by $BLM^{642-1290}$ (square) and $BLM^{642-1108}$ (circle) as a function of protein concentration. DNA substrates were prepared as described in Materials and Methods. Reactions (10 μl) were carried out in buffer H containing 2 mM ATP. After 30 minutes incubation at 37 °C, reaction products were quantified as described in Materials and Methods. The lines in the graphs are drawn just to guide the eye. Individual datum points represent the mean of at least three independent measurements.

domain that are conserved among RecQ family members (Figure 5(a)) and characterized the biochemical properties of the resulting mutant proteins. The following amino acid residues were chosen for mutagenesis of the $BLM^{642-1290}$ fragment: C1036, R1038, F1045, E1047, C1063, D1064 and C1066 (Figure 5(a)). We have created alanine mutants at all those residues. The acidic residues E1047 and D1064 were replaced also by a glutamine and an asparagine, respectively. The mutants were prepared in the same way as the wild-type enzyme. Under these conditions, all the three cysteine mutants exhibited a high level of susceptibility to degradation, being degraded almost completely following purification on the chitin column and were, therefore, not further analyzed.

Substitutions at all residues were found to impair the ssDNA-dependent ATPase activity of $BLM^{642-1290}$ (Table 3). Interestingly, at position 1064, the value of k_{cat} was found to be related to the nature of the present residue. While the neutral D1064A mutant displayed a very poor k_{cat} value, the polar D1064N mutant had a k_{cat} value similar to that of the wild-type enzyme. (The same dependence was observed for helicase and ssDNA binding activities; see below.) All of the mutants had a K_M for ATP similar to that of the wild-type enzyme, with the exception of the E1047A mutant, which exhibited about twofold higher value of K_M than the wild-type enzyme (Table 3). The helicase activity of the mutants was measured using partial M13 duplex (25 bp) and four-way junction substrates. With the exception of the D1064N mutant, all mutants had reduced strand displacement activity on both substrates, with R1038A and D1064A mutants being affected most dramatically (Figure 6(a) and (b)). The ability of the BLM mutants to bind ssDNA was again investigated by EMSA using a 5′ end-labeled 30mer oligonucleotide. Figure 7 shows that all mutants displayed a reduction in their affinity for ssDNA compared to $BLM^{642-1290}$ from about twofold decrease (in apparent K_d) for the D1064N mutant to more than 20-fold decrease for the D1064A mutant.

Together, these data indicate that the RecQ-Ct domain of BLM plays an important role in the helicase function of the enzyme.

Site-directed mutagenesis of the region connecting the RecQ-Ct and HRDC domains of BLM

Multiple sequence alignment of RecQ family members also reveals a number of conserved residues in the region connecting the RecQ-Ct and HRDC domains (Figure 5(b)). To investigate the importance of this region for helicase activity of BLM, we have produced single alanine mutants of $BLM^{642-1290}$ at R1108 and K1125, two highly conserved residues in this region. Biochemical characterization of these mutants indicated that they do not show significant differences from the wild-type enzyme in ATPase or helicase activities (Table 3 and Figure 6(b)), or in the ability to bind ssDNA (not shown). These data suggest that the defects observed in the $BLM^{642-1108}$ mutant, which lacks a large part of this region, are rather due to the absence of the HRDC domain.

Discussion

In this work, we have characterized a recombinant fragment of the Bloom syndrome protein including the entire RecQ homology region and investigated the role of its RecQ-Ct and HRDC domains in the helicase activity of the enzyme.

Analysis of $BLM^{642-1290}$ using size-exclusion chromatography revealed that it exists as a monomer both in solution and in its ssDNA-bound form (in the presence and in the absence of ATPγS/Mg^{2+}) (Table 1). In contrast, the full-size

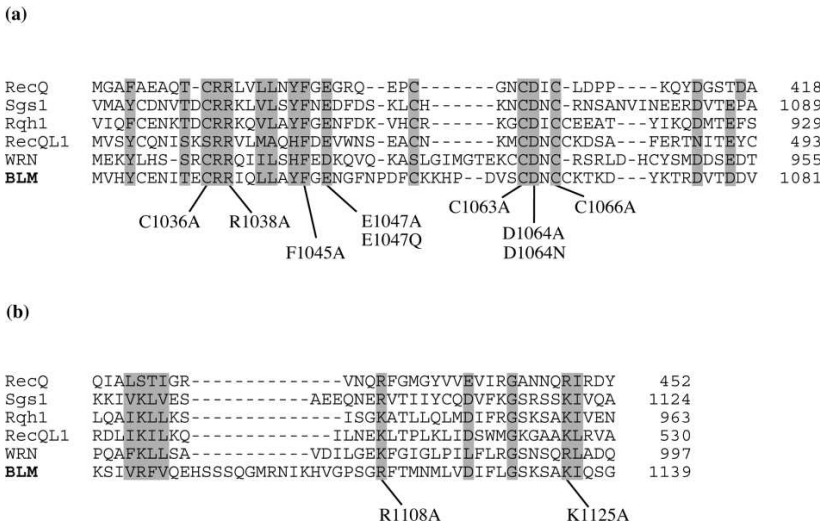

Figure 5. Amino acid sequence alignment of several RecQ helicases. The regions corresponding to (a) the RecQ-Ct domain and (b) the proximal part of the domain connecting the RecQ-Ct and HRDC domains are shown. The multiple alignment was performed with the program ClustalX and refined manually. The numbers at the end of each sequence correspond to the position of the last amino acid residue. Highly conserved amino acid residues are shadowed in grey. Amino acid substitutions generated in $BLM^{642-1290}$ are shown. The protein accession numbers used by the National Center for Biotechnology Information are: Sgs1, P35187; Rqh1, Q09811; RecQL1, NP_002898; WRN, NP_000544; BLM, A57570.

BLM protein forms an oligomeric ring structure in solution.[35] The oligomerization of BLM is mediated by the N-terminal region of the protein[36], which is absent in the $BLM^{642-1290}$ fragment. Since $BLM^{642-1290}$ retained all the enzymatic activities found in the full-size protein, including the ability to function as a structure-specific DNA helicase, it seems that the ring structure of BLM is probably required for other functions: perhaps it is involved in the formation of specific multiprotein–DNA repair complexes.

The rates of both ATP hydrolysis and DNA unwinding by $BLM^{642-1290}$ showed a hyperbolic dependence on ATP concentration (Figures 2(b) and 3(b)), which argues against a co-operative interaction between ATP-binding sites during unwinding and suggests that the enzyme may act as a monomer. This assumption may be supported by a hyperbolic nature of the dependence of DNA unwinding by $BLM^{642-1290}$ on enzyme concentration (Figure 4(a) and (b)). As mentioned above, however, the issue of the functional form of non-hexameric helicases has been debated over the last years. Studies of the PcrA (SF1) and RecG (SF2) helicases have led to suggestions that these enzymes as well as other SF1 and SF2 members function as monomeric helicases.[8,41] In contrast, pre-steady-state kinetic studies of DNA unwinding by the UvrD and Rep helicases, SF1 members, of which the latter has been shown to be a structural homologue of PcrA,[42] demonstrated that enzyme oligomers are required to initiate unwinding.[10,11] Recent single-molecule studies employing fluorescence resonance energy transfer technique to measure unwinding indicated that a Rep monomer can use ATP hydrolysis to move towards the junction between ssDNA and dsDNA (in agreement with the PcrA model), but then displays conformational fluctuations that do not lead to DNA unwinding.[12] DNA unwinding initiates only when the translocating enzyme interacts with additional enzyme molecule(s).[12] Similar studies will be required for RecQ DNA helicases to gain deeper insight into the mechanism of unwinding by these enzymes.

RecQ helicases mechanistically belong to the 3′-5′ class of helicases that generally require the presence of a 3′ single-stranded tail to initiate unwinding of a DNA duplex. However, our experiments revealed that BLM can unwind efficiently forked duplexes having 3′ arm double-stranded and 5′ arm single-stranded (5′-ssDNA-flap duplex), indicating that the enzyme does not essentially require the 3′ tail to be single-stranded to initiate DNA unwinding on a forked duplex (Figure 3(c)). Recently, the WRN helicase also has been shown to posses such an activity.[43] Moreover, both BLM and WRN helicases can unwind synthetic four-way junctions with blunt-ended arms and are able to promote the movement of a branched point along a long stretch of dsDNA.[6,39,44] Thus, it appears that the mode of DNA translocation and unwinding by RecQ helicases is different from that of the 3′-5′ helicases such as PcrA which translocate along ssDNA to mediate duplex unwinding.[8] On the basis of similarity in substrate specificity, one can predict that RecQ helicases may be mechanistically related to the RecG

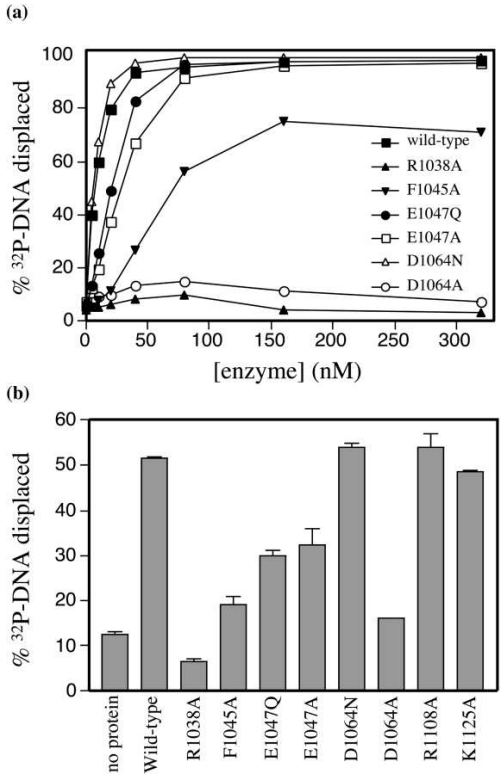

Figure 6. DNA helicase activity of BLM$^{642-1290}$ point mutants. (a) Unwinding of 0.5 nM 25 bp partial M13 duplex by wild-type and mutant BLM$^{642-1290}$ proteins as a function of protein concentration. (b) Unwinding of 1 nM synthetic four-way junction by wild-type and mutant BLM$^{642-1290}$ proteins each at a concentration of 40 nM. DNA substrates were prepared as described in Materials and Methods. Reactions (10 μl) were carried out in buffer H containing 2 mM ATP. After 30 minutes incubation at 37 °C, reaction products were quantified as described in Materials and Methods. The data shown represent the mean of at least three independent measurements.

helicase, which is believed to mediate strand separation *via* translocation on dsDNA.[45]

A deletion of 182 C-terminal amino acid residues from the BLM$^{642-1290}$ fragment including the HRDC domain and a part of the region connecting this domain with the RecQ-Ct domain substantially reduced the helicase activity of the enzyme on both partial duplex and four-way junction substrates (Figure 4(a) and (b)). Detailed analysis of the BLM$^{642-1108}$ mutant revealed that it had a severe defect in the ability to bind ssDNA (Figure 7), whereas its kinetic parameters for ATP hydrolysis at saturating concentrations of ssDNA were close to the BLM$^{642-1290}$ values (Table 3). Thus, it appears that the deleted region significantly contributes to ssDNA binding but plays no direct role in ATP hydrolysis by the enzyme. The characteristics of the BLM$^{642-1108}$ mutant are consistent with the prediction that the HRDC domain serves as an auxiliary DNA-binding domain, which was made on the basis of similarity of the three-dimensional structure of the Sgs1 HRDC domain to an ssDNA-binding domain of the human DNA polymerase β or the domain 1B of PcrA.[33] However, the BLM$^{642-1108}$ fragment also lacks a large part of the region connecting the RecQ-Ct and HRDC domain that contains a number of amino acid residues conserved among RecQ family members, raising the possibility that the absence of this region rather than the absence of the HRDC domain is responsible for the observed defects. Nevertheless, we have found that single alanine substitutions at two highly conserved basic residues, R1108 and K1125 of BLM located in this region, had no effect on the activity of BLM$^{642-1290}$, supporting the assumption that the defects of the BLM$^{642-1108}$ mutant are due to the absence of the HRDC domain. A recombinant fragment of the Sgs1 helicase ending at the beginning of the HRDC domain failed to bind to a synthetic oligonucleotide, although it was able to function as an ATP-dependent DNA helicase.[46] Moreover, the small isoform of the *Drosophila melanogaster* RecQ5 helicase containing only the DEAH and RecQ-Ct domains showed significantly reduced DNA helicase activity compared to the large RecQ5 isoform, which contains the entire RecQ homology region, whereas the ATPase characteristics of these proteins were quite similar.[47,48] Thus, all these findings suggest that the HRDC domain of RecQ helicases is involved in modulating the helicase activity of the enzyme through ssDNA binding, but is not absolutely required for the activity.

Biochemical characterization of BLM$^{642-1290}$ mutants at several conserved amino acid residues in the RecQ-Ct domain demonstrated that this domain is essential for the helicase activity of the enzyme (Figure 6). In particular, the R1038A, F1045A and D1064A mutants exhibited severe helicases defects. All alanine mutants displayed reduction in both ATP hydrolysis and ssDNA binding of magnitudes similar to those of the reduction in their helicase activity (compare Figure 6, Figure 7 and Table 3). Since DNA-dependent ATPase activity is a prerequisite of the DNA-unwinding function of the enzyme, ATPase defects of these mutants seem to be the cause of their helicase defects. It is less likely that the R1038, F1045 and D1064 residues are involved in DNA binding directly, because in such a scenario mutants would not exhibit significant ATPase defects under conditions of a saturating concentration of DNA. Instead, it is possible that the mutations at R1038, F1045 and D1064 induced local conformational changes in the protein that impaired coupling between DNA binding and ATPase activities of the enzyme or that these residues are involved directly in coupling of these activities.

Modeling of BLM structure using the crystal structure of the PcrA helicase as a template revealed that the DEAH domain of BLM consists

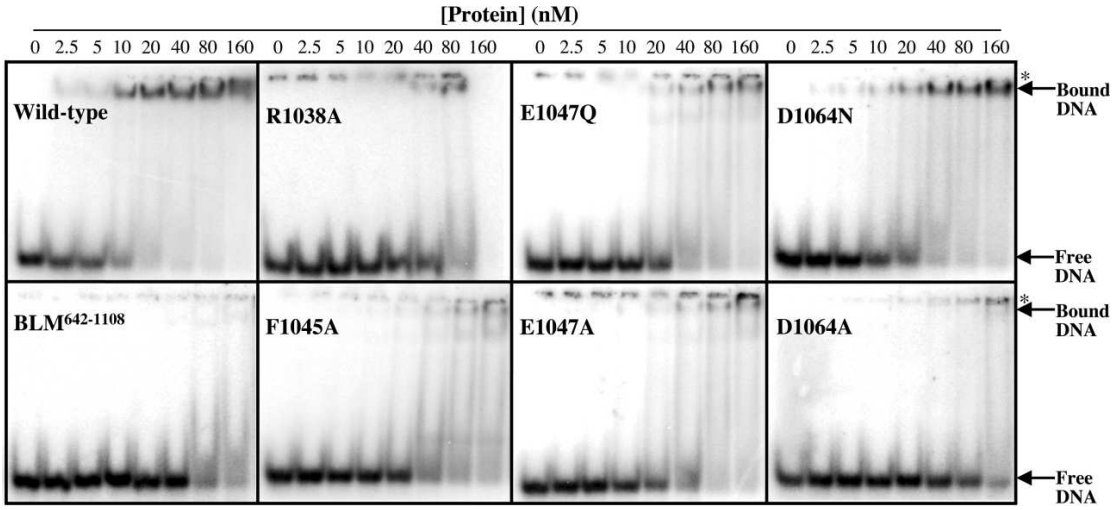

Figure 7. Electrophoretic mobility-shift assays of wild-type and mutant forms of $BLM^{642-1290}$. Proteins at the concentrations indicated were incubated with 0.5 nM 5′ end-labeled, single-stranded 30mer in buffer B at room temperature for 20 minutes. Bound and free DNA were separated by electrophoresis through a non-denaturing 15% polyacrylamide gel and visualized using a PhosphorImager. Positions of free DNA and DNA–protein complexes are indicated on the right by arrowheads. Asterisks (*) indicate the positions of the wells.

of two RecA-like subdomains that are found in all SF1 and SF2 helicases for which structural information is available.[49] The cleft between these domains forms the ATP-binding site, with residues from seven helicase signature motifs mediating protein–nucleotide interactions.[8,41,42] The structures showed also that DNA is bound along a groove on the top of the RecA-like domains and that the cleft closes and opens in response to ATP binding and hydrolysis, which suggested a mechanism for how protein translocates along DNA.[8] It has been postulated that the RecA domains of SF1 and SF2 helicases represent the motor capable of translocating along DNA, and that the additional, diverse domains are determinants of the specificity of the enzyme.[4] Thus, the domains 1B and 2B of PcrA are thought to be involved in destabilization of DNA duplex ahead of the motor translocating along ssDNA.[8] The N-terminal domain of RecG, forming a large fold that is divided into three subdomains linked to the C-terminal RecA-like motor by a long helix, was shown to bind to a three-way DNA junction in a manner that would allow duplex separation.[41] Thus, it is tempting to speculate that the region C-terminal to the DEAH domain of RecQ helicases including the RecQ-Ct and the HRDC domains have such a "specificity" function. Structural studies of a RecQ family member combined with biochemical analysis of mutants will certainly clarify this issue. The recombinant fragment of BLM described here seems to be a good candidate for these studies, since it can be prepared in large amounts at a high level of purity.

The fact that the $BLM^{642-1290}$ fragment could reduce the frequency of the λ Spi^- phage formation in a *recQ* mutant (Table 2) suggests that the RecQ function to suppress illegitimate recombination has been conserved throughout the evolution from bacteria to humans. In *E. coli*, RecQ plays a role in suppression of RecET-mediated illegitimate recombination.[15,24] It has been proposed that the RecQ helicase may unwind intermediates of the DNA end-joining reaction that involves annealing of 3′ single-stranded tails, generated by the RecE-mediated exonucleolytic processing of a DSB, at sites of microhomology.[24] BLM has been shown to unwind forked DNA duplexes efficiently,[39] suggesting that it may indeed act on intermediates of illegitimate recombination to promote non-mutagenic repair of DSBs. However, experiments using mutants in the chicken cell line DT40 suggested that these DNA transactions are mediated rather by the WRN helicase, whereas BLM is probably involved in restarting DNA replication at stalled replication forks, which prevents generation of DSBs.[22] However, recent evidence from plasmid rejoining assays using BLM proficient and deficient cell extracts demonstrated that BLM can suppress mutagenic repair of DSBs by illegitimate recombination,[26] suggesting an overlap between cellular functions of BLM and WRN. Our data support this assumption.

In contrast to the suppressive effect of the BLM fragment in a recQ mutant, its over-expression in the wild-type strain rather enhanced illegitimate recombination. A similar effect has been observed following over-expression of the DnaB helicase in *E. coli*.[50] A model has been proposed for initiation of illegitimate recombination in which over-production of DnaB helicase results in excessive DNA unwinding at replication forks and induction of DSBs.[50] A similar scenario might happen in the case of high levels of BLM, as it efficiently unwinds forked DNA duplexes.[39]

Materials and Methods

DNA manipulations

All restriction and other DNA-modifying enzymes were purchased from New England Biolabs (NEB). The pJP71 expression vector was constructed by a PCR amplification of the region of *BLM* cDNA comprising the codons 642–1290 with primers introducing *Nco*I and *Sap*I sites, respectively, and inserting the PCR product after digestion with *Nco*I and *Sap*I between the *Nco*I and *Sap*I sites in pTXB3 (NEB). This resulted in a translational fusion of $BLM^{642-1290}$ with a self-cleaving affinity tag composed of the Mxe intein and a chitin-binding domain (CBD) present in pTXB3. An additional methionine residue was introduced between the BLM fragment and the intein according to the manufacturer's instructions. The plasmids pJP71S1167, pJP71S1108, pJP71S1056, pJP71S1036, pJP71S997 producing the C-terminal truncated variants of $BLM^{642-1290}$: $BLM^{642-1167}$, $BLM^{642-1108}$, $BLM^{642-1056}$, $BLM^{642-1036}$ and $BLM^{642-997}$, respectively, as Mxe–CBD fusions were constructed in the same way as pJP71. All constructs were verified by sequencing to eliminate any possible mutations introduced by PCR. An origin repair method was employed for site-directed mutagenesis of BLM.[51,52] Mutagenesis was performed using the plasmid pJP74, a derivative of pGLamB[52] in which the *Xba*I–*Bam*HI fragment containing the *lam*B gene was replaced by the *Xba*I–*Bam*HI fragment of pJP71 encoding for the $BLM^{642-1290}$–intein–CBD fusion. For production of mutants, the resulting point mutations were transferred to pJP71 by replacing the *Xba*I–*Bam*HI region in this plasmid with the corresponding *Xba*I–*Bam*HI fragments from the mutant derivatives of pJP74. The plasmid pJP79 was constructed by introducing the *Xba*I–*Bsa*BI fragment of pJP71 encoding for $BLM^{642-1290}$ into pBluescript SK(+) digested with *Xba*I and *Bam*HI. The *Bam*HI end of the pBluescript SK(+) vector was filled in using Klenow fragment in this construction. In pJP79, $BLM^{642-1290}$ is under control of the *lac* promoter and, as in pJP71, contains an additional methionine codon at the C terminus, which is followed by a TGA stop codon.

λ Spi^- assay

HI2776 Δ*recQ101* :: *cat* λ *cI857* lysogen was constructed by transduction of HI1162 λ *cI857* lysogen[53] with P1 phage prepared from N1126 Δ*recQ101* :: *cat* (kindly provided by Dr J. Kato). The HI1162 and HI2776 strains were transformed with either pBluescript SK(+) or pJP79. The frequency of the λ Spi^- phages in these strains was measured as described.[40] Briefly, cells were grown to 2×10^8 cells/ml at 30 °C in λYP broth containing 20 μg/ml of ampicillin. If necessary, 2 ml of the culture was irradiated with a UV lamp (15 W) at a wavelength of 254 nm. Immediately after UV irradiation, the thermal induction of λ phage was carried out by incubation at 42 °C for 15 minutes with aeration. The culture was then incubated at 37 °C for two hours and the phage lysate was prepared. The titer of Spi^- phage was measured by plating on *E. coli* WL95 P2 lysogen. The titer of total phage was measured by plating on *E. coli Yme*I. The frequency of Spi^- phage was obtained by dividing the titer of Spi^- phage by the titer of total phage. Burst size was determined by dividing the number of total λ phages in a lysate by the number of total cells in the culture before heat induction.

Protein purifications

$BLM^{642-1290}$ was produced as a fusion with a Mxe–CBD self-cleaving affinity tag in the *E. coli* BL21-CodonPlus-(DE3)-RIL strain (Stratagene) containing the plasmid pJP71. Cells were grown at 37 °C in 1 l of LB medium supplemented with ampicillin and chloramphenicol at concentrations of 150 μg/ml and 25 μg/ml, respectively. At an A_{600} of 0.3, the cultivation temperature was reduced to 18 °C and protein synthesis was induced by adding isopropyl-β,D-thiogalactopyranoside (IPTG) to a final concentration of 0.2 mM and subsequent incubation for 16 hours. All protein purification steps were carried out at 4 °C. Cells were harvested by centrifugation, suspended in 50 ml of buffer CH (50 mM Tris–HCl (pH 8), 500 mM NaCl, 1 mM EDTA, 10% (v/v) glycerol, 0.1% (v/v) Triton X-100) and disrupted by sonication. The cell extract was clarified by centrifugation in an SS-34 rotor (Sorvall) at 18,000 rpm for 30 minutes. The supernatant was loaded onto a 15 ml chitin column (NEB) at a flow-rate of 12 ml/hour. The column was washed with 20 column volumes of buffer CH. Cleavage of $BLM^{642-1290}$ from the Mxe intein was induced by flushing the column with three column volumes of buffer CH supplemented with 50 mM DTT, with a subsequent incubation overnight at 4 °C. The protein was eluted with buffer CH. Fractions containing $BLM^{642-1290}$ (as judged from SDS-PAGE) were pooled, diluted 2.5 times with 50 mM Tris–HCl (pH 7.5) and loaded onto a 5 ml HiTrap heparin cartridge (Amersham Pharmacia Biotech) equilibrated with buffer HP (50 mM Tris–HCl (pH 7.5), 0.1 mM EDTA, 1 mM DTT, 10% (v/v) glycerol, 200 mM NaCl). The protein was eluted with a linear concentration gradient of NaCl (0.2 M–0.6 M; 50 ml) in buffer HP. Fractions containing $BLM^{642-1290}$ were pooled, diluted three times with 20 mM Tris–HCl (pH 8) and loaded onto a 50 ml CM-Sepharose FF column (Amersham Pharmacia Biotech) equilibrated with buffer CM (20 mM Tris–HCl (pH 8.0), 0.1 mM EDTA, 1 mM DTT, 10% (v/v) glycerol, 150 mM NaCl). The protein was eluted with a linear concentration gradient of NaCl (0.15 M–0.35 M; 500 ml) in buffer CM. Fractions containing $BLM^{642-1290}$ with >95% homogeneity were pooled and concentrated by dialysis against storage buffer (50 mM Tris–HCl (pH 7.5), 200 mM NaCl, 50% (v/v) glycerol, 1 mM DTT). Other BLM variants were produced and purified according to the same protocol. The $BLM^{642-1108}$ protein as well as the R1038A and D1064A mutants of $BLM^{642-1290}$ did not bind to the heparin column under these conditions. However, sufficient purification of these proteins to more than 90% homogeneity could be achieved by combining chromatographies on the chitin and CM-Sepharose FF columns. Protein concentration was determined from absorption at 280 nm using molar extinction coefficients derived from amino acid composition. The full-size BLM protein was kindly provided by Professor Ian D. Hickson from the University of Oxford.

Size-exclusion chromatography

Size-exclusion chromatography of $BLM^{642-1290}$ was performed at room temperature on a Superdex 200 PC3.2/30 column using a SMART system (Amersham Pharmacia Biotech). The column was equilibrated with buffer GF (20 mM Tris–HCl (pH 7.5), 150 mM NaCl, 0.1 mM EDTA, 1 mM DTT). Samples were prepared by dilution of the protein tenfold in GF buffer to a final

concentration of 3 μM. Where required, samples were supplemented with 0.5 μM single-stranded 30mer oligonucleotide: 5′-CCGTCGACTGACCGATATCCTCG GTACCCC-3′, 1 mM ATPγS and 5 mM $MgCl_2$. Samples were incubated at room temperature for 15 minutes prior to injection of 50 μl aliquots onto the column. The column was run at a flow-rate of 40 μl/minute and absorbance was monitored at 215 nm, 260 nm and 280 nm. The following size markers were used for calibration of the column: thyroglobulin (669 kDa), ferritin (440 kDa), catalase (232 kDa), aldolase (158 kDa), bovine serum albumin (67 kDa), ovalbumin (43 kDa) and chymotrypsinogen (25 kDa).

DNA helicase assays

DNA helicase activity of BLM and its mutants was measured using either partial DNA duplexes prepared by annealing oligonucleotides to circular M13mp18 ssDNA or using various synthetic duplex substrates. The following oligonucleotides were used for preparation of the partial M13 duplex substrates: 43mer 5′-CTTGCATGCCTGCAGGTCGACTCTAGAGGATCCCC GGGTACCG-3′ and 24mer: 5′-CATTAAAGCCAGAATG GAAAGCGC-3′. The oligonucleotides were annealed to M13mp18 ssDNA at molar ratio of 10:1 by heating at 95 °C for five minutes and then cooling to 30 °C at 0.2 deg.C/second. Non-annealed oligonucleotides were removed using a QIAquick PCR purification kit (QIAGEN). Annealed oligonucleotides were radioactively labeled at the 3′ end by a filling-in reaction catalyzed by Klenow fragment (NEB) in the presence of [α-^{32}P]ATP (3000 Ci/mmol; Amersham Pharmacia Biotech) under standard conditions (NEB). The oligonucleotides A_{20} (50mer), A_0 (30mer), B_{19} (49mer), B_0 (30mer) and C_{19} (19mer) were used for the generation of the blunt-ended duplex ($A_0 + B_0$), 3′-ssDNA-tailed duplex ($A_0 + B_{19}$), splayed arm ($A_{20} + B_{19}$), 5′-ssDNA flap duplex ($A_{20} + B_{19} + C_{19}$) and nicked duplex ($A_0 + B_{19} + C_{19}$) have been described.[54] The oligonucleotides A_{20} and A_0 were labeled at the 5′ end using [γ-^{32}P]ATP (3000 Ci/mmol; Amersham Pharmacia Biotech) and phage T4 polynucleotide kinase (NEB), and annealed to appropriate complementary strands at a molar ratio of 1:1.25 by incubation at 95 °C for five minutes and then cooling to 30 °C at 0.2 deg.C/second. The 50mer oligonucleotides used to prepare the four-way junction substrate have been described.[6] One of the oligonucleotides was radiolabeled at the 5′ end using [γ-^{32}P]ATP and T4 polynucleotide kinase. The labeled oligonucleotide was annealed with the other three strands at a molar ratio of 1:4 by incubation at 95 °C for five minutes and then cooling to 30 °C at 0.2 deg.C/second. The radiolabeled four-way junction substrate was separated from other species on a non-denaturing 15% (w/v) polyacrylamide gel (acrylamide to bis-acrylamide, 19:1 (w/w)) run in TBE buffer (90 mM Tris–borate (pH 8.3), 2 mM EDTA) and recovered from the gel by electroelution.

DNA helicase reactions were carried out at 37 °C in buffer H (50 mM Tris–HCl (pH 7.5), 50 mM NaCl, 5 mM $MgCl_2$, 50 μg/ml of bovine serum albumin (BSA), 2 mM ATP, 1 mM DTT). DNA substrates were present at a concentration of 0.5 nM for partial M13 duplexes or 1 nM for synthetic substrates. After two minutes preincubation, reactions were started with enzyme and later terminated by addition of 0.5 reaction volume of buffer S (150 mM EDTA, 2% (w/v) SDS, 30% (v/v) glycerol, 0.1% (w/v) bromophenol blue). In protein titration experiments, reactions were usually carried out in a volume of 10 μl using various quantities of protein (as indicated in the Figure legends) and an incubation time of 30 minutes. To measure the rate of DNA unwinding by $BLM^{642-1290}$ as a function of ATP concentration, 50 μl time-course reactions were carried out for concentrations of ATP ranging from 10 μM to 2000 μM using 25 bp partial duplex as DNA substrate (0.5 nM) and an enzyme concentration of 20 nM. Reaction aliquots (10 μl) at time-points of 0.5, one, two and three minutes were analyzed.

For all reactions, the displaced radiolabeled oligonucleotide was separated from its annealed form by electrophoresis through a non-denaturing 15% polyacrylamide gel (acrylamide to bis-acrylamide, 37.5:1 (w/w)) run in TBE buffer at 100 V for two hours. Gels were dried and subjected to autoradiography and/or quantified using a PhosphorImager and ImageQuant software (Molecular Dynamics). The $K_{1/2}$ value for ATP (concentration of ATP at which the rate of unwinding was half of the maximal rate) was derived by fitting data by the Michaelis–Menten equation using Prism 2.0 software.

ATPase assays

DNA-dependent ATPase activity was measured using a malachite green assay based on a colorimetric estimation of inorganic phosphate produced by ATP hydrolysis.[55] Reactions were carried out at 37 °C in buffer H in the presence of saturating amounts of DNA cofactors, including M13mp18 ssDNA, supercoiled pTZ18R plasmid DNA and a 43mer oligonucleotide (see above) as indicated in the Figure and Table legends. Reactions were initiated by adding ATP. Aliquots (5–20 μl) were removed from reactions at various time-points (1, 2, 4, 8, 16, and 32 minutes) and mixed with 20 μl of 0.1 M EDTA to terminate ATP hydrolysis. After appropriate dilution, samples (40 μl) were subjected to malachite green assay in a 96-well microplate as described[56] along with a series of KH_2PO_4 dilutions ranging from 10 μM to 140 μM that served for calibration. Steady-state kinetic parameters K_M and k_{cat} for ATP were measured at a protein concentration of 20 nM, with the exception of D1064A and R1038A mutants, which were present at concentrations of 40 nM and 100 nM, respectively. The concentration of ATP was varied from 10 μM to 2 mM in these measurements. The K_M and k_{cat} values were derived by fitting data by the Michaelis–Menten equation using Prism 2.0 software.

DNA binding assay

Protein at concentrations ranging from 5 to 640 nM was incubated with 2.5 nM 30mer oligonucleotide (the same as in the gel-filtration experiments) labeled at the 5′ end using [γ-^{32}P]ATP and T4 polynucleotide kinase. Incubations were carried out at room temperature for 20 minutes in buffer B (50 mM Tris–HCl (pH 7.5), 1 mM DTT, 50 mM NaCl, 10% (v/v) glycerol). Samples were subsequently subjected to electrophoresis through a non-denaturing 15% polyacrylamide gel (acrylamide to bis-acrylamide, 37.5:1 (w/w)) run in TBE buffer at 100 V to separate protein–DNA complex from free DNA. Gels were dried and analyzed by a PhosphorImager. The apparent dissociation constant (K_d) was determined as the protein concentration at which 50% of DNA was bound.

Acknowledgements

We thank Hagop Youssoufian for providing us with BLM cDNA, Ian Hickson for supplying the full-size BLM protein, Marcel Hohl for help with preparation of DNA helicase substrates, Ilana Camargo for help with plasmid constructions, Mark Szczelkun and Sergey Korolev for critical reading of the manuscript. This work was supported by the Swiss National Foundation.

References

1. Lohman, T. M. & Bjornson, K. P. (1996). Mechanisms of helicase-catalyzed DNA unwinding. *Annu. Rev. Biochem.* **65**, 169–214.
2. Hall, M. C. & Matson, S. W. (1999). Helicase motifs: the engine that powers DNA unwinding. *Mol. Microbiol.* **34**, 867–877.
3. von Hippel, P. H. & Delagoutte, E. (2001). A general model for nucleic acid helicases and their coupling within macromolecular machines. *Cell*, **104**, 177–190.
4. Singleton, M. R. & Wigley, D. B. (2002). Modularity and specialization in superfamily 1 and 2 helicases. *J. Bacteriol.* **184**, 1819–1826.
5. West, S. C. (1996). The RuvABC proteins and Holliday junction processing in *Escherichia coli*. *J. Bacteriol.* **178**, 1237–1241.
6. Karow, J. K., Constantinou, A., Li, J. L., West, S. C. & Hickson, I. D. (2000). The Bloom's syndrome gene product promotes branch migration of Holliday junctions. *Proc. Natl Acad. Sci. USA*, **97**, 6504–6508.
7. Gorbalenya, A. E. & Koonin, E. V. (1993). Helicases: amino acid sequence comparisons and structure–function relationships. *Curr. Opin. Struct. Biol.* **3**, 419–429.
8. Velankar, S. S., Soultanas, P., Dillingham, M. S., Subramanya, H. S. & Wigley, D. B. (1999). Crystal structures of complexes of PcrA DNA helicase with a DNA substrate indicate an inchworm mechanism. *Cell*, **97**, 75–84.
9. Levin, M. K. & Patel, S. S. (1999). The helicase from hepatitis C virus is active as an oligomer. *J. Biol. Chem.* **274**, 31839–31846.
10. Ali, J. A., Maluf, N. K. & Lohman, T. M. (1999). An oligomeric form of *E. coli* UvrD is required for optimal helicase activity. *J. Mol. Biol.* **293**, 815–834.
11. Cheng, W., Hsieh, J., Brendza, K. M. & Lohman, T. M. (2001). *E. coli* Rep oligomers are required to initiate DNA unwinding *in vitro*. *J. Mol. Biol.* **310**, 327–350.
12. Ha, T., Rasnik, I., Cheng, W., Babcock, H. P., Gauss, G. H., Lohman, T. M. & Chu, S. (2002). Initiation and re-initiation of DNA unwinding by the *Escherichia coli* Rep helicase. *Nature*, **419**, 638–641.
13. Patel, S. S. & Picha, K. M. (2000). Structure and function of hexameric helicases. *Annu. Rev. Biochem.* **69**, 651–697.
14. Courcelle, J. & Hanawalt, P. C. (1999). RecQ and RecJ process blocked replication forks prior to the resumption of replication in UV-irradiated *Escherichia coli*. *Mol. Gen. Genet.* **262**, 543–551.
15. Hanada, K., Ukita, T., Kohno, Y., Saito, K., Kato, J. & Ikeda, H. (1997). RecQ DNA helicase is a suppressor of illegitimate recombination in *Escherichia coli*. *Proc. Natl Acad. Sci. USA*, **94**, 3860–3865.
16. Enomoto, T. (2001). Functions of RecQ family helicases: possible involvement of Bloom's and Werner's syndrome gene products in guarding genome integrity during DNA replication. *J. Biochem. (Tokyo)*, **129**, 501–507.
17. Ellis, N. A., Groden, J., Ye, T. Z., Straughen, J., Lennon, D. J., Ciocci, S., Proytcheva, M. & German, J. (1995). The Bloom's syndrome gene product is homologous to RecQ helicases. *Cell*, **83**, 655–666.
18. Yu, C. E., Oshima, J., Fu, Y. H., Wijsman, E. M., Hisama, F., Alisch, R. *et al.* (1996). Positional cloning of the Werner's syndrome gene. *Science*, **272**, 258–262.
19. Kitao, S., Shimamoto, A., Goto, M., Miller, R. W., Smithson, W. A., Lindor, N. M. & Furuichi, Y. (1999). Mutations in RECQL4 cause a subset of cases of Rothmund–Thomson syndrome. *Nature Genet.* **22**, 82–84.
20. Furuichi, Y. (2001). Premature aging and predisposition to cancers caused by mutations in RecQ family helicases. *Ann. NY Acad. Sci.* **928**, 121–131.
21. Myung, K., Datta, A., Chen, C. & Kolodner, R. D. (2001). SGS1, the *Saccharomyces cerevisiae* homologue of BLM and WRN, suppresses genome instability and homeologous recombination. *Nature Genet.* **27**, 113–116.
22. Imamura, O., Fujita, K., Itoh, C., Takeda, S., Furuichi, Y. & Matsumoto, T. (2002). Werner and Bloom helicases are involved in DNA repair in a complementary fashion. *Oncogene*, **21**, 954–963.
23. Shimizu, H., Yamaguchi, H., Ashizawa, Y., Kohno, Y., Asami, M., Kato, J. & Ikeda, H. (1997). Short-homology-independent illegitimate recombination in *Escherichia coli*: distinct mechanism from short-homology-dependent illegitimate recombination. *J. Mol. Biol.* **266**, 297–305.
24. Shiraishi, K., Hanada, K., Iwakura, Y. & Ikeda, H. (2002). Roles of RecJ, RecO, and RecR in RecET-mediated illegitimate recombination in *Escherichia coli*. *J. Bacteriol.* **184**, 4715–4721.
25. Kamath-Loeb, A. S., Loeb, L. A., Johansson, E., Burgers, P. M. & Fry, M. (2001). Interactions between the Werner syndrome helicase and DNA polymerase delta specifically facilitate copying of tetraplex and hairpin structures of the d(CGG)n trinucleotide repeat sequence. *J. Biol. Chem.* **276**, 16439–16446.
26. Gaymes, T. J., North, P. S., Brady, N., Hickson, I. D., Mufti, G. J. & Rassool, F. V. (2002). Increased error-prone non homologous DNA end-joining—a proposed mechanism of chromosomal instability in Bloom's syndrome. *Oncogene*, **21**, 2525–2533.
27. Oshima, J., Huang, S., Pae, C., Campisi, J. & Schiestl, R. H. (2002). Lack of WRN results in extensive deletion at nonhomologous joining ends. *Cancer Res.* **62**, 547–551.
28. Pause, A. & Sonenberg, N. (1992). Mutational analysis of a DEAD box RNA helicase: the mammalian translation initiation factor eIF-4A. *EMBO J.* **11**, 2643–2654.
29. Hall, M. C., Ozsoy, A. Z. & Matson, S. W. (1998). Site-directed mutations in motif VI of *Escherichia coli* DNA helicase II result in multiple biochemical defects: evidence for the involvement of motif VI in the coupling of ATPase and DNA binding activities *via* conformational changes. *J. Mol. Biol.* **277**, 257–271.
30. Dillingham, M. S., Soultanas, P. & Wigley, D. B. (1999). Site-directed mutagenesis of motif III in PcrA helicase reveals a role in coupling ATP hydrolysis to strand separation. *Nucl. Acids Res.* **27**, 3310–3317.
31. Dillingham, M. S., Soultanas, P., Wiley, P., Webb, M. R.

& Wigley, D. B. (2001). Defining the roles of individual residues in the single-stranded DNA binding site of PcrA helicase. *Proc. Natl Acad. Sci. USA*, **98**, 8381–8387.
32. Morozov, V., Mushegian, A. R., Koonin, E. V. & Bork, P. (1997). A putative nucleic acid-binding domain in Bloom's and Werner's syndrome helicases. *Trends Biochem. Sci.* **22**, 417–418.
33. Liu, Z., Macias, M. J., Bottomley, M. J., Stier, G., Linge, J. P., Nilges, M. *et al.* (1999). The three-dimensional structure of the HRDC domain and implications for the Werner and Bloom syndrome proteins. *Struct. Fold. Des.* **7**, 1557–1566.
34. Wu, L. & Hickson, I. D. (2001). RecQ helicases and topoisomerases: components of a conserved complex for the regulation of genetic recombination. *Cell. Mol. Life Sci.* **58**, 894–901.
35. Karow, J. K., Newman, R. H., Freemont, P. S. & Hickson, I. D. (1999). Oligomeric ring structure of the Bloom's syndrome helicase. *Curr. Biol.* **9**, 597–600.
36. Beresten, S. F., Stan, R., van Brabant, A. J., Ye, T., Naureckiene, S. & Ellis, N. A. (1999). Purification of overexpressed hexahistidine-tagged BLM N431 as oligomeric complexes. *Protein Expr. Purif.* **17**, 239–248.
37. Xue, Y., Ratcliff, G. C., Wang, H., Davis-Searles, P. R., Gray, M. D., Erie, D. A. & Redinbo, M. R. (2002). A minimal exonuclease domain of WRN forms a hexamer on DNA and possesses both 3′-5′ exonuclease and 5′-protruding strand endonuclease activities. *Biochemistry*, **41**, 2901–2912.
38. Harmon, F. G. & Kowalczykowski, S. C. (2001). Biochemical characterization of the DNA helicase activity of the *Escherichia coli* RecQ helicase. *J. Biol. Chem.* **276**, 232–243.
39. Mohaghegh, P., Karow, J. K., Brosh, R. M., Jr, Bohr, V. A. & Hickson, I. D. (2001). The Bloom's and Werner's syndrome proteins are DNA structure-specific helicases. *Nucl. Acids Res.* **29**, 2843–2849.
40. Ikeda, H., Shimizu, H., Ukita, T. & Kumagai, M. (1995). A novel assay for illegitimate recombination in *Escherichia coli*: stimulation of lambda bio transducing phage formation by ultra-violet light and its independence from RecA function. *Advan. Biophys.* **31**, 197–208.
41. Singleton, M. R., Scaife, S. & Wigley, D. B. (2001). Structural analysis of DNA replication fork reversal by RecG. *Cell*, **107**, 79–89.
42. Korolev, S., Hsieh, J., Gauss, G. H., Lohman, T. M. & Waksman, G. (1997). Major domain swiveling revealed by the crystal structures of complexes of *E. coli* Rep helicase bound to single-stranded DNA and ADP. *Cell*, **90**, 635–647.
43. Brosh, R. M., Jr, Waheed, J. & Sommers, J. A. (2002). Biochemical characterization of the DNA substrate specificity of Werner syndrome helicase. *J. Biol. Chem.* **277**, 23236–23245.
44. Constantinou, A., Tarsounas, M., Karow, J. K., Brosh, R. M., Bohr, V. A., Hickson, I. D. & West, S. C. (2000). Werner's syndrome protein (WRN) migrates Holliday junctions and co-localizes with RPA upon replication arrest. *EMBO Rep.* **1**, 80–84.
45. Mahdi, A. A., Briggs, G. S., Sharples, G. J., Wen, Q. & Lloyd, R. G. (2003). A model for dsDNA translocation revealed by a structural motif common to RecG and Mfd proteins. *EMBO J.* **22**, 724–734.
46. Bennett, R. J., Sharp, J. A. & Wang, J. C. (1998). Purification and characterization of the Sgs1 DNA helicase activity of *Saccharomyces cerevisiae*. *J. Biol. Chem.* **273**, 9644–9650.
47. Ozsoy, A. Z., Sekelsky, J. J. & Matson, S. W. (2001). Biochemical characterization of the small isoform of *Drosophila melanogaster* RECQ5 helicase. *Nucl. Acids Res.* **29**, 2986–2993.
48. Kawasaki, K., Maruyama, S., Nakayama, M., Matsumoto, K. & Shibata, T. (2002). *Drosophila melanogaster* RECQ5/QE DNA helicase: stimulation by GTP binding. *Nucl. Acids Res.* **30**, 3682–3691.
49. Rong, S. B., Valiaho, J. & Vihinen, M. (2000). Structural basis of Bloom syndrome (BS) causing mutations in the BLM helicase domain. *Mol. Med.* **6**, 155–164.
50. Yamashita, T., Hanada, K., Iwasaki, M., Yamaguchi, H. & Ikeda, H. (1999). Illegitimate recombination induced by overproduction of DnaB helicase in *Escherichia coli*. *J. Bacteriol.* **181**, 4549–4553.
51. Ohmori, H. (1994). A new method for strand discrimination in sequence-directed mutagenesis. *Nucl. Acids Res.* **22**, 884–885.
52. Prilipov, A., Phale, P. S., Van, G. P., Rosenbusch, J. P. & Koebnik, R. (1998). Coupling site-directed mutagenesis with high-level expression: large scale production of mutant porins from *E. coli*. *FEMS Microbiol. Letters*, **163**, 65–72.
53. Ukita, T. & Ikeda, H. (1996). Role of the recJ gene product in UV-induced illegitimate recombination at the hotspot. *J. Bacteriol.* **178**, 2362–2367.
54. Hohl, M., Thorel, F., Clarkson, S. G. & Scharer, O. D. (2003). Structural determinants for substrate binding and catalysis by the structure-specific endonuclease XPG. *J. Biol. Chem.* **278**, 19500–19508.
55. Chan, K. M., Delfert, D. & Junger, K. D. (1986). A direct colorimetric assay for Ca^{2+}-stimulated ATPase activity. *Anal. Biochem.* **157**, 375–380.
56. Janscak, P., Abadjieva, A. & Firman, K. (1996). The type I restriction endonuclease R.*Eco* R124I: over-production and biochemical properties. *J. Mol. Biol.* **257**, 977–991.

Edited by J. O. Thomas

(Received 6 January 2003; received in revised form 16 April 2003; accepted 18 April 2003)

Article II

Human RECQ5β, a protein with DNA helicase and
strand-annealing activities in a single polypeptide

Patrick L. Garcia, Ylun Liu, Josef Jiricny, Stephen C. West and Pavel Janscak

The EMBO Journal 2004, **23**: 2882-2891

In this work, I have performed all experiments except those for figures 3 and 4.

The EMBO Journal (2004) 23, 2882–2891 | © 2004 European Molecular Biology Organization | All Rights Reserved 0261-4189/04
www.embojournal.org

THE EMBO JOURNAL

Human RECQ5β, a protein with DNA helicase and strand-annealing activities in a single polypeptide

Patrick L Garcia[1], Yilun Liu[2], Josef Jiricny[1], Stephen C West[2] and Pavel Janscak[1,*]

[1]Institute of Molecular Cancer Research, University of Zürich, Zürich, Switzerland and [2]Cancer Research UK, London Research Institute, Clare Hall Laboratories, Herts, UK

Proteins belonging to the highly conserved RecQ helicase family are essential for the maintenance of genomic stability. Here, we describe the biochemical properties of the human RECQ5β protein. Like BLM and WRN, RECQ5β is an ATP-dependent 3′–5′ DNA helicase that can promote migration of Holliday junctions. However, RECQ5β required the single-stranded DNA-binding protein RPA in order to mediate the efficient unwinding of oligonucleotide-based substrates. Surprisingly, we found that RECQ5β possesses an intrinsic DNA strand-annealing activity that is inhibited by RPA. Analysis of deletion variants of RECQ5β revealed that the DNA helicase activity resides in the conserved N-terminal portion of the protein, whereas strand annealing is mediated by the unique C-terminal domain. Moreover, the strand-annealing activity of RECQ5β was strongly inhibited by ATPγS, a poorly hydrolyzable analog of ATP. This effect was alleviated by mutations in the ATP-binding motif of RECQ5β, indicating that the ATP-bound form of the protein cannot promote strand annealing. This is the first demonstration of a DNA helicase with an intrinsic DNA strand-annealing function residing in a separate domain.

The EMBO Journal (2004) **23,** 2882–2891. doi:10.1038/sj.emboj.7600301; Published online 8 July 2004
Subject Categories: genome stability & dynamics
Keywords: DNA helicase; genomic instability; Holliday junctions; RecQ; single-strand annealing

Introduction

Helicases are ubiquitous enzymes that use the free energy of nucleotide triphosphate hydrolysis to separate nucleic acid duplexes into the constituent single strands (reviewed in Lohman and Bjornson, 1996; Hall and Matson, 1999; von Hippel and Delagoutte, 2001). They play essential roles in nearly all DNA metabolic processes, including DNA replication, recombination and repair. Helicases often contain additional functional domains or interact with other proteins to mediate complex DNA transactions.

*Corresponding author. Institute of Molecular Cancer Research, University of Zürich, August Forel-Strasse 7, 8008 Zürich, Switzerland. Tel.: +41 1 634 8941; Fax: +41 1 634 8904;
E-mail: pjanscak@imr.unizh.ch

Received: 22 April 2004; accepted: 9 June 2004; published online: 8 July 2004

DNA helicases of the RecQ family, named after the 3′–5′ DNA helicase RecQ of *Escherichia coli*, unwind a wide variety of potentially recombinogenic DNA structures, including four-way junctions, D-loops and G-quadruplex DNA. RecQ helicases are highly conserved from bacteria to humans, but while prokaryotes and unicellular eukaryotes such as *Saccharomyces cerevisiae* or *Schizosaccharomyces pombe* possess only a single RecQ homolog, multicellular organisms have several (for recent reviews, see Bachrati and Hickson, 2003; Hickson, 2003; Khakhar *et al*, 2003). In humans, five RecQ homologs have been identified to date: RECQ1, BLM/RECQ2, WRN/RECQ3, RECQ4 and RECQ5. In all organisms, defective RecQ helicase function is associated with genomic instability, which is generally manifested as an increase in the frequency of inappropriate recombination events. Mutations in genes encoding the human RecQ helicases BLM, WRN and RECQ4 give rise to the hereditary disorders Bloom's syndrome, Werner's syndrome and Rothmund–Thomson syndrome, respectively (Bachrati and Hickson, 2003). These diseases are associated with cancer predisposition and variable aspects of premature aging. Although the precise DNA transactions mediated by RecQ helicases remain elusive, the enzymes have been implicated in the processing of aberrant DNA structures arising during DNA replication and repair (Bachrati and Hickson, 2003).

RecQ helicases possess the so-called DExH helicase and RecQ-Ct (RecQ C-terminal) regions, which form the catalytic core of the enzyme (Bachrati and Hickson, 2003; Bernstein and Keck, 2003). The former domain is homologous to the superfamily 2 helicases, while the latter is unique to the RecQ family. Recent structural studies on the *E. coli* RecQ helicase have shown that the RecQ-Ct region forms two subdomains (Bernstein *et al*, 2003). The proximal part of this region folds into a platform of four helices containing a Zn^{2+}-binding site and the distal part forms a specialized helix–turn–helix motif, called the winged-helix (WH) domain, which serves as a double-stranded DNA (dsDNA)-binding motif in several proteins including the catabolite gene activator protein (Bernstein *et al*, 2003). Some RecQ helicases also contain the so-called HRDC (Helicase and RNAseD C-terminal) region, which may serve as an auxiliary DNA-binding domain (Liu *et al*, 1999; Bernstein and Keck, 2003). The eukaryotic members of the RecQ family usually have additional N- and C-terminal domains flanking the RecQ core, which are involved in protein–protein interactions (Bachrati and Hickson, 2003).

Although defects in WRN, BLM and RECQ4 are associated with heritable human disease, such an association has not been demonstrated for RECQ5. Targeted disruption of *RECQ5* in chicken DT40 cells, which have proven to be a valuable model system to study the cellular functions of BLM and WRN, does not result in genomic instability (Imamura *et al*, 2002; Wang *et al*, 2003). However, a $RECQ5^{-/-}$ $BLM^{-/-}$ DT40 double mutant exhibits much higher levels of sister chromatid exchanges (SCEs) than a $BLM^{-/-}$ mutant, suggesting that

RECQ5 may serve as backup for BLM (Wang *et al*, 2003). RECQ5 deficiency in *Caenorhabditis elegans* reduces lifespan and increases cellular sensitivity to ionizing radiation (Jeong *et al*, 2003). Together, these findings support the notion that the product of the human *RECQ5* gene may be important for the maintenance of genomic stability.

The human RECQ5 protein exists in at least three different isoforms, which result from alternative splicing of the *RECQ5* transcript (Shimamoto *et al*, 2000). In addition to the conserved helicase and RecQ-Ct regions, the largest isoform, RECQ5β, contains a long C-terminal region that displays no homology to the other family members (Figure 7A). Also, in contrast to the other RecQ helicases, RECQ5β lacks the WH domain. The other two isoforms, RECQ5α and RECQ5γ, are almost identical. RECQ5α terminates inside the RecQ-Ct region, just upstream of the putative Zn^{2+}-binding site. RECQ5γ contains 25 additional amino acids at the C-terminus that are not present in RECQ5β. The RECQ5β isoform localizes to the nucleus, whereas the two smaller isoforms are cytoplasmic (Shimamoto *et al*, 2000).

The biochemical functions of these isoforms are unknown. To gain an insight into the potential role of *RECQ5* in the maintenance of genomic stability, we have carried out an extensive biochemical analysis of the RECQ5β protein. We found that RECQ5β is monomeric and contains two separate functional domains: the N-terminal half of the protein comprising the conserved DExH and Zn^{2+}-binding domains functions as a DNA-dependent ATPase and an ATP-dependent 3′–5′ DNA helicase. The unique C-terminal portion possesses an efficient DNA strand-annealing activity. To our knowledge, this is the first demonstration of a DNA helicase with an intrinsic DNA strand-annealing function residing in a separate domain of the same polypeptide.

Results

DNA-dependent ATPase and 3′–5′ DNA helicase activities of RECQ5β

RECQ5β was overproduced in *E. coli* as a fusion protein with a self-cleaving affinity tag composed of an intein fragment and a chitin-binding domain (CBD), and purified to more than 95% homogeneity (Figure 1A). To determine the quaternary structure of the RECQ5β protein in solution, analytical ultracentrifugation experiments were conducted with 0.5 μM protein. The sedimentation velocity profile of RECQ5β preparation revealed the presence of a single species with an $S_{20,W}$ value of 5.6. Sedimentation equilibrium measurements yielded an apparent molecular mass of 134 kDa indicating that RECQ5β exists as a monomer in solution (the predicted value for the monomer is 108.9 kDa). Size-exclusion chromatography on a Superdex 200 column revealed no change in the quaternary structure of the protein upon addition of a 30-mer oligonucleotide and/or ATPγS-Mg^{2+} (data not shown).

The ATPase activity of RECQ5β was analyzed in the presence of various DNA molecules, including short oligonucleotides, circular single-stranded DNA (ssDNA), linear dsDNA or supercoiled plasmid DNA. RECQ5β was found to exhibit robust ATPase activity with both ssDNA and dsDNA, whereas little ATPase activity was observed in the absence of

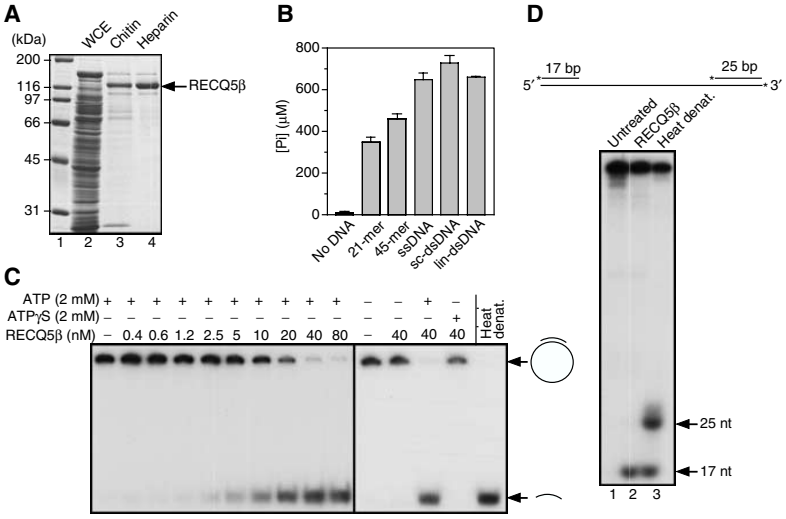

Figure 1 ATPase and DNA helicase activities of RECQ5β. (**A**) A 10% SDS–polyacrylamide gel showing individual RECQ5β purification steps. RECQ5β was overproduced in *E. coli* as a fusion with a self-cleaving affinity tag. Lane 1, molecular size marker; lane 2, soluble fraction of whole-cell extract (WCE); lane 3, pooled fractions from the chitin column; lane 4, pooled fractions from the heparin column. (**B**) ATPase activity of RECQ5β in the presence of the indicated DNA effectors. Reactions were carried out at 37°C for 30 min and contained 20 nM RECQ5β, 2 mM ATP and 25 μg/ml DNA effector. The amount of inorganic phosphate (P_i) released by ATP hydrolysis was determined as described in Materials and methods. sc-dsDNA, supercoiled dsDNA; lin-dsDNA, linear dsDNA. (**C**) Conventional DNA helicase assay using a 44 bp M13mp18-based duplex radiolabeled at the 3′-end. Reactions were carried out at 37°C for 30 min and contained 0.5 nM DNA, varying concentrations of RECQ5β and 2 mM ATP (or ATPγS) as indicated. The reaction products were analyzed by 10% nondenaturing PAGE. Radiolabeled species were visualized by autoradiography. The last lane contains heat-denatured substrate. (**D**) Helicase polarity assay using a linearized M13mp18-based DNA substrate with partial-duplex termini. Radiolabeled 3′-ends in this DNA substrate are indicated by asterisks (top panel). Reactions were carried out at 37°C for 30 min and contained 0.5 nM DNA substrate, 40 nM RECQ5β and 2 mM ATP. The products were analyzed as in (C). Lane 1, substrate incubated without enzyme; lane 2, substrate plus enzyme; lane 3, heat-denatured substrate.

DNA (Figure 1B). In addition to ATP, RECQ5β could hydrolyze dATP with a specific activity similar to that observed with ATP (data not shown). We also found that GTP and dGTP could be hydrolyzed in the presence of ssDNA and dsDNA, but the specific activities were approximately 10-fold lower than that observed with ATP (data not shown). No significant hydrolytic activity was observed with other nucleotides.

To determine whether RECQ5β possesses a DNA helicase activity, we first tested its ability to disrupt an M13mp18-based partial duplex of 44 bp. Using 0.5 nM DNA substrate and increasing amounts of RECQ5β in the presence of ATP, we observed that RECQ5β displaced the annealed oligonucleotide in a concentration-dependent manner (Figure 1C). At a protein concentration of approximately 15–20 nM, 50% strand displacement occurred. DNA helicase activity was dependent on ATP hydrolysis, as strand displacement was not observed when ATP was replaced with poorly hydrolyzable ATP analog, ATPγS (Figure 1C). We found that dATP could substitute for ATP, but failed to observe DNA helicase activity when other nucleotides were used.

To determine the polarity of the RECQ5β helicase, we employed a linear DNA substrate consisting of M13mp18 ssDNA with short ^{32}P-labeled (17 and 25 bp) duplex regions at the 5′- and 3′-ends, respectively (Figure 1D, top panel). We found that RECQ5β could only displace the 17-mer, indicating 3′–5′ polarity, which is a general characteristic of the RecQ helicase family (Figure 1D, lower panel).

RECQ5β requires RPA to unwind oligonucleotide-based partial duplexes

Further analysis of the DNA helicase activity of RECQ5β revealed that the unwinding of oligonucleotide-based substrates was poor compared with the M13-based partial duplexes. Using a 30-bp forked duplex with single-stranded splayed arms, we observed that the formation of unwound products increased proportionally with protein concentration, peaking at 10 nM with about 20% of the substrate dissociated (Figure 2A). Interestingly, at higher protein concentrations (10–40 nM), the strand displacement activity dropped below the level of spontaneous dissociation of the substrate. At even greater protein concentrations (40–320 nM), the activity again increased gradually with protein concentration (Figure 2A). The inability of RECQ5β to promote efficient unwinding of an oligonucleotide-based fork structure was surprising since other RecQ helicases such as BLM or WRN exhibit a preference for this substrate (Mohaghegh *et al*, 2001).

To explore the possibility that RECQ5β requires additional factors to mediate unwinding of oligonucleotide-based substrates, we first examined the effect of the human replication protein A (RPA), an ssDNA-binding protein, on this reaction. RPA has been shown to enhance specifically the unwinding of long DNA duplexes by WRN and BLM (Brosh *et al*, 1999, 2000). We observed that addition of RPA greatly stimulated RECQ5β-mediated unwinding of the splayed-arm structure in a concentration-dependent manner (Figure 2B). Time-course studies, carried out at 1 nM DNA and 20 nM RECQ5β, showed that in the presence of 24 nM RPA (trimer) the unwinding reaction was completed in $<$16 min (Figure 2C). The *E. coli* ssDNA-binding (SSB) protein (120 nM) could partially substitute for RPA, but the efficiency of unwinding was reduced

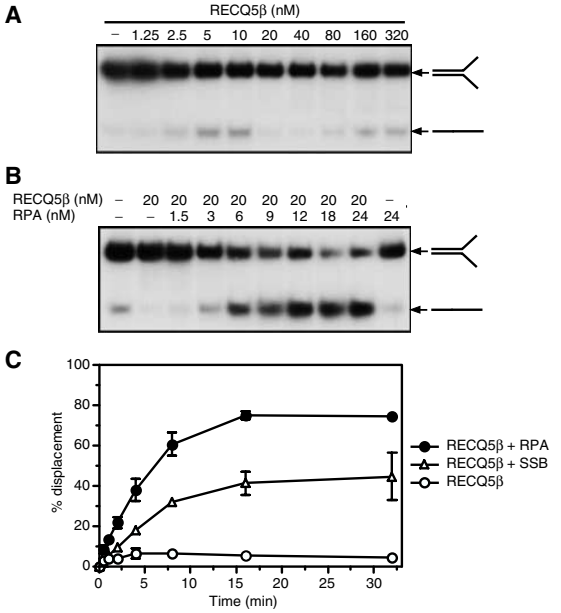

Figure 2 Stimulation of RECQ5β helicase activity on oligonucleotide-based partial duplexes by ssDNA-binding proteins. (**A**) Unwinding of 1 nM 30-bp forked duplex, ^{32}P-end labeled in the 5′-ssDNA arm, by RECQ5β at concentrations ranging from 0 to 320 nM. Reactions were incubated at 37°C for 20 min, and the products were analyzed by 10% nondenaturing PAGE. Radiolabeled species were visualized by autoradiography. (**B**) Unwinding of 1 nM 30-bp forked duplex by 20 nM RECQ5β in the presence of the indicated concentrations of RPA. Reactions were carried out and analyzed as in (A). (**C**) Kinetics of unwinding of 1 nM 30-bp forked duplex by 20 nM RECQ5β in the presence of 24 nM RPA, 120 nM *E. coli* SSB or without any ssDNA-binding protein. The percentage strand displacement was estimated as described in Materials and methods.

(Figure 2C). These results indicate that the stimulatory effect of RPA may involve specific interactions between RPA and RECQ5β, in addition to its effect in binding the ssDNA products.

RECQ5β promotes Holliday junction branch migration

The BLM and WRN proteins interact with Holliday junctions (HJs) and promote their migration (Constantinou *et al*, 2000; Karow *et al*, 2000). To determine whether RECQ5β could catalyze similar reactions, we analyzed its activity with the synthetic HJ substrate X26 that contains a 26-bp core of homologous sequences flanked by heterologous arm sequences. In the presence of ATP, we observed concentration-dependent branch migration that generated splayed-arm products (Figure 3A, lanes 2–6). Branch migration was stimulated by the presence of RPA (Figure 3A, lanes 8–11, and Figure 3B).

In these reactions, comparatively few three-strand junctions or single-stranded products were observed, indicating that the primary RECQ5β-mediated reaction involved recognition of the HJ followed by its movement and dissociation into splayed-arm products. This proposal was supported by the analysis of RECQ5β-mediated branch migration reactions in which the DNA substrate was preincubated with *E. coli* RuvA, a protein known to bind HJs with high specificity.

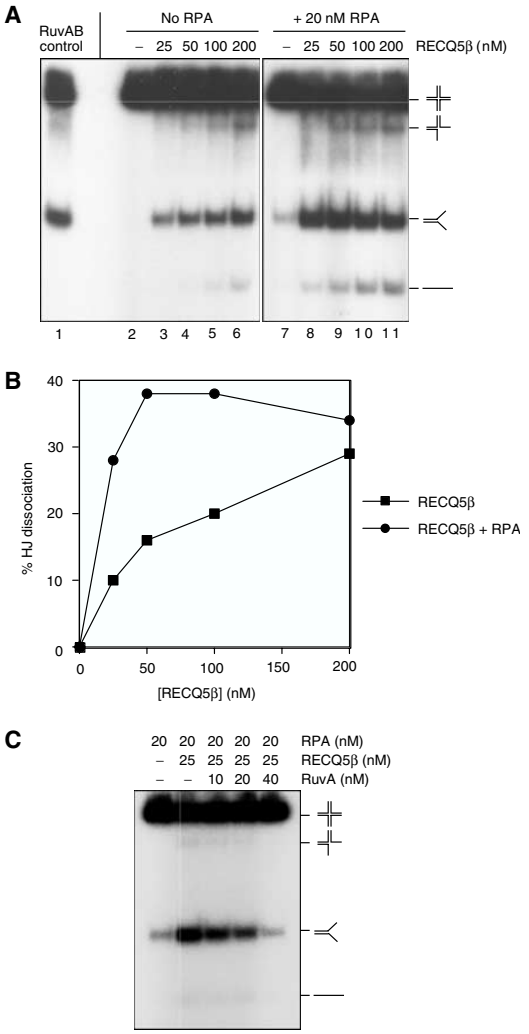

Figure 3 Branch migration of HJs by RECQ5β. (**A**) RECQ5β-mediated branch migration in the presence or absence of RPA. Reactions contained 0.5 nM synthetic junction X26, and the indicated amounts of RECQ5β protein in the presence or absence of 20 nM RPA. Reactions were carried out at 37°C for 15 min, and the DNA products were analyzed by neutral PAGE. Lane 1, control reaction with *E. coli* RuvA (25 nM) and RuvB (50 nM). (**B**) Quantification of the data shown in (A). The relative concentration of the dissociated products is expressed as percentage of total DNA. The dissociated products include three-way junctions, splayed arms (the products of branch migration) and ssDNA. Background levels of dissociated species have been subtracted. (**C**) Inhibition of RECQ5β branch migration activity by the *E. coli* HJ-binding protein RuvA. RuvA was preincubated with the junction in reaction buffer for 1 min prior to the addition of the RECQ5β protein. Incubation was then continued, and the products were assayed as described in (A).

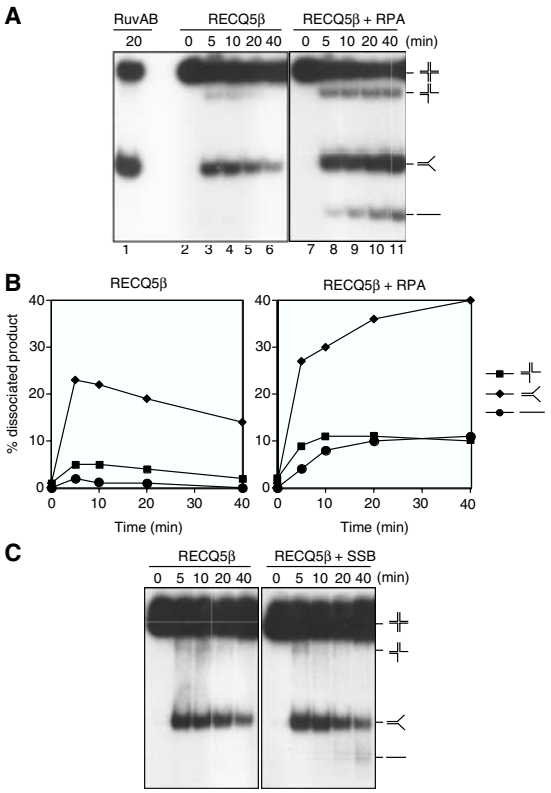

Figure 4 RPA stimulates RECQ5β-mediated branch migration by inhibiting DNA reannealing. (**A**) Time course of branch migration of 0.5 nM X26 mediated by 50 nM RECQ5β either in the presence or absence of 20 nM RPA. Reactions were carried out at 37°C, and the DNA products were analyzed by neutral PAGE. (**B**) Quantification of products (three-way junction, splayed-arm branch migration products and single strands) formed during the reactions shown in (A). The relative concentration of the products is expressed as percentage of total dissociated products. (**C**) Time course of branch migration of 0.5 nM X26 mediated by 50 nM RECQ5β in the presence or absence of excess *E. coli* SSB protein (1 μM). Reactions were carried out and analyzed as in (A).

We found that the presence of 40 nM RuvA imposed a complete block to branch migration mediated by 25 nM RECQ5β (Figure 3C).

The ability of RPA to stimulate branch migration could be a consequence of its ability to bind the single-stranded arms of reaction products thereby (i) stimulating the forward reaction or (ii) blocking a reverse reaction in which the splayed-arm structures reannealed to reform the HJ structure. To distinguish between these possibilities, time-course studies were carried out in the presence and absence of RPA. Without RPA, formation of the splayed-arm branch migration products was greater after 5 min than at later time points (Figure 4A, lanes 3–6, and Figure 4B). This surprising result contrasts with data obtained with reactions carried out in the presence of RPA, in which splayed-arm products accumulated in a time-dependent manner (Figure 4A, lanes 7–11, and Figure 4B). As observed in the helicase assays described earlier, SSB could only partially substitute for RPA (Figure 4C). Taken together, these results indicate that RPA plays a specific role in the branch migration reaction, by specifically inhibiting the reannealing of the splayed-arm products. RPA stimulation therefore involves inhibition of annealing, rather than stimulation of branch migration.

RECQ5β possesses DNA strand-annealing activity

The finding that the RECQ5β-mediated dissociation of four-way junctions to splayed-arm products was followed by a

slow reannealing reaction (Figure 4A) encouraged us to test whether RECQ5β itself possesses the ability to promote the annealing of complementary single strands. We therefore incubated two partially complementary oligonucleotides (those used to make the splayed-arm helicase substrate) with increasing amounts of RECQ5β in the absence of ATP, and subsequently analyzed the reaction products by 10% nondenaturing polyacrylamide gel electrophoresis (PAGE). We found that RECQ5β promoted an efficient annealing reaction (Figure 5). Using 1 nM ssDNA, we found that annealing was dependent on protein concentration, with the reaction being most efficient at around 40 nM RECQ5β (Figure 5A). A large excess of RECQ5β over DNA slightly inhibited single-strand annealing, possibly as a consequence of protein aggregation (Figure 5A). Time-course experiments conducted at the optimal concentration of RECQ5β (40 nM) revealed that the RECQ5β-promoted annealing reaction was rapid, with 50% of the single-stranded substrate being converted into the double-stranded product within 2 min (Figure 5B). In contrast, spontaneous DNA annealing was slow, with only 15% of the substrate being converted to dsDNA after 32 min (Figure 5B). These findings provide an explanation for the apparent poor helicase activity displayed by RECQ5β on oligonucleotide-based substrates.

RECQ5β was also tested for its ability to promote the annealing of a short oligonucleotide to a target sequence in M13mp18 ssDNA, which contains a large excess of heterologous sequences. In this experiment, a ^{32}P-end-labeled 43-mer oligonucleotide (also used in the helicase assays shown in Figure 1C) was preincubated with RECQ5β followed by the addition of M13mp18 ssDNA. RECQ5β promoted the annealing of the oligonucleotide to the M13mp18 ssDNA (Figure 5C). However, the yield of the annealed product in this reaction was significantly lower than that of the RECQ5β-promoted annealing of complementary oligonucleotides (compare Figure 5A and C). This negative effect of heterologous DNA sequences on RECQ5β-mediated strand annealing correlates with our earlier studies in which it was shown that RECQ5β efficiently unwinds M13mp18-based partial duplexes (Figure 1C).

To gain further insight into the mechanism of RECQ5β-mediated DNA strand annealing, we investigated whether coating of the oligonucleotides with RPA would affect the annealing reaction. Assuming that the size of the DNA-binding site for RPA is about 30 nucleotides (nt) (Kim *et al*, 1992), we anticipated that the two partially complementary oligonucleotides (with lengths of 50 and 49 nt) would each be occupied by 1–2 RPA heterotrimers. The oligonucleotides (1 nM) were first preincubated with RPA at a concentration ranging from 0 to 24 nM for 2 min. After this DNA-binding reaction, RECQ5β was added to a final concentration of 40 nM and incubation was continued for 20 min. This protein titration experiment revealed that the presence of RPA at concentrations above 3 nM completely inhibited the DNA strand-annealing activity of RECQ5β (Figure 5D). This result correlates with the observation that RPA enhances the DNA helicase activity of RECQ5β on the oligonucleotide-based substrates (Figure 2C) and also blocks the reassociation of splayed-arm products resulting from RECQ5β-promoted HJ branch migration on the X26 structure (Figure 4A and B).

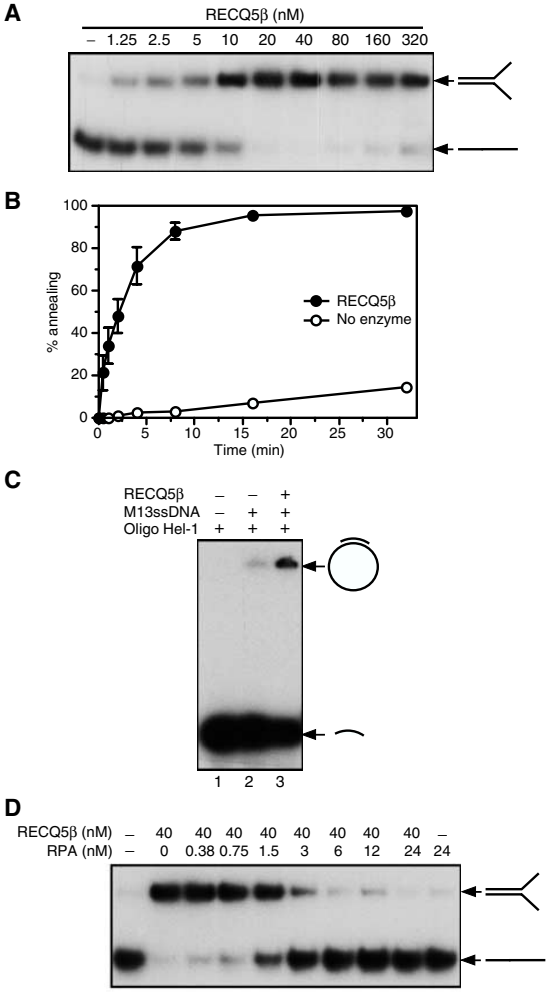

Figure 5 RECQ5β promotes DNA strand annealing. (**A**) Formation of 30-bp forked duplex in the presence of varying concentrations of RECQ5β. The A20 and B19 complementary oligonucleotides (1 nM), of which A20 was radiolabeled at its 5′-end, were incubated with the indicated concentrations of RECQ5β for 20 min at 37°C. The reaction products were separated by 10% nondenaturing PAGE and visualized by autoradiography. (**B**) Kinetics of RECQ5β-mediated and spontaneous formation of 30-bp forked duplex. Reactions were carried out at 37°C. The component strands A20 and B19 were present at a concentration of 1 nM and RECQ5β was at a concentration of 40 nM. Reactions were initiated by the addition of unlabeled B19 oligonucleotide. The relative concentration of the strand-annealing product was determined as described in Materials and methods. (**C**) Annealing of 1 nM ^{32}P-end-labeled Hel-1 oligonucleotide (43-mer) to 2 nM M13mp18 ssDNA in the absence or presence of 100 nM RECQ5β. Reactions were carried out at 37°C for 20 min and analyzed as in (A). RECQ5β was preincubated with Hel-1 for 2 min at room temperature prior to the addition of M13mp18 ssDNA. Lane 1, Hel-1 alone; lane 2, Hel-1 and M13mp18 ssDNA; lane 3, Hel-1, M13mp18 ssDNA and RECQ5β. (**D**) Effect of RPA on RECQ5β-mediated DNA strand annealing. The complementary oligonucleotides A20 and B19 (1 nM), of which A20 was radiolabeled, were incubated with or without RPA for 5 min at room temperature. RECQ5β was added to a final concentration of 40 nM and incubation was continued at 37°C for 20 min. The reaction products were analyzed as in (A).

ATP binding to the helicase domain of RECQ5β suppresses strand annealing

We next sought to examine the effect of ATP on the strand-annealing activity of RECQ5β. Since ATP can be hydrolyzed by RECQ5β under the conditions of the strand-annealing assay, we also employed the poorly hydrolyzable analog of ATP, ATPγS, in order to trap RECQ5β in its ATP-bound form. Using the two partially complementary oligonucleotides, we found that the presence of ATP or ADP had little or no effect on the RECQ5β-mediated strand-annealing reaction (Figure 6A). In contrast, ATPγS dramatically inhibited the efficient strand-annealing activity of RECQ5β (Figure 6A). These data imply that the observed inhibitory effect is the consequence of ATP binding rather than hydrolysis.

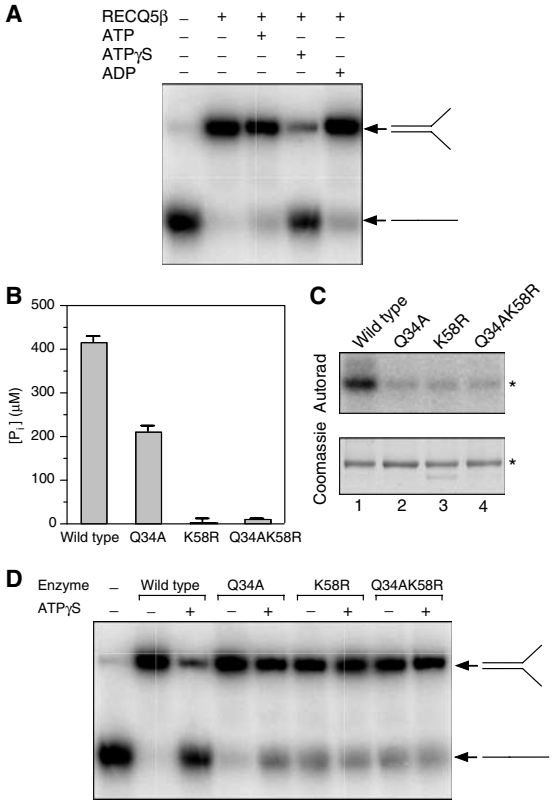

Figure 6 The ATP-bound form of RECQ5β does not promote DNA strand annealing. (**A**) Effect of ATP, ATPγS and ADP on RECQ5β-promoted annealing of the A20 and B19 oligonucleotides. Reactions were carried out at 37°C for 20 min and contained 40 nM RECQ5β, 1 nM DNAs and 2 mM nucleotides as indicated. The reaction products were analyzed by 10% nondenaturing PAGE. Radiolabeled species were visualized by autoradiography. (**B**) Comparative ATPase assay for wild-type, Q34A, K58R and Q34AK58R RECQ5β. ATPase reactions were carried out essentially as described in Figure 1B using A20 oligonucleotide as a DNA effector. (**C**) Comparative ATP-binding assay for wild-type, Q34A, K58R and Q34AK58R RECQ5β. ATP binding was measured using the ATP photo-crosslinking assay described in Materials and methods. The material was resolved on a 10% SDS–polyacrylamide gel, stained with Coomassie brilliant blue (bottom panel) and subjected to autoradiography (top panel). The asterisks indicate the position of the RECQ5β protein. (**D**) Effect of ATPγS on DNA strand-annealing activities of the wild-type, Q34A, K58R and Q34AK58R RECQ5β. Reaction conditions and analyses were as described in (A).

We next used a mutational approach to prove that the inhibitory effect of ATPγS on RECQ5β-mediated strand annealing was due to its binding to the ATP-binding site of the RECQ5β helicase domain. In the crystal structure of the complex of the *E. coli* RecQ catalytic core with ATPγS and Mn^{2+}, the adenine moiety forms hydrogen bonds with Gln-30 of motif 0 while the triphosphate is bound to Lys-53 of motif I (Bernstein *et al*, 2003). We therefore generated mutants in the corresponding residues of RECQ5β, Gln-34 and Lys-58, by replacing them with alanine and arginine, respectively. Both single and double mutants were generated, purified essentially as the wild-type enzyme and tested for their ability to bind and hydrolyze ATP. We found that the Q34A mutant retained partial ATPase activity (about 50% of wild type), whereas the K58A mutant and the double mutant failed to show any significant ATPase activity (Figure 6B). Using a UV crosslinking assay with [γ-^{32}P]ATP, we found that all three mutants exhibited reduced ATP binding relative to the wild-type enzyme (Figure 6C).

The partially complementary oligonucleotides were then used to assess the effect of ATPγS on the strand-annealing activity of the mutant RECQ5β proteins. We found that, in the absence of ATPγS, all mutant proteins promoted DNA annealing, although the activities of the K58R mutant and the double mutant were slightly reduced compared to that of the wild-type enzyme (Figure 6D). However, in contrast to the dramatic inhibitory effect seen with the wild-type enzyme, ATPγS only partially inhibited the strand-annealing activity of the Q34A mutant and had no effect on the strand-annealing activities of the K58R and Q34AK58R mutants (Figure 6D). These results correlate nicely with the observed ATPase activities of these proteins (Figure 6B), and show that the ATP-bound form of RECQ5β does not possess the ability to promote the reannealing of two complementary DNA strands.

DNA strand-annealing activity resides in the C-terminal region of RECQ5β

To define the region of RECQ5β responsible for the observed strand-annealing activity, the RECQ5$^{1-475}$ and RECQ5$^{411-991}$ deletion variants (Figure 7A) were tested for their ability to promote this reaction. The former mutant consists of the conserved portion of RECQ5β including the DExH and the Zn^{2+}-binding domains while the latter includes the unique C-terminal half of RECQ5β. In these reactions, we used two fully complementary 50-mer oligonucleotides. We found that the annealing activity promoted by RECQ5$^{1-475}$ was only slightly greater than that observed in the absence of added protein and 30-fold lower than that of the wild-type enzyme (Figure 7B). In contrast, RECQ5$^{411-991}$ displayed a significant strand-annealing activity although the rate of this reaction was reduced (four-fold) with respect to the wild-type enzyme (Figure 7B). From these data, we suggest that the observed DNA strand-annealing activity resides in the unique C-terminal part of the RECQ5β polypeptide, although it is evident that the helicase domain increases this activity possibly by enhancing the affinity of the enzyme for ssDNA.

Because RECQ5$^{1-475}$ does not display a significant DNA strand-annealing activity and contains the entire helicase catalytic core, we anticipated that it would unwind oligonucleotide substrates more efficiently than the full-size protein. To address this question, we compared the helicase activities of RECQ5β and RECQ5$^{1-475}$ on the 30-bp splayed-arm sub-

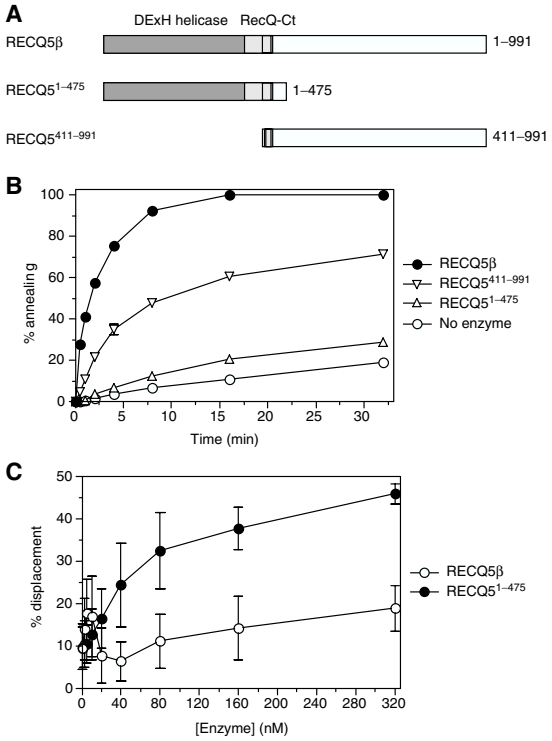

Figure 7 The DNA strand-annealing activity resides in the unique C-terminal portion of the RECQ5β polypeptide. (**A**) Schematic diagrams indicating RECQ5β and the variant proteins used in this study. The DExH helicase and RecQ-Ct domains conserved among the members of the RecQ family are shown as dark- and light-gray boxes, respectively. The location of the putative Zn^{2+}-binding site within the RecQ-Ct region is indicated as a checkered box. The remaining portion represents the region that is not conserved in the RecQ family. The numbers on the right refer to the primary amino-acid sequence of RECQ5β. (**B**) Kinetics of annealing of 1 nM 50-mer complementary oligonucleotides A20 and B20 (A20 was radioactively labeled at its 5′-end) in the presence of 20 nM RECQ5β, 20 nM $RECQ5^{1-475}$, 20 nM $RECQ5^{411-991}$ or without protein. Reactions were carried at 37°C. The relative concentration of the strand-annealing product was determined as described in Materials and methods. (**C**) Unwinding of a 30-bp forked duplex by RECQ5β and $RECQ5^{1-475}$ as a function of enzyme concentration. Reactions were carried out at 37°C for 20 min and contained 1 nM DNA, 2 mM ATP and varying amounts of enzyme. The percentage of unwound DNA was determined as described in Materials and methods.

strate at a wide range of protein concentrations (0–320 nM). We found that $RECQ5^{1-475}$ exhibited a significantly greater DNA helicase activity than the wild-type enzyme at protein concentrations >20 nM, at which RECQ5β displayed efficient strand-annealing activity (compare Figures 5A and 7C). As mentioned above, the helicase activity of RECQ5β displayed a biphasic dependence on protein concentration. In contrast, the helicase activity of $RECQ5^{1-475}$ gradually increased within the protein concentration range used (Figure 7C). The increase in helicase activity of RECQ5β at enzyme concentrations above 40 nM presumably reflects an inhibitory effect of ATP on the RECQ5β-mediated reannealing reaction, which we have observed to become more pronounced at elevated protein concentrations (data not shown).

We conclude that RECQ5β contains two separate functional domains: a DNA helicase domain and a DNA strand-annealing domain.

Discussion

In this work, we have defined the biochemical characteristics of the human RECQ5β protein, a member of the RecQ family of DNA helicases. Our work revealed that RECQ5β functions as an ssDNA/dsDNA-dependent ATPase and an ATP-dependent 3′–5′ DNA helicase with the ability to promote branch migration of HJs. These characteristics are shared by other members of the RecQ helicase family (Bachrati and Hickson, 2003). However, in contrast to BLM and WRN that form oligomeric structures (Karow *et al*, 1999; Xue *et al*, 2002), the RECQ5β helicase exists as a monomer both in free and DNA/ATP-bound forms. Most importantly, our analyses revealed that RECQ5β exhibits an efficient DNA strand-annealing activity, residing in the unique C-terminal half of the protein. Such a feature has not been seen for any DNA helicase characterized so far.

The observed inhibition of RECQ5β-mediated DNA strand annealing by RPA indicates that the annealing mechanism is likely to be distinct from the mode of action of classical single-strand-annealing proteins such as RAD52, which involves a cooperative interaction with the complex of the cognate ssDNA-binding protein and ssDNA (Sugiyama *et al*, 1998). Moreover, classical strand-annealing proteins are known to form oligomeric ring structures (Van Dyck *et al*, 1998; Passy *et al*, 1999; Stasiak *et al*, 2000), whereas RECQ5β protein is monomeric. Structural analyses of the mechanism of RAD52-mediated strand annealing revealed that multiple RAD52 rings appear to be the active catalytic species in the reaction, with ssDNA bound around each ring with the bases exposed on the surface of the protein (Van Dyck *et al*, 2001; Singleton *et al*, 2002).

The strand-annealing mechanism exhibited by RECQ5β may be more closely related to that of MRE11, which is also strongly inhibited by RPA (de Jager *et al*, 2001). MRE11 is thought to promote DNA annealing by bridging two complementary DNA segments such that their close proximity results in base pairing and duplex DNA formation. Consistent with this mode of annealing, RECQ5β-mediated annealing of complementary DNA strands was dramatically reduced by the presence of a large excess of heterologous DNA sequence, as found by measuring the annealing of a short oligonucleotide to the complementary region in M13mp18 ssDNA.

We also found that the DNA strand-annealing activity of RECQ5β was inhibited by the binding of ATPγS to the helicase domain of the enzyme. Since helicases are known to translocate along DNA in a reaction driven by ATP binding and hydrolysis, we suggest that ATPγS binding may lead to the formation of an intermediate DNA–protein complex that is incapable of DNA translocation. Alternatively, the binding of ATPγS may induce an allosteric change in RECQ5β leading to inactivation of the putative DNA strand-annealing domain. The fact that ATP did not produce a significant inhibitory effect is presumably due to its hydrolysis by the ssDNA–enzyme complex that drives protein translocation and release from the ssDNA template, allowing the strand-annealing domain to mediate duplex formation. These findings are

consistent with a model in which the helicase and the strand-annealing domains of RECQ5β act in a coordinated fashion.

In the case of oligonucleotide-based partial duplexes as well as four-way junctions, the strand-annealing activity of RECQ5β dominated over its helicase activity, unless the annealing reaction was blocked by coating of the displaced DNA strands with RPA. In contrast, RECQ5β displayed an efficient DNA helicase activity with the M13-based partial duplexes. We suggest that the M13-ssDNA substrate may trap the strand-annealing moiety of RECQ5β, thus effectively disabling the annealing activity. Under these conditions, RECQ5β could act as a DNA helicase. With oligonucleotide substrates, the strand-annealing domain is free to mediate DNA reannealing during, or immediately after, the strand displacement reaction.

Previous biochemical analysis of the large RECQ5 isoform of *Drosophila melanogaster* (DmRECQ5/QE) did not reveal the presence of an intrinsic DNA strand-annealing activity (Kawasaki *et al*, 2002). However, it should be noted that the helicase activity of DmRECQ5/QE was tested solely on M13-based substrates. In addition, the C-terminal half of human RECQ5β that is responsible for the observed strand-annealing activity shows extensive amino-acid sequence homology to the corresponding part of the DmRECQ5/QE polypeptide (Shimamoto *et al*, 2000). Therefore, the existence of this activity in the *Drosophila* protein cannot be excluded.

At the present time, the biological significance of our findings cannot be readily assessed because of the lack of information on the phenotypic consequences of *RECQ5* deficiency in human cells. It is known that targeted inactivation of the chicken *RECQ5* homolog results in a dramatic increase in the frequency of SCEs, albeit solely in a $BLM^{-/-}$ background (Wang *et al*, 2003). BLM and DNA topoisomerase IIIα (TOPOIIIα) have been shown to affect the dissolution of double HJ recombination intermediates using a strand-passage mechanism. This reaction yields only non-crossover products, explaining the observed high levels of SCEs in BLM-deficient cells (Wu and Hickson, 2003). Our observation that the human RECQ5β protein can promote HJ branch migration, an essential step in HJ or replication intermediate processing, in combination with the finding that RECQ5β co-immunoprecipitates with TOPOIIIα and TOPOIIIβ from human cell extracts (Shimamoto *et al*, 2000) is consistent with a model in which RECQ5β serves as a backup for BLM. However, we show here that RECQ5β has substantially different biochemical properties compared to those of BLM. It is therefore plausible that it has alternative and possibly more specialized cellular roles.

The biochemical properties of RECQ5β led us to suggest that the protein may be involved in a DNA repair pathway that requires the coordinated action of DNA helicase and DNA strand-annealing activities. Depletion of the RECQ5 homolog in *C. elegans* results in hypersensitivity to γ-radiation (Jeong *et al*, 2003), indicating that RECQ5β may play a role in the repair of radiation-induced lesions such as DNA double-strand breaks, or may be active at stalled replication forks that arise through radiation damage. One attractive possibility is that the DNA helicase and reannealing activities of RECQ5β are coordinated to mediate fork regression, such that the helicase promotes movement of the branch point while the annealing activity facilitates base pairing of the newly synthesized strands during the regression reaction. In agreement with this hypothesis, the small *Drosophila* RECQ5 isoform was found to unwind preferentially the 'lagging-strand arm' in a synthetic DNA molecule resembling a stalled replication fork (Ozsoy *et al*, 2003). Further analysis of the precise cellular roles of RECQ5β will shed light on the functions of the RecQ helicases in maintenance of genomic stability.

Materials and methods

Plasmid construction

The PP1045 cDNA including the RECQ5β codons 411–991 (GenBank accession no. AF193041, kindly provided by Dr Gu) and the RECQ5γ cDNA (kindly provided by Dr J Sekelsky) were used as PCR templates to reconstruct the full-size RECQ5β coding region. In the first step, the 5′- and 3′-halves of the RECQ5β coding region overlapping in the codons 403–417 were amplified and the resulting DNA fragments were fused in a second round of PCR amplification to yield the entire RECQ5β coding region. The coding region of RECQ5β was then inserted between the *Nde*I and *Sap*I sites of the plasmid pTXB1 (NEB) to construct a translational fusion between RECQ5β and a self-cleaving affinity tag composed of an Mxe intein fragment and the CBD. The resulting plasmid was named pPG10. An additional methionine codon was placed between RECQ5β and the affinity tag according to the manufacturer's instructions. The plasmids pPG16 and pPG19 encoding the deletion variants of RECQ5β ($RECQ5^{411-991}$ and $RECQ5^{1-475}$, respectively) were constructed in the same way as pPG10. Site-directed mutagenesis of the ATP-binding motifs of RECQ5β was performed using a QuickChange™ site-directed mutagenesis kit (Stratagene) essentially according to the manufacturer's protocol with pPG10 as template.

Protein purifications and analysis

The RECQ5β protein and its variants were produced as C-terminal fusions with the self-cleaving Mxe-CBD affinity tag in the *E. coli* BL21-CodonPlus-(DE3)-RIL cells (Stratagene) and purified essentially as previously described for the production and purification of the $BLM^{642-1290}$ fragment (Janscak *et al*, 2003). *E. coli* RuvA and RuvB were purified as described (Eggleston *et al*, 1997) and *E. coli* SSB was purchased from USB. Human RPA protein was prepared essentially as described, but the purification procedure also included chromatography on an ssDNA–cellulose column (Henricksen *et al*, 1994). Concentrations of proteins are expressed in moles of monomer except for RPA, which is expressed in moles of trimeric complex.

Gel filtration chromatography on a Superdex 200 PC3.2/30 column was performed using an ÄKTA system (Amersham Pharmacia Biotech) under the conditions described previously (Janscak *et al*, 2003). Sedimentation velocity and sedimentation equilibrium runs were carried out in a buffer containing 20 mM Tris–HCl (pH 7.5), 75 mM NaCl, 0.1 mM EDTA and 1 mM DTT as described previously (Janscak *et al*, 2001).

DNA substrates

All oligonucleotides used in the helicase and strand-annealing assays were purchased from Microsynth (Switzerland) and purified by PAGE. The oligonucleotides A20 (50-mer) and B19 (49-mer) are described elsewhere (Hohl *et al*, 2003). The 43-mer Hel-1 (5′-CTTGCATGCCTGCAGGTCGACTCTAGAGGATCCCCGGGTACCG-3′) is complementary to the M13mp18 viral strand. The 50-mer B20 (5′-GAGGTCACTCCAGTGAATTCGAGCTCGCAGTGTCTAGGTCGTGACTT TGA-3′) is the complement of A20. The M13mp18-based partial-duplex substrate for conventional helicase assays was prepared by annealing the Hel-1 43-mer to circular M13mp18 ssDNA (NEB) and by extension of this molecule by 1 nt using the Klenow fragment (NEB) and [α-^{32}P]dATP (Amersham Pharmacia Biotech) as described previously (Janscak *et al*, 2003). The substrate for the helicase polarity assay was prepared by cutting the 43-bp M13mp18/Hel-1 partial duplex with *Acc*I to produce a linear ssDNA molecule with short duplex regions at both ends. All available 3′-ends in this molecule were radioactively labeled using the Klenow fragment, [α-^{32}P]dATP and [α-^{32}P]dCTP. For oligonucleotide-based helicase substrates, one of the oligonucleotides was labeled at the

5′-end using T4 polynucleotide kinase (NEB) and [γ-^{32}P]ATP, and annealed to the appropriate complementary strand as described (Janscak *et al*, 2003). The synthetic HJ X26, which contains a 26 base pair region of homology flanked by heterologous arms, was made by annealing four oligonucleotides as described (Constantinou *et al*, 2001).

ATPase assays

ATPase activity was determined by colorimetric estimation of the concentration of inorganic phosphate released by ATP hydrolysis using the malachite green assay in a 96-well microplate setup (Chan *et al*, 1986; Janscak *et al*, 1996). Reactions were carried out at 37°C in a buffer containing 50 mM Tris–HCl (pH 7.5), 50 mM NaCl, 2 mM $MgCl_2$, 1 mM DTT and 50 μg/ml BSA. Reaction mixtures (typically 20 μl) contained 20 nM wild-type or mutant RECQ5β in the presence or absence of saturating concentrations of DNA effectors (25 μg/ml). Supercoiled pGEM-13Zf(+) DNA (Stratagene), *Nde*I-linearized pGEM-13Zf(+) DNA, single-stranded pGEM-13Zf(+) DNA, and 45- and 21-mer oligonucleotides were used as DNA effectors. Reactions were usually initiated by adding ATP to a final concentration of 2 mM and terminated after 30 min by adding one reaction volume of 0.1 M EDTA (pH 8.0).

Helicase assays

Helicase reactions were carried out at 37°C in buffer HA (20 mM Tris-acetate, pH 7.9, 50 mM KOAc, 10 mM $Mg(OAc)_2$, 1 mM DTT, 50 μg/ml BSA). Reaction mixtures (10 μl) contained either 0.5 nM M13mp18-based or 1 nM oligonucleotide-based partial duplexes, 2 mM ATP and indicated concentrations of RECQ5β (or its mutants). Where required, RPA or SSB was added at indicated concentrations. Reactions were started with enzyme and terminated typically after 20 min by adding 0.5 reaction volumes of solution S (150 mM EDTA, 2% (w/v) SDS, 30% (v/v) glycerol, 0.1% (w/v) bromophenol blue). In time-course experiments, the reaction volume was 50 μl, and 5 μl aliquots were removed at 0.5, 1, 2, 4, 8, 16 and 32 min. The reaction mixtures were resolved using a 10% (w/v) polyacrylamide gel (acrylamide to bis-acrylamide ratios 19:1 for oligonucleotide substrates and 37.5:1 for M13mp18-based substrates) run in TBE buffer (90 mM Tris-borate (pH 8.3), 2 mM EDTA) at 100 V and room temperature. Radiolabeled DNA species were visualized by autoradiography and quantified using a Molecular Dynamics Typhoon 9400 scanner with associated IMAGEQUANT software. The relative concentration of displaced products was expressed as percentage of total DNA.

Branch migration assay

Reactions were carried out at 37°C in a buffer containing 50 mM Tris–HCl (pH 8.0), 2 mM $MgCl_2$, 2 mM ATP, 1 mM DTT and 100 μg/ml BSA. Reaction mixtures (10 μl) contained 0.5 nM 5′-^{32}P-labeled synthetic HJ DNA (X26) and indicated amounts of RECQ5β. RPA (20 nM) or SSB (1 μM) was added as indicated. For the inhibition experiment, RuvA was preincubated with the HJ in reaction buffer for 1 min at room temperature before the addition of RECQ5β protein. The DNA products were deproteinized and electrophoresed through 10% neutral polyacrylamide gels. Control reactions with RuvAB (25 nM RuvA, 50 nM RuvB) were carried out in a buffer containing 20 mM Tris-acetate (pH 7.5), 15 mM $Mg(OAc)_2$, 2 mM ATP, 1 mM DTT and 100 μg/ml BSA.

DNA strand-annealing assays

The DNA strand-annealing activity of RECQ5β was measured using complementary synthetic oligonucleotides (each at a concentration of 1 nM) of which one was labeled at the 5′-end using [γ-^{32}P]ATP and T4 polynucleotide kinase. Annealing of a ^{32}P-labeled oligonucleotide (1 nM) to M13mp18 ssDNA (2 nM) was also measured. Annealing reactions (typically 10 μl) were carried out at 37°C in buffer HA and contained the indicated amounts of RECQ5β (or its mutants). Where required, RPA (0.38–24 nM), ATP (2 mM), ATPγS (2 mM) and ADP (2 mM) were added. Reactions were usually initiated by adding the unlabeled DNA strand and were incubated for 20 min. In time-course experiments, 50 μl reactions were initiated and 5 μl aliquots were removed at 0.5, 1, 2, 4, 8, 16 and 32 min. Reactions were analyzed essentially as the helicase reactions (see above).

ATP photo-crosslinking

Purified protein (1 μg) was incubated in a volume of 10 μl of buffer HA with 25 μM ATP and 2 μCi of [γ-^{32}P]ATP (3000 Ci/mmol; Amersham Pharmacia Biotech) for 5 min at 37°C. Reactions were spotted onto Parafilm, placed on ice and irradiated for 5 min using a UV-Stratalinker 1800 lamp (Stratagene). The covalent protein–ATP complex was separated from free ATP by electrophoresis in a 10% SDS–polyacrylamide gel. Radiolabeled species were visualized by autoradiography. The gel was subsequently stained with Coomassie brilliant blue to determine the position of the protein.

Acknowledgements

We thank Jian-ren Gu for generously providing us with PP1045 cDNA, Jeff Sekelsky for RECQ5γ cDNA, Ariel Lustig for analytical ultracentrifugation measurements, Marcel Hohl for help with preparation of DNA substrates and Christiane Koenig for technical assistance. This work was supported by the Cancer League of Kanton Zürich and Cancer Research UK. YL is a recipient of a postdoctoral fellowship from the American Cancer Society.

References

Bachrati CZ, Hickson ID (2003) RecQ helicases: suppressors of tumorigenesis and premature aging. *Biochem J* **374:** 577–606

Bernstein DA, Keck JL (2003) Domain mapping of *Escherichia coli* RecQ defines the roles of conserved N- and C-terminal regions in the RecQ family. *Nucleic Acids Res* **31:** 2778–2785

Bernstein DA, Zittel MC, Keck JL (2003) High-resolution structure of the *E.coli* RecQ helicase catalytic core. *EMBO J* **22:** 4910–4921

Brosh Jr RM, Li JL, Kenny MK, Karow JK, Cooper MP, Kureekattil RP, Hickson ID, Bohr VA (2000) Replication protein A physically interacts with the Bloom's syndrome protein and stimulates its helicase activity. *J Biol Chem* **275:** 23500–23508

Brosh Jr RM, Orren DK, Nehlin JO, Ravn PH, Kenny MK, Machwe A, Bohr VA (1999) Functional and physical interaction between WRN helicase and human replication protein A. *J Biol Chem* **274:** 18341–18350

Chan KM, Delfert D, Junger KD (1986) A direct colorimetric assay for Ca^{2+} -stimulated ATPase activity. *Anal Biochem* **157:** 375–380

Constantinou A, Davies AA, West SC (2001) Branch migration and Holliday junction resolution catalyzed by activities from mammalian cells. *Cell* **104:** 259–268

Constantinou A, Tarsounas M, Karow JK, Brosh RM, Bohr VA, Hickson ID, West SC (2000) Werner's syndrome protein (WRN) migrates Holliday junctions and co-localizes with RPA upon replication arrest. *EMBO Rep* **1:** 80–84

de Jager M, Dronkert ML, Modesti M, Beerens CE, Kanaar R, van Gent DC (2001) DNA-binding and strand-annealing activities of human Mre11: implications for its roles in DNA double-strand break repair pathways. *Nucleic Acids Res* **29:** 1317–1325

Eggleston AK, Mitchell AH, West SC (1997) *In vitro* reconstitution of the late steps of genetic recombination in *E. coli*. *Cell* **89:** 607–617

Hall MC, Matson SW (1999) Helicase motifs: the engine that powers DNA unwinding. *Mol Microbiol* **34:** 867–877

Henricksen LA, Umbricht CB, Wold MS (1994) Recombinant replication protein A: expression, complex formation, and functional characterization. *J Biol Chem* **269:** 11121–11132

Hickson ID (2003) RecQ helicases: caretakers of the genome. *Nat Rev Cancer* **3:** 169–178

Hohl M, Thorel F, Clarkson SG, Scharer OD (2003) Structural determinants for substrate binding and catalysis by the structure-specific endonuclease XPG. *J Biol Chem* **278:** 19500–19508

Imamura O, Fujita K, Itoh C, Takeda S, Furuichi Y, Matsumoto T (2002) Werner and Bloom helicases are involved in DNA repair in a complementary fashion. *Oncogene* **21:** 954–963

Janscak P, Abadjieva A, Firman K (1996) The type I restriction endonuclease R.*Eco*R124I: over-production and biochemical properties. *J Mol Biol* **257:** 977–991

Janscak P, Garcia PL, Hamburger F, Makuta Y, Shiraishi K, Imai Y, Ikeda H, Bickle TA (2003) Characterization and mutational

analysis of the RecQ core of the Bloom syndrome protein. *J Mol Biol* **330:** 29–42

Janscak P, Sandmeier U, Szczelkun MD, Bickle TA (2001) Subunit assembly and mode of DNA cleavage of the type III restriction endonucleases *Eco*P1I and *Eco*P15I. *J Mol Biol* **306:** 417–431

Jeong YS, Kang Y, Lim KH, Lee MH, Lee J, Koo HS (2003) Deficiency of *Caenorhabditis elegans* RecQ5 homologue reduces life span and increases sensitivity to ionizing radiation. *DNA Repair (Amst)* **2:** 1309–1319

Karow JK, Constantinou A, Li JL, West SC, Hickson ID (2000) The Bloom's syndrome gene product promotes branch migration of Holliday junctions. *Proc Natl Acad Sci USA* **97:** 6504–6508

Karow JK, Newman RH, Freemont PS, Hickson ID (1999) Oligomeric ring structure of the Bloom's syndrome helicase. *Curr Biol* **9:** 597–600

Kawasaki K, Maruyama S, Nakayama M, Matsumoto K, Shibata T (2002) *Drosophila melanogaster* RECQ5/QE DNA helicase: stimulation by GTP binding. *Nucleic Acids Res* **30:** 3682–3691

Khakhar RR, Cobb JA, Bjergbaek L, Hickson ID, Gasser SM (2003) RecQ helicases: multiple roles in genome maintenance. *Trends Cell Biol* **13:** 493–501

Kim C, Snyder RO, Wold MS (1992) Binding properties of replication protein A from human and yeast cells. *Mol Cell Biol* **12:** 3050–3059

Liu Z, Macias MJ, Bottomley MJ, Stier G, Linge JP, Nilges M, Bork P, Sattler M (1999) The three-dimensional structure of the HRDC domain and implications for the Werner and Bloom syndrome proteins. *Struct Fold Des* **7:** 1557–1566

Lohman TM, Bjornson KP (1996) Mechanisms of helicase-catalyzed DNA unwinding. *Annu Rev Biochem* **65:** 169–214

Mohaghegh P, Karow JK, Brosh Jr RM, Bohr VA, Hickson ID (2001) The Bloom's and Werner's syndrome proteins are DNA structure-specific helicases. *Nucleic Acids Res* **29:** 2843–2849

Ozsoy AZ, Ragonese HM, Matson SW (2003) Analysis of helicase activity and substrate specificity of *Drosophila* RECQ5. *Nucleic Acids Res* **31:** 1554–1564

Passy SI, Yu X, Li Z, Radding CM, Egelman EH (1999) Rings and filaments of beta protein from bacteriophage lambda suggest a superfamily of recombination proteins. *Proc Natl Acad Sci USA* **96:** 4279–4284

Shimamoto A, Nishikawa K, Kitao S, Furuichi Y (2000) Human RecQ5beta, a large isomer of RecQ5 DNA helicase, localizes in the nucleoplasm and interacts with topoisomerases 3alpha and 3beta. *Nucleic Acids Res* **28:** 1647–1655

Singleton MR, Wentzell LM, Liu Y, West SC, Wigley DB (2002) Structure of the single-strand annealing domain of human RAD52 protein. *Proc Natl Acad Sci USA* **99:** 13492–13497

Stasiak AZ, Larquet E, Stasiak A, Muller S, Engel A, Van Dyck E, West SC, Egelman EH (2000) The human Rad52 protein exists as a heptameric ring. *Curr Biol* **10:** 337–340

Sugiyama T, New JH, Kowalczykowski SC (1998) DNA annealing by RAD52 protein is stimulated by specific interaction with the complex of replication protein A and single-stranded DNA. *Proc Natl Acad Sci USA* **95:** 6049–6054

Van Dyck E, Hajibagheri NM, Stasiak A, West SC (1998) Visualisation of human rad52 protein and its complexes with hRad51 and DNA. *J Mol Biol* **284:** 1027–1038

Van Dyck E, Stasiak AZ, Stasiak A, West SC (2001) Visualization of recombination intermediates produced by RAD52-mediated single-strand annealing. *EMBO Rep* **2:** 905–909

von Hippel PH, Delagoutte E (2001) A general model for nucleic acid helicases and their 'coupling' within macromolecular machines. *Cell* **104:** 177–190

Wang W, Seki M, Narita Y, Nakagawa T, Yoshimura A, Otsuki M, Kawabe Y, Tada S, Yagi H, Ishii Y, Enomoto T (2003) Functional relation among RecQ family helicases RecQL1, RecQL5, and BLM in cell growth and sister chromatid exchange formation. *Mol Cell Biol* **23:** 3527–3535

Wu L, Hickson ID (2003) The Bloom's syndrome helicase suppresses crossing over during homologous recombination. *Nature* **426:** 870–874

Xue Y, Ratcliff GC, Wang H, Davis-Searles PR, Gray MD, Erie DA, Redinbo MR (2002) A minimal exonuclease domain of WRN forms a hexamer on DNA and possesses both 3′–5′ exonuclease and 5′-protruding strand endonuclease activities. *Biochemistry* **41:** 2901–2912

Article III

RPA alleviates the inhibitory effect of vinylphosphonate internucleotide linkages on DNA unwinding by BLM and WRN helicases

Patrick L. Garcia, Glyn Bradley, Christopher J. Hayes, Sussie Krintel, Panos Soultanas and Pavel Janscak *Nucleic Acids Res.* 2004, **32(12)s**: 3771-8

For this work, only the modified DNA substrates were provided by our collaborators.

Nucleic Acids Research, 2004, Vol. 32, No. 12 ***3771–3778***
doi:10.1093/nar/gkh709

RPA alleviates the inhibitory effect of vinylphosphonate internucleotide linkages on DNA unwinding by BLM and WRN helicases

Patrick L. Garcia, Glyn Bradley[1], Christopher J. Hayes[1], Sussie Krintel[1], Panos Soultanas[1] and Pavel Janscak*

Institute of Molecular Cancer Research, University of Zürich, August Forel-Strasse 7, CH-8008 Zürich, Switzerland and [1]School of Chemistry, Centre for Biomolecular Sciences (CBS), University of Nottingham, University Park, Nottingham NG7 2RD, UK

Received May 18, 2004; Revised and Accepted June 29, 2004

ABSTRACT

Bloom (BLM) and Werner (WRN) syndrome proteins are members of the RecQ family of SF2 DNA helicases. In this paper, we show that restricting the rotational DNA backbone flexibility, by introducing vinylphosphonate internucleotide linkages in the translocating DNA strand, inhibits efficient duplex unwinding by these enzymes. The human single-stranded DNA binding protein replication protein A (RPA) fully restores the unwinding activity of BLM and WRN on vinylphosphonate-containing substrates while the heterologous single-stranded DNA binding protein from *Escherichia coli* (SSB) restores the activity only partially. Both RPA and SSB fail to restore the unwinding activity of the SF1 PcrA helicase on modified substrates, implying specific interactions of RPA with the BLM and WRN helicases. Our data highlight subtle differences between SF1 and SF2 helicases and suggest that although RecQ helicases belong to the SF2 family, they are mechanistically more similar to the SF1 PcrA helicase than to other SF2 helicases that are not affected by vinylphosphonate modifications.

INTRODUCTION

Helicases are motor proteins that use free energy from nucleotide triphosphate hydrolysis for unwinding of nucleic acid duplexes (1–4). Helicases can be classified as one of two types: those that translocate along a nucleic acid strand in a 3′ to 5′ direction and those that operate with the opposite polarity. Based on amino acid sequence homology, helicases have been grouped into five superfamilies (SF1–5) (5). Most of the known 3′–5′ DNA helicases are members of SF1 or SF2. These two superfamilies have similar sets of conserved motifs that are responsible for coupling of ATP hydrolysis to DNA translocation and unwinding. The SF1 and SF2 proteins are mostly monomeric, but the oligomeric state of the functional form of these enzymes remains to be clarified, since both monomeric and oligomeric models have been proposed (6–11). Out of various models proposed for DNA unwinding by helicases, the so-called inchworm model (12) seems to be the most plausible for the SF1 and SF2 enzymes (6,13). This model is reminiscent of a 'snowplow' which is pushed or pulled along the nucleic acid duplex mechanically forcing the duplex to dissociate into the constituent strands. Extensive structural and biochemical studies on the SF1 helicase PcrA suggested the mechanism of how the free energy of ATP hydrolysis is converted to the mechanical force required for the motion. The ATP binding site of the enzyme is located in the cleft between two RecA-like domains, with residues from seven helicase signature motifs mediating protein–nucleotide interactions (6). DNA is bound along a groove on the top of the RecA-like domain and the cleft closes and opens in response to ATP binding and hydrolysis, suggesting a mechanism for DNA translocation (6). A similar situation exists also in the other SF1 and SF2 helicases which have been analyzed to atomic resolution (14–16). However, it appears that there is a mechanistic distinction between the SF1 and SF2 helicases in the nature of contacts between the translocating motor and the DNA substrate (4). Structural studies of the SF1 helicases PcrA and Rep revealed that they bind to the substrate via hydrophobic interactions with the bases and thus translocate along single-stranded DNA (ssDNA). In contrast, structural data available for SF2 helicases suggest that these enzymes bind nucleic acids rather via contacts with the phosphodiester backbone, which would allow the helicase motor to translocate on both single-stranded DNA (ssDNA) and double-stranded DNA (dsDNA) (4). In agreement with the structural data, ATP hydrolysis by SF1 helicases is stimulated only by ssDNA, whereas the ATPase activity of SF2 helicases is stimulated by both ssDNA and dsDNA (4).

The proposed base-flipping mechanism of ssDNA translocation by PcrA helicase has been examined using DNA substrates containing vinylphosphonate internucleotide linkages, which confer reduced rotational flexibility to the DNA backbone with minimal steric hindrance (17). In agreement with the model derived from structural studies, vinylphosphonate linkages have been found to completely inhibit the helicase activity of PcrA as long as they are situated in the translocating

*To whom correspondence should be addressed. Tel: +41 0 16348941; Fax: +41 0 16348904; Email: pjanscak@imr.unizh.ch

772 Nucleic Acids Research, 2004, Vol. 32, No. 12

trand either at the single-strand/double-strand junction or nside the duplex region (18). The precise mechanism of this nhibitory effect is not known, but such data are consistent with nidirectional translocation of the enzyme along ssDNA nediated via base-stacking interactions between bases and romatic residues of the enzyme, which is likely to depend n rotational flexibility of various bonds in the DNA ackbone.

Here we have examined the effect of vinylphosphonate nternucleotide linkages on DNA unwinding activity of two uman SF2 helicases BLM and WRN. BLM and WRN belong o the highly-conserved RecQ family of 3′–5′ helicases that are ssential for maintenance of genomic stability (19). Inherited nutations in both alleles of the *BLM* and *WRN* genes are asso-iated with the cancer-prone disorders Bloom and Werner yndromes, respectively (19). BLM and WRN are DNA-tructure-specific helicases that preferentially unwind G-quad-uplex DNA and various branched DNA structures such as our-way junctions, D-loops and forked duplexes as compared o 3′-ssDNA-tailed duplexes (20). They can also promote ranch migration of Holliday junctions along long stretches f dsDNA (21,22).

We present evidence that vinylphosphonate internucleotide inkages inhibit the helicase activity of both BLM and WRN s long as they are placed on the translocating strand. The bserved inhibitory effect is not as drastic as in the case of 'crA but nevertheless it is significant. Moreover we show that he human ssDNA-binding factor replication protein A (RPA) elieves the inhibitory effect of vinylphosphonate modifica-ions on BLM- and WRN-mediated unwinding, whereas it oes not affect the PcrA-catalyzed reaction. We conclude hat the rotational backbone flexibility of the DNA substrate s important for the action of the BLM and WRN helicases. he mechanism of DNA translocation by these enzymes may nvolve some base flipping but it is not based entirely on base-lipping as is the case of the SF1 PcrA helicase.

MATERIALS AND METHODS

DNA substrates

Unmodified oligonucleotides were purchased from Micro-ynth (Switzerland) and purified by PAGE. The sequences f the oligonucleotides used were as follows (5′ to 3′): VP7 45mer), TCAAAGTCACGACCTAGACAATCCCCAAAA-AAAAAGCTCGAATTC; VP8 (45mer), TCAAAGTCACG-ACCTAGACAAGCTCGAATTCGTAATCATGGTCAT; VP9 59mer), TCAAAGTCACGACCTAGACAATCCCCAA-AAAAAAAGCTCGAATTCGTAATCATGGTCAT; VP10 38mer), TCTAGAGGATCCCCAAAAAAAAACGAGCTT-AAGCATTA; VP11 (19mer), TGCATGCCTGCAGGTCGAC; RB15 (66mer), ATGACCATGATTACGAATTCGAGCTTT-TTTTTTGGGGATCCTCTAGAGTCGACCTGCAGGCAT-GCA. A derivative of RB15, named 4mod, containing a andem of four vinylphosphonate internucleotide linkages ATGACCATGATTACGAATTCGAGCTT*TT*TT*TT* TGGGGATCCTCTAGAGTCGACCTGCAGGCATGCA; positions of modifications are indicated by asterisks) was ynthesized using 5′-DMTO-T*T-3′CEP phosphoramidite uilding blocks as described previously (17). It was purified sing ABI OPC cartridges according to the manufacturer's

Table 1. DNA substrates used in this study

Name	Oligonucleotides	Schematic
A1 A2	VP7 + RB15 VP7 + 4mod	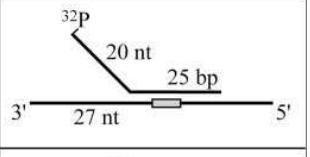
B1 B2	VP8 + RB15 VP8 + 4mod	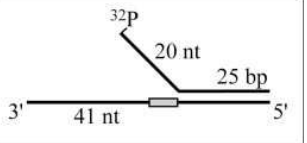
C1 C2	VP9 + RB15 VP9 + 4mod	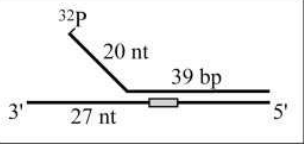
D1 D2	VP10 + VP11 + RB15 VP10 + VP11 + 4mod	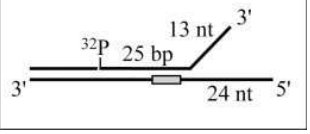

Sequences of the constituent oligonucleotides are described in Materials and Methods. A1, B1, C1 and D1 are unmodified substrates. A2, B2, C2 and D2 are modified substrates. Positions of the four tandem vinylphosphonate modifications in the schemes of individual substrates are indicated as light gray boxes. Note that in substrates D1 and D2, a 19mer oligonucleotide, VP11, was annealed to the 3′ end of RB15 and 4mod, respectively, to ensure that the enzymes enters the duplex only from the splayed-arm side and thereby translocates only along unmodified strand.

instructions. To prepare the splayed-arm DNA substrates shown in Table 1, the VP7, VP8, VP9 and VP10 oligonucleotides were radioactively labeled at the 5′ end using T4 polynucleotide kinase (New England Biolabs) and [γ-^{32}P]ATP (Amersham Pharmacia Biotech), and annealed to either RB15 (unmodified substrates) or 4mod (modified substrates) under previously described conditions (23).

Protein purifications

$BLM^{642\text{-}1290}$, WRN and PcrA helicases were prepared as previously described (23–26). *Escherichia coli* single-stranded DNA binding (SSB) protein was purchased from Promega. Human RPA was prepared essentially as described in (27). Concentrations of proteins are expressed in moles of monomer except for RPA, which is expressed in moles of heterotrimeric complex.

Oligonucleotide-displacement assays

Reactions were carried out at 37°C in a buffer containing 50 mM Tris–HCl (pH 7.5), 50 mM NaCl, 2 mM $MgCl_2$, 2 mM ATP, 1 mM DTT and 50 μg/ml BSA. Reaction mixtures contained 1 nM 5′ ^{32}P-labeled DNA substrate and 20 nM $BLM^{642–1290}$ or 5 nM WRN. Control reactions with 100 nM PcrA and 0.5 nM DNA substrate were carried out in a

Nucleic Acids Research, 2004, Vol. 32, No. 12 3773

buffer containing 20 mM Tris (pH 7.5), 10 mM $MgCl_2$, 50 mM NaCl, 4 mM DTT, 2.5 mM ATP. Where required, RPA was added to a concentration of 24 nM and SSB to a concentration of 120 nM. Reactions were started with enzyme. Aliquots of 10 µl were removed at indicated time points and mixed with 5 µl of stop solution containing 150 mM EDTA, 2% (w/v) SDS, 30% (v/v) glycerol and 0.1% (w/v) bromophenol blue. The reaction mixtures were resolved on 10% (w/v) polyacrylamide gels (acrylamide to bis-acrylamide ratio 19:1) run in TBE buffer (90 mM Tris–borate, pH 8.3, and 2 mM EDTA) at 7 V/cm and room temperature. Radiolabeled DNA species were visualized by autoradiography and quantified using a Molecular Dynamics Typhoon 9400 scanner with associated IMAGEQUANT software. The relative concentration of displaced products was expressed as a percentage of total DNA.

RESULTS

Inhibition of the DNA helicase activity of BLM by vinylphosphonate internucleotide linkages in the translocating strand

To investigate the effect of vinylphosphonate internucleotide linkages on the helicase activity of BLM, we prepared a series of splayed-arm DNA substrates containing four consecutive modifications either in the translocating or displaced strands at varying positions relative to the single-strand/double-strand junction (Table 1). A fragment of BLM comprising the helicase catalytic core (residues 642–1290, $BLM^{642–1290}$) was used in these experiments. This variant was found to exhibit a similar specific activity as the full-size BLM protein on a number of DNA structures including splayed arm (23). Using a simple gel-based, oligonucleotide displacement assay, we observed that the $BLM^{642–1290}$-mediated unwinding of a 25 bp duplex was inhibited when the modifications were located inside the duplex region on the translocating strand (Figure 1A and B). Modifications incorporated just prior to the duplex on the translocating strand also reduced the helicase activity of $BLM^{642–1290}$ though to a much lesser extent than the modifications inside the duplex (Figure 1C and D). No inhibitory effect was apparent when the modifications were present on the displaced strand inside the duplex (Figure 1E). Overall, these data indicate that restricting the rotational DNA backbone flexibility in the translocating DNA strand impairs BLM-mediated DNA unwinding.

RPA relieves the inhibitory effect of vinylphosphonate internucleotide linkages on BLM-mediated DNA unwinding

The human RPA has been shown to specifically promote unwinding of long DNA duplexes by BLM and WRN. This stimulatory effect is mediated by physical interaction between RPA and these helicases (28,29). We set up to determine whether RPA can alleviate the inhibitory effect of vinylphoshonate internucleotide linkages on the helicase activity of BLM. In these experiments, we used 39 bp forked duplex substrates with or without four consecutive modifications on the translocating strand located inside the duplex (Table 1; substrates C1 and C2). Under the conditions used, $BLM^{642–1290}$ alone could only partially unwind the unmodified substrate and showed no detectable helicase activity on the modified substrate (Figure 2A; compare lanes 2 and 9). In contrast, in the presence of RPA, both unmodified and modified substrates were unwound by $BLM^{642–1290}$ efficiently (Figure 2A; lanes 3 and 10). Substitution of RPA with the *E.coli* SSB protein also resulted in a stimulation of BLM-catalyzed unwinding of both modified and unmodified substrates, but to a lesser extent than in the case of the RPA-promoted reactions (Figure 2A; lanes 4 and 11). Time-course experiments revealed that the RPA-promoted unwinding reaction on the modified substrate displayed similar kinetics as that with unmodified substrate (Figure 2B and C). Thus, these data indicate that RPA completely relieves the inhibitory effect of vinylphosphonate internucleotide linkages on BLM-catalyzed DNA unwinding.

Single-stranded DNA binding proteins do not stimulate the helicase activity of PcrA on DNA substrates containing vinylphosphonate linkages

As mentioned above the helicase activity of PcrA has been shown to be inhibited by vinylphosphonate internucleotide linkages located in the translocating DNA strand (18). In agreement with these findings, the 39 bp splayed arm substrate containing modifications inside the duplex region was not unwound by PcrA, although unmodified substrate was unwound efficiently (Figure 3A, B and C). In contrast to BLM, RPA did not alleviate the inhibitory effect of vinylphosphonate modifications on PcrA-mediated DNA unwinding reaction (Figure 3D). In addition, PcrA helicase activity on modified substrate was not stimulated by *E.coli* SSB protein (data not shown). These data provide further evidence that the RPA-promoted bypass of regions containing vinyphosphonate internucleotide linkages by BLM is a specific reaction.

Effect of vinylphosphonate internucleotide linkages on the helicase activity of WRN

Next we sought to examine whether other RecQ DNA helicases display the same characteristics as BLM on DNA substrates containing vinylphosphonate internucleotide linkages. To this end, we tested the WRN helicase for the ability to unwind these substrates in the absence and presence of RPA. Similar to BLM, we found that vinylphosphonate modifications significantly reduced the helicase activity of WRN if located in the translocating strand (Figure 4A and B), but did not produce an inhibitory effect when located on the displaced strand (Figure 4D). In fact, the substrate with modifications in the displaced strand was unwound by WRN more efficiently than the corresponding unmodified substrate. This could be explained partly by an assumption that the vinylphosphonate modifications decrease somewhat the stability of the DNA duplex, since DNA melting studies have revealed that such modifications decrease the melting temperature of DNA duplexes by ~3.5°C per modification (data not shown). In the case of BLM, such striking differences was not apparent as the reactions were nearly completed at the first time point analyzed (Figure 1E). It should also be emphasized that these modifications do not affect the overall structure of normal B-DNA as revealed by NMR studies (18).

774 Nucleic Acids Research, 2004, Vol. 32, No. 12

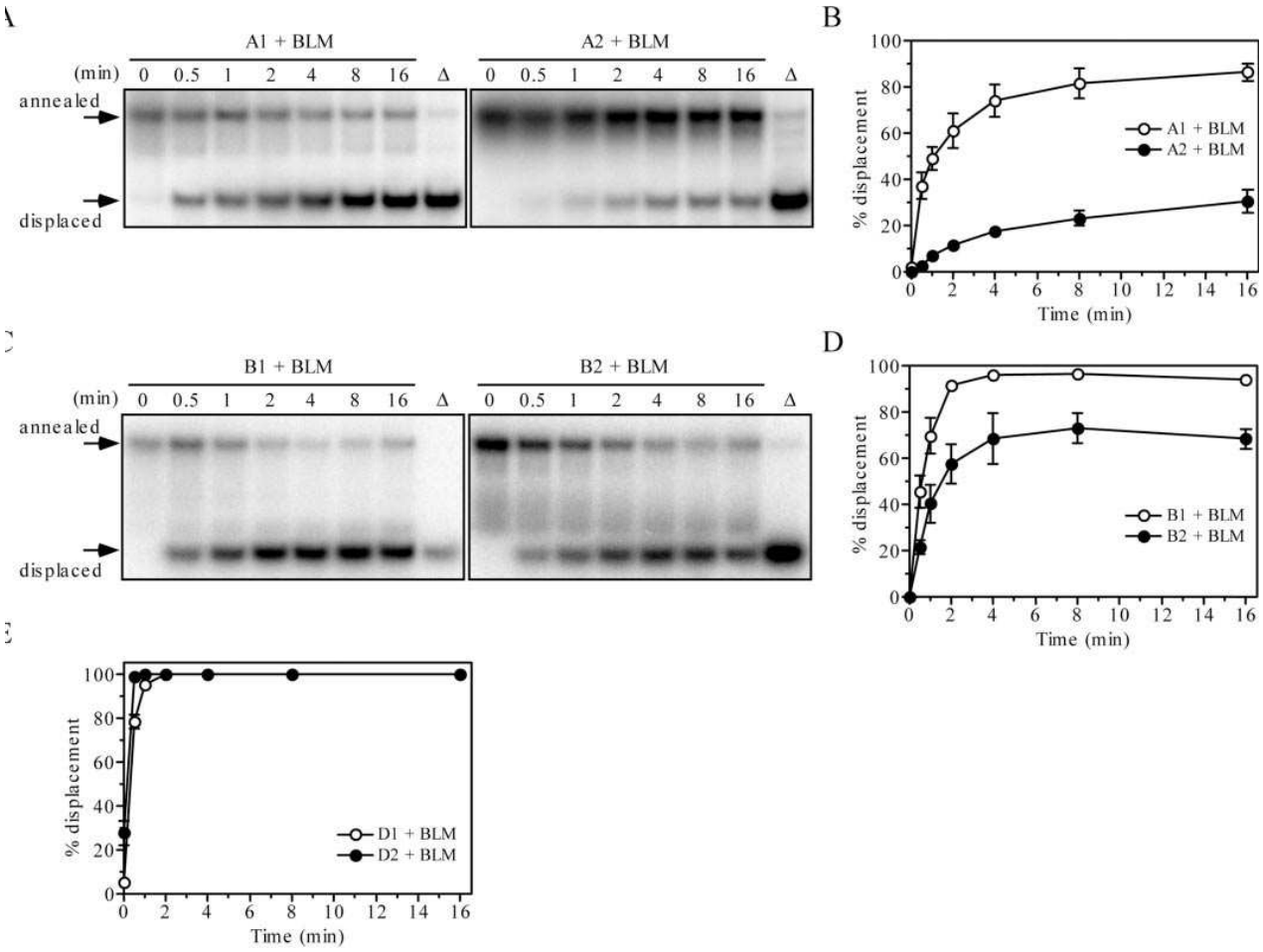

Figure 1. Effect of vinylphosphonate internucleotide linkages on helicase activity of $BLM^{642–1290}$. (**A**) Kinetics of unwinding of 1 nM A1 (left panel) and 1 nM A2 (right panel) by 20 nM $BLM^{642–1290}$. (**B**) Quantification of the reactions shown in (A). Data points represent mean values from three independent experiments. (**C**) Kinetics of unwinding of 1 nM B1 (left panel) and 1 nM B2 (right panel) by 20 nM $BLM^{642–1290}$. (**D**) Quantification of the reactions shown in (C). Data points represent mean values from three independent experiments. (**E**) Kinetics of unwinding of 1 nM D1 (open circles) and 1 nM D2 (filled circles) by 20 nM $BLM^{642–1290}$. The graph shows mean values from three independent experiments. All reactions were carried out at 37°C and analyzed as described in Materials and Methods. The relative concentration of the strand-displacement products is expressed as a percentage of total DNA. Lanes labeled with triangles contain heat-denatured substrate. DNA substrates are shown in Table 1.

The inhibitory effect of vinylphosphonate modifications on WRN-catalyzed unwinding was lost upon addition of RPA (Figure 4C), again highlighting differences between RecQ helicases and PcrA in the mode of DNA translocation.

DISCUSSION

Based on amino acid sequence homology, the RecQ proteins belong to the SF2 superfamily of helicases (5). Several crystal structures of SF2 helicases, including *E.coli* RecQ (16), HCV NS3 (15,30), UvrB (31), RecG (13) and eIF4a (32) have been solved and revealed structural similarities, but also intriguing differences from the SF1 helicases PcrA (6,33) and Rep (14). While the SF1 helicases interact with ssDNA using mainly hydrophobic interactions with the DNA bases, the SF2 helicases seem to interact with the DNA via non-specific electrostatic interactions with the phosphodiester backbone (4,34). These differences may reflect mechanistic differences, with SF1 helicases apparently able to translocate along ssDNA and the SF2 helicases along both ssDNA and dsDNA.

The translocation mechanism of helicases has been a contentious issue (35), but in the case of PcrA a base-flipping unidirectional mode of translocation with one ATP molecule utilized per base translocated has been suggested (6,36). The base-flipping mechanism requires the DNA base to flip in and out of certain pockets on the surface of the protein as it moves along the ssDNA, which is enabled by rotational flexibility of the DNA backbone. Consistent with this model, restricting backbone rotational freedom by introducing vinylphosphonate internucleotide linkages has a detrimental effect on the PcrA helicase activity (18). Vinylphosphonate backbone modifications do not affect regular bending and 'stiffness' of DNA, unless there are sharp kinks induced by the translocating

Nucleic Acids Research, 2004, Vol. 32, No. 12 3775

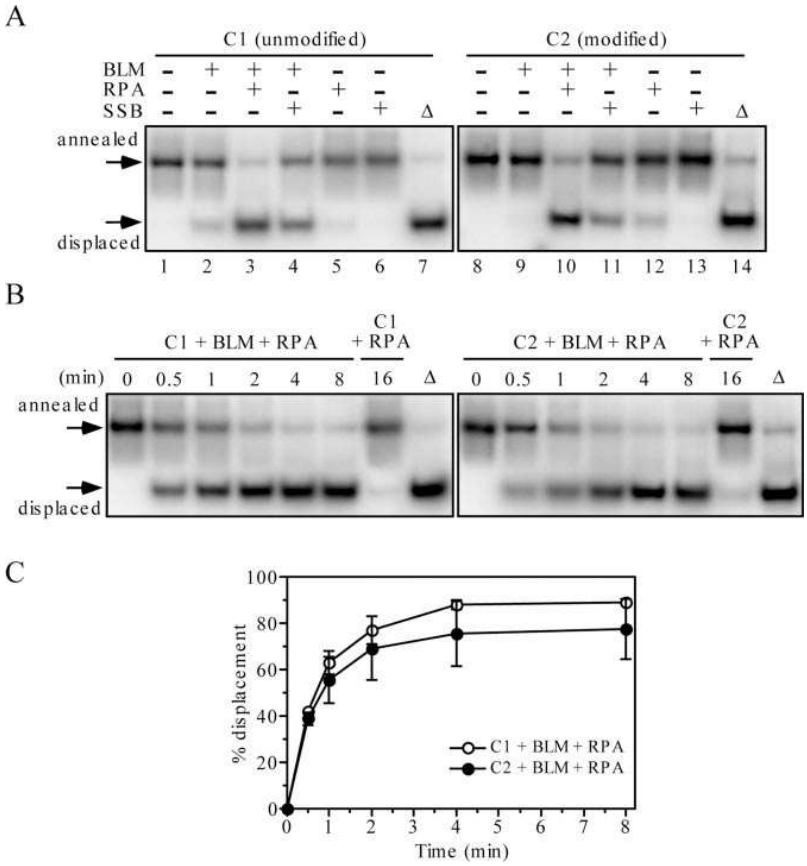

Figure 2. Single-stranded DNA binding proteins promote unwinding of vinylphosphonate-containing DNA substrates by $BLM^{642–1290}$. (**A**) Effect of 24 nM human RPA and 120 nM *E.coli* SSB on unwinding of 1 nM C1 and 1 nM C2 by 20 nM $BLM^{642–1290}$. Reactions were incubated for 20 min. (**B**) Kinetics of unwinding of 1 nM C1 (left panel) and 1 nM C2 (right panel) by 20 nM $BLM^{642–1290}$ in the presence of 24 nM RPA. In control reactions, 1 nM DNA was incubated with 24 nM RPA for 16 min. (**C**) Quantification of the reactions shown in (B). Data points represent mean values from three independent experiments. The relative concentration of the strand-displacement products is expressed as a percentage of total DNA. All reactions were carried out at 37°C and analyzed as described in Materials and Methods. Lanes labelled with triangles contain heat-denatured substrate. DNA substrates are shown in Table 1.

helicase that also require rotational backbone freedom. There is no structural or functional evidence that such sharp kinks are part of the translocation mechanism of any helicase.

Helicases that interact with DNA mainly via the phosphodiester backbone, such as the SF2 HCV NS3 (Eckhard Jankowsky, personal communication) and RecG (Robert G. Lloyd, personal communication), are able to translocate over vinylphosphonate modifications without apparent problems. In contrast, here we show that two other SF2 helicases, BLM and WRN, are inhibited by vinylphosphonate modifications. As these modifications in the A2 and C2 substrates reside inside the duplex region, it is unlikely that they will inhibit the initial binding of BLM and WRN proteins to the ssDNA/dsDNA junction. Instead, the inhibition must be related to the actual translocation process. Although the inhibitory effect of vinylphosphonate internucleotide linkages on BLM- and WRN-mediated DNA unwinding is not as drastic as that observed for PcrA, it is significant, suggesting that rotational DNA backbone freedom is an essential requirement for efficient helicase activity in these helicases. Therefore, the translocation mechanism of BLM and WRN seems to involve some base-flipping aspect, as in PcrA, but it is not entirely dependent on base-flipping, unlike PcrA (partial inhibition versus complete inhibition). As mentioned above, other SF2 helicases such as HCV NS3 and RecG are unaffected by vinylphosphonate modifications, suggesting that their mechanism of translocation does not involve base-flipping and is instead based upon interaction with the phosphodiester backbone in agreement with structural studies. Moreover, the SF2 helicase NPH-II has been recently shown to tolerate abasic sites in the translocating strand, while it essentially requires physical continuity of the phosphodiester linkage, again suggesting a mechanism in which the protein makes contact with the sugar-phosphate backbone during translocation (37). The recent crystal structure of the *E.coli* RecQ revealed a patch of conserved aromatic and charged residues (residues 156–159, C-terminal to motif II) mapping to the same relative surface location as similar residues in PcrA that are used in DNA binding (residues 257–260, C-terminal to motif III) (16). This structural feature suggests that *E.coli* RecQ may utilize a combination of base-flipping and phosphodiester backbone interactions to translocate along ssDNA, although the structure

'776 Nucleic Acids Research, 2004, Vol. 32, No. 12

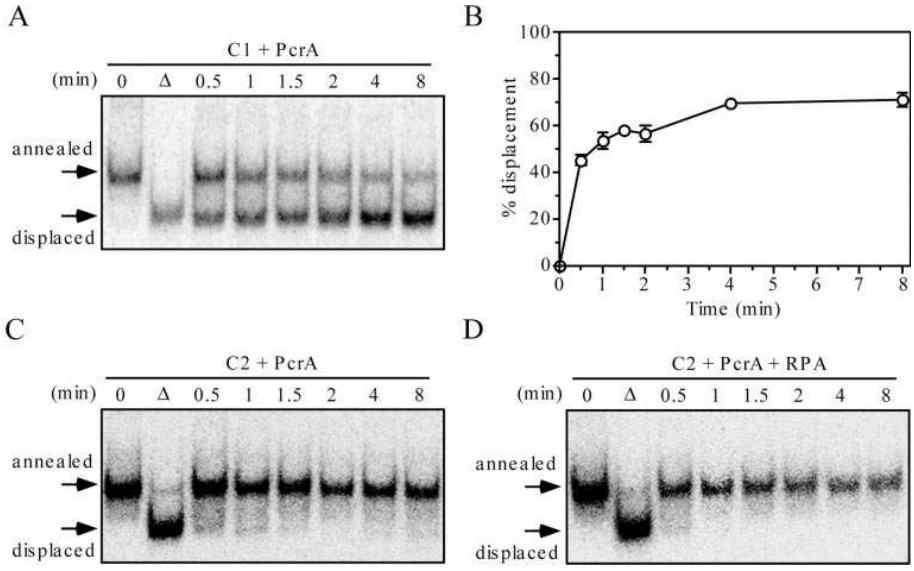

igure 3. RPA does not alleviate inhibitory effect of vinylphosphonate internucleotide linkages on PcrA-catalyzed DNA unwinding. (**A**) Kinetics of unwinding of .5 nM C1 by 100 nM PcrA. (**B**) Quantification of the reaction shown in (A). Data points represent mean values from two independent experiments. (**C**) Time course f the reaction of 100 nM PcrA with 0.5 nM C2. (**D**) Time course of the reaction of 100 nM PcrA with 0.5 nM C2 in the presence of 24 nM RPA. Reactions were carried ut at 37°C and analyzed as described in Materials and Methods. The relative concentration of the strand-displacement products is expressed as a percentage of total)NA. Lanes labelled with triangles contain heat-denatured substrate. DNA substrates are shown in Table 1.

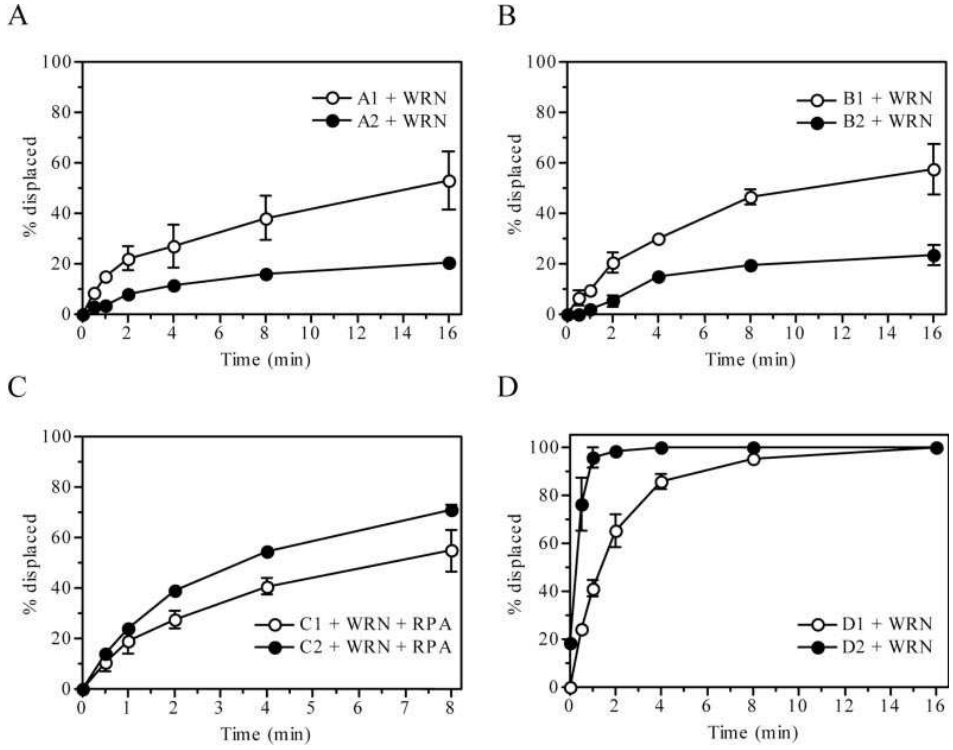

igure 4. Effect of vinylphosphonate internucleotide linkages on helicase activity of WRN in the absence and the presence of RPA. (**A**) Kinetics of unwinding of nM A1 (open circles) and 1 nM A2 (filled circles) by 5 nM WRN. (**B**) Kinetics of unwinding of 1 nM B1 (open circles) and 1 nM B2 (filled circles) by 5 nM WRN. C) Kinetics of unwinding of 1 nM C1 (open circles) and 1 nM C2 (filled circles) by 5 nM WRN in the presence of 24 nM RPA. (**D**) Kinetics of unwinding of 1 nM D1)pen circles) and 1 nM D2 (filled circles) by 5 nM WRN. Reactions were carried out at 37°C and analyzed as described in Materials and Methods. The relative oncentration of the strand-displacement products is expressed as a percentage of total DNA. Data points represent mean values from three independent experi- ients. DNA substrates are shown in Table 1.

Nucleic Acids Research, 2004, Vol. 32, No. 12 3777

of RecQ complexed with DNA is required to confirm these observations.

The stimulatory effect of RPA on BLM- and WRN-mediated unwinding of vinylphosphonate-containing DNA substrates and the failure of RPA to stimulate PcrA imply a specific interaction between RPA and both BLM and WRN helicases. This is further supported by the fact that heterologous SSB from *E.coli* stimulated BLM and WRN helicases on modified substrates only marginally. This effect is likely to reflect a simple non-specific trapping of displaced strands by SSB. BLM and WRN helicases exhibit a very low processivity (28,29). RPA has been shown to specifically stimulate BLM- and WRN-mediated unwinding through direct protein–protein interactions (28,29). It has been postulated that in addition to trapping displaced single-strands, RPA may tether the helicase to the DNA substrate at the single-strand/double-strand junction to facilitate the progression of the enzyme through relatively long DNA duplex tracts (28,29). Such a mechanism would explain the observed stimulatory effect of RPA on BLM- and WRN-mediated unwinding of vinylphosphonate-linked substrates. Providing that the modifications cause a pause in enzyme translocation followed by its dissociation from the DNA substrate, one can assume that tethering the enzyme to the translocating strand via interaction with ssDNA-bound RPA would allow it to cope with a more rotationally rigid region in the DNA template during the unwinding reaction.

Our study provides evidence of subtle differences and similarities between SF1 and SF2 helicases. Although RecQ helicases belong to SF2, they appear to be different from other SF2 helicases such as HCV NS3, RecG and NPH-II. They may translocate along ssDNA by using a combination of base-flipping (characteristic of the SF1 PcrA helicase) and non-specific phosphodiester–backbone interactions (characteristic of SF2 HCV NS3, RecG and NPH-II helicases). In that sense RecQ helicases may mechanistically belong to a sub-family of SF2 helicases.

ACKNOWLEDGEMENTS

We thank Richard Bertram and John Keyte for help with the preparation of vinylphosphonate DNA substrates. This work was supported by a Swiss National Science Foundation grant to P.J. and a Wellcome Trust grant (064751/Z/01/Z) to P.S.

REFERENCES

1. Lohman,T.M. and Bjornson,K.P. (1996) Mechanisms of helicase-catalyzed DNA unwinding. *Annu. Rev. Biochem.*, **65**, 169–214.
2. Hall,M.C. and Matson,S.W. (1999) Helicase motifs: the engine that powers DNA unwinding. *Mol. Microbiol.*, **34**, 867–877.
3. von Hippel,P.H. and Delagoutte,E. (2001) A general model for nucleic acid helicases and their 'coupling' within macromolecular machines. *Cell*, **104**, 177–190.
4. Singleton,M.R. and Wigley,D.B. (2002) Modularity and specialization in superfamily 1 and 2 helicases. *J. Bacteriol.*, **184**, 1819–1826.
5. Gorbalenya,A.E. and Koonin,E.V. (1993) Helicases: amino acid sequence comparisons and structure-function relationships. *Curr. Opin. Struct. Biol.*, **3**, 419–429.
6. Velankar,S.S., Soultanas,P., Dillingham,M.S., Subramanya,H.S. and Wigley,D.B. (1999) Crystal structures of complexes of PcrA DNA helicase with a DNA substrate indicate an inchworm mechanism. *Cell*, **97**, 75–84.
7. Levin,M.K. and Patel,S.S. (1999) The helicase from hepatitis C virus is active as an oligomer. *J. Biol. Chem.*, **274**, 31839–31846.
8. Cheng,W., Hsieh,J., Brendza,K.M. and Lohman,T.M. (2001) *E.coli* Rep oligomers are required to initiate DNA unwinding *in vitro*. *J. Mol. Biol.*, **310**, 327–350.
9. Ha,T., Rasnik,I., Cheng,W., Babcock,H.P., Gauss,G.H., Lohman,T.M. and Chu,S. (2002) Initiation and re-initiation of DNA unwinding by the *Escherichia coli* Rep helicase. *Nature*, **419**, 638–641.
10. Maluf,N.K., Fischer,C.J. and Lohman,T.M. (2003) A dimer of *Escherichia coli* UvrD is the active form of the helicase *in vitro*. *J. Mol. Biol.*, **325**, 913–935.
11. Levin,M.K., Wang,Y.H. and Patel,S.S. (2004) The functional interaction of the hepatitis C virus helicase molecules is responsible for unwinding processivity. *J. Biol. Chem.*, **279**, 26005–26012.
12. Yarranton,G.T. and Gefter,M.L. (1979) Enzyme-catalyzed DNA unwinding: studies on *Escherichia coli* Rep protein. *Proc. Natl Acad. Sci. USA*, **76**, 1658–1662.
13. Singleton,M.R., Scaife,S. and Wigley,D.B. (2001) Structural analysis of DNA replication fork reversal by RecG. *Cell*, **107**, 79–89.
14. Korolev,S., Hsieh,J., Gauss,G.H., Lohman,T.M. and Waksman,G. (1997) Major domain swiveling revealed by the crystal structures of complexes of *E.coli* Rep helicase bound to single-stranded DNA and ADP. *Cell*, **90**, 635–647.
15. Kim,J.L., Morgenstern,K.A., Griffith,J.P., Dwyer,M.D., Thomson,J.A., Murcko,M.A., Lin,C. and Caron,P.R. (1998) Hepatitis C virus NS3 RNA helicase domain with a bound oligonucleotide: the crystal structure provides insights into the mode of unwinding. *Structure*, **6**, 89–100.
16. Bernstein,D.A., Zittel,M.C. and Keck,J.L. (2003) High-resolution structure of the *E.coli* RecQ helicase catalytic core. *EMBO J.*, **22**, 4910–4921.
17. Abbas,S., Bertram,R.D. and Hayes,C.J. (2001) Commercially available 5′-DMT phosphoramidites as reagents for the synthesis of vinylphosphonate-linked oligonucleic acids. *Org. Lett.*, **3**, 3365–3367.
18. Bertram,R.D., Hayes,C.J. and Soultanas,P. (2002) Vinylphosphonate internucleotide linkages inhibit the activity of PcrA DNA helicase. *Biochemistry*, **41**, 7725–7731.
19. Bachrati,C.Z. and Hickson,I.D. (2003) RecQ helicases: suppressors of tumorigenesis and premature aging. *Biochem. J.*, **374**, 577–606.
20. Mohaghegh,P., Karow,J.K., Brosh,R.M.Jr., Bohr,V.A. and Hickson,I.D. (2001) The Bloom's and Werner's syndrome proteins are DNA structure-specific helicases. *Nucleic Acids Res.*, **29**, 2843–2849.
21. Constantinou,A., Tarsounas,M., Karow,J.K., Brosh,R.M., Bohr,V.A., Hickson,I.D. and West,S.C. (2000) Werner's syndrome protein (WRN) migrates Holliday junctions and co-localizes with RPA upon replication arrest. *EMBO Rep.*, **1**, 80–84.
22. Karow,J.K., Constantinou,A., Li,J.L., West,S.C. and Hickson,I.D. (2000) The Bloom's syndrome gene product promotes branch migration of Holliday junctions. *Proc. Natl Acad. Sci. USA*, **97**, 6504–6508.
23. Janscak,P., Garcia,P.L., Hamburger,F., Makuta,Y., Shiraishi,K., Imai,Y., Ikeda,H. and Bickle,T.A. (2003) Characterization and mutational analysis of the RecQ core of the Bloom syndrome protein. *J. Mol. Biol.*, **330**, 29–42.
24. Orren,D.K., Brosh,R.M.,Jr, Nehlin,J.O., Machwe,A., Gray,M.D. and Bohr,V.A. (1999) Enzymatic and DNA binding properties of purified WRN protein: high affinity binding to single-stranded DNA but not to DNA damage induced by 4NQO. *Nucleic Acids Res.*, **27**, 3557–3566.
25. Gray,M.D., Shen,J.C., Kamath-Loeb,A.S., Blank,A., Sopher,B.L., Martin,G.M., Oshima,J. and Loeb,L.A. (1997) The Werner syndrome protein is a DNA helicase. *Nature Genet.*, **17**, 100–103.
26. Bird,L.E., Brannigan,J.A., Subramanya,H.S. and Wigley,D.B. (1998) Characterisation of *Bacillus stearothermophilus* PcrA helicase: evidence against an active rolling mechanism. *Nucleic Acids Res.*, **26**, 2686–2693.
27. Henricksen,L.A., Umbricht,C.B. and Wold,M.S. (1994) Recombinant replication protein A: expression, complex formation, and functional characterization. *J. Biol. Chem.*, **269**, 11121–11132.
28. Brosh,R.M.,Jr, Li,J.L., Kenny,M.K., Karow,J.K., Cooper,M.P., Kureekattil,R.P., Hickson,I.D. and Bohr,V.A. (2000) Replication protein A physically interacts with the Bloom's syndrome protein and stimulates its helicase activity. *J. Biol. Chem.*, **275**, 23500–23508.
29. Brosh,R.M.,Jr, Orren,D.K., Nehlin,J.O., Ravn,P.H., Kenny,M.K., Machwe,A. and Bohr,V.A. (1999) Functional and physical interaction

between WRN helicase and human replication protein A. *J. Biol. Chem.*, **274**, 18341–18350.
0. Yao,N., Hesson,T., Cable,M., Hong,Z., Kwong,A.D., Le,H.V. and Weber,P.C. (1997) Structure of the hepatitis C virus RNA helicase domain. *Nature Struct. Biol.*, **4**, 463–467.
1. Machius,M., Henry,L., Palnitkar,M. and Deisenhofer,J. (1999) Crystal structure of the DNA nucleotide excision repair enzyme UvrB from *Thermus thermophilus*. *Proc. Natl Acad. Sci. USA*, **96**, 11717–11722.
2. Caruthers,J.M., Johnson,E.R. and McKay,D.B. (2000) Crystal structure of yeast initiation factor 4A, a DEAD-box RNA helicase. *Proc. Natl Acad. Sci. USA*, **97**, 13080–13085.
3. Subramanya,H.S., Bird,L.E., Brannigan,J.A. and Wigley,D.B. (1996) Crystal structure of a DExx box DNA helicase. *Nature*, **384**, 379–383.
34. Korolev,S., Yao,N., Lohman,T.M., Weber,P.C. and Waksman,G. (1998) Comparisons between the structures of HCV and Rep helicases reveal structural similarities between SF1 and SF2 super-families of helicases. *Protein Sci.*, **7**, 605–610.
35. Soultanas,P. and Wigley,D.B. (2001) Unwinding the 'Gordian knot' of helicase action. *Trends Biochem. Sci.*, **26**, 47–54.
36. Dillingham,M.S., Wigley,D.B. and Webb,M.R. (2000) Demonstration of unidirectional single-stranded DNA translocation by PcrA helicase: measurement of step size and translocation speed. *Biochemistry*, **39**, 205–212.
37. Kawaoka,J., Jankowsky,E. and Pyle,A.M. (2004) Backbone tracking by the SF2 helicase NPH-II. *Nature Struct. Mol. Biol.*, **11**, 526–530.

Article IV

The HRDC domain of BLM is required for the recognition, processing and dissolution of double Holliday junctions

Leonard Wu, Kok Lung Chan, Christine Ralf, Douglas A. Bernstein, Patrick L. Garcia, Vilhelm A. Bohr, Alessandro Vindigni, Pavel Janscak, James L. Keck and Ian D. Hickson *EMBO J. - in press* 2005

I have contributed to this work by performing initial double holliday junction dissolution experiments with WRN and RECQ5β in conjunction with TOPOIIIα and providing RECQ5β protein.

The EMBO Journal (2005) 24, 2679–2687 | © 2005 European Molecular Biology Organization | All Rights Reserved 0261-4189/05
www.embojournal.org

THE EMBO JOURNAL

The HRDC domain of BLM is required for the dissolution of double Holliday junctions

Leonard Wu[1], Kok Lung Chan[1], Christine Ralf[1], Douglas A Bernstein[2], Patrick L Garcia[3], Vilhelm A Bohr[4], Alessandro Vindigni[5], Pavel Janscak[3], James L Keck[2] and Ian D Hickson[1,*]

[1]Cancer Research UK Laboratories, Weatherall Institute of Molecular Medicine, John Radcliffe Hospital, University of Oxford, Oxford, UK, [2]Department of Biomolecular Chemistry, University of Wisconsin, Madison, WI, USA, [3]Institute of Molecular Cancer Research, University of Zürich, Zürich, Switzerland, [4]Laboratory of Molecular Gerontology, NIA, National Institutes of Health, Baltimore, MD, USA and [5]International Centre for Genetic Engineering and Biotechnology, Padriciano, Trieste, Italy

Bloom's syndrome is a hereditary cancer-predisposition disorder resulting from mutations in the *BLM* gene. In humans, *BLM* encodes one of five members of the RecQ helicase family. One function of BLM is to act in concert with topoisomerase IIIα (TOPO IIIα) to resolve recombination intermediates containing double Holliday junctions by a process called double Holliday junction dissolution, herein termed dissolution. Here, we show that dissolution is highly specific for BLM among human RecQ helicases and critically depends upon a functional HRDC domain in BLM. We show that the HRDC domain confers DNA structure specificity, and is required for the efficient binding to and unwinding of double Holliday junctions, but not for the unwinding of a simple partial duplex substrate. Furthermore, we show that lysine-1270 of BLM, which resides in the HRDC domain and is predicted to play a role in mediating interactions with DNA, is required for efficient dissolution.

The EMBO Journal (2005) **24,** 2679–2687. doi:10.1038/sj.emboj.7600740; Published online 30 June 2005
Subject Categories: genome stability & dynamics
Keywords: Bloom's syndrome; Holliday junction resolution; HRDC domain; RecQ DNA helicases; topoisomerase III

Introduction

Mutations in the *BLM* gene give rise to Bloom's syndrome (BS) in humans (Ellis *et al*, 1995). This rare genetic disorder is characterized by short stature, sunlight sensitivity, immunodeficiency and a predisposition to the development of many different types of malignancies (Bachrati and Hickson, 2003; Hickson, 2003). *BLM* encodes a DNA helicase that belongs to a highly conserved family, the prototypical member of which is encoded by the *recQ* gene of *Escherichia coli* (Figure 1A) (Bachrati and Hickson, 2003). Germline mutations in two other human RecQ family helicase genes also give rise to cancer-predisposition disorders: *WRN* mutations give rise to Werner's syndrome and *RECQ4* mutations are associated with some cases of Rothmund–Thomson syndrome (Yu *et al*, 1996; Kitao *et al*, 1999).

The existence of clinically distinct disorders associated with inactivation of any of three different RecQ family helicases indicates that the human RecQ family helicases have specialized functions in the cell (Oakley and Hickson, 2002; Bachrati and Hickson, 2003; Wang *et al*, 2003). In the budding yeast, *Saccharomyces cerevisiae,* mutation of the sole RecQ helicase gene, *SGS1*, results in elevated levels of genome-wide genetic recombination (Gangloff *et al*, 1994; Watt *et al*, 1996). This role in regulating homologous recombination levels appears to have been conserved in humans, at least in the case of BLM, since BS cells also show excessive levels of genome-wide homologous recombination. This is particularly apparent for recombination events between sister chromatids, giving rise to a characteristically elevated level of sister chromatid exchanges (SCEs) that is sufficiently specific for BS to be used in the diagnosis of the disorder (Chaganti *et al*, 1974). The hyper-recombination phenotype of certain RecQ helicase mutants is likely due to aberrant processing of recombination intermediates (Wu and Hickson, 2002b) since RecQ helicases from several organisms have been purified, and have been shown to act upon DNA intermediates that arise during the process of homologous recombination (Bachrati and Hickson, 2003).

RecQ helicases all contain a conserved helicase domain that defines the family (Bachrati and Hickson, 2003). There are, however, additional sequence motifs that flank the signature helicase domain (Figure 1A). In certain cases, additional enzymatic activities reside in these flanking domains. In the case of WRN, a 3′–5′ exonuclease domain is located in the N-terminal region, whereas the C-terminal domain of RECQ5β directs a DNA strand annealing function (Huang *et al*, 1998; Kamath-Loeb *et al*, 1998; Garcia *et al*, 2004) (Figure 1A). Other sequence motifs identified in RecQ helicases include the RQC domain, which is situated C-terminal to the helicase domain and appears to be found exclusively in some RecQ helicases, and the HRDC domain, which is found C-terminal to the RQC domain of some RecQ helicases and in RNaseD homologs (Figure 1A and B) (Bachrati and Hickson, 2003). The structures of the RQC and HRDC domains have been determined for RecQ and Sgs1, respectively (Liu *et al*, 1999; Bernstein *et al*, 2003). The RQC domain resembles a so-called winged-helix domain, which is a member of the helix–turn–helix superfamily, and plays a role in binding duplex DNA (Bernstein *et al*, 2003). Interestingly, in BLM and WRN, the RQC domain has been implicated also in the orchestration of protein–protein interactions (Brosh *et al*, 2001; von Kobbe *et al*, 2002; Bachrati and

*Corresponding author. Cancer Research UK Laboratories, Oxford Cancer Centre, Weatherall Institute of Molecular Medicine, John Radcliffe Hospital, University of Oxford, Oxford OX3 9DS, UK.
Tel.: +44 1865 222 417; Fax: +44 1865 222 431;
E-mail: ian.hickson@cancer.org.uk

Received: 19 April 2005; accepted: 10 June 2005; published online: 30 June 2005

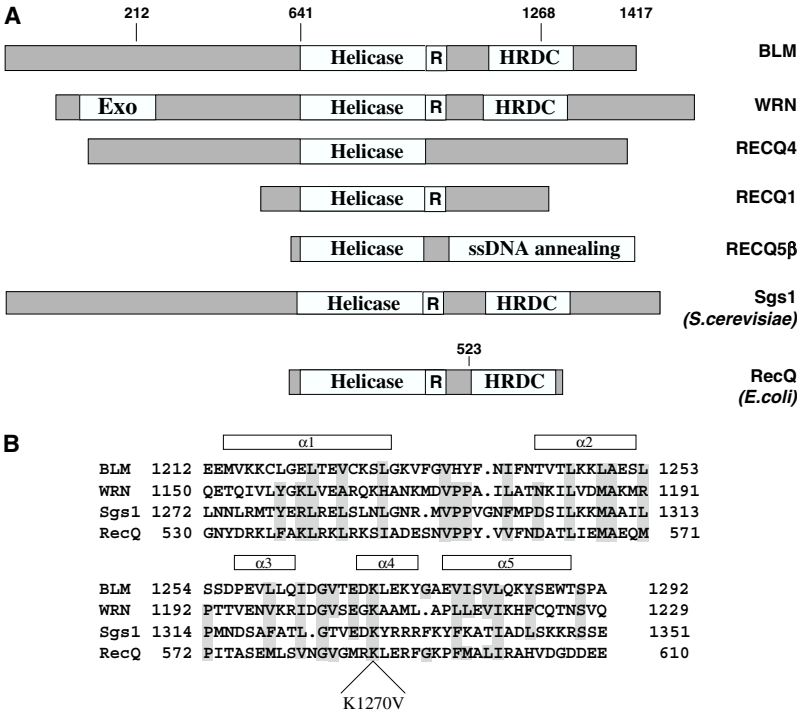

Figure 1 (**A**) Schematic representation of selected members of the RecQ helicase family. All proteins are from humans, except *E. coli* RecQ and *S. cerevisiae* Sgs1, and are aligned about the conserved helicase domain. Also shown are the relative positions of the exonuclease (Exo) and ssDNA annealing domains of WRN and RECQ5β, respectively, and the RQC (R) and HRDC domains. Nonconserved regions are shaded in gray. Relevant amino-acid residue positions of truncation mutants used in this study are indicated above BLM and RecQ. See text for details. (**B**) Alignment of the HRDC domain of BLM, WRN, Sgs1 and *E. coli* RecQ. Residues comprising α-helices in the three-dimensional structure of Sgs1 are indicated by boxes above. Identical or similar residues are shaded in gray. Shown below is the amino-acid substitution K1270V used in the generation of BLM(K1270V). See text for details. The figure was adapted from Liu *et al* (1999).

Hickson, 2003). The HRDC domain is thought to function as an auxiliary DNA-binding domain and, structurally, it resembles domains found in many DNA-metabolizing enzymes such as helicases, polymerases and recombinases (Morozov *et al*, 1997; Liu *et al*, 1999). How these conserved motifs impact on the biochemical properties of RecQ helicases and affect the *in vivo* function of these enzymes has not been determined.

In addition to the presence or absence of the aforementioned functional domains, the different cellular functions of the various vertebrate RecQ helicases likely depend on their ability to form specific interactions with different protein partners. BLM is proposed to act in a complex with replication protein A and the type IA topoisomerase, topoisomerase IIIα (hTOPO IIIα) (Brosh *et al*, 2000; Johnson *et al*, 2000; Wu *et al*, 2000; Meetei *et al*, 2003). This association with a type IA topoisomerase is evolutionarily conserved, since Sgs1p also acts together with Top3p, the only type IA topoisomerase expressed in budding yeast (Gangloff *et al*, 1994; Bennett and Wang, 2001; Fricke *et al*, 2001). *top3* mutant cells have elevated levels of recombination (Wallis *et al*, 1989), which can be suppressed, at least partially, by inactivation of either Sgs1p or Rad52p, the latter of which is required for all forms of homologous recombination (Gangloff *et al*, 1994; Oakley *et al*, 2002; Shor *et al*, 2002). The conserved coupling of a RecQ helicase and a type IA topoisomerase, therefore, appears to have a central role in regulating recombination levels in the cell (Wu and Hickson, 2001). In particular, Sgs1p and BLM appear to suppress the formation of crossover products that arise from the resolution of homologous recombination intermediates containing Holliday junctions (Ira *et al*, 2003; Wu and Hickson, 2003). We have recently proposed a mechanism by which this is achieved by BLM. Together with hTOPO IIIα, BLM can catalyze double Holliday junction dissolution (DHJ), a reaction mechanism in which DHJs are resolved exclusively into non-crossover recombinant products (Wu and Hickson, 2003). Here, we have demonstrated that BLM cannot by substituted by other RecQ helicases in dissolution reactions containing hTOPO IIIα. Furthermore, we reveal the first biochemical function for the HRDC domain of a RecQ helicase through the demonstration of a requirement for this domain in the specific recognition, processing and dissolution of DHJs.

Results

Double Holliday junction dissolution is specific for BLM

Despite the similar biochemical properties of many RecQ helicases *in vitro,* and their ability to act upon a wide variety of DNA structures, an elevated frequency of SCEs is thought to be a feature unique to BLM-deficient cells among human RecQ helicase mutants. We set out, therefore, to examine the apparent contradiction between, on the one hand, the promiscuous and redundant biochemical activities of RecQ

helicases *in vitro* and, on the other, the distinct cellular phenotypes of RecQ helicase mutants. To do this, we analyzed the ability of three other human RecQ helicases to catalyze dissolution in conjunction with hTOPO IIIα. Dissolution was assessed using an oligonucleotide-based molecule (DHJ) that we had used previously to assay for dissolution activity (Figure 2) (Fu *et al*, 1994; Wu and Hickson, 2003). Using this substrate, we found that WRN, RECQ1 and RECQ5β could not substitute for BLM in dissolution reactions with hTOPO IIIα, indicating that the reaction mechanism of dissolution displays a high degree of specificity for BLM (Figure 3).

The N-terminal domain of BLM is not required to catalyze dissolution

The apparently specific ability of BLM to catalyze dissolution indicated that the BLM protein itself must possess biochemical functions that are not present in the other human RecQ helicases. To identify structural features of BLM that are required for catalysis of dissolution, we generated a series of truncated versions of BLM that all retained the catalytic core of BLM (Figure 1) and assessed the ability of these BLM variants to catalyze dissolution. Residues 1–133 of BLM contain an hTOPO IIIα-interaction domain (Hu *et al*, 2001). We therefore wanted to determine if this interaction domain was required for dissolution. Deletion of residues 1–212 of BLM, and thus removal of this hTOPO IIIα-interaction domain, did not affect the ability of BLM to catalyze dissolution (Figure 4A). Moreover, a truncated BLM protein generated by removal of the entire nonconserved N-terminal domain of BLM (residues 1–641) was still able to catalyze dissolution (data not shown). Dissolution of DHJ is a symmetrical reaction and generates two circular products in an ATP-dependent manner. To eliminate the possibility that both of the N-terminally truncated proteins catalyze a pseudodissolution reaction by, for instance, asymmetric nicking of the substrate in the unlabeled oligonucleotide, we monitored the

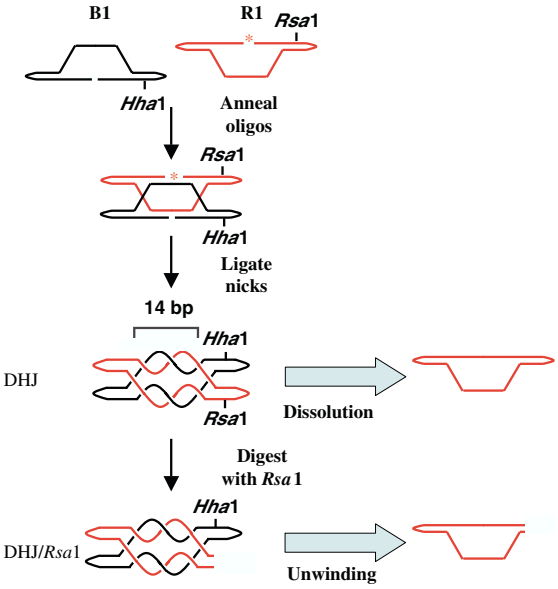

Figure 2 Outline of the strategy used in the generation of the DHJ-containing substrates analyzed in this study, DHJ and DHJ/*Rsa*1. DHJ comprises two oligonucleotides (B1 and R1), each of which contains two regions of complementary sequences giving rise to two 11 bp internal duplex arms. When incubated together, B1 and R1 anneal to form a molecule that contains two juxtaposed HJs separated by two 14 bp heteroduplex regions (Fu *et al*, 1994; Wu and Hickson, 2003). These heteroduplexes contain approximately 1.5 helical turns, which results in the catenation of B1 and R1 when both oligonucleotides are circularized by ligation. Topologically relevant helical turns are shown. Each oligonucleotide can be detected individually by the 5′ end-labeling of one of the oligonucleotides prior to annealing. In this scheme, oligonucleotide R1 has been labeled, as indicated by the asterisk. Blue arrows indicate the enzymatic activity each substrate was used to assess and the detectable product generated from each substrate. Dissolution of DHJ results in the decatenation of B1 and R1 releasing the two oligonucleotides as circular DNA species, each of which has a faster mobility on denaturing PAGE than the DHJ substrate (Wu and Hickson, 2003). Unwinding of DHJ/*Rsa*1 by BLM releases linear R1 and circular B1.

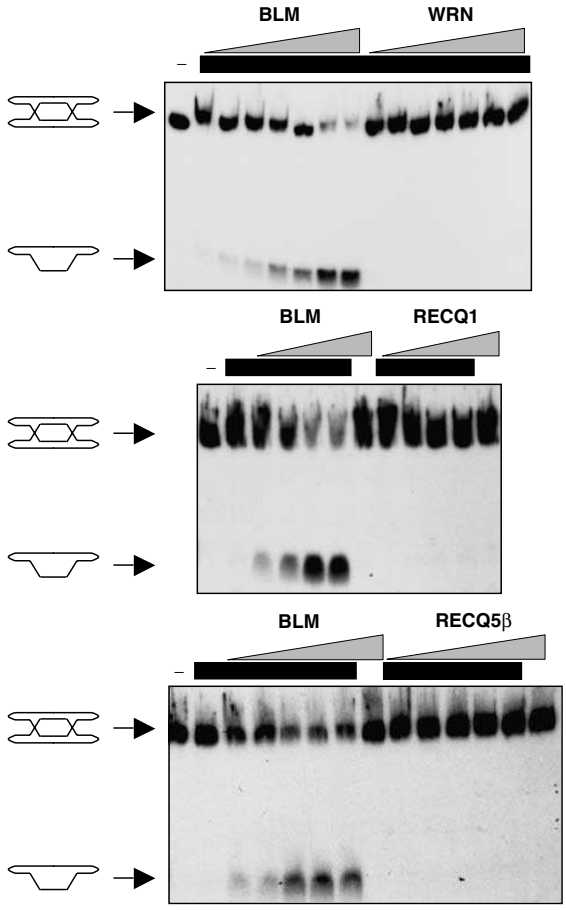

Figure 3 Dissolution is specifically catalyzed by BLM. Dissolution reactions containing a series of two-fold dilutions of BLM (upper panel, 5, 2.5, 1.25, 0.625, 0.3125, 0.15 and 0.075 nM; the middle and lower panels did not contain the three and two lowest concentrations, respectively), WRN (15, 7.5, 3.75, 1.87, 0.94, 0.47 and 0.24 nM), RECQ1 (100, 50, 25 and 12.5 nM) or RECQ5β (80, 40, 20, 10 and 5 nM), as indicated above the panels. Lanes containing hTOPO IIIα (250 nM) are indicated above by black bars. Positions of the DHJ substrate and the dissolution product are shown on the left. For simplicity, the intertwining of the strands of DHJ is omitted.

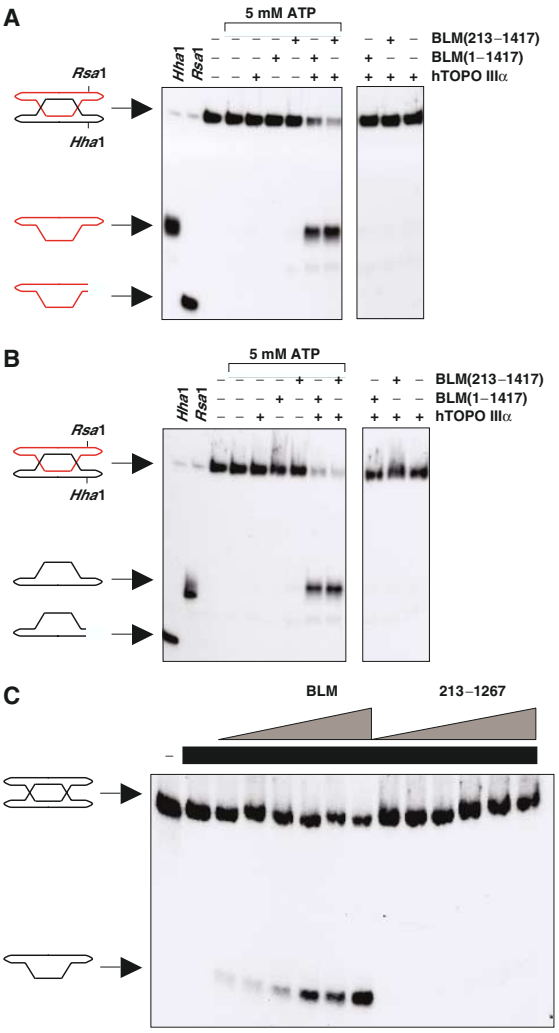

Figure 4 The C- but not the N-terminal domain of BLM is required for dissolution. (**A**) Dissolution reactions in the presence or absence of 5 mM ATP and containing hTOPO IIIα and full-length BLM(1–1417) or BLM(213–1417), as indicated. In the DHJ substrate, oligonucleotide R1 is labeled. Positions of the DHJ substrate, dissolution product and products of the indicated restriction digests, confirming the identity of the labeled oligonucleotide, are shown on the left. (**B**) Identical reactions to those shown in (A) were carried out except that a DHJ molecule was used in which oligonucleotide B1 was labeled. (**C**) Dissolution reactions containing a series of two-fold dilutions of BLM (highest concentration, 5 nM) or BLM(213–1267) (highest concentration, 7 nM). Lanes containing hTOPO IIIα (250 nM) are indicated by black bars. Positions of the DHJ substrate and dissolution product are shown on the left.

fate of both oligonucleotides by performing dissolution reactions on the two forms of DHJ in which either oligonculeotide R1 or B1 was labeled. The reaction catalyzed by both of the N-terminal BLM truncation mutants on each DHJ substrate was indistinguishable from that carried out by full-length BLM with regard to ATP dependency and the structure of the reaction products, that is, two intact circular species (Figure 4A and B and data not shown). Together, these data indicate that the N-terminal domain of BLM, and thus a physical

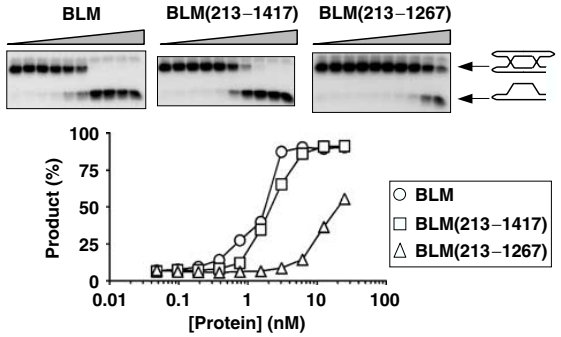

Figure 5 The C-terminal domain of BLM is required for efficient unwinding of DHJs. Helicase assays using DHJ/*Rsa*1 and a series of two-fold dilutions of BLM, BLM(213–1417) or BLM(213–1267) on DHJ/*Rsa*1, as indicated. The positions of DHJ/*Rsa*1 and the unwound product are shown on the right. The graph shows quantification of the level of unwound product generated by BLM (circles), BLM(213–1417) (squares) and BLM(213–1267) (triangles) on DHJ/*Rsa*1. Note that the scale on the horizontal axis is logarithmic.

association of hTOPO IIIα with this portion of BLM, is not required for the catalysis of dissolution.

The C-terminal domain of BLM is essential for dissolution

The dispensable nature of the N-terminal domain of BLM for dissolution led us to examine the role of the C-terminal domain of BLM using a previously described, truncated version of BLM that consists of residues 213–1267, herein designated BLM(213–1267) (Wu and Hickson, 2002a). Despite being an active helicase, we found that BLM(213–1267), in contrast to BLM(213–1417), which contains the natural C-terminus of BLM, was defective in catalyzing dissolution (Figure 4C). This indicates that in addition to the helicase domain, residues 1268–1417 of BLM are required for dissolution (Figure 4).

The RecQ family HRDC domain is required for the binding to and unwinding of double Holliday junctions

The deletion of residues 1268–1417 to generate BLM(213–1267) resulted in truncation of the HRDC domain, which consists of residues 1210–1290 in BLM (Figure 1A and B). We reasoned, therefore, that the failure of BLM(213–1267) to catalyze dissolution might be reflected in a diminished ability to interact with and/or process DHJs as a result of the inactivation of the DNA-binding function of the BLM HRDC domain. To address this, we compared the ability of BLM and BLM(213–1267) to unwind, in the absence of hTOPO IIIα, a modified DHJ molecule (DHJ/*Rsa*1) in which DHJ had been digested with *Rsa*1 (Wu and Hickson, 2003). The linearization of oligonucleotide R1 by *Rsa*1 results in the topological unlinking of the two constituent oligonucleotides of DHJ and thus creates a substrate that can be disrupted by thermal denaturation or by a helicase activity (Figure 2) (Wu and Hickson, 2003). The intact DHJ substrate is resistant to conventional unwinding due to its covalently closed nature. While we found that both BLM and BLM(213–1267) were able to unwind DHJ/*Rsa*1, BLM(213–1267) displayed an approximately 10-fold reduction in helicase activity toward this substrate compared to that of full-length BLM (Figure 5).

This impaired helicase activity was solely due to the loss of residues 1268–1417 of BLM, since BLM(213–1417), which lacks only the N-terminal 1–212 residues, displayed helicase activity on this substrate that was equivalent to that displayed by full-length BLM (Figure 5).

One possible explanation for the reduced helicase activity displayed by BLM(213–1267) was that the truncated protein has a reduced affinity for DHJs. To analyze this, we employed two independent means to compare the binding affinities of BLM(213–1417) and BLM(213–1267) for the DHJ substrate: a filter-binding assay, in which we measured protein-dependent retention of DHJ on a nitrocellulose membrane, and an electrophoretic mobility shift assay (EMSA), in which potentially different protein/DHJ complexes were visualized as a result of their reduced electrophoretic mobility compared to protein-free DHJ. Using the filter-binding assay, we found that BLM(213–1267) had a significantly reduced ability to bind DHJ as compared to BLM(213–1417) (Figure 6A). Using EMSAs, BLM(213–1417) was found to generate two differentially retarded species and a small amount of material that could not be resolved and was retained in the gel wells (Figure 6B). The level of all retarded species was dramatically reduced when BLM(213–1267) replaced BLM(213–1417) in the EMSA analyses (Figure 6B), thus confirming the conclusion of the filter-binding assay.

Next, we addressed the question of whether the observed reduction in DNA-binding affinity and helicase activity of BLM(213–1267) was specific for DHJ structures. To do this, we compared the helicase activities of BLM, BLM(213–1417) and BLM(213–1267) on a conventional helicase substrate, a forked partial duplex. Interestingly, all three proteins displayed very similar levels of helicase activity on this substrate and, in contrast to the results with the DHJ substrate, BLM and BLM(213–1267) displayed similar binding affinities for the forked duplex substrate (Figure 7). Together, these data strongly suggest that the C-terminal domain of BLM contains a DNA structure-specific binding motif, and implicate residues 1268–1417 of BLM in the processing of DHJ structures.

To provide further support for the proposal that it is loss of the HRDC domain that is responsible for the reduced ability of BLM(213–1267) to unwind DHJ/*Rsa*1, a comparison was made between the activities of *E. coli* RecQ and a truncated version of this protein (residues 1–523) that lacks the entire HRDC domain, RecQ(1–523) (Figure 1A and B) (Bernstein and Keck, 2003). Both proteins were able to unwind DHJ/*Rsa*1 to some extent, but RecQ(1–523) had a much reduced ability to unwind this molecule compared to full-length RecQ (>10-fold reduction; Figure 8). As was the case with BLM, loss of the RecQ HRDC domain appeared to specifically affect the helicase activity of RecQ on the DHJ/*Rsa*1 substrate since

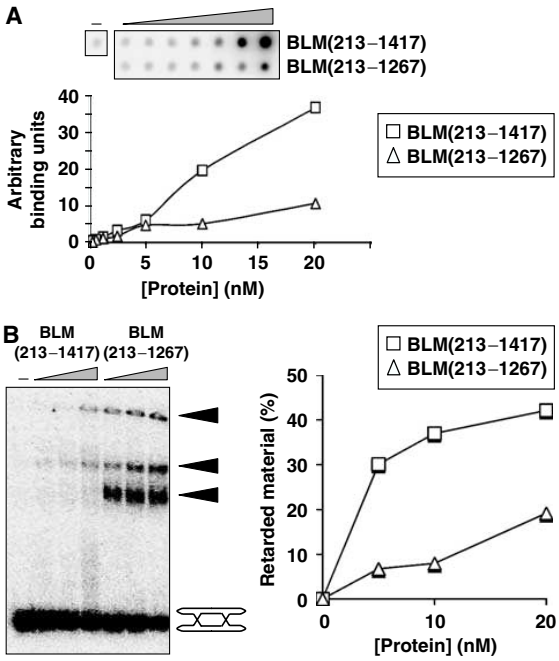

Figure 6 The C-terminal domain of BLM is required for efficient binding to DHJs. (**A**) DNA filter-binding assay using a series of two-fold dilutions of BLM(213–1417) or BLM(213–1267) on DHJ. The graph shows the quantification of the relative level of DNA bound to the filter in reactions containing either BLM(213–1417) (squares) or BLM(213–1267) (triangles). (**B**) DNA EMSA using a series of two-fold dilutions of BLM(213–1417) or BLM(213–1267) on DHJ, as indicated above the lanes. The positions of the unbound substrate and protein–DNA complexes (black arrowheads) are indicated on the right. The graph shows the quantification of the total amount of DNA bound by BLM(213–1417) (squares) or BLM(213–1267) (triangles).

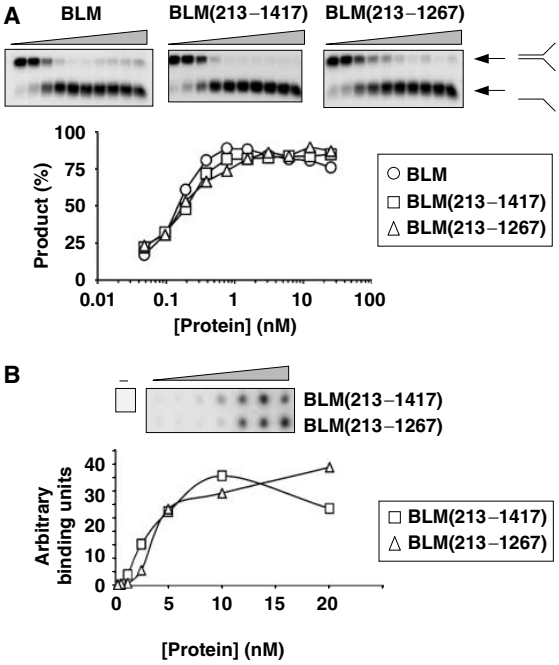

Figure 7 The C-terminal domain of BLM is not required for the unwinding or binding of forked duplexes. (**A**) Helicase assays using a series of two-fold dilutions of BLM, BLM(213–1417) and BLM(213–1267) on a forked partial duplex substrate. The positions of the forked duplex and the unwound product are shown on the right. The graph shows quantification of the amount of unwound product generated by BLM (circles), BLM(213–1417) (squares) or BLM(213–1267) (triangles). (**B**) DNA filter-binding assay using a series of two-fold dilutions of BLM or BLM(213–1267) on a forked partial duplex substrate. The graph shows quantification of the relative amount of DNA bound to the filter in reactions containing BLM(213–1417) (squares) or BLM(213–1267) (triangles).

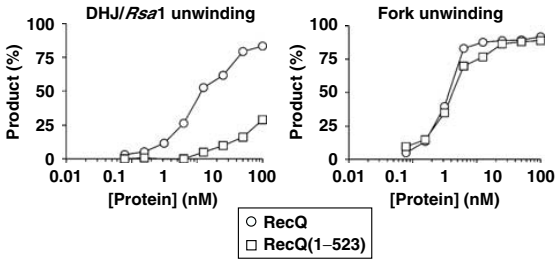

Figure 8 The *E. coli* RecQ HRDC domain is required for the unwinding of DHJ/*Rsa*1 but not of a forked duplex. Helicase assays using RecQ and RecQ(1–523) on either DHJ/*Rsa*1 (left) or a forked partial duplex (right) substrate. The graphs show the quantification of unwound product for each substrate for RecQ (circles) and RecQ(1–523) (squares). Note that the scale on the horizontal axis is logarithmic.

it had no significant effect on its helicase activity on a forked DNA substrate (Figure 8). These data suggest a conserved function for the HRDC domain of RecQ family helicases in the specific processing of DHJs. The fact that the RecQ and BLM HRDC domains apparently have similar functions in facilitating the efficient unwinding of DHJ/*Rsa*1 raised the possibility that RecQ might also catalyze dissolution together with bacterial Top3. RecQ and Top3 have been shown to cooperate in the mediation of a strand passage activity that facilitates the catenation and decatenation of covalently closed plasmid DNAs (Harmon *et al*, 1999). However, we found that RecQ and Top3 could not catalyze dissolution under conditions that supported dissolution by BLM and hTOPO IIIα (data not shown).

Lysine-1270 of BLM is required for efficient dissolution activity

Thus far, we conclude that the inability of BLM(213–1267) to catalyze dissolution is likely due to the absence of a functional HRDC domain, which had been inactivated by truncation. However, to demonstrate this directly and to eliminate the possibility that the truncation of the C-terminal 150 residues to generate BLM(213–1267) might have had long-range effects on other portions of the BLM protein and thereby led to inactivation of non-HRDC-mediated functions, we sought to abrogate the HRDC domain function in the context of the full-length protein. The similarity of the predicted secondary structure of the HRDC domain in RecQ helicases to motifs in unrelated DNA-metabolizing enzymes suggests that it is the conserved protein fold of the HRDC domain that is important for function. We set out, therefore, specifically to disrupt the conformation of the HRDC domain in BLM by site-directed mutagenesis. Initial attempts involved either the substitution of proline for the highly conserved alanine-1250 residue in order to destabilize α-helix 2 of the HRDC domain, or the creation of an internal deletion removing residues 1251–1262 to truncate α-helix 2 and remove α-helix 3 (Figure 1B). However, neither of these proteins could be expressed successfully, indicating that disruption of the fold of the HRDC domain likely reduces the solubility and/or stability of BLM. As an alternative, we chose to mutate highly conserved residues that, in the predicted three-dimensional structure of the BLM HRDC domain, reside on the protein surface. We reasoned that such residues

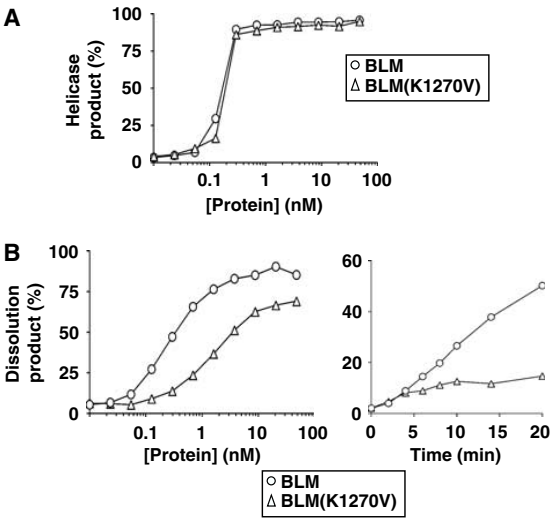

Figure 9 Lysine-1270 is required for efficient catalysis of dissolution. (**A**) Graph of relative helicase activity for BLM (circles) and BLM(K1270V) (triangles) on a forked partial duplex substrate. (**B**) Graph of relative dissolution activity catalyzed by BLM (circles) and BLM(K1270V) (triangles) as a function of either protein concentration (left) with a logarithmic scale on the horizontal axis or time in the presence of a fixed protein concentration of 0.8 nM (right).

were less likely to be essential for the overall structural integrity of the HRDC domain, but may be important for function through the mediation of intermolecular interactions. Lysine-1329 of Sgs1 has been shown to contact ssDNA, consistent with the role of the HRDC domain as an auxiliary DNA-binding domain (Liu *et al*, 1999). This residue is conserved among RecQ helicases and corresponds to residue 1270 in BLM (Figure 1B). We therefore mutated the *BLM* cDNA to convert lysine-1270 to valine in the full-length BLM protein to generate BLM(K1270V). BLM(K1270V) could be expressed and purified to give protein yields that were comparable to those seen with wild-type BLM (data not shown). Purified BLM(K1270V) was active as a helicase, and had a level of activity on a forked partial duplex substrate that was indistinguishable from that of wild-type BLM (Figure 9A). The substitution of lysine-1270 to valine, therefore, did not appear to have any gross effect on the overall stability or the helicase activity of BLM. However, BLM(K1270V) had a substantially reduced ability in comparison with wild-type BLM to support dissolution together with hTOPO IIIα (Figure 9B). Time-course experiments performed with a fixed concentration of protein indicated an approximately eight-fold reduction in the rate of dissolution for BLM(K1270V) (Figure 9B). Taken together, these data reveal that lysine-1270 of the HRDC domain in BLM is essential for the efficient dissolution of DHJ.

Discussion

A cellular marker of BLM deficiency used in the diagnosis of BS is an abnormally high frequency of spontaneous SCEs. In normal cells, it has been proposed that SCEs are suppressed by the ability of BLM, together with hTOPO IIIα, to catalyze dissolution. This is an alternative mechanism to that of

endonuclease-mediated resolution of HJs, such as that catalyzed by RuvC, Mus81 or the XRCC3/RAD51C complex (Chen *et al*, 2001; Osman *et al*, 2003; West, 2003; Liu *et al*, 2004). Here, we have shown that despite being one of five highly related human RecQ helicases, BLM could not be substituted by WRN, RECQ1 or RECQ5β in dissolution reactions containing hTOPO IIIα. Structurally, proteins of the RecQ helicase family are modular in nature. Several members, including BLM, contain, in addition to the signature helicase domain, a number of identifiable sequence motifs. Previously (and in this study), we have shown that BLM-mediated dissolution requires ATP hydrolysis, indicating a requirement for the helicase domain of BLM in this reaction (Wu and Hickson, 2003). In this study, we have identified the HRDC domain of BLM as also being required for dissolution. The structural similarity of the HRDC domain found in RecQ helicases to domains found in other DNA-metabolizing enzymes strongly indicates a role in mediating contacts with DNA. However, the RecQ helicase HRDC domain is clearly not required for intrinsic helicase activity since we demonstrated that variants of both BLM and RecQ that lack HRDC domains have a helicase activity on forked duplexes that is similar to that of their respective full-length proteins. Rather, we propose that the HRDC domain found in RecQ helicases performs a more specialized role in the recognition of alternate DNA structures, and, more specifically, that it is required for the efficient unwinding of DHJ structures. In particular, we have shown that the amino-acid substitution K1270V in BLM, which is predicted to alter the charge of the DNA-binding face of the HRDC domain, resulted in a diminished ability to mediate dissolution. This is the first specific biochemical function to have been ascribed to the HRDC domain. We did not attempt to complement the hyper-SCE phenotype of BS cells by expression of the *BLM(K1270V)* cDNA since we and others (Ellis *et al*, 1999; Hu *et al*, 2001; Davies *et al*, 2004) have made the observation that complementation with the wild-type *BLM* cDNA is often only partial and results in a broad range of SCE frequencies. Therefore, given that the BLM(K1270V) mutant is only partially defective for HRDC function and can still catalyze dissolution, to some extent, we think it is unlikely that any statistically significant difference between BLM(K1270V) and BLM to correct the elevated SCEs seen in BS cells will be demonstrable. However, Yankiwski *et al* (2001) have shown that expression of a mutant BLM cDNA, which contains an internal deletion that removes the whole of the HRDC domain and thus will be completely defective for HRDC function, is unable to complement the hyper-SCE phenotype of BS cells. This observation is consistent with the proposal that there is a direct link between the dissolution of DHJs and the suppression of SCEs *in vivo*.

While the HRDC domain is necessary for BLM to catalyze dissolution, its presence in other RecQ helicases is not sufficient to facilitate dissolution. One question that arises from this study, therefore, is does the HRDC domain function in a similar manner in those RecQ helicases where it is present or has it evolved different but related auxiliary functions that contribute to the functional diversification of RecQ helicases? Superficially, the BLM and RecQ HRDC domains appear to have a similar role, *in vitro*, in the specific recognition of DHJs. An HRDC domain is also present in WRN. However, unlike BS cells, Werner syndrome cells do not show obvious alterations in the levels of genome-wide recombination, but do have telomere maintenance defects (Wyllie *et al*, 2000; Crabbe *et al*, 2004). Indeed, in murine models of WS, many of the phenotypes of WS are only manifested in the presence of a second mutation that inactivates telomerase (Chang *et al*, 2004; Du *et al*, 2004). Therefore, one role for WRN may be in a recombination-dependent pathway that acts to maintain telomeres in the absence of telomerase. The HRDC domain of WRN may therefore have evolved a role in the specific recognition of recombination structures that arise at telomeres (Opresko *et al*, 2004). Structural comparisons of the RecQ and Sgs1 HRDC domains indicate that the domain is a highly versatile DNA-binding module that can support several different DNA-binding modes (Liu *et al*, 1999; DA Bernstein and JL Keck, unpublished data). Indeed, the distribution of surface charge of the HRDC domain, to which lysine-1270 of BLM contributes, is quite distinct between Sgs1, BLM and WRN, which is consistent with the notion that the HRDC domain may have evolved different roles in different RecQ helicases (Liu *et al*, 1999, DA Bernstein and JL Keck, unpublished data).

We have demonstrated that the entire N-terminal domain of BLM is dispensable for dissolution. This result was somewhat surprising since this portion of BLM contains an hTOPO IIIα-interaction domain that is essential *in vivo* for the interaction with hTOPO IIIα and for the suppression of SCEs (Hu *et al*, 2001). Moreover, a similar functional domain organization exists in Sgs1, where the N-terminal domain of Sgs1p is required for the interaction with Top3p (Gangloff *et al*, 1994; Bennett *et al*, 2000; Fricke *et al*, 2001). One possible explanation for these apparently contradictory *in vitro* and *in vivo* requirements for a physical association of BLM and hTOPO IIIα is that, *in vivo*, the physical association between hTOPO IIIα and the N-terminal domain of BLM may facilitate, not a biochemical activity, but rather the recruitment of hTOPO IIIα to its correct subcellular localization. This proposal is consistent with the mislocalization of hTOPO IIIα observed in BS cells (Wu *et al*, 2000).

RecQ and Top3, respectively, constitute the sole RecQ helicase family member and topoisomerase III enzyme in *E. coli*. The fact that these two enzymes were unable to catalyze DHJ dissolution suggests that the ancestral function of coupling the activities of a RecQ helicase and topoisomerase III may not be to catalyze dissolution. Indeed, in contrast to BS cells, RecQ mutants have decreased, not increased, levels of crossovers (Kusano *et al*, 1994). Dissolution results exclusively in non-crossover products and therefore suppresses the exchange of genetic material between molecules engaged in the process of homologous recombination. We propose that this mechanism to resolve recombination intermediates evolved with the advent of diploid organisms with large genomes containing repetitive sequences. In such organisms, the suppression of crossover events during recombinational repair is paramount for the prevention of mutagenic genomic rearrangements that can arise when the DNA molecules participating in recombinational repair are nonsisters. In particular, crossing-over in mammalian cells between sequences lying on homologous chromosomes can lead to loss of heterozygosity, a known driver of the tumorigenesis process. Notably, Blm-deficient mice show excessive loss of heterozygosity and accelerated tumor development (Luo *et al*, 2000).

In summary, we have shown that the RecQ helicase family HRDC domain confers DNA structure specificity and, in BLM, is required for the dissolution of DHJs. Further analyses to elucidate how the HRDC domain confers structural specificity and how it may function differentially in the various RecQ helicase family members will be crucial in our understanding of the role played by these enzymes in the maintenance of genome integrity and the suppression of tumorigenesis in man.

Materials and methods

Proteins

BLM, BLM (K1270V), BLM(213–1267) and BLM(213–1417) proteins were expressed in yeast and purified by nickel-chelate affinity chromatography using methods described previously (Karow *et al*, 1997). WRN, RECQ1, RECQ5β, RecQ and RecQ(1–523) were expressed and purified as described previously (Brosh *et al*, 1999; Bernstein and Keck, 2003; Bernstein *et al*, 2003; Cui *et al*, 2004; Garcia *et al*, 2004). The expression construct for BLM(K1270V) was generated by replacing in the yeast expression vector, pJK1, the *Hin*dIII/*Bam*HI fragment, internal to the BLM cDNA, with a PCR-generated mutant fragment containing the desired single codon substitution. hTOPO IIIα was a kind gift from Drs Hélène Goulaouic and Jean-François Riou (Goulaouic *et al*, 1999).

DNA substrates

DHJ, DHJ/*Rsa*1 and partial duplex fork substrates were prepared and purified as described previously (Mohaghegh *et al*, 2001; Wu and Hickson, 2003).

Dissolution and unwinding assays

Reactions were carried out in a buffer containing 50 mM Hepes–KOH, pH 7.2, 50 mM NaCl, 4 mM $MgCl_2$, 5 mM ATP, 1 mM DTT and various combinations of proteins and DNA substrates, as indicated in the figure legends. Reactions were incubated at 37°C for 60 min, unless otherwise stated, and stopped by the addition of 1% SDS and 50 mM EDTA. Samples were deproteinized by the addition of proteinase K and a further incubation at 37°C for 15 min. Dissolution and unwinding reactions were subjected, respectively, to 8% denaturing and 10% native PAGE. Gels were dried and subjected to PhosphorImage analysis using a STORM 840 scanner and ImageQuant software.

DNA-binding filter assays

DHJ was incubated with varying concentrations of protein, as indicated in the figure legends, in reaction buffer containing 20 mM triethanolamine–HCl, pH 7.5, 4 mM $MgCl_2$, 10 μg/ml BSA, 2 mM ATPγS and 1 mM DTT at 37°C for 20 min. Reactions containing the forked duplex were performed as described above for the DHJ, with the exception that the reaction buffer contained 2 mM $MgCl_2$. Reactions were then adsorbed under vacuum onto a nitrocellulose membrane using a dot-blot manifold apparatus. Each reaction spot was then washed with 500 μl reaction buffer under vacuum before the membrane was air-died and subjected to PhosphorImage analysis using a STORM 840 scanner and ImageQuant software.

DNA-binding EMSA

DHJ was incubated with varying concentrations of protein, as indicated in the figure legends, in reaction buffer containing 20 mM triethanolamine–HCl, pH 7.5, 4 mM $MgCl_2$, 10 μg/ml BSA, 2 mM ATPγS and 1 mM DTT at 37°C for 20 min. Samples were then fixed by the addition of 0.25% glutaraldehyde before being subjected to 5% PAGE. Gels were dried and subjected to PhosphorImage analysis using a STORM 840 scanner and ImageQuant software.

Acknowledgements

We thank members of the Genome Integrity group for useful discussions, and Dr Peter McHugh for comments on the manuscript. This work was funded by Cancer Research UK and The Croucher Foundation (Hong Kong).

References

Bachrati CZ, Hickson ID (2003) RecQ helicases: suppressors of tumorigenesis and premature aging. *Biochem J* **374:** 577–606

Bennett RJ, Noirot-Gros MF, Wang JC (2000) Interaction between yeast sgs1 helicase and DNA topoisomerase III. *J Biol Chem* **275:** 26898–26905

Bennett RJ, Wang JC (2001) Association of yeast DNA topoisomerase III and Sgs1 DNA helicase: studies of fusion proteins. *Proc Natl Acad Sci USA* **98:** 11108–11113

Bernstein DA, Keck JL (2003) Domain mapping of *Escherichia coli* RecQ defines the roles of conserved N- and C-terminal regions in the RecQ family. *Nucleic Acids Res* **31:** 2778–2785

Bernstein DA, Zittel MC, Keck JL (2003) High-resolution structure of the *E. coli* RecQ helicase catalytic core. *EMBO J* **22:** 4910–4921

Brosh Jr RM, Li JL, Kenny MK, Karow JK, Cooper MP, Kureekattil RP, Hickson ID, Bohr VA (2000) Replication protein A physically interacts with the Bloom's syndrome protein and stimulates its helicase activity. *J Biol Chem* **275:** 23500–23508

Brosh Jr RM, Orren DK, Nehlin JO, Ravn PH, Kenny MK, Machwe A, Bohr VA (1999) Functional and physical interaction between WRN helicase and human replication protein A. *J Biol Chem* **274:** 18341–18350

Brosh Jr RM, von Kobbe C, Sommers JA, Karmakar P, Opresko PL, Piotrowski J, Dianova I, Dianov GL, Bohr VA (2001) Werner syndrome protein interacts with human flap endonuclease 1 and stimulates its cleavage activity. *EMBO J* **20:** 5791–5801

Chaganti RS, Schonberg S, German J (1974) A manyfold increase in sister chromatid exchanges in Bloom's syndrome lymphocytes. *Proc Natl Acad Sci USA* **71:** 4508–4512

Chang S, Multani AS, Cabrera NG, Naylor ML, Laud P, Lombard D, Pathak S, Guarente L, DePinho RA (2004) Essential role of limiting telomeres in the pathogenesis of Werner syndrome. *Nat Genet* **36:** 877–882

Chen XB, Melchionna R, Denis CM, Gaillard PH, Blasina A, Van de Weyer I, Boddy MN, Russell P, Vialard J, McGowan CH (2001) Human Mus81-associated endonuclease cleaves Holliday junctions *in vitro*. *Mol Cell* **8:** 1117–1127

Crabbe L, Verdun RE, Haggblom CI, Karlseder J (2004) Defective telomere lagging strand synthesis in cells lacking WRN helicase activity. *Science* **306:** 1951–1953

Cui S, Arosio D, Doherty KM, Brosh Jr RM, Falaschi A, Vindigni A (2004) Analysis of the unwinding activity of the dimeric RECQ1 helicase in the presence of human replication protein A. *Nucleic Acids Res* **32:** 2158–2170

Davies SL, North PS, Dart A, Lakin ND, Hickson ID (2004) Phosphorylation of the Bloom's syndrome helicase and its role in recovery from S-phase arrest. *Mol Cell Biol* **24:** 1279–1291

Du X, Shen J, Kugan N, Furth EE, Lombard DB, Cheung C, Pak S, Luo G, Pignolo RJ, DePinho RA, Guarente L, Johnson FB (2004) Telomere shortening exposes functions for the mouse Werner and Bloom syndrome genes. *Mol Cell Biol* **24:** 8437–8446

Ellis NA, Groden J, Ye TZ, Straughen J, Lennon DJ, Ciocci S, Proytcheva M, German J (1995) The Bloom's syndrome gene product is homologous to RecQ helicases. *Cell* **83:** 655–666

Ellis NA, Proytcheva M, Sanz MM, Ye TZ, German J (1999) Transfection of BLM into cultured bloom syndrome cells reduces the sister-chromatid exchange rate toward normal. *Am J Hum Genet* **65:** 1368–1374

Fricke WM, Kaliraman V, Brill SJ (2001) Mapping the DNA topoisomerase III binding domain of the Sgs1 DNA helicase. *J Biol Chem* **276:** 8848–8855

Fu TJ, Tse-Dinh YC, Seeman NC (1994) Holliday junction crossover topology. *J Mol Biol* **236:** 91–105

Gangloff S, McDonald JP, Bendixen C, Arthur L, Rothstein R (1994) The yeast type I topoisomerase Top3 interacts with Sgs1, a DNA helicase homolog: a potential eukaryotic reverse gyrase. *Mol Cell Biol* **14:** 8391–8398

Garcia PL, Liu Y, Jiricny J, West SC, Janscak P (2004) Human RECQ5β, a protein with DNA helicase and strand-annealing activities in a single polypeptide. *EMBO J* **23:** 2882–2891

Goulaouic H, Roulon T, Flamand O, Grondard L, Lavelle F, Riou JF (1999) Purification and characterization of human DNA topoisomerase IIIα. *Nucleic Acids Res* **27:** 2443–2450

Harmon FG, DiGate RJ, Kowalczykowski SC (1999) RecQ helicase and topoisomerase III comprise a novel DNA strand passage function: a conserved mechanism for control of DNA recombination. *Mol Cell* **3:** 611–620

Hickson ID (2003) RecQ helicases: caretakers of the genome. *Nat Rev Cancer* **3:** 169–178

Hu P, Beresten SF, van Brabant AJ, Ye TZ, Pandolfi PP, Johnson FB, Guarente L, Ellis NA (2001) Evidence for BLM and Topoisomerase IIIα interaction in genomic stability. *Hum Mol Genet* **10:** 1287–1298

Huang S, Li B, Gray MD, Oshima J, Mian IS, Campisi J (1998) The premature ageing syndrome protein, WRN, is a 3′→5′ exonuclease [letter]. *Nat Genet* **20:** 114–116

Ira G, Malkova A, Liberi G, Foiani M, Haber JE (2003) Srs2 and Sgs1–Top3 suppress crossovers during double-strand break repair in yeast. *Cell* **115:** 401–411

Johnson FB, Lombard DB, Neff NF, Mastrangelo MA, Dewolf W, Ellis NA, Marciniak RA, Yin Y, Jaenisch R, Guarente L (2000) Association of the Bloom syndrome protein with topoisomerase IIIα in somatic and meiotic cells. *Cancer Res* **60:** 1162–1167

Kamath-Loeb AS, Shen JC, Loeb LA, Fry M (1998) Werner syndrome protein. II. Characterization of the integral 3′→5′ DNA exonuclease. *J Biol Chem* **273:** 34145–34150

Karow JK, Chakraverty RK, Hickson ID (1997) The Bloom's syndrome gene product is a 3′–5′ DNA helicase. *J Biol Chem* **272:** 30611–30614

Kitao S, Shimamoto A, Goto M, Miller RW, Smithson WA, Lindor NM, Furuichi Y (1999) Mutations in RECQL4 cause a subset of cases of Rothmund–Thomson syndrome. *Nat Genet* **22:** 82–84

Kusano K, Sunohara Y, Takahashi N, Yoshikura H, Kobayashi I (1994) DNA double-strand break repair: genetic determinants of flanking crossing-over. *Proc Natl Acad Sci USA* **91:** 1173–1177

Liu Y, Masson JY, Shah R, O'Regan P, West SC (2004) RAD51C is required for Holliday junction processing in mammalian cells. *Science* **303:** 243–246

Liu Z, Macias MJ, Bottomley MJ, Stier G, Linge JP, Nilges M, Bork P, Sattler M (1999) The three-dimensional structure of the HRDC domain and implications for the Werner and Bloom syndrome proteins. *Struct Fold Des* **7:** 1557–1566

Luo G, Santoro IM, McDaniel LD, Nishijima I, Mills M, Youssoufian H, Vogel H, Schultz RA, Bradley A (2000) Cancer predisposition caused by elevated mitotic recombination in Bloom mice. *Nat Genet* **26:** 424–429

Meetei AR, Sechi S, Wallisch M, Yang D, Young MK, Joenje H, Hoatlin ME, Wang W (2003) A multiprotein nuclear complex connects Fanconi anemia and Bloom syndrome. *Mol Cell Biol* **23:** 3417–3426

Mohaghegh P, Karow JK, Brosh Jr RM, Bohr VA, Hickson ID (2001) The Bloom's and Werner's syndrome proteins are DNA structure-specific helicases. *Nucleic Acids Res* **29:** 2843–2849

Morozov V, Mushegian AR, Koonin EV, Bork P (1997) A putative nucleic acid-binding domain in Bloom's and Werner's syndrome helicases. *Trends Biochem Sci* **22:** 417–418

Oakley TJ, Goodwin A, Chakraverty RK, Hickson ID (2002) Inactivation of homologous recombination suppresses defects in topoisomerase III-deficient mutants. *DNA Repair (Amst)* **1:** 463–482

Oakley TJ, Hickson ID (2002) Defending genome integrity during S-phase: putative roles for RecQ helicases and topoisomerase III. *DNA Repair (Amst)* **1:** 175–207

Opresko PL, Otterlei M, Graakjaer J, Bruheim P, Dawut L, Kolvraa S, May A, Seidman MM, Bohr VA (2004) The Werner syndrome helicase and exonuclease cooperate to resolve telomeric D loops in a manner regulated by TRF1 and TRF2. *Mol Cell* **14:** 763–774

Osman F, Dixon J, Doe CL, Whitby MC (2003) Generating crossovers by resolution of nicked Holliday junctions: a role for Mus81–Eme1 in meiosis. *Mol Cell* **12:** 761–774

Shor E, Gangloff S, Wagner M, Weinstein J, Price G, Rothstein R (2002) Mutations in homologous recombination genes rescue top3 slow growth in *Saccharomyces cerevisiae*. *Genetics* **162:** 647–662

von Kobbe C, Karmakar P, Dawut L, Opresko P, Zeng X, Brosh Jr RM, Hickson ID, Bohr VA (2002) Colocalization, physical, and functional interaction between Werner and Bloom syndrome proteins. *J Biol Chem* **277:** 22035–22044

Wallis JW, Chrebet G, Brodsky G, Rolfe M, Rothstein R (1989) A hyper-recombination mutation in *S. cerevisiae* identifies a novel eukaryotic topoisomerase. *Cell* **58:** 409–419

Wang W, Seki M, Narita Y, Nakagawa T, Yoshimura A, Otsuki M, Kawabe Y, Tada S, Yagi H, Ishii Y, Enomoto T (2003) Functional relation among RecQ family helicases RecQL1, RecQL5, and BLM in cell growth and sister chromatid exchange formation. *Mol Cell Biol* **23:** 3527–3535

Watt PM, Hickson ID, Borts RH, Louis EJ (1996) SGS1, a homologue of the Bloom's and Werner's syndrome genes, is required for maintenance of genome stability in *Saccharomyces cerevisiae*. *Genetics* **144:** 935–945

West SC (2003) Molecular views of recombination proteins and their control. *Nat Rev Mol Cell Biol* **4:** 435–445

Wu L, Davies SL, North PS, Goulaouic H, Riou JF, Turley H, Gatter KC, Hickson ID (2000) The Bloom's syndrome gene product interacts with topoisomerase III. *J Biol Chem* **275:** 9636–9644

Wu L, Hickson ID (2001) RecQ helicases and topoisomerases: components of a conserved complex for the regulation of genetic recombination. *Cell Mol Life Sci* **58:** 894–901

Wu L, Hickson ID (2002a) The Bloom's syndrome helicase stimulates the activity of human topoisomerase IIIα. *Nucleic Acids Res* **30:** 4823–4829

Wu L, Hickson ID (2002b) RecQ helicases and cellular responses to DNA damage. *Mutat Res* **509:** 35–47

Wu L, Hickson ID (2003) The Bloom's syndrome helicase suppresses crossing over during homologous recombination. *Nature* **426:** 870–874

Wyllie FS, Jones CJ, Skinner JW, Haughton MF, Wallis C, Wynford-Thomas D, Faragher RG, Kipling D (2000) Telomerase prevents the accelerated cell ageing of Werner syndrome fibroblasts. *Nat Genet* **24:** 16–17

Yankiwski V, Noonan JP, Neff NF (2001) The C-terminal domain of the Bloom syndrome helicase is essential for genomic stability. *BMC Cell Biol* **2:** 11

Yu CE, Oshima J, Fu YH, Wijsman EM, Hisama F, Alisch R, Matthews S, Nakura J, Miki T, Ouais S, Martin GM, Mulligan J, Schellenberg GD (1996) Positional cloning of the Werner's syndrome gene. *Science* **272:** 258–262

Article V

The Bloom's syndrome helicase promotes the annealing of complementary single-stranded DNA

Chit Fang Cheok, Leonard Wu, Patrick L. Garcia, Pavel Janscak and Ian D. Hickson *Nucleic Acids Res. - in press* 2005

To this work I have contributed by providing BLM variant proteins and expression constructs.

Published online July 15, 2005

3932–3941 *Nucleic Acids Research, 2005, Vol. 33, No. 12*
doi:10.1093/nar/gki712

The Bloom's syndrome helicase promotes the annealing of complementary single-stranded DNA

Chit Fang Cheok, Leonard Wu, Patrick L. Garcia[1], Pavel Janscak[1] and Ian D. Hickson*

Cancer Research UK Laboratories, Weatherall Institute of Molecular Medicine, University of Oxford, John Radcliffe Hospital, Oxford OX3 9DS, UK and [1]Institute of Molecular Cancer Research, University of Zürich, August Forel-Strasse 7, CH-8008, Zürich, Switzerland

Received May 31, 2005; Revised and Accepted June 30, 2005

ABSTRACT

The product of the gene mutated in Bloom's syndrome, BLM, is a 3′–5′ DNA helicase belonging to the highly conserved RecQ family. In addition to a conventional DNA strand separation activity, BLM catalyzes both the disruption of non-B-form DNA, such as G-quadruplexes, and the branch migration of Holliday junctions. Here, we have characterized a new activity for BLM: the promotion of single-stranded DNA (ssDNA) annealing. This activity does not require Mg^{2+}, is inhibited by ssDNA binding proteins and ATP, and is dependent on DNA length. Through analysis of various truncation mutants of BLM, we show that the C-terminal domain is essential for strand annealing and identify a 60 amino acid stretch of this domain as being important for both ssDNA binding and strand annealing. We present a model in which the ssDNA annealing activity of BLM facilitates its role in the processing of DNA intermediates that arise during repair of damaged replication forks.

INTRODUCTION

Bloom's syndrome (BS) is a rare genetic disorder associated with several abnormalities, including proportional dwarfism, sunlight sensitivity and a predisposition to cancers of most types. The gene mutated in BS, *BLM*, encodes a protein comprising 1417 amino acids that is a member of the highly conserved RecQ family (1,2). This family includes Sgs1p of *Saccharomyces cerevisiae*, Rqh1p of *Schizosaccharomyces pombe*, and the WRN, RECQ1, RECQ4 and RECQ5 proteins in humans. WRN and RECQ4 are defective in Werner's and Rothmund–Thomson syndromes, respectively, which are disorders not only associated with cancer predisposition but also with some features of premature aging (2). Where tested, all RecQ family members are DNA helicases that translocate along DNA strands in the 3′–5′ direction. A number of studies have shown that RecQ helicases unwind a wide variety of different oligonucleotide-based DNA substrates, including forked duplexes, four-way junctions modeling the Holliday junction, and simple 3′-tailed duplexes. Moreover, RecQ helicases can even unwind non-B-form DNA structures, such as G-quadruplexes (3–7).

RecQ helicases are defined by a highly conserved domain that contains seven signature motifs (hereafter referred to as the helicase domain) (2). These sequence motifs are also found, in a related form, in many other RNA or DNA helicases from different families. Outside of the helicase domain there is much less sequence similarity between RecQ family members. Nevertheless, there are two additional identifiable domains that are found in some, but not all, RecQ family proteins. One of these, the RQC (RecQ C-terminal) domain, is apparently unique to the RecQ family and is found in BLM. Recent X-ray crystallographic analysis of *Escherichia coli* RecQ protein indicates that the RQC domain forms a so-called winged-helix structure that is implicated in the binding of DNA (8). Indeed, a previous study showed that the RQC domain of WRN binds several DNA structures, including a forked duplex and a four-way junction (9). Interestingly, in some RecQ helicases, the RQC domain also seems to direct protein–protein interactions (10–12). A second sequence feature found in certain RecQ helicases, including BLM, is the HRDC (helicase and RNaseD C-terminal) domain (13). This domain is poorly conserved at the primary sequence level, but seemingly has a well-conserved structural fold comprising five α-helices and a number of basic residues that constitute a putative DNA binding surface (14). This domain is not unique to RecQ helicases, being present also in RNaseD homologs and, in a related form, in some DNA polymerases and recombinases. In those RecQ helicases where the RQC and HRDC domains are present, it is possible that interactions with different DNA substrates are influenced by either or both of these putative auxiliary DNA binding regions in the enzyme. Nevertheless, because some RecQ enzymes only

*To whom correspondence should be addressed. Tel: +44 0 1865 222 417; Fax: +44 0 1865 222 431; Email: ian.hickson@cancer.org.uk

Nucleic Acids Research, 2005, Vol. 33, No. 12 3933

contain the helicase domain, and lack the RQC and HRDC domains, it seems highly likely that the helicase domain is both necessary and sufficient for at least some enzymatic activities. The functional role(s) of the RQC and HRDC domains can only be the subject of speculation at this stage, but a possible candidate is to extend the range of alternate DNA structures, such as G-quadruplexes or Holliday junctions, that can be recognized by a particular RecQ helicase.

Our studies of the RecQ helicase family are focused on the BLM protein. We have previously shown that BLM is a DNA structure-specific helicase that unwinds a wide variety of DNA molecules, although it is incapable of unwinding a blunt-ended DNA duplex (3,15). Nevertheless, it can disrupt a four-way junction modeling the Holliday junction recombination intermediate even if that substrate has blunt termini (15). Consistent with this activity being dependent upon branch migration, BLM has been shown to catalyze branch migration of bona fide Holliday junctions generated by the RecA recombinase (15). Here, we report a new activity for the BLM protein: the promotion of single-stranded DNA (ssDNA) annealing. We have characterized the biochemical properties of this strand annealing activity and have identified a short region of the C-terminal domain of BLM that is essential for this function. We provide evidence that strand annealing is influenced by ssDNA binding proteins, by nucleotide co-factors and by DNA length.

MATERIALS AND METHODS

Plasmids

Plasmids pJP71, pJP74 and pJP75, which were used for the expression of the truncated BLM variants, BLM642-1290, BLM642-1417 and BLM642-1350, respectively, were constructed as described previously (16). Briefly, the region of the *BLM* cDNA encoding residues 642–1290, 642–1350 or 642–1417 was amplified by PCR with primers introducing NcoI and SapI sites. The PCR product was digested with NcoI and SapI, and inserted between the NcoI and SapI sites of pTXB3 (NEB). Constructs for the expression of BLM213-1417 and BLM213-1267 have been described previously (17).

Protein purification

BLM, BLM213-1417 and BLM213-1267 were expressed as C-terminally hexahistidine-tagged proteins in the protease-deficient yeast strain JEL1 (MATα *leu2 trp1 ura3-52 prb1-1122 pep4-3 his3::PGAL10-GAL4*) and were purified as described previously (18). BLM642-1290, BLM642-1350 and BLM642-1417 were produced as C-terminal fusion proteins with the Mxe-CBD affinity tag in the *E.coli* BL21-Codonplus-(DE3)-RIL strain (Stratagene) and were purified as described previously (16). Human replication protein A (RPA) was kindly provided by Dr A Vindigni. *E.coli* ssDNA binding protein (SSB) was purchased from USB. All concentrations of proteins are given in terms of moles of monomer.

DNA substrates

All oligonucleotides used in this study were purchased from Sigma Genosys and were purified by PAGE. X12-1 (5′-CGGGTCAACGTGGGCAAAGATGTCCTAGCAATG-TAATCGTCTATGAGACG-3′) and its complement X12-2 (5′-GACGCTGCCGAATTCTGGCTTGCTAGGACATCTT-TGCCCACGTTGACCCG-3′) were used for the generation of the 31 bp forked duplex. DF-1 (5′-TGTAATCGTCTAT-GAGACGCGGGTCAACGTGGACATCTGCAAAGATGT-CCTAGCAATGTAATCGTCTATGAGACG-3′) and its complement DF-2 (5′-GACGCTGCCGAATTCTGGCTTGC-TAGGACATCTTTGCAGATGTCCACGTTGACCCGGAC-GCTGCCGAATTCTGGC-3′) were used for the generation of the twin-forked duplex. DS-50-1 (5′-GGCAAAGATGTC-CTAGCAACGGGTCAACGTGGGCAAAGATGTCCTAG-CAA-3′) and its complement DS-50-2 (5′-TTGCTAGGAC-ATCTTTGCCCACGTTGACCCGTTGCTAGGACATCTTT-GCC-3′) were used for the generation of the 50 bp duplex; DS-31-1 (5′-CGGGTCAACGTGGGCAAAGATGTCCTAG-CAA-3′) and its complement DS-31-2 (5′-TTGCTAGGA-CATCTTTGCCCACGTTGACCCG-3′) were used for the generation of 31 bp duplex; DS-15-1 (5′-GGCAAAGATG-TCCTA-3′) and its complement DS-15-2 (5′-TAGGACA-TCTTTGCC-3′) were used for the generation of the 15 bp duplex. X12-1, DF-1 DS-50-1, DS-31-1 and DS-15-1 were labeled at the 5′ end using T4 polynucleotide kinase (NEB) and [γ-^{32}P]ATP. The forked duplex used in helicase assays was generated by the annealing of X12-1 and X12-2. X12-1 was 5′-^{32}P-labeled before annealing. All concentrations of DNA substrates are given in terms of moles of oligonucleotides.

Helicase assays

The 31 bp forked duplex was prepared as described previously (18). Reactions (20 μl) were carried out at 37°C in buffer H (50 mM Tris–HCl, pH 7.5, 50 mM NaCl, 1 mM DTT and 0.1 mg/ml BSA) supplemented with 2 mM $MgCl_2$ and 2 mM ATP for 30 min in the presence of the indicated amounts of BLM and 1 nM of ^{32}P-end-labeled forked duplex substrate. Where indicated, SSB and RPA were added at a concentration of 60 and 3 nM, respectively. Reactions were stopped, and the samples were de-proteinized by the addition of stop buffer (50 mM EDTA, 1% SDS and 0.1 mg/ml proteinase K) and incubated at 37°C for 10 min. The reaction products were resolved on a native 10% (w/v) polyacrylamide gel (acrylamide to bis-acrylamide ratios 19:1) run in TBE at 30 mA per gel for 1 h at 4°C. The radiolabeled DNA was visualized using a PhosphorImager and the percentage DNA unwinding was quantified using ImageQuant software.

Strand annealing assays

DNA strand annealing activity was measured using fully or partially complementary oligonucleotides (at a concentration of 1 nM each), one of which was 5′-^{32}P-end-labeled. Reactions (20 μl) were carried out in buffer H supplemented with 2 mM $MgCl_2$ unless otherwise indicated for 30 min at 37°C with the indicated concentrations of BLM. For time-course experiments, an 80 μl reaction was initiated and 10 μl aliquots were removed at defined time points. Reactions were stopped by the addition of stop buffer (50 mM EDTA, 1% SDS and 0.1 mg/ml of proteinase K) and incubated for 10 min at 37°C. Where indicated, RPA was added (0.75–48 nM) to the reaction. The reaction products were analyzed as described for the helicase assay.

3934 *Nucleic Acids Research, 2005, Vol. 33, No. 12*

Gel retardation assays

Radiolabeled oligonucleotide (1 nM) was incubated with BLM or its truncated derivatives in 50 mM triethanolamine, pH 7.5, 2 mM $MgCl_2$, 2 mM ATPγS, 50 mM NaCl, 1 mM DTT and 0.1 μg/ml BSA for 20 min at 37°C. Glutaraldehyde (0.25%) was then added and the reaction was incubated for a further 10 min at 37°C. The protein–DNA complexes were resolved on a 5% (w/v) native polyacrylamide gel (acrylamide to bis-acrylamide ratios 19:1) run in TBE at 150 V for 70 min at 4°C. The radiolabeled DNA was visualized using a PhosphorImager and the percentage ssDNA bound was quantified using ImageQuant software.

RESULTS

During an analysis of the DNA helicase activity of BLM, we observed that the appearance of the ssDNA product of unwinding followed an unusual pattern. The extent of ssDNA product formation increased with increasing enzyme concentration up to a point, beyond which the level of unwound product declined substantially. An example of such a pattern is shown in Figure 1a and quantified in Figure 1d for a forked DNA duplex substrate. In this particular case, the level of the ssDNA product of unwinding peaked in reactions containing ~10 nM BLM and then declined significantly until it was only marginally above background in reactions containing 80 nM BLM (Figure 1a and quantified in Figure 1d). One explanation for this phenomenon was that high concentrations of BLM were able to promote the re-annealing of the ssDNA products of the unwinding reaction. Consistent with this was the observation that addition of either *E.coli* SSB or human RPA, two unrelated ssDNA binding proteins, could overcome the apparent decline in helicase activity seen at high BLM concentrations (Figure 1b–d). Previously, it was shown that BLM helicase activity is stimulated by RPA (19), but not by SSB, making it unlikely that the similar effects of RPA and SSB shown in Figure 1 involved direct stimulation of BLM helicase activity.

To analyze this putative ssDNA annealing activity of BLM more directly, we incubated different concentrations of BLM with the two single-stranded 50mer oligonucleotides (each at 1 nM) that were utilized to create the forked duplex used in the experiment shown in Figure 1. One of these oligonucleotides was 5′-end-labeled to allow strand annealing to be monitored. We found that BLM promoted efficient annealing of the two oligonucleotides. Using BLM concentrations of ⩾20 nM, ~90% of the labeled ssDNA was annealed to its complement (Figure 2a). Analysis of the kinetics of this reaction using a fixed BLM concentration (20 nM) indicated that 50% of the labeled oligonucleotide was annealed in <4 min (Figure 2b), using the reaction conditions described in Materials and Methods. Consistent with the notion that this reaction reflected genuine ssDNA annealing, addition of increasing concentrations of RPA progressively diminished the level of the annealed forked duplex product (Figure 2c). This confirmed that the ability of RPA to overcome the decline in helicase activity seen at high BLM concentrations (Figure 1c) was due to the inhibition of the ssDNA annealing activity of BLM.

BLM requires Mg^{2+} and ATP to catalyze DNA unwinding (18). We tested whether there was a similar co-factor

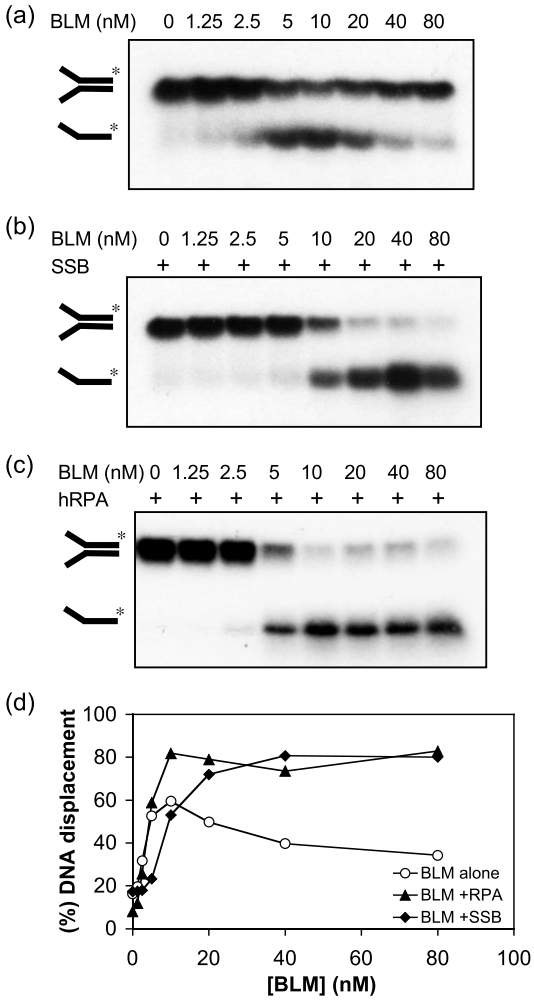

Figure 1. Inhibition of BLM helicase activity occurs at high protein concentrations, which is relieved by ssDNA binding proteins. (**a**) Unwinding of 1 nM of a 31 bp forked duplex catalyzed by different concentrations of BLM, as indicated above the lanes. (**b**) Unwinding of 1 nM of a 31 bp forked duplex catalyzed by BLM in the presence of 60 nM SSB or (**c**) in the presence of 3 nM RPA. In (a–c), the positions of the forked duplex and the ssDNA product of unwinding are indicated on the left. (**d**) Quantification of the helicase activity of BLM from the data in (a–c). All reactions were incubated for 30 min at 37°C.

requirement for the strand annealing function. As shown in Figure 3a, strand annealing promoted by BLM did not depend on the presence of Mg^{2+}. Indeed, the strand annealing activity was resistant to incubation with 50 mM EDTA (data not shown). Although there was a slight stimulation of strand annealing activity at a Mg^{2+} concentration of 1 mM, Mg^{2+} concentrations >4 mM caused a mild inhibition of the reaction. In marked contrast to the absolute requirement for ATP hydrolysis in DNA unwinding, increasing ATP concentrations strongly inhibited the DNA strand annealing reaction (Figure 3b). A similar, if slightly less dramatic, inhibition was seen with the poorly hydrolyzable ATP analog, ATPγS. In contrast, concentrations of ADP up to 20 mM had no detectable inhibitory effect on the reaction (Figure 3b). Hence, the ssDNA annealing reaction promoted by BLM has different

Nucleic Acids Research, 2005, Vol. 33, No. 12 3935

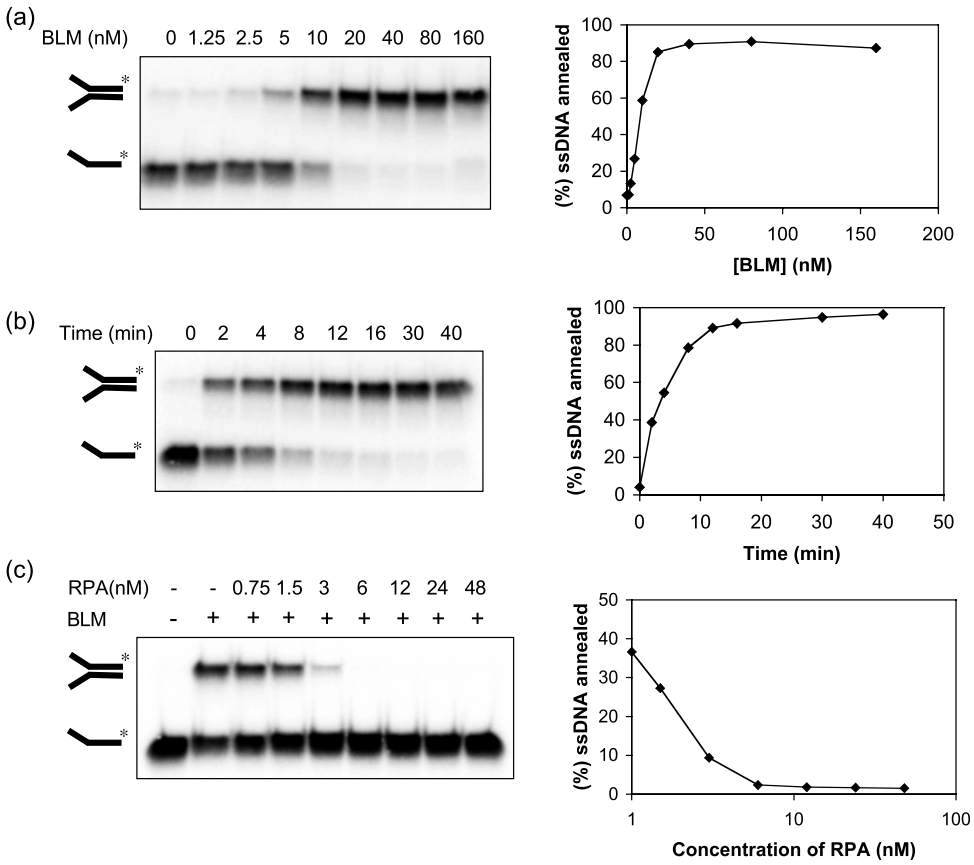

Figure 2. BLM promotes annealing of ssDNA. (**a**) Effect of BLM concentration on the annealing of two ssDNA molecules to generate a forked duplex. Reactions were incubated for 30 min. (**b**) Time course of ssDNA annealing in reactions containing 20 nM BLM. (**c**) Effect of increasing concentrations of RPA on ssDNA annealing catalyzed by 10 nM BLM. In (a–c), the percentage of ssDNA annealed was quantified and the data are presented graphically on the right of the corresponding dataset.

Mg^{2+} and adenine nucleotide co-factor requirements from those needed to support BLM helicase activity.

Next, we asked whether oligonucleotide length influenced the efficiency of BLM-mediated strand annealing (Figure 4). We found that complementary 15mer oligonucleotides were not annealed to any detectable extent, while a 31mer pair could be annealed, albeit very inefficiently, requiring a BLM concentration of >40 nM. Increasing the oligonucleotide length to 50 nt substantially increased the extent of annealing, particularly in reactions containing a low BLM concentration (<20 nM). We then asked whether the annealing reaction required that the two oligonucleotides be fully complementary. To analyze this, we used two related oligonucleotide pairs. One pair comprised a 31mer complementary region and a non-complementary 19mer tail, which could form a forked partial duplex, and the other comprised the same 31mer complementary region flanked by two 19mer non-complementary regions that could form a twin-forked duplex (Figure 4a). Both oligonucleotide pairs could be annealed efficiently by BLM (Figure 4a and b), indicating that the annealing reaction does not require the oligonucleotides to be fully complementary, and that the complementary portion of the oligonucleotide need not be located at the ends of the DNA molecule. Despite containing only 31 nt of complementary sequence, these oligonucleotides were annealed as efficiently as the fully complementary 50mers, and far more efficiently than the fully complementary 31mer pair (Figure 4a and b). These data indicate that, for a fixed length of complementary sequence, the overall length of the oligonucleotide strongly influences the efficiency of the annealing reaction.

Next, we addressed whether the differences in annealing efficiency noted above for different lengths of ssDNA were reflected in differences in the ability of BLM to form a stable complex with each DNA substrate. To achieve this, we used gel retardation assays with a 15mer, a 31mer and a 50mer single-stranded oligonucleotide. As shown in Figure 4c and d, BLM formed a stable complex with the 50mer and, to a much lesser extent, with the 31mer, but no complex with the 15mer could be detected. These data suggest that the DNA length-dependence of the ssDNA annealing reaction may be a reflection of the relative ability of BLM to bind stably to DNA molecules of different length.

In order to identify functional domains in BLM required for the ssDNA annealing reaction, we purified a series of truncated versions of BLM, which are shown diagrammatically in Figure 5. These variants all contain the central helicase and

3936 Nucleic Acids Research, 2005, Vol. 33, No. 12

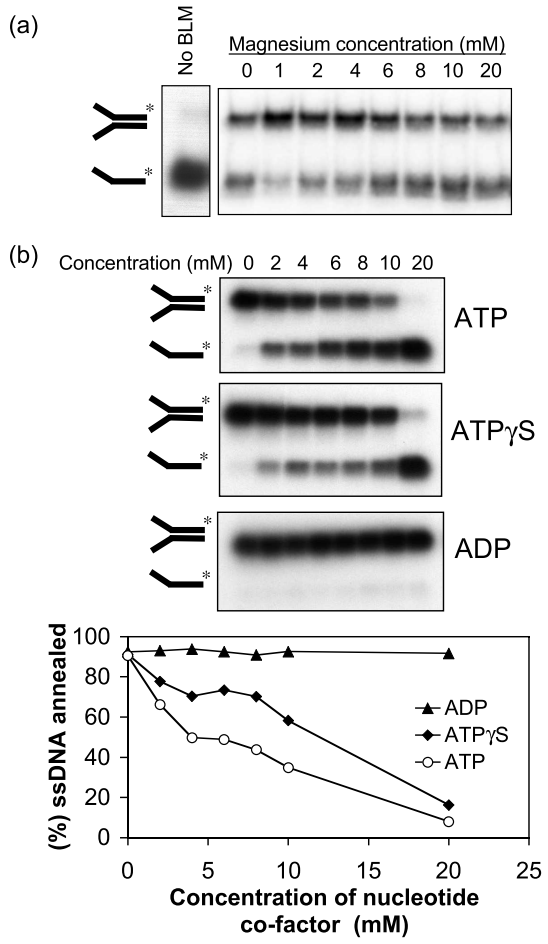

Figure 3. Effect of Mg^{2+} and adenine nucleotide co-factors on ssDNA annealing. (**a**) Strand annealing by BLM (10 nM) as a function of increasing Mg^{2+} concentration. The reaction shown in the left panel was performed in the absence of BLM. (**b**) Strand annealing by BLM (10 nM) as a function of increasing concentration of ATP, ATPγS or ADP, as indicated. Graph below shows quantification of the data.

RQC domains, but lack part or all of the N-terminal domain, and in some cases also part of the C-terminal domain. Initially, we analyzed whether strand annealing required the N- and C-terminal portions of BLM. A BLM variant lacking the N-terminal 212 amino acids (BLM213–1417) was proficient at strand annealing (Figure 6a and b), as indeed was BLM642–1417 that lacked the entire N-terminal domain (data not shown). In contrast, BLM213–1267 was barely able to catalyze strand annealing above the background level seen in the absence of BLM (Figure 6a and b) and showed a >10-fold reduced rate of strand annealing in comparison with BLM213–1417. This difference between these two BLM variants was specific for the strand annealing function of BLM, since the intrinsic helicase activity of each protein was comparable (Figure 6c). Importantly, these helicase assays were performed in the presence of SSB in order to prevent ssDNA annealing.

The results presented thus far would indicate that the C-terminal domain of BLM between residues 1267 and 1417 is important for its strand annealing function. Given that the entire N-terminal domain of BLM is dispensable for ssDNA annealing, we used BLM variants commencing at residue 642 to analyze whether the annealing function could be localized to a particular region of the C-terminal domain of BLM. We found that a protein truncated by only 67 C-terminal residues (BLM642–1350) could promote efficient strand annealing (Figure 6d). In contrast, removal of an additional 60 residues (to create BLM642–1290) generated a protein that had no detectable annealing activity (Figure 6d). The removal of residues 1291–1350 appear to specifically affect the strand annealing function of BLM since BLM642–1290 protein is an active helicase (16).

Since we had shown above that a correlation exists between DNA binding efficiency and an ability to promote annealing of different lengths of ssDNA, we next asked if those truncation mutants of BLM that were unable to promote annealing might have an alteration in their intrinsic ssDNA binding properties. Using gel retardation assays we found that, although there was no quantitative difference in the total amount of ssDNA bound by full-length BLM and its truncated derivatives, there was a clear qualitative difference in the nature of the retarded complexes when comparing strand annealing-proficient and -deficient variants. Using BLM, BLM213–1417, BLM642–1417 or BLM642–1350 at concentrations that promote efficient strand annealing, most of the retarded DNAs could not be resolved in the gel, indicative of the formation of large protein–DNA complexes (Figure 7). In contrast, the retarded species seen in reactions with the two strand annealing-defective variants, BLM213–1267 and BLM642–1290, were readily resolved within the gel (Figure 7). Taken together, these data indicate that the first 641 amino acids of BLM are not important for ssDNA binding or annealing, but that the 60 residues between positions 1290 and 1350 are essential for strand annealing and for the formation of higher-order protein–DNA complexes.

DISCUSSION

We report a new activity for the BLM helicase in showing that BLM promotes efficient annealing of complementary ssDNA molecules. This activity does not require Mg^{2+} or ATP, the co-factors essential for BLM to perform its helicase function. We have shown that significant DNA length dependence exists for the BLM strand annealing activity, which appears to derive from differences in the ability of BLM to form stable complexes with ssDNA of different lengths. Most interestingly, this length dependence does not require that the annealed strands be fully complementary. This may suggest that the mechanism by which BLM promotes ssDNA annealing is for it to bind non-specifically to the two ssDNA molecules and then to bring them into close proximity via protein–protein interactions between BLM molecules bound to the individual oligonucleotides. The length dependence may, therefore, reflect the number of BLM molecules that can bind simultaneously to each ssDNA molecule. Using different BLM variants, we found a strong correlation exists between ssDNA annealing activity and an ability to form higher-order protein–DNA complexes that were not resolved on polyacrylamide gels. In line with the comments above, we would propose that the formation of these large molecular

Nucleic Acids Research, 2005, Vol. 33, No. 12 3937

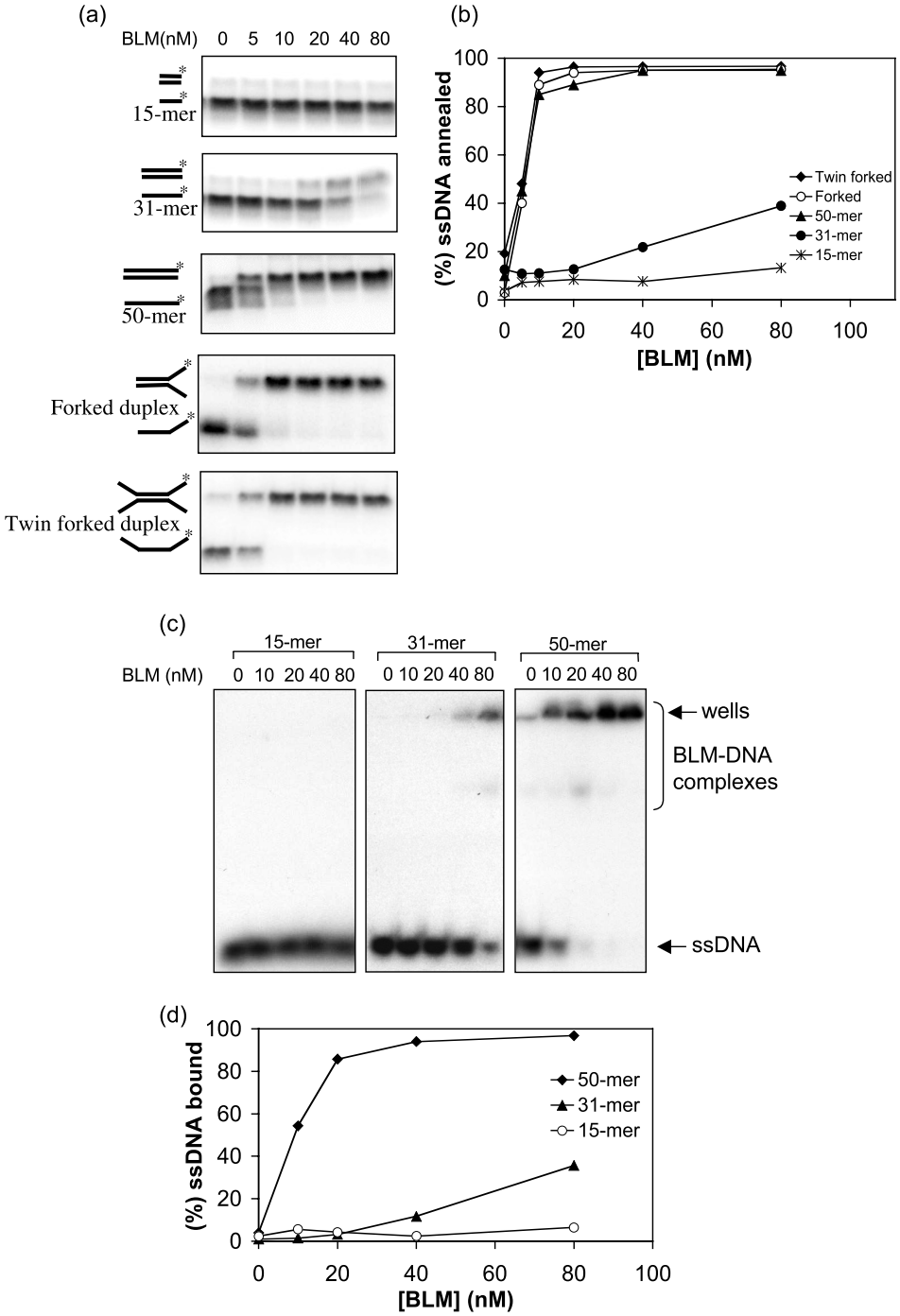

Figure 4. Strand annealing of different ssDNA structures by BLM. (**a**) In each case, different concentrations of BLM (indicated above the lanes) were incubated with the ssDNA species indicated on the left of each autoradiogram. The positions of the unannealed ssDNA and the annealed fully duplex or partial duplex products are indicated on the left. (**b**) Quantification of the data in (a). (**c**) Gel retardation assays with increasing quantities of BLM and the ssDNA oligonucleotides indicated above the wells. The positions of the ssDNA and the retarded BLM–DNA complexes are shown on the right. (**d**) Quantification of the data from (c).

weight complexes is a function of the binding of multiple BLM molecules to each ssDNA oligonucleotide.

BLM may promote ssDNA annealing in a manner similar to that of the RAD52 recombination protein. RAD52 forms oligomeric rings that bind ssDNA on their outer surface, and the annealing reaction requires that multiple rings engage their bound ssDNA in a large complex (20,21). BLM is oligomeric in solution, and previous studies have identified

3938 Nucleic Acids Research, 2005, Vol. 33, No. 12

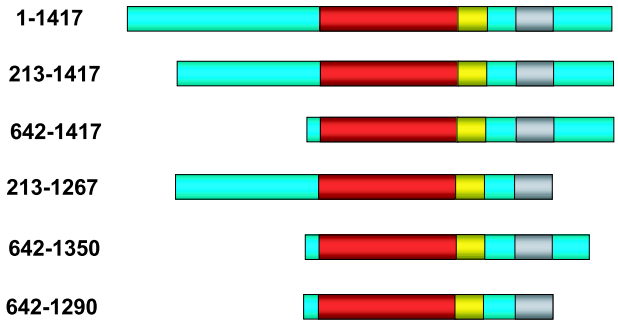

Figure 5. Schematic representation of the full-length BLM (1–1417) and truncated BLM variants used in this study. Amino acid residue numbers of each protein are indicated on the left. The positions of the helicase (red), RQC (yellow), HRDC (gray) domains are indicated. Green boxes denote poorly conserved regions.

4- and 6-fold symmetric ring structures that can form in the absence of DNA (22). However, the oligomeric state of the catalytically active form of BLM remains to be confirmed. Certain truncated forms of BLM are monomeric in solution and yet can still perform DNA unwinding (16), suggesting that the ability to form oligomers is not obligatory for helicase function. An interesting avenue for future research will be to address whether oligomerization of BLM is required for its ssDNA annealing function.

Recent data indicate that BLM is not alone among RecQ helicases in promoting strand annealing. Garcia *et al.* (23) showed that human RECQ5β also possesses a DNA strand annealing activity that is strongly inhibited by RPA. However, we have data to indicate that such a strand annealing activity is not conserved in *E.coli* RecQ (C.F. Cheok, L. Wu and I.D. Hickson, unpublished data). This suggests that the annealing function is unlikely to be intrinsic to the highly conserved

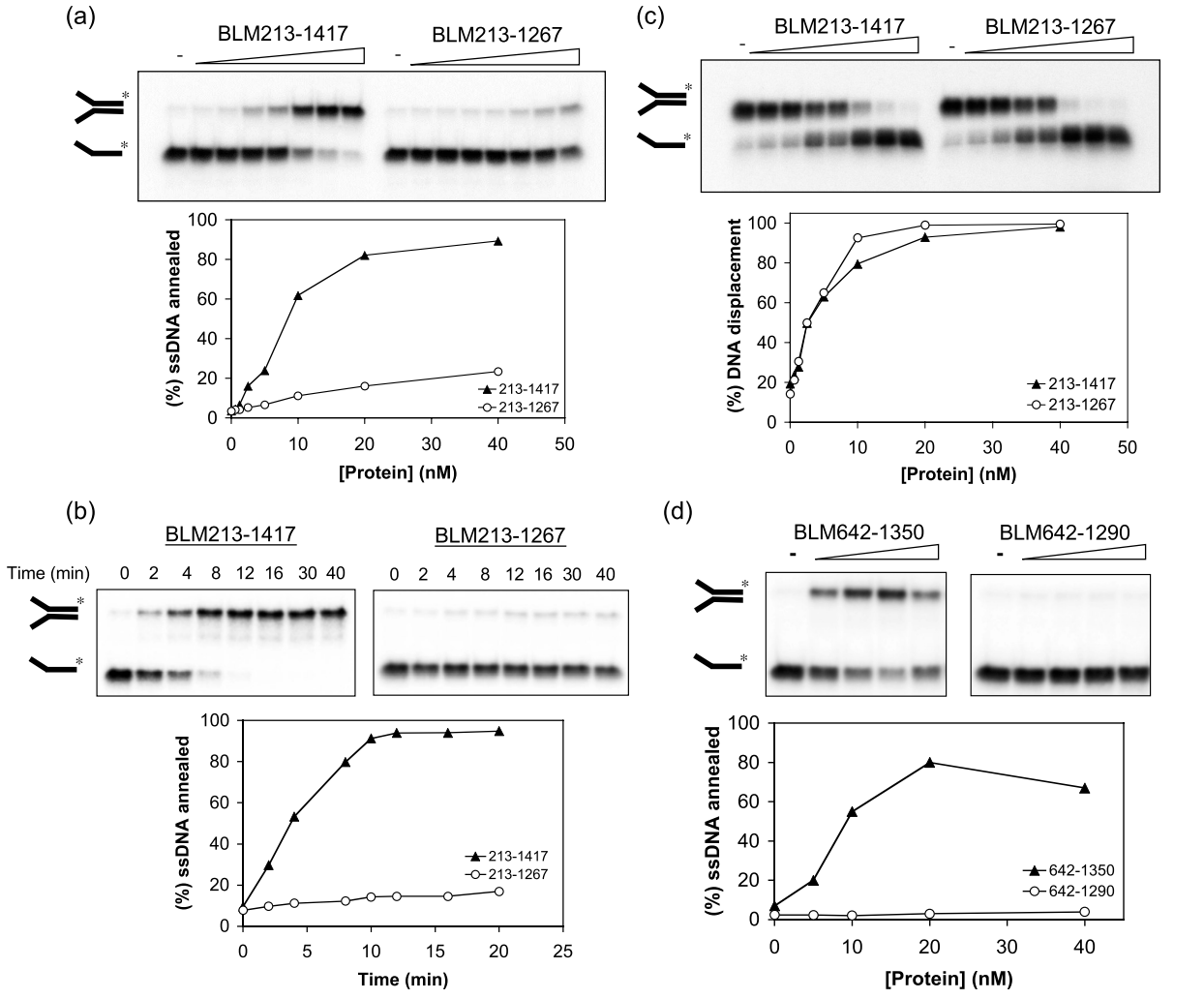

Figure 6. The C-terminal domain of BLM, between residues 1290 and 1350, is required for ssDNA annealing. (**a**) Strand annealing as a function of increasing protein concentration for BLM213–1417 and BLM213–1267. Reactions were incubated for 30 min. The graph below shows quantification of the data. (**b**) Time course of ssDNA annealing by 20 nM BLM213–1417 or BLM213–1267. The graph below shows quantification of the data. (**c**) Comparison of the helicase activity of BLM213–1417 and BLM213–1267. Assays were as described in Figure 1. Graph below shows quantification of the data. (**d**) Strand annealing as a function of increasing protein concentration for BLM642–1290 and BLM642–1350. Graph below shows quantification of the data.

Nucleic Acids Research, 2005, Vol. 33, No. 12 3939

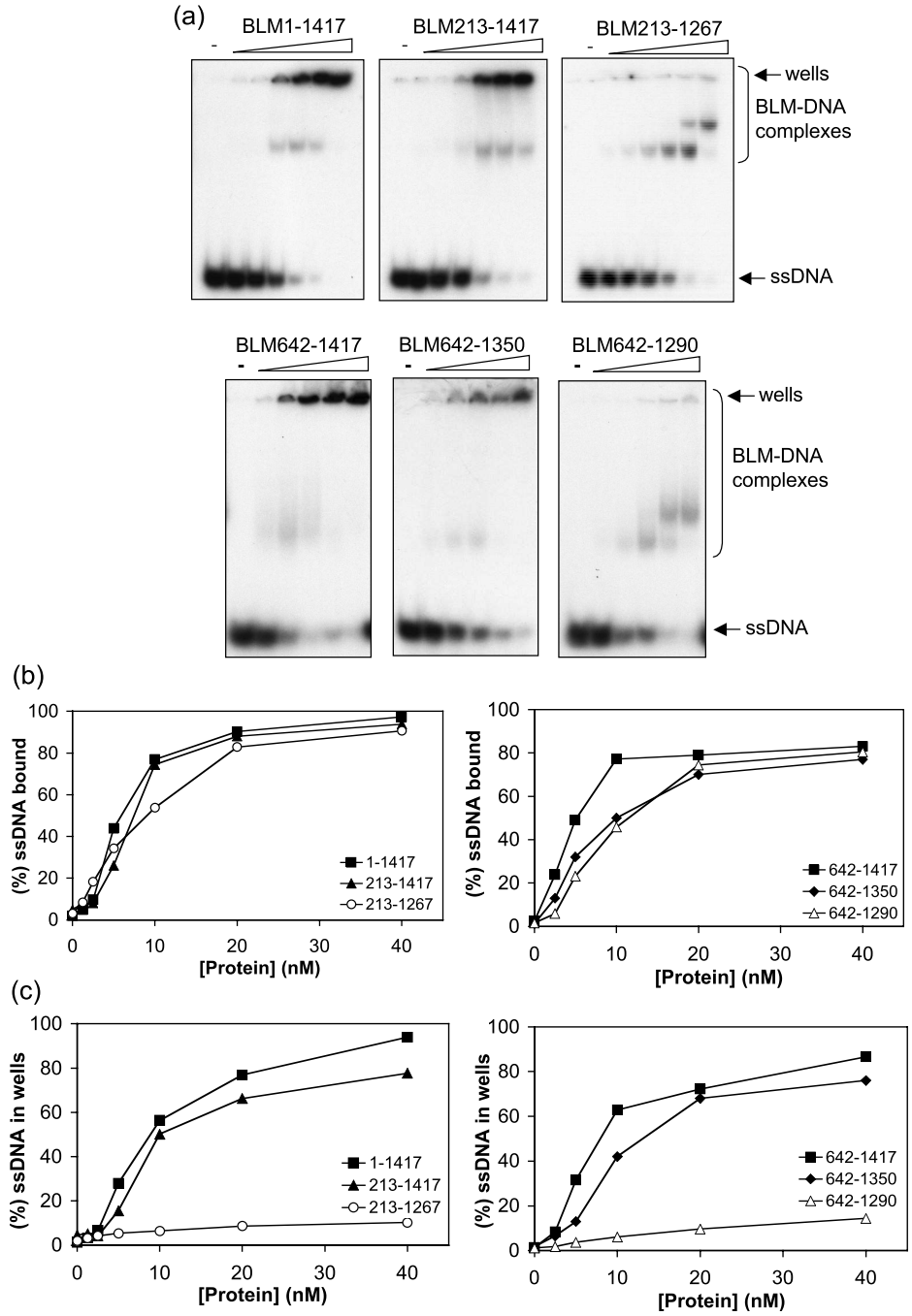

Figure 7. The C-terminal domain of BLM is required for the formation of higher-order protein–DNA complexes. (**a**) Gel retardation assays of BLM1–1417, BLM213–1417, BLM213–1267 (upper panel), BLM642–1417, BLM642–1350 and BLM642–1290 (lower panel) using a 50mer ssDNA oligonucleotide. The positions of the gel wells and of BLM–DNA complexes that could be resolved in the gel are indicated on the right. (**b**) Quantification of total ssDNA bound by BLM and its truncated derivatives. (**c**) Quantification of the ssDNA that was retarded in the gel wells. For clarity, the data are represented on two graphs in each case.

helicase and RQC domains, but rather is dictated by one of the poorly conserved N- or C-terminal regions that flank these domains in BLM. Consistent with this, the C-terminal domains of BLM and RecQ5β are required for ssDNA annealing activity. Interestingly, the C-terminal domains of these two proteins, however, show little sequence similarity. Notably, the RecQ5β C-terminal domain lacks both the 60 amino acid region found in the C-terminal domain of BLM, which we have shown is essential for ssDNA annealing activity, and an HRDC domain, which in BLM lies adjacent to the critical

3940 Nucleic Acids Research, 2005, Vol. 33, No. 12

60 amino acid region. Moreover, there are obvious differences in the effects of nucleotide analogs on the respective activities of the two proteins. Most notably, the annealing activity of RECQ5β is inhibited by ATPγS, but not by ATP or ADP, whereas BLM is inhibited by both ATPγS and ATP. While this manuscript was in preparation, we became aware of an electronic paper in press containing findings that overlap with those presented here. Machwe *et al.* (24) reported that RecQ family members, including BLM, promote DNA strand pairing as well as DNA unwinding. Our findings are in general agreement with those of Machwe *et al.* (24), except we did not find that BLM requires Mg^{2+} for its strand annealing activity. Moreover, in the present work, we have significantly extended our knowledge of the strand annealing function of BLM. In particular, we have mapped a domain in BLM vital for strand annealing activity and have defined structural features of the DNA substrates that are required for BLM to mediate this function.

An important issue to address is why should RecQ helicases catalyze apparently antagonistic reactions: DNA unwinding and ssDNA annealing? Although the precise cellular role of any RecQ helicases is not fully elucidated, our previously published evidence indicates that BLM co-operates with topoisomerase IIIα to resolve DNA intermediates that arise during recombinational repair of replication forks (25). The ability of BLM to promote strand annealing of molecules with non-complementary ends indicates that BLM can promote strand annealing at internal sites in DNA and may not require DNA end recognition. One potential role for ssDNA annealing activity may be to promote the processing of Holliday junctions. BLM and topoisomerase IIIα together catalyze double Holliday junction dissolution (25), a process that requires the juxtaposition of two individual Holliday junctions. As two Holliday junctions are brought together in close proximity, the torsional stress generated by the convergence of the two junctions may be relieved by topoisomerases acting ahead of each migrating Holliday junction. The strand annealing activity of BLM acting on the strands behind each junction may function to overcome the torsional constraints imposed by two converging Holliday junctions (Figure 8a). Furthermore, as the two junctions are brought together in close proximity, steric hindrance may prevent either junction from being able

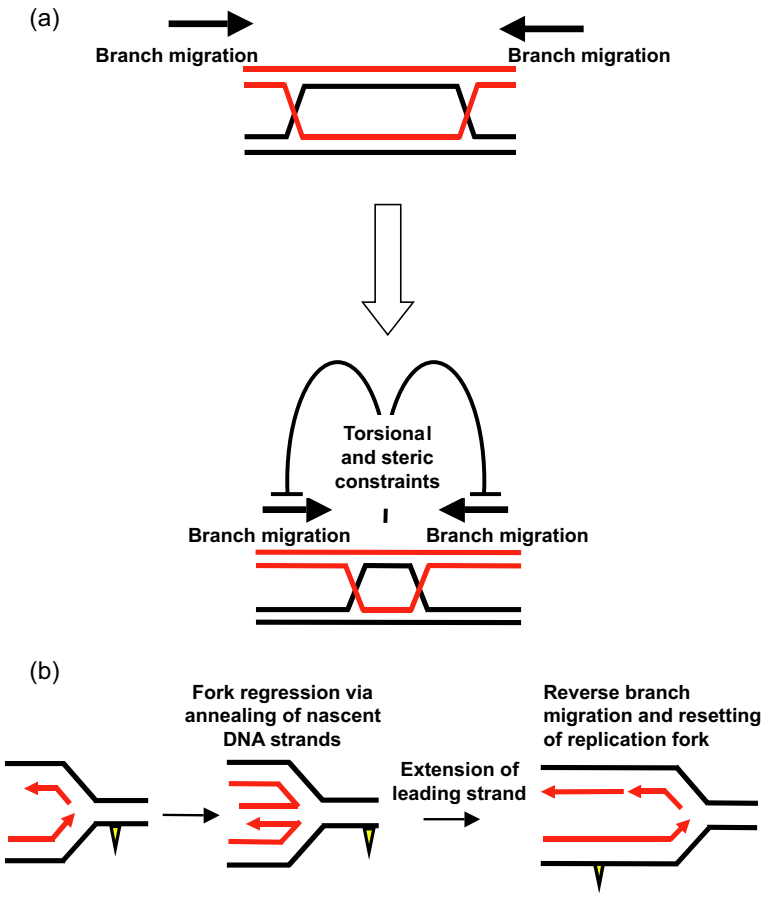

Figure 8. Models for the possible role of the strand annealing function of BLM in replication fork maintenance. (**a**) Branch migration model. Schematic representation of how torsional stress and steric hindrance may impede the convergence of two Holliday junctions by branch migration. The strand annealing activity of BLM acting on strands behind each junction may act to overcome these constraints and thereby facilitate the juxtaposition of two Holliday junctions. See text for details. (**b**) Fork regression model. Template strands are shown in black and nascent strands in red. The yellow triangle depicts a fork-blocking adduct on the leading strand template. See text for details.

to assume the necessary square planar configuration. Rather, each junction may assume the configuration in which the two duplexes are stacked, which is inhibitory to classical branch migration. Under these conditions, the ssDNA annealing activity of BLM may be required to promote an atypical form of Holliday junction branch migration in order to generate a hemicatenane, the presumed substrate for double Holliday junction dissolution. Our recent data indicate that the two strand annealing defective derivatives of BLM described here are also defective in catalyzing Holliday junction dissolution (26), although whether there is a mechanistic link between these two functions is unclear at this stage.

A second possible model (Figure 8b) for the role of the ssDNA annealing function specifically links BLM function with repair of damaged replication forks. Lesions on the leading strand template for DNA replication likely block fork progression. One proposal is that lesion bypass can occur via template switching in which the fork regresses via the annealing of the nascent strands to form a so-called chicken-foot structure (15,27). After extension of the leading strand and/or lesion removal, the regressed fork (a four-way junction) can be reversed by branch migration to re-set an active fork. We propose that BLM could catalyze both the fork regression step, by promoting annealing of the nascent strands, and the reversal of the regressed fork, using its helicase/branch migration function. In this way, BLM recruited to the arrested fork could promote repair and hence restoration of productive DNA replication. Clearly, further work is needed to identify whether these models have validity.

ACKNOWLEDGEMENTS

The authors thank Dr A.Vindigni for human RPA, Dr P. McHugh for helpful comments on the manuscript and members of the Genome Integrity Group for useful discussions and technical help. This work was supported by Cancer Research UK and the Swiss National Science Foundation. Funding to pay the Open Access publication charges for this article was provided by JISC. C.F.C. acknowledges the support of A*STAR (Singapore).

Conflict of interest statement. None declared.

REFERENCES

1. German,J. (1995) Bloom's syndrome. *Dermatol. Clin.*, **13**, 7–18.
2. Hickson,I.D. (2003) RecQ helicases: caretakers of the genome. *Nature Rev. Cancer*, **3**, 169–178.
3. Mohaghegh,P., Karow,J.K., Brosh,R.M.,Jr, Bohr,V.A. and Hickson,I.D. (2001) The Bloom's and Werner's syndrome proteins are DNA structure-specific helicases. *Nucleic Acids Res.*, **29**, 2843–2849.
4. Huber,M.D., Lee,D.C. and Maizels,N. (2002) G4 DNA unwinding by BLM and Sgs1p: substrate specificity and substrate-specific inhibition. *Nucleic Acids Res.*, **30**, 3954–3961.
5. Li,J.L., Harrison,R.J., Reszka,A.P., Brosh,R.M.,Jr, Bohr,V.A., Neidle,S. and Hickson,I.D. (2001) Inhibition of the Bloom's and Werner's syndrome helicases by G-quadruplex interacting ligands. *Biochemistry*, **40**, 15194–15202.
6. Sun,H., Karow,J.K., Hickson,I.D. and Maizels,N. (1998) The Bloom's syndrome helicase unwinds G4 DNA. *J. Biol. Chem.*, **273**, 27587–27592.
7. Wu,X. and Maizels,N. (2001) The substrate-specific inhibition of RecQ helicases. *Nucleic Acids Res.*, **29**, 1765–1771.
8. Bernstein,D.A., Zittel,M.C. and Keck,J.L. (2003) High-resolution structure of the *E.coli* RecQ helicase catalytic core. *EMBO J.*, **22**, 4910–4921.
9. von Kobbe,C., Thoma,N.H., Czyzewski,B.K., Pavletich,N.P. and Bohr,V.A. (2003) Werner syndrome protein contains three structure-specific DNA binding domains. *J. Biol. Chem.*, **278**, 52997–53006.
10. von Kobbe,C., Harrigan,J.A., May,A., Opresko,P.L., Dawut,L., Cheng,W.H. and Bohr,V.A. (2003) Central role for the Werner syndrome protein/poly(ADP-ribose) polymerase 1 complex in the poly(ADP-ribosyl)ation pathway after DNA damage. *Mol. Cell. Biol.*, **23**, 8601–8613.
11. Opresko,P.L., von Kobbe,C., Laine,J.P., Harrigan,J., Hickson,I.D. and Bohr,V.A. (2002) Telomere-binding protein TRF2 binds to and stimulates the Werner and Bloom syndrome helicases. *J. Biol. Chem.*, **277**, 41110–41119.
12. Brosh,R.M.,Jr, von Kobbe,C., Sommers,J.A., Karmakar,P., Opresko,P.L., Piotrowski,J., Dianova,I., Dianov,G.L. and Bohr,V.A. (2001) Werner syndrome protein interacts with human flap endonuclease 1 and stimulates its cleavage activity. *EMBO J.*, **20**, 5791–5801.
13. Morozov,V., Mushegian,A.R., Koonin,E.V. and Bork,P. (1997) A putative nucleic acid-binding domain in Bloom's and Werner's syndrome helicases. *Trends Biochem. Sci.*, **22**, 417–418.
14. Liu,Z., Macias,M.J., Bottomley,M.J., Stier,G., Linge,J.P., Nilges,M., Bork,P. and Sattler,M. (1999) The three-dimensional structure of the HRDC domain and implications for the Werner and Bloom syndrome proteins. *Structure Fold Des.*, **7**, 1557–1566.
15. Karow,J.K., Constantinou,A., Li,J.L., West,S.C. and Hickson,I.D. (2000) The Bloom's syndrome gene product promotes branch migration of Holliday junctions. *Proc. Natl Acad. Sci. USA*, **97**, 6504–6508.
16. Janscak,P., Garcia,P.L., Hamburger,F., Makuta,Y., Shiraishi,K., Imai,Y., Ikeda,H. and Bickle,T.A. (2003) Characterization and mutational analysis of the RecQ core of the Bloom's syndrome protein. *J. Mol. Biol.*, **330**, 29–42.
17. Wu,L., Davies,S.L., North,P.S., Goulaouic,H., Riou,J.F., Turley,H., Gatter,K.C. and Hickson,I.D. (2000) The Bloom's syndrome gene product interacts with topoisomerase III. *J. Biol. Chem.*, **275**, 9636–9644.
18. Karow,J.K., Chakraverty,R.K. and Hickson,I.D. (1997) The Bloom's syndrome gene product is a 3′–5′ DNA helicase. *J. Biol. Chem.*, **272**, 30611–30614.
19. Brosh,R.M.,Jr, Li,J.L., Kenny,M.K., Karow,J.K., Cooper,M.P., Kureekattil,R.P., Hickson,I.D. and Bohr,V.A. (2000) Replication protein A physically interacts with the Bloom's syndrome protein and stimulates its helicase activity. *J. Biol. Chem.*, **275**, 23500–23508.
20. Singleton,M.R., Wentzell,L.M., Liu,Y., West,S.C. and Wigley,D.B. (2002) Structure of the single-strand annealing domain of human RAD52 protein. *Proc. Natl Acad. Sci. USA*, **99**, 13492–13497.
21. Lloyd,J.A., Forget,A.L. and Knight,K.L. (2002) Correlation of biochemical properties with the oligomeric state of human rad52 protein. *J. Biol. Chem.*, **277**, 46172–46178.
22. Karow,J.K., Newman,R.H., Freemont,P.S. and Hickson,I.D. (1999) Oligomeric ring structure of the Bloom's syndrome helicase. *Curr. Biol.*, **9**, 597–600.
23. Garcia,P.L., Liu,Y., Jiricny,J., West,S.C. and Janscak,P. (2004) Human RECQ5beta, a protein with DNA helicase and strand-annealing activities in a single polypeptide. *EMBO J.*, **23**, 2882–2891.
24. Machwe,A., Xiao,L., Groden,J., Matson,S.W. and Orren,D.K. (2005) RECQ family members combine strand pairing and unwinding activities to catalyze strand exchange. *J. Biol. Chem.*, **280**, 23397–23407.
25. Wu,L. and Hickson,I.D. (2003) The Bloom's syndrome helicase suppresses crossing over during homologous recombination. *Nature*, **426**, 870–874.
26. Wu,L., Chan,K.L., Ralf,C., Bernstein,D.A., Garcia,P.L., Bohr,V.A., Janscak,P., Keck,J.L. and Hickson,I.D. (2005) The HRDC domain of BLM is required for the dissolution of double Holliday junctions. *EMBO J.*, doi:10.1083/sj.emboj.7600740.
27. McGlynn,P., Lloyd,R.G. and Marians,K.J. (2001) Formation of Holliday junctions by regression of nascent DNA in intermediates containing stalled replication forks: RecG stimulates regression even when the DNA is negatively supercoiled. *Proc. Natl Acad. Sci. USA*, **98**, 8235–8240.

4 Conclusions and Perspectives

The human genome is constantly challenged with endogenous and exogenous DNA damage and requires a set of mechanisms to preserve its integrity. The human RECQ helicases seem to play an important role in resolution of aberrant structures that arise from different repair pathways and are likely to mediate other functions as well. The fact that there are five different RecQ family members in humans, whereas unicellular organisms only contain a sole RecQ helicase, points to the evolutionary split-up and extension of the RecQ-mediated processes. Many groups have contributed to unravelling the roles of the RecQ helicases but the DNA transactions mediated by these proteins are diverse and are not fully understood yet.

Yet, to elucidate the roles of the human RecQ helicases, different approaches must be combined. The observation that BLM and RECQ5 have non-redundant roles in suppressing is further supported by our finding that RECQ5β cannot perform the DHJ dissolution in conjunction with TOPOIIIα which is consistent with our finding that the HRDC domain of BLM - absent in RECQ5β - is essential for efficient binding and unwinding of DHJs. As we have found that RECQ5β exhibits strand-annealing activity in addition to its helicase activity, it may be that RECQ5 acts in the recovery of damaged replication forks by promoting fork regression, whereas BLM suppresses cross-overs that would appear from the repair of non-meiotic DHJs that arise from HR-dependent repair of daughter strand gaps formed during replications. To address this possibility, the next steps would be to knock down the protein levels of RECQ5β in human cells and to characterise the phenotypic consequence with regard to sensitivities to DNA damaging agents and SCE frequency. A further evidence for the non-redundant roles of RECQ5β and BLM could be obtained by knocking down RECQ5β in BS cells and monitoring sensitivity to DNA damaging agents and the rate of SCEs. Furthermore, with experiments established for RecA and RecG to assay for fork-regression activity, RECQ5β should be tested for its potential ability to regress forks.

Surprisingly, the functions of the human RecQ helicases are more global than only restricted to resolve aberrant DNA structure, as has been shown with RECQ4 that plays a role in replication initiation. The question arises if the role of RECQ4 in replication initiation is an evolutionarily acquired function, or if it is conserved in bacteria as well. Therefore, this aspect may be studied in *E. coli* and *S. cervisiae*.

5 Acknowledgements

I’d like to thank Pavel for having given me the opportunity to do my PhD in his group and for guiding me along the way.

I’m grateful to Joe for all his support.

I thank everybody at IMCR, especially the friends I have found here.

Furthermore, I thank Steve West and Panos Soultanas for the collaborations and especially Ian Hickson for collaborations and discussions.

Last but not least, those without whom I would not have had the opportunity to grow and develop: my parents, family and friends. I thank them for all their support and love.

6 Curriculum Vitae

Patrick L. Garcia
Schützenstrasse 9
CH-8702 Zollikon
Switzerland
mobile: +41(0)765829902
patrick.l.garcia@gmail.com

Place and date of birth, marital status, nationality

Born 23.10.1975 in Vevey, VD (Switzerland), single, swiss and spanish nationalities

Profession

Ph.D. student in biochemistry/molecular biology at the Institute for Molecular Cancer Research at the University of Zürich, Switzerland.

Awards

Charles Rodolphe Brupbacher Young Investigator's Award 2005

Languages

German	mother tongue	Spanish	good
English	accent free	Italian	good
Dutch	accent free	Portuguese	basic knowledge
French	very good	Swedish	basic knowledge

Education

1997-2002	Diploma studies of Biologie II (Biochemistry) at the Biocentre of the University of Basel, Switzerland.
1991-1997	High school, Gymnasium Interlaken Type C (focus on Mathematics and Physics), Interlaken BE.
1986-1991	Secondary school Unterseen, Unterseen BE
1982-1986	Primary school Unterseen, Unterseen BE

Scientific education

2002-	PhD thesis in the research group of Dr. P. Janscak at the Institute of Molecular Cancer Research (IMCR) of the University of Zürich, Switzerland on the biochemical and cellular functions of the human RECQ5β helicase. Responsible member of faculty: Prof. Dr. J. Jiricny

2001-2002 Diploma thesis in the group of Prof. Dr. T.A. Bickle in the department of Molecular Microbiology at the Biocentre, University of Basel, Switzerland under the supervision of Dr. P. Janscak with the title "Exploring the molecular mechanisms of the methyl-dependent restriction enzymes McrA and Mrr."

Other subject-related activities

2003- 2005 Translation of scientific articles for the official bulletin from English to German, interpreting and writing summaries of public talks on cancer for the website of the cancer league of the canton of Zürich. Contact person: C. de Capitani.

Summer 2001 One month training at the Microbial Quality Control of the Laboratories of Dr. G. Bichsel AG in Unterseen, Switzerland. Adjustment of SOPs and room-classifications to comply with GMP and pharmaceutical regulations (Pharmakopö) under the supervision of Dr. M. Eisenhawer.

Publications

Garcia,P.L., Bradley,G., Hayes,C.J., Krintel,S., Soultanas,P. and Janscak,P. (2004) RPA alleviates the inhibitory effect of vinylphosphonate internucleotide linkages on DNA unwinding by BLM and WRN helicases. *Nucl. Acids. Res.* **32**(12), 3771-3778

Garcia,P.L., Liu,Y., Jiricny,J., West,S.C., and Janscak,P., (2004) Human RECQ5b, a protein with DNA helicase and strand-annealing activities in the same polypeptide. *EMBO J.* 2004 Jul 21;**23**(14):2882-91.

Janscak,P., **Garcia,P.L.**, Hamburger,F., Makuta,Y., Shiraishi,K., Imai,Y., Ikeda,H. and Bickle,T.A. (2003) Characterization and mutational analysis of the RecQ core of the Bloom syndrome protein. *J. Mol. Biol.*, **330,** 29-42.

Employment whilst studying

Migros Interlaken, Bühler Spielwaren Interlaken, Mc Donald's Interlaken, Camping Manor Farm Interlaken-Unterseen, Coop Basel, Promoter Pool, Zürich (worked as a promoter in Yverdon, Rapperswil und Basel).

Hobbies

Playing the guitar, music, basketball, squash, tennis, volleyball, sailing, literature, painting, Salsa dancing